UNIVERSIDAD DE ANTIOQUIA

DYNAMIC QUANTITATIVE DESCRIPTION OF THE METABOLIC CAPABILITIES OF *STREPTOMYCES CLAVULIGERUS* FOR CLAVULANIC ACID PRODUCTION

Autor

David Andrés Gómez Ríos

Universidad de Antioquia

Facultad de Ingeniería, Departamento (Escuela, etc.)

Ciudad, Colombia

Año

CC BY NC ND

Dynamic Quantitative Description of the Metabolic Capabilities of *Streptomyces clavuligerus* for Clavulanic Acid Production

David Andrés Gómez Ríos

Tesis presentada como requisito para optar al título de:
Doctor en Ingeniería Química

Co- Directores.

Prof. Rigoberto Ríos Estepa Ingeniero Químico. MSc. PhD.
Prof. Silvia Mercedes Ochoa Cáceres. Ingeniera Química. MSc. Dr. Ing
Prof. Howard Diego Ramírez Malule. Ingeniero Químico. Dr.

Universidad de Antioquia
Facultad de Ingeniería, Departamento de Ingeniería Química
Medellín, Colombia
2020.

UNIVERSIDAD DE ANTIOQUIA
FACULTY OF ENGINEERING
DEPARTMENT OF CHEMICAL ENGINEERING

Dynamic Quantitative Description of the Metabolic Capabilities of *Streptomyces clavuligerus* for Clavulanic Acid Production

Thesis submitted in partial fulfillment of the requirements for the degree of
DOCTOR IN CHEMICAL ENGINEERING

By

DAVID ANDRÉS GÓMEZ RÍOS

Chemical Engineer. M.Sc

Prof. Rigoberto Ríos Estepa
Prof. Silvia Ochoa Cáceres
Prof. Howard Ramírez Malule

Grupo de Bioprocesos
Grupo de Investigación en Simulación, Diseño,
Control y Optimización de Procesos

UNIVERSIDAD DE ANTIOQUIA
Faculty of Engineering
Department of Chemical Engineering

Medellín, Colombia

2020

Acknowledgements

It is still strange to complete a four-year, hard-working process in the midst of such extraordinary circumstances on a global scale. This process does not refer only to reaching the highest degree in a field, but goes back to the entire chain of situations, people, purposes, interests and ideals that end up determining the chosen course. For this reason, there is probably no space to name and thank all the people who contributed to achieving the objectives and goals initially set.

At the risk of leaving someone out of these words, it is necessary to name those who come to mind at this time. First of all, to my family, the first and the most important thing I have: Dolly, José, Sebastián and Lida... even to Odín, this new and old dog spent many of its nights and early mornings by my side working on this. Each one with their love, patience, support, understanding, encouragement, help ... and even loans, contributed to have the required additional strength. I cannot forget to mention to my grandfather, Ing. Leonel de Jesus Ríos, who passed away before starting the program. He definitely influenced my decision to take this long journey through chemical engineering. In a small family, everyone has some influence, my grandparents, uncles, cousins; even friends, sometimes distanced due to the circumstances, but who can certainly be counted on.

I was fortunate to have three professors, something unusual. Their knowledge and experience contributed to outlining the correct path of this work, furthermore, they also gave me big support in the difficult circumstances that sometimes emerged during the course of the program. Many thanks to professors Dr. Rigoberto Ríos Estepa and Dr. Ing. Silvia Ochoa Cáceres at the University of Antioquia. Also to professor Dr. Howard Ramírez at the Universidad del Valle, with whom I have a close friendship as well as a productive scientific collaboration since that Chem. Eng. conference in Cartagena. Prof. Ramírez gave himself to this work from the beginning, even with his own resources and when the possibilities of recognition for it were scarce. Also thanks to Dr. Victor López Agudelo with whom I also gained a friendship so does a scientific collaboration as a result of this doctorate. Dr. López contributed importantly with his knowledge and experience in the final stages of this work in relation to metabolic modeling. To the research groups of Bioprocesos and Simulación, Diseño y Control de Procesos (SIDCOP), to the Department of Chemical Engineering, in it, to professors César Botache, Felipe Bustamante and Lina María Rodríguez for their support in different situations arisen during this program. To the postgraduate office staff who helped me on many occasions with my particular administrative situations; possibly they got rid of me.

It is also necessary to mention and to thank the members of the Fachgebiet Bioverfahrenstechnik in TU Berlin: Dr. Ing. Stefan Junne and Prof. Dr. Peter Neubauer, they have supported and put big efforts, time and resources to maintain this collaboration with Colombian partners. To the technical staff of the laboratory Dipl. Ing. Brigitte Burckhardt, Dipl. Thomas Högl and Irmgard Maue-Mohn for their assistance during experiments and analytics. Of course, to the “Latinos” in the laboratory: Dr. Ing. Klaus Pellicer, MSc. Roger Paixau, MSc. Marly Katherine Erazo, MSc. Lara Santolini, Dr. Ing. Carlos Gómez Camacho, Dr. Ing. Anika Bockisch and Dr. Ing. Anna Maria Marbà, all they made Berlin not look very "German".

I acknowledge the financial support of the Departamento Administrativo de Ciencia, Tecnología e Innovación—COLCENCIAS (Grants number 111577657246 CT 432-2017 and CTO 654-2015 ABioPro), as well as the Federal German Ministry of Education and Research (BMBF) (grant number 01DN16018).

Finally to the evaluation committee: Prof. Dr. Claudio Avignone-Rossa (University of Surrey, UK) , Prof. Dr. Camilo Suárez Mendez (Universidad Nacional de Colombia, Sede Medellín) and Prof. Dr. Carlos Martinez Riascos (Universidad Nacional de Colombia, Sede Bogotá), who dedicated their valuable time and contributed to improve the quality of this doctoral thesis.

To the Faculty of Engineering of University of Antioquia:

The members of the evaluation committee appointed to examine the Doctoral Dissertation presented by David Andrés Gómez Ríos find it satisfactory and recommend its acceptance, as well as a *Cum Laude* distinction for being considered a significant contribution to the field of research.

Members of the Evaluation Committee

Prof. Dr. Claudio Avignone Rossa
University of Surrey

Prof. Dr. Camilo Alberto Suárez Méndez
Universidad Nacional de Colombia

Prof. Dr. Carlos Arturo Martínez Riascos
Universidad Nacional de Colombia

Table of contents

Abstract

Clavulanic acid (CA) is a β-lactam antibiotic with potent inhibitory activity against β-lactamase enzymes, which are responsible for the antibiotic resistance phenomenon in several pathogenic bacteria. CA is a secondary metabolite of pharmaceutical and industrial interest naturally produced by the filamentous Gram-positive bacterium *Streptomyces clavuligerus* (*S. clavuligerus*) under limited nutritional conditions. CA has limited availability in the market, and its high cost is a consequence of the complexity of the production process. It is determined mainly by the low titers of CA obtained in submerged cultivations of *S. clavuligerus* and the difficulties associated with the down-stream process. Several authors have applied experimental approaches to study the influence of some variables, especially those of nutritional nature, on CA accumulation. Nevertheless, the effect of variables relevant to the bioprocess operation, as the reactor hydrodynamics and shear stress conditions, has not been well explored.

Fluxomic approaches have been recently applied to *S. clavuligerus* aimed to improve the understanding of its metabolism. Such approaches were mostly developed under steady-state assumptions, resulting in a limited comprehension of the metabolism under the dynamic conditions of batch and fed-batch processes. In this thesis, the reconstruction of a new and enhanced genome-scale model of *S. clavuligerus,* the successful combination of experimental studies in the shake flask and bioreactor scales coupled with constraint-based modeling in pseudo-steady (flux balance analysis) and dynamic (dynamic flux balance analysis) conditions were used as strategies for studying the metabolic response of *S. clavuligerus* to environmental and nutritional perturbations in connection with CA biosynthesis.

Experimental studies in stirred tank and 2-D rocking-motion bioreactors provided valuable information on the strain's metabolic response to environmental conditions, especially regarding the effect of shear forces. Moreover, the experimental data obtained allowed to test different *in silico* scenarios by using constraint-based modeling with a new and enhanced reconstruction of a genome-scale metabolic network of *S. clavuligerus,* aimed to understand the carbon fluxes distribution during the different environmental conditions attained during the cultivations. The use of constrained-based modeling under pseudo-steady state conditions (Flux Balance Analysis, FBA) and dynamic conditions (Dynamic Flux Balance Analysis, DFBA) allowed to explain the role of primary metabolism and revealed the dynamics of intracellular carbon fluxes distribution during CA biosynthesis. Furthermore, the *in silico* simulation of metabolic scenarios and experimental testing showed that fed-batch operation with glutamate supplementation is a favorable condition for increasing the CA production. Potential genetic engineering targets were identified and evaluated *in silico, aiming* to improve the CA titers in *S. clavuligerus* cultures. This is the first work considering the cultivation dynamics on experimental and *in silico* studies of *S. clavuligerus* metabolism.

Keywords: *Streptomyces clavuligerus*, clavulanic acid, dynamic flux balance analysis, genome-scale metabolic network, stirred tank reactor, single-use bioreactor, fed-batch, antibiotic resistance

Introduction

The finding that microorganisms are able to synthesize compounds with antibiotic activity is considered as one of the most important discoveries in the history of medicine since they made possible the effective treatment of infectious diseases saving millions of human lives in about seven decades. However, the inappropriate use of commercial antibiotics in humans and agriculture, along with the evolution and spread of mobile genetic resistance elements, has triggered the increase of antibiotics, multidrug and extremely drug resistance in the last decades.

Clavulanic acid (CA) is a β-lactam antibiotic with potent inhibitory activity against β-lactamase enzymes responsible, which is responsible for the hydrolysis of the β-lactam ring present in several wide-spectrum antibiotics. CA is a secondary metabolite naturally produced by the filamentous bacterium *Streptomyces clavuligerus* (*S. clavuligerus*) under limited nutritional conditions. CA is an analog of the penicillin ring, in which the characteristic sulfur atom has been substituted by an oxygen atom. The combined effective inhibition of β-lactamase and antibacterial activity of CA in combination with other β-lactam antibiotics make it very important, both clinically and economically. CA mechanism of action involves the irreversible bonding of the β-lactam ring, present in the CA molecule, with a serine residue part of the active site of β-lactamase enzymes, thus preventing the inactivation of the main antimicrobial agent.

CA has limited availability in the market and its high cost is a consequence of the complexity of the production process which is determined mainly by the low titers of CA obtained in submerged cultivations of *S. clavuligerus.* Different studies aiming at the improvement of the yield of CA production have been carried out in shake flasks and/or pilot-scale stirred tank reactors (STR), in which the maximum CA concentrations are in the range of 0.4-1.5 $g.L^{-1}$ depending on the nutritional conditions of cultivation and the operation mode (batch or fed-batch). So far, it is known that cultivation conditions can lead to changes in the carbon flux distribution along the metabolic networks of an organism. Nevertheless, the variability in CA titers reported by different authors reveals that the metabolic response of *S. clavuligerus,* under different environmental conditions and operation modes, is not clearly understood.

Currently, there are uncertainties concerning the causes of CA low titers in *S. clavuligerus* submerged cultures and how to overcome them. The modeling approaches and fluxomic studies regarding *S. clavuligerus* have been performed under steady state assumptions, resulting in a limited comprehension of the metabolism under the intrinsic dynamic conditions of batch and fed-batch processes. The previous experimental approaches have studied the influence of some variables, especially those of nutritional nature, on CA accumulation. Nevertheless, effect of variables relevant to the bioprocess operation, as the case of the reactor hydrodynamics and shear stress conditions, have been not explored beyond the traditional STR and airlift reactors. Moreover, the environmental conditions of cultivation could potentially induce metabolic phenotypical changes that would affect extracellular metabolites accumulation, including our product of interest, CA. The initially stated objectives to be achieved during this doctoral research are as follows:

General objective

To study the dynamics of the metabolic response of *S. clavuligerus* exposed to different environmental conditions, so as to propose strategies that eventually lead to enhanced CA titers.

Specific objectives

To set up an experimental design that allows characterizing the kinetics of *S. clavuligerus* cell cultures through batch and fed-batch cultivations in STR and 2-D single-use rocking-wave bioreactors.

To develop a genome-scale dynamic model of *S. clavuligerus*, as a tool for appraising the dynamic response of cell system exposed to different operating conditions.

To perform *in silico* studies at different bioprocessing scenarios (i.e. operating conditions and strain modifications) aimed at inducing *S. clavuligerus* physiological responses potentially leading to larger CA accumulation.

Consistent with the objectives declared, in this thesis, a successful combination of experimental studies in the shake flask and bioreactor scales with constraint-based modeling in pseudo-steady and dynamic conditions was used as strategy for studying the metabolic response of *S. clavuligerus* to environmental and nutritional perturbations in connection with CA biosynthesis. The experimental studies in shake flask scale, stirred tank and 2-D rocking-motion bioreactors provided valuable information of the metabolic response on the strain to environmental conditions, especially regarding the effect of shear forces. Moreover, the experimental data obtained allowed to test different *in silico* scenarios by using constraint-based modeling with a new and enhanced reconstruction of a genome-scale metabolic network of *S. clavuligerus*, aimed to understand the carbon fluxes distribution during the different environmental conditions attained during the cultivations.

The use of constrained-based modeling under pseudo-steady state conditions (Flux Balance Analysis, FBA) and dynamic conditions (Dynamic Flux Balance Analysis, DFBA) helps to explain metabolite accumulation profiles and their relationship with intracellular carbon fluxes distribution and accumulation of intermediates in the different metabolic scenarios arisen during non-steady state cultivations, as the case of batch and fed-batch operations. Furthermore, the *in silico* simulation of metabolic scenarios was applied for the study of genetic engineering targets as strategy for further design of a CA-overproducer strain.

This thesis is a compilation of six manuscripts that details the research process in the shake flask and bioreactor scales, so as the development of a new and enhanced genome-scale metabolic network for *S. clavuligerus* and the implementation of a methodological approach involving constraint-based modeling in pseudo-steady state (FBA) and dynamic conditions (DFBA) aimed to characterize the metabolic capabilities of *S. clavuligerus* for CA production. A summary of the chapters comprising this thesis and the contributions in peer-reviewed scientific journals and academic events is presented below.

1. Chapter 1: describes the importance of CA as a pharmaceutical compound of clinical and industrial importance. Additionally, a review of the current application of systemic approaches in CA and *S. clavuligerus* studies is presented.
2. Chapter 2: the use of different media was explored for determination of the most favorable cultivation conditions regarding the CA production. The study was aimed to identify the best experimental condition for obtaining stable growth of the microorganism and detectable concentrations of CA for the further studies at bioreactor scale regarding the nutritional limitation and impact of oxygen mass transfer and agitation on CA production.
3. Chapter 3: a comparative analysis of the metabolic response *of S. clavuligerus* and CA production in STR (high-shear stress conditions) and 2-D rocking-motion (low-shear stress conditions) bioreactors is presented. The shear stress conditions affected considerably the morphology of the strain, the metabolites accumulation and the oxygen transfer, all impacting the CA production.
4. Chapter 4: a new and improved genome-scale model of the *S. clavuligerus* metabolism (iDG1237) was presented. This model was used in a combined modeling-experimental based approach for investigating the link between the different nutritional conditions observed in *S. clavuligerus* cultivations and CA biosynthesis.
5. Chapter 5: presents the implementation of a DFBA framework for the analysis of dynamic characteristics of *S. clavuligerus* metabolism in connection with CA production and cultivation

operation mode, aimed to explore potential metabolic scenarios that might lead to the enhancement of CA production in wild-type and engineered strains.

6. Chapter 6**:** the experimental-based modeling of CA degradation kinetics in fermentation broth at low temperatures (−80, −20, 4, and 25 °C) as well as during the imidazole–derivatized conditions are presented. Determination of kinetic constants for predicting the degradation rate of CA under fermentation conditions is of interest for the bioprocess operation and downstream processing.

List of contributions

Scientific papers

- Gómez-Ríos, D.; Junne, S.; Neubauer, P.; Ochoa, S.; Ríos-Estepa, R.; Ramírez-Malule, H. Characterization of the Metabolic Response of Streptomyces clavuligerus to Shear Stress in Stirred Tanks and Single-Use 2D Rocking Motion Bioreactors for Clavulanic Acid Production. *Antibiotics* **2019**, *8*, 168, doi:10.3390/antibiotics8040168

- Gómez-Ríos, D.; Ramírez-Malule, H.; Neubauer, P.; Junne, S.; Ríos-Estepa, R. Degradation kinetics of clavulanic acid in fermentation broths at low temperatures. *Antibiotics* **2019**, *8*, 6, doi:10.3390/antibiotics8010006.

- Gómez-Ríos, D.; Ramírez-Malule, H.; Neubauer, P.; Junne, S.; Ríos-Estepa, R. Data of clavulanic acid and clavulanate-imidazole stability at low temperatures. *Data Br.* **2019**, *23*, 103775, doi:10.1016/j.dib.2019.103775.

- Gómez-Ríos, D.; Ramírez-Malule, H. Bibliometric analysis of recent research on multidrug and antibiotics resistance (2017–2018). *J. Appl. Pharm. Sci.* **2019**, *9*, doi:10.7324/JAPS.2019.90515

- Gómez-Rios, D; López-Agudelo, V; Ramírez-Malule, H.; Neubauer, P.; Junne, S.; Ochoa, S.; Ríos-Estepa, R. A combined constraint-based modeling and experimental approach clears up the metabolic relationship during clavulanic acid production between the tricarboxylic acid cycle intermediates, amino acid biosynthesis, phosphate and oxygen uptake. *Microorganisms* **2020**, (under evaluation)

Scientific and academic presentations

- 2nd Bioprocess Winter School. "Modeling of the Central Carbon Metabolism of *Streptomyces Clavuligerus*: a kinetic approach". October 19th-21st , 2016. Medellín, Colombia.

- 10th World Congress of Chemical Engineering & 4th European Congress of Applied Biotechnology. "Kinetic modeling of accumulation of TCA cycle intermediates during clavulanic acid biosynthesis in batch cultures of *Streptomyces clavuligerus"*. October 1st- 5th, 2017. Barcelona, Spain.

- 29 Congreso Colombiano de Ingeniería Química. "Acumulación de intermedios del ciclo de los ácidos tricarboxílicos en la biosíntesis de ácido clavulánico en cultivos en lote de *Streptomyces clavuligerus*". October 18th-20th, 2017. Manizales, Colombia.

- 5th BioProScale Symposium. "Comparison of *Streptomyces clavuligerus* cultivations in Stirred Tank and Single Use Rocking Wave Bioreactors for Production of Clavulanic Acid". March 20th-23th, 2018. Berlin, Germany.

- 3rd Biochemical Process Winter School. "Metabolic response of *Streptomyces clavuligerus* to environmental conditions in stirred tank and single use 2-D rocking-motion bioreactors". August 21st-23rd, 2019. Medellín, Colombia.

- 12th European Congress of Chemical Engineering & 5th European Congress of Applied Biotechnology. "Physiological Response of *Streptomyces clavuligerus* to shear forces in 2-D Rocking Motion and Stirred Tank Bioreactors". September 15th-19th, 2019. Florence, Italy.

- V Congreso Colombiano de Biología Computacional y Bioinformática. "Modelado dinámico a escala genómica del metabolismo de *Streptomyces clavuligerus*: análisis de la respuesta metabólica al efecto de la captación de oxígeno en la biosíntesis de ácido clavulánico". November 5th-8th, 2019. Ibagué, Colombia.

Chapter 1

Systemic Approaches in Clavulanic Acid Production and *Streptomyces clavuligerus* Studies

Abstract: Antibiotic resistance is considered nowadays, as a severe public health problem. Among the bacterial defense against antibiotics action, the production of specific antibiotic-hydrolyzing enzymes is one of the most spread mechanisms. β-lactamase inhibitors are antibiotic compounds that inactivate the β-lactamase enzymes produced by several bacterial species as defense mechanisms against the action of wide-spectrum β-lactam antibiotics like penicillins. Clavulanic acid is a β-lactam antibiotic with modest activity, produced by the filamentous bacterium *Streptomyces clavuligerus* and it is also a potent inhibitor of β-lactamases. Clavulanic acid production has been widely studied and the adoption of systemic approaches aid to improve the understanding of the diverse metabolic phenotypes and carbon flux distribution during CA biosynthesis. This review focuses on CA production and the implementation of systemic approaches for studying *S. clavuligerus* metabolism and CA production as well as genetic engineering for strain improvement.

1.1. Introduction

The finding that microorganisms are able to synthesize compounds with antibiotic activity is considered as one of the most important discoveries in the history of medicine since they made possible the effective treatment of infectious diseases saving millions of human lives in approximately seven decades since its discovery. However, the inappropriate use of commercial antibiotics in humans and agriculture, along with the evolution and spread of mobile genetic resistance elements, has triggered the increase of antibiotics, multidrug and extremely drug resistance in the last decades [1]. The increase in resistance generated by bacteria to antibiotics is a worldwide phenomenon and there is no hospital or health institution that could escape from this reality.

Currently, three mechanisms used by bacteria to create resistance to antibiotics have been identified: (i) putative changes in penicillin-fixing proteins (PBP) making inaccessible the proteins to the antibiotics, (ii) in Gram-negative bacteria, development of a antibiotics-non-permeable membrane, together with the presence of an efflux pump that takes the antibiotic out from the periplasmic space to the extracellular environment, and (iii) production of drug-hydrolyzing enzymes [2]. In this last mechanism we can distinguish two forms. One is production of an enzyme specifically directed towards a particular antibiotic, such as chloramphenicol acetyl transferase, which is an enzyme capable of destroying the chloramphenicol molecule. The other is the production of β-lactamases, enzymes that hydrolyze the β-lactam ring of penicillin-type antibiotics, cephalosporins and their derivatives [2]. β-lactamases are produced by both Gram-negative and Gram-positive bacteria, as well as aerobic, facultative and anaerobic bacteria.

The pharmaceutical industry plays a key role in the development of effective treatments against multidrug-resistant bacteria. The class of compounds referred to as β-lactam antibiotics are currently the most widely used class of antibiotics, since the discovery of benzylpenicillin in the 1920s,a significant number of cephalosporins, cephamycins, monobactams, and carbapenems have been discovered and implemented in the clinical practice [3]. The new combinations of antibiotics are aimed to increase their spectrum of activity and overcome the resistance barriers developed by the bacteria. In order to mitigate the bacterial resistance to β-lactam antibiotics, several compounds have been identified as β-lactamase inhibitors. Those compounds can irreversibly inactivate the

β-lactamases allowing the β-lactam antibiotics to act against the infection. The main β-lactamase inhibitors are Sulbactam, Tazobactam and Clavulanic acid (CA).

CA is a secondary metabolite with a modest antibacterial activity against Gram positive and Gram negative bacteria; it is naturally produced by the filamentous organism *Streptomyces clavuligerus*[4–6]. CA is an analog of the penicillin ring, in which the characteristic sulfur atom has been substituted by an oxygen atom. The combined effective inhibition of β-lactamase and antibacterial activity of CA in combination with other β-lactam antibiotics make it very important, both clinically and economically [7]. This review focuses on the current application of systemic approaches in CA and *S. clavuligerus* studies.

1.2. Antibiotic resistance and CA

The emergence of an antibiotics, multidrug resistance (MDR) and extremely drug resistance (XDR) phenomenon in the last decades constitutes one of the most important challenges for the health and wellbeing. The inappropriate use of commercial antibiotics in humans and agriculture, along with the evolution and spread of mobile genetic resistance elements, has triggered the increase of MDR and XDR pathogenic species that implies serious risks for the human and animals life [1]. In February 2017, the World Health Organization (WHO) published the global priority list of antibiotic-resistant bacteria aiming to guide the research and development efforts of new and effective antibiotic treatments in the next years [8]. The report classified 12 bacteria and bacterial families in three categories of priority: (i) critical, (ii) high and (iii) medium. The classification of those bacterial groups and their specific resistance are presented in Table 1.1 [8,9]. The pathogenicity level of those priority bacteria and their resistance to most of the recent antibiotic treatments suggest that an effective scientific collaboration between different disciplines in several fields is necessary to face this resistance phenomenon.

Table 1.1. Global priority list of antibiotic-resistant bacteria reported by the World Health Organization in 2017 (adapted from [8]).

Priority level	Strain	Resistance
Critical	*Acinetobacter baumannii*	Carbapenem
	Pseudomonas aeruginosa	Carbapenem
	*Enterobacteriaceae***	Carbapenem, 3rd generation cephalosporin
High	*Enterococcus faecium*	Vancomycin
	Staphylococcus aureus	Methicillin, Vancomycin
	Helicobacter pylori	Clarithromycin
	Campylobacter	Fluoroquinolone
	Salmonella spp.	Fluoroquinolone
	Neisseria gonorrhoeae	3rd generation cephalosporin, fluoroquinolone
Medium	*Streptococcus pneumoniae*	Penicillin non-susceptible
	Haemophilus influenza	Ampicillin
	Shigella spp.	Fluoroquinolone

**Mycobacteria* (including *Mycobacterium tuberculosis*, the cause of human tuberculosis), was not included in the study carried out by World Health Organization. **Enterobacteriaceae include: *Klebsiella pneumonia*, *Escherichia coli*, *Enterobacter* spp., *Serratia* spp., *Proteus* spp., *Providencia* spp and *Morganella* spp [8]

A brief bibliometric analysis of research regarding the antibiotics and multidrug resistance in the last two years reveals that main area contributing with the research in this field (Figure 1.1) is *medicine* (38.8%), since a considerable number of reports are focused on clinical studies, appearance of new clinical cases and emergence of new resistant pathogens and the increase of morbidity rates [10]. The areas of *immunology* and *microbiology* contributed with 20.5% and *pharmacology, toxicology and pharmaceutics* with 11.9% of the published reports including the research in novel drugs and antibiotic compounds. Moreover an increasing number of studies in the areas of *biochemistry, genetics*

and molecular biology evidence the application of systemic approaches in the development of new antibiotic compounds, genetic improvement of producer strains and molecular studies.

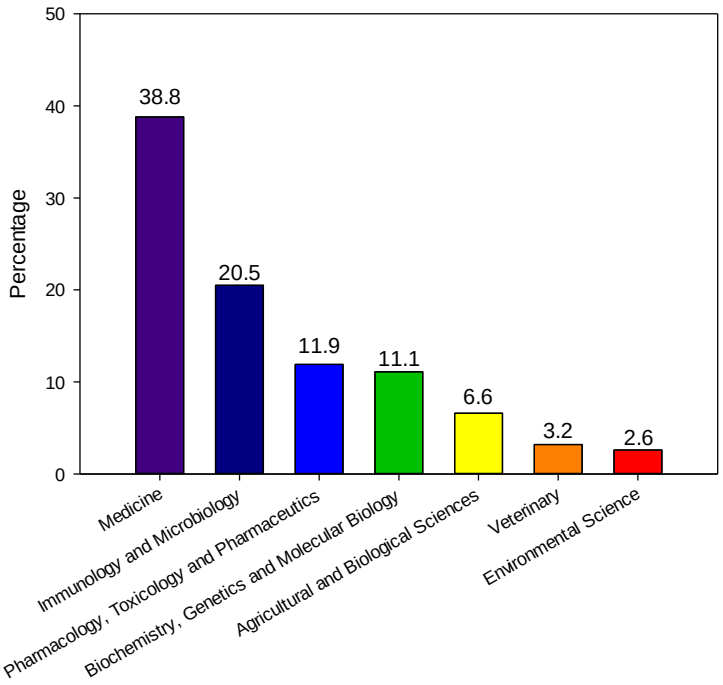

Figure 1.1. Contributions in multidrug resistance and antibiotics resistance per area of knowledge between 2017 and 2018. Other areas contributed 5.3%.

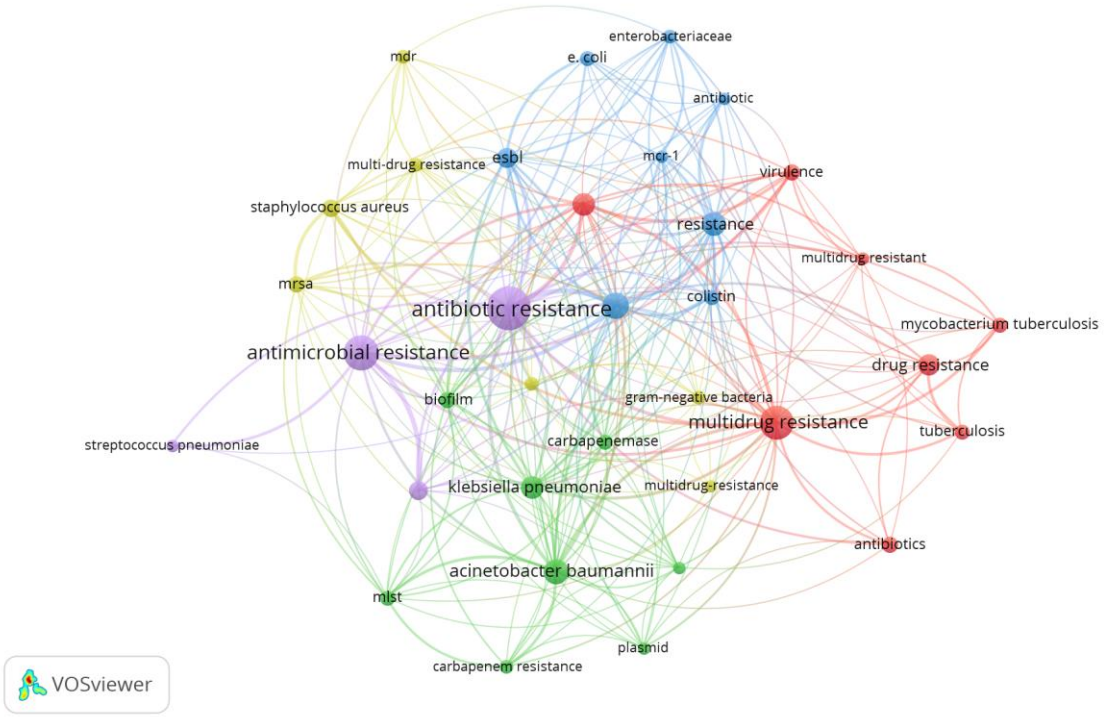

Figure 1.2. Research-topic network visualization of publications related to multidrug resistance and antibiotics resistance.

Figure 1.2 shows the research-topic network of publications regarding multidrug resistance and antibiotics resistance in the last year. A significant number of studies were focused on four pathogenic bacteria: *Escherichia coli, Pseudomonas aeruginosa, Acinetobacter baumannii* and *Klebsiella pneumoniae*, which are included in the critical priority level according to the WHO (Table 1.1). This information suggests that important scientific efforts have been dedicated, in the last two years, to the study of multidrug and antibiotics resistance in those bacteria [11–14]. Although most of the bacteria considered in the critical priority level (Table 1.1) has received attention, considerably less importance has been given to those of high and medium priority levels as the case of *Staphylococcus aureus*, *Neisseria gonorrhoeae* and *Streptococcus pneumoniae* that also represent a high risk for human and animal health.

Currently, the β-lactamase inhibitor CA is used in combination with β-lactam antibiotics as an effective treatment against some of the resistant pathogenic bacteria previously mentioned and included in the WHO priority list, namely *Escherichia coli, Staphylococcus aureus, Neisseria gonorrhoeae, Streptococcus pneumoniae* and all *Enterobacteriaceae and Klebsiella* species, among many other antibiotic resistant species. Pharmaceutical combinations of CA with β-lactam antibiotics amoxicillin or ticarcillin are widely used in clinical practice for the treatment of infections caused by such resistant pathogenic bacteria. CA is part of the so-called clavam metabolites, most of those metabolites have the characteristic fused bicyclic β-lactam/oxazolidine ring. Nevertheless, CA molecule (Figure 1.3) has 3R, 5R stereochemistry, opposite to the 3S, 5S configuration present in the other clavam metabolites, which do not exhibit β-lactamase inhibition activity, although some of them have antibacterial or antifungal properties [7]. In addition to the stereochemistry, the inhibitory effect of CA has been explained by the presence of the β-lactam/oxazolidine ring that bonds irreversibly with a serine residue in the catalytic center of the β-lactamase enzyme, thus rendering it inactive [15]. Nowadays CA is produced worldwide on a large scale by several pharmaceutical companies, it is also prescribed in more than 150 countries [16] and it has relatively limited market availability and high cost because of its complex production process, both concerning the technology and intellectual property rights associated [7].

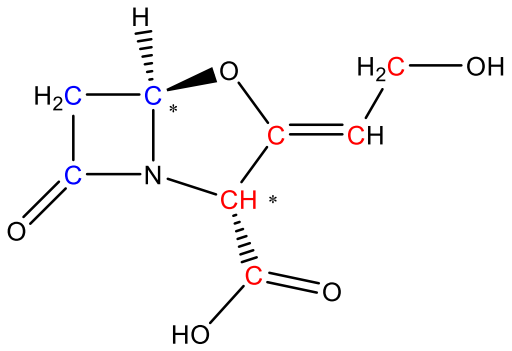

Clavulanic acid

Figure 1.3. CA structure. Red and blue C atoms correspond to those coming from C-3 and C-5 precursors, respectively. * Stereochemical center on CA structure.

1.3. CA biosynthesis in *S. clavuligerus*

The Streptomyces genus is known for its extraordinary ability to produce secondary metabolites of antibiotic activity, nearly two-thirds of which occur naturally [17]. *Streptomyces clavuligerus* is a Gram-positive filamentous bacterium first described by Higgens and Kartsner in 1971 as producer of two cephalosporin antibiotics [18]. Later in 1977, *S. clavuligerus* was also reported as the producer of CA as a β-lactam secondary metabolite with a potent inhibitory activity of β-lactamases enzymes.

CA is a secondary metabolite, referred to also as specialized metabolite, secreted by *S. clavuligerus* under nutritional restriction [7] as product of the so-called clavam pathway. The clavam pathway is usually divided into the early steps including the reactions from *N*2-(2-carboxy-ethyl) L-arginine to (*3S*, *5S*)-clavaminic acid and the late steps comprising the reactions up to CA and the clavam 5S compounds [19–21]. CA biosynthesis is summarized in Figure 1.4. The first reaction of the pathway involves a condensation reaction between L-arginine and glyceraldehyde-3-phosphate to produce N2-(2-carboxy-ethyl) L-arginine in a reaction catalyzed by N2-(2-carboxyethyl) arginine synthase (CEAS). Subsequently, deoxyguanidinoproclavaminic acid, a β-lactam compound, is formed by intramolecular reaction of *N*2-(2-carboxy-ethyl) L-arginine by action of β-lactam synthetase (BLS) [22–24]. Enzyme clavaminate synthase (CAS) is a 2-oxoglutarate dependent oxygenase catalyzing three reaction of the clavam pathway, the first of them being the hydroxylation of deoxyguanidinoproclavaminic acid forming guanidinoproclavaminic acid [24–27]. The amidino group in the residue of arginine in guanidinoproclavaminic acid is removed by action of proclavaminate amidino hydrolase (PAH) producing proclavaminic acid [28,29]. Proclavaminic acid forms dihydroclavaminic acid following an oxidative cyclization mechanism in the second reaction catalyzed by CAS, which is followed by an oxidative desaturation catalyzed by CAS, yielding the (3S, 5S)-clavaminic acid [24,30]. At this point, the clavam pathway bifurcates in two branches, one leading to CA having clavulanate-9-aldehyde as intermediate, and the other producing several clavam 5S compounds. Notice that 3S, 5S stereochemistry of clavaminic acid is conserved in the synthesis of clavams 5S; nevertheless, stereochemical inversion is required in the late steps leading to CA. Some authors suggested that N-glycyl-clavaminic acid might be an intermediate in the late steps of CA biosynthesis, which also would have a key role in the stereochemical inversion of 3S, 5S configuration into 3R, 5R of clavulanate-9-aldehyde and CA [4,31]. However, more experimental evidence is required for the elucidation of intermediate reactions connecting clavaminic acid with clavulanate-9-aldehyde [4,31], which is finally reduced by the clavulanate dehydrogenase (CAD) into CA [32].

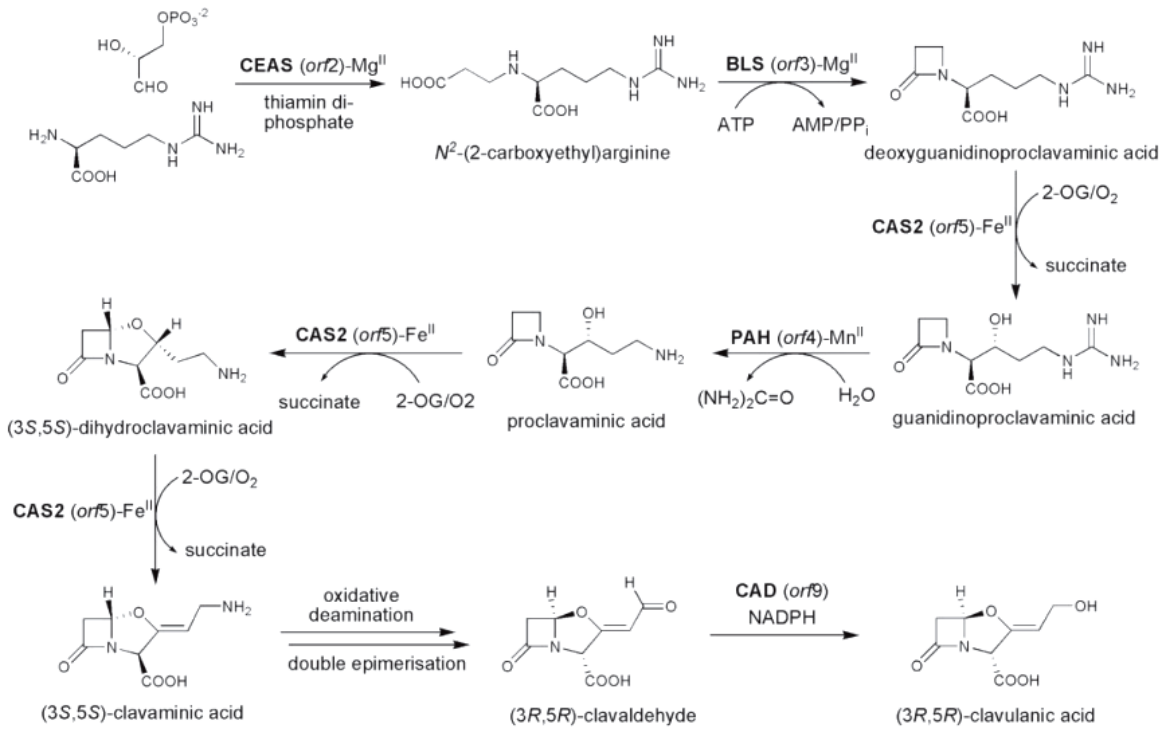

Figure 1.4. Condensed scheme of the CA biosynthetic pathway in *S. clavuligerus* [31].

Apart from CA, other metabolites derived from (3S, 5S)-clavaminic acid have been identified as side compounds of this biosynthetic pathway, namely N-glycyl-clavaminic acid, N-acetylglycyl-clavaminic acid and N-acetyl-clavaminic acid. It has been suggested that those compounds might be the result of intermediate steps participating in the stereochemical inversion from 3S,5S configuration into 3R, 5R present in CA [4]. Additionally, 2-hydroxymethylclavam, 2-formyloxymethylclavam, clavam-2-carboxylic acid and alanylclavam are grouped as clavams 5S compounds due to their 3S, 5S stereochemistry [31,33,34]. Despite the structural similarity and common precursors, only the clavams presenting a bicyclic nucleus formed by a β-lactam ring and an oxazolidine ring with 3R,5R stereochemistry can effectively inhibit the β-lactamases activity [17,33].

Glycerol is the preferred substrate for production of CA by *S. clavuligerus* because of its direct incorporation into glycolysis by forming glyceraldehyde 3-phosphate which is the C-3 precursor of CA [35,36]. At this point, the carbon flux splits into three pathways: (i) gluconeogenesis and pentoses phosphate pathway, (ii) glycolysis and tricarboxylic acid (TCA) cycle and (iii) clavam and CA biosynthesis pathway [36–38]. In addition to glyceraldehyde 3-phosphate, the need for a C-5 precursor implies the constant demand for L-arginine. L-arginine is synthetized in the urea cycle and amino acids like L-glutamate or L-aspartate promote its biosynthesis by fueling the urea cycle in the oxidative direction [35–37].

1.4. *S. clavuligerus* and CA production studies

CA production is commonly carried out in submerged cultivations of *S. clavuligerus* and different operation modes and media compositions have been explored aimed to increase the characteristic low titers of this compound obtained during the bioprocess as Ser et al. [39] reviewed recently. As previously mentioned, glycerol is the preferred carbon source for CA production given the direct formation of glyceraldehyde 3-phosphate as early CA precursor [39–41]. When comparing the CA production using glycerol and sucrose as carbon sources, glycerol promotes higher CA titers up to 5-fold than those observed in cultivations with starch [40,42]. Nevertheless, substrate inhibition can occur at concentrations of glycerol higher than 50 $g.L^{-1}$ [42]. The production of CA is enhanced by amino-acids supplementation [35,43] and complex nitrogen sources such as soy protein and soy flour [40,42]. Conversely, the use of dextrose or starch promote the secretion of Cephamycin C [40,44]. Recently, in a screening of media for CA production da Silva et al. [45] observed in batch submerged cultivations with the wild-type strain that the highest CA production (437 $mg.L^{-1}$) was attained in medium having glycerol as the main carbon source and isolated soy protein, in which the amino acids supplementation did not enhance the CA productivity. Neto et al. [46] reported CA concentrations in batch, fed batch and continuous cultivations of 195, 404 and 293 $mg.L^{-1}$. The highest CA concentrations obtained in bioreactor cultivations with the wild-type strain were reported by Teodoro et al. [47]. In that study, batch and fed-batch operation modes were tested using a complex medium prepared with glycerol, malt and yeast extracts, peptone and trace elements. Batch cultivations yielded 430-530 $mg.L^{-1}$ of CA while fed-batch cultivations with ornithine (3.7 g/L) led to a CA accumulation of 1560 $mg.L^{-1}$ [47,48]. A complex culture medium is a source of important amounts of free or hydrolyzed amino acids, which act not only as nitrogen sources but also as secondary carbon sources. Complex nitrogen sources, as those containing soy protein, favor considerably the CA accumulation in contrast to the chemically defined media [42]. Phosphate has a potential repressive effect on CA production; thus culture media are commonly designed with phosphate limitation [7,35,39]. In this regard, Saudagar and Singhal [43] found CA biosynthesis repression when increasing the phosphate concentration in the media over 100 $mmol.L^{-1}$. The studies indicate that CA accumulation is favored by fed-batch operation under controlled conditions of pH, aeration and stirring. Those conditions are more easily controllable in stirred tank bioreactors (STR), although the CA production studies are not restricted only to this configuration.

Other factors apart from culture media could affect the CA accumulation in submerged cultures of *S. clavuligerus.* The CA molecule shows susceptibility to temperature and ionic strength in

aqueous solutions, which compromises the CA titers attained during cultivations [49,50]. The pH culture conditions seem to affect CA yield, possibly more linked to molecule degradation than biosynthesis inhibition [51]. The highest concentration of CA has been reported at neutral or slightly acidic pH conditions (6.8), regardless the substrates used during the cultivations [39]. Low temperatures favor the molecule stability; in this regard, higher titers have been reported during operating fermentations at 20°C but the growth rate at such temperature is lower than that observed at 28°C [52].

Regarding the operational variables associated to fermentative processes in *Streptomyces* species, the nutritional effects have been more studied than the effects of hydrodynamic conditions and reactor geometry [53]. The conventional cultivations are generally carried out in STR, since this traditional geometry has been proven to be reliable since it assures good mixing, mass and heat transfer rates [54]. Novel impeller geometries for STR have been studied as feasible alternatives for improving the oxygen dissolution and nutrient dispersion [55] during the fermentative process. Studies involving the hydrodynamic patterns of reactor in addition to growth, morphology and mass transfer in *Streptomyces* cultures have not been performed. Such studies are required for a more precise description of antibiotics biosynthesis in bioreactors [53]. The reactor geometry, impeller configuration and velocity of mixing have impact on the oxygen availability of the system; it has been demonstrated that higher mixing velocities and turbulence gives better volumetric oxygen transfer coefficients (K_La), increasing the specific growth rate of the microorganism [54,56]. The reactor design must be focused on balancing mass and heat transfer with shear rates, since the latter can cause hydrodynamic stress on cells, affecting their growth and productivity [53] and single use technologies can offer some advantages in this field.

In bioreactors the agitation rate is related not only to dissolved oxygen and mass transfer conditions, but also to the shear conditions. The effects of shear forces are particularly important in microbial cultivations, since they affect growth rate, broth rheology and transport of nutrients that might lead to specific metabolic and morphological responses. In the case of *S. clavuligerus* agitation and aeration are also considered as factors potentially affecting the CA production. An increase of 50% in oxygen transfer in shake flask cultures increased 2-fold the CA production [57]. For the case of bioreactor operation, Rosa et al. [58] found that intense agitation rates as high as 800 - 1000 rpm, favored CA accumulation in STR. The volumetric mass transfer coefficient (k_La) observed in airlift reactors operated in the range from 3 to 5 vvm, is comparable to those arisen in STR, operating in the range of 600 to 1000 rpm; both conditions promote CA accumulation. Some studies have explored the impact of mechanical stress on *Streptomyces* morphology in suspension cultures, showing that high shear stress typically leads to the formation of small mycelial particles while clumping or pellet formation occurs at low shear stress [59,60]. Such pellets favor the accumulation of actinorhodin in *S. coelicolor*, nystatin in *S. noursei*, retamycin in *S. olindensis*, and nikkomycin in *S. tendae* as Manteca et al. [61] previously reviewed. In the case of *S. clavuligerus*, little is known about the relationship between shear stress, growth, morphology and metabolites secretion. Dispersed mycelial morphology has been observed more often in *S. clavuligerus* cultivations performed in bioreactors and, in contrast to other phylogenetically related species, pellet formation seems to be related with a decrease in the CA production rate [36,62]. The effect of reactor geometry has not been yet considered apart from the experiments involving STR [58] and airlift reactors [63], which presented similar performance in terms of shear forces and mass transfer .

1.5. Systemic approaches in *S. clavuligerus* and CA studies

The rational comprehension and improvement of the biological behavior of organisms in bioprocesses requires a detailed understanding of the metabolic pathways involved. In this regard, the efforts for enhancing CA productivity in bioprocess *S. clavuligerus* cover different disciplines such as biology, engineering, biochemistry, molecular biology, analytical chemistry and computational biology are contributing to unravel the metabolic complexity of this organism. As showed in Figure 1.5, the studies regarding CA and S. *clavuligerus* considering systemic approaches

were concentrated in three knowledge areas: bioengineering (fermentation and adsorption), pharmaceutics (pharmacokinetic, pharmacodynamics, antibiotics and antibiotics resistance), and molecular biology and biochemistry (biosynthesis, regulation and strain improvement), showing the spectrum of application and the multidisciplinary nature of this kind of studies.

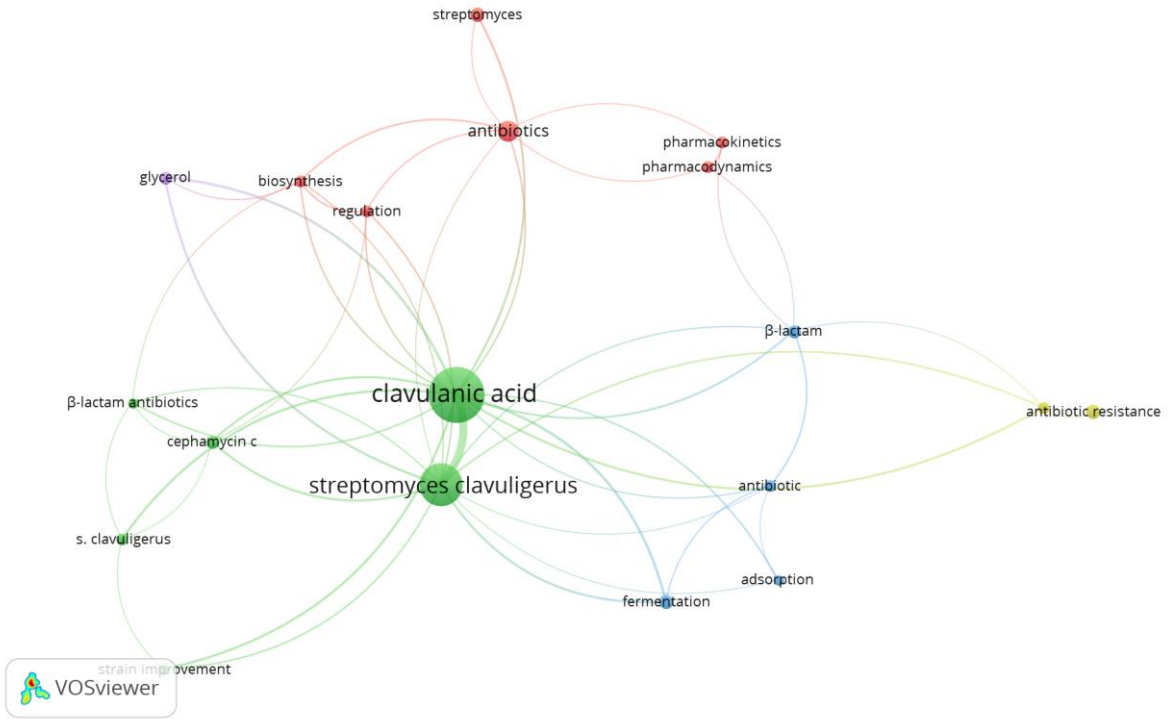

Figure 1.5. Keywords co-occurrence network of CA and *S. clavuligerus* with systemic approaches-related publications

Among the systemic approaches, systems biology has emerged as one of the most important frameworks aimed to decipher the complexity of biological systems. This approach postulates that the different networks conforming the living organisms are more than the sum of their parts. Thus, systems biology is a multidisciplinary and holistic approach that implements analytical tools and computational models that are supported and inspired by real biological systems and usually integrate empirical knowledge. Through the implementation of sophisticated models, systems biology aims to predict how the biological systems change over time and under varying conditions in order to develop solutions in those fields in which living organisms are involved.

In systems biology, metabolic modeling constitutes a rational framework for studying the effect of genetic and environmental perturbations on metabolism through the application of mathematical, biochemical and biological knowledge. In this regard, the large-scale genome analyses and the genome-scale constraint-based modeling allow the in silico evaluation of the global physiology of a cell with respect to nutritional and environmental perturbations in connection with cellular regulations at different levels, e.g. gene expression, transcriptional regulation and metabolic fluxes distribution [64]. This analysis can provide information of suitable bioprocessing conditions or it can be used to predict potential metabolic targets for further application of genetic engineering approaches. Moreover, computer aided process simulation can be integrated with system biology approaches for development of technoeconomic analysis in bioprocesses design and assessment [65,66].

The pseudo-steady state modeling through application of flux balance analysis (FBA) has contributed to understand the physiology of several organisms regarding nutritional conditions,

gene essentiality, activation of secondary metabolism, antibiotics secretion, host-pathogen interactions, genetic perturbations, among others. Kirk et al. [67] studied the metabolic flux distribution in a chemostat culture of *S. clavuligerus* at a dilution rate of 0.05 h^{-1}. The authors evaluated the effect of carbon, nitrogen and phosphate limitations on CA production, and obtained specific productivities of 0, 0.32 and 3.65 mg.(g DCW.h^{-1}) of CA, respectively. FBA results indicated that under carbon limitation the anaplerotic metabolism was restricted, affecting the TCA cycle intermediates oxaloacetate and 2-oxoglutarate, which are directly connected with the urea cycle. Moreover, nitrogen limitation affected amino acid biosynthesis, including L-arginine, the C-5 precursor of CA. Conversely, under phosphate limitation, CA production achieved its highest specific production rate coinciding with the highest flux of the C-3 and C-5 precursors.

Bushell et al [35] used FBA to formulate feeding conditions in chemostat cultures of *S. clavuligerus*. In this regard, the combination of amino acids formulated with the aid of FBA, resulted in an 18-fold increase of CA compared with the batch cultures. The FBA indicated that feeding with single amino acids limited the antibiotic yield, suggesting that the urea cycle, was capable to provide an excess of C5 precursors. A metabolic model reported by Sanchez *et al*. [37,68] consisted of 100 reactions and 91 metabolites. The maximization of three metabolic objective functions was studied: (i) specific growth rate, (ii) ATP yield and (iii) CA production. The effects of carbon, nitrogen, phosphate and oxygen limitation were best represented by the maximization of ATP as objective function. *In silico* results indicated the phosphate limitation as the best scenario for CA production. The calculated metabolic flux distribution indicated that metabolic fluxes involved in the urea cycle were highly favored when CA achieved its highest specific production rate.

Cavallieri et al. [38] through application of FBA considering ATP maximization as objective function, observed that the production of CA and cephamycin C could be connected despite being synthesized in different pathways, namely the clavam and cephalosporin biosynthesis pathways. The authors carried out continuous cultivation of *S. clavuligerus* at a dilution rate of 0.013 h^{-1} and employed lysine and maltose as nitrogen and carbon sources in the feed medium, respectively. Those sources were expected to favor the cephamycin C production, however, the CA production also increased despite lysine being a cephamycin C precursor.

In the case of *S. clavuligerus*, few genome-scale models of the metabolism have been reconstructed and/or updated for the *in silico* analysis of metabolic phenotypes [36,69–71]. Those works have provided some insights about the metabolic features of the species and possible genetic targets for further strain improvement. The first genome-scale model of *S. clavuligerus* metabolism (iMM865) was reported by Medema et al [72], this model included 1492 reactions and 1173 metabolites and it was checked for biomass synthesis under minimal growth medium conditions (glycerol, ammonia, phosphate and sulfate). Ramirez-Malule et al. [73] reconstructed a genome-scale metabolic model (iHR1510) taking as basis the model published by Medema et al. This new model consisted of 1510 reactions and 1187 metabolites and it explained under pseudo-state conditions the experimental observations of TCA cycle intermediates at different feeding conditions in chemostat cultures of *S. clavuligerus* and determined the metabolic flux distribution during CA production [36]. This genome-scale model was recently updated (iGG1534) for the *in silico* study of metabolic phenotypes under different conditions leading to secretion of CA and cephamycin C [71]. Similarly, Toro et al [70] expanded and updated the genome-scale metabolic model published by Medema et al. This new model (iLT1021) included 1021 genes-protein rules and 1494 reactions. The gene-protein information was curated and new features related to clavam pathway and biomass synthesis equation were incorporated. FBA showed that limiting concentrations of phosphate and an excess of ammonia accumulation are unfavorable for growth and CA biosynthesis. The evaluation of different objective functions for FBA showed that maximization of ATP generated better predictions for chemostat cultures, while the maximization of growth rate provides better predictions for batch cultures. Through gene essentiality analysis, 130 essential genes were found using a limited in silico media, while 100 essential genes were identified in amino acid supplemented media and *in silico* strain design was explored for the identification of potential

targets to increase the CA biosynthesis. Nevertheless, the genome-scale models iHR1510, iLT1021 and iGG1534 reconstructions are based in the genome assembly reported by Medema et al [72] leading to models with a low number of gene-protein interactions and potentially to missed reactions and pathways. *De novo S. clavuligerus* genome assemblies recently reported by Cao et al [74] and Wang et al [75] might help to generate new genome-scale reconstructions with increased biochemical information.

Despite the extensive studies performed on media optimization and cultures conditions, a high number of bioprocessing factors affect the CA productivity when using the wild-type strain. Therefore, CA titers in cultivation processes are still low, undoubtedly increasing the production costs. The potential application of systemic approaches in strain improvement aimed to increase the antibiotics yield in *S. clavuligerus* cultures implies the connection between the new genetic regulatory information, *in silico* prediction of suitable phenotypes and experimental construction of transformants. The understanding of the clavam pathway has been deduced from genetic studies that also have been applied to the metabolic engineering of the species for improvement of CA production [76]. In many cases, CA overproduction has been achieved from manipulation of genes encoding biosynthetic enzymes or transcriptional regulators.

Hung et al. [77] showed that CA production was increased by combined overexpression of a positive regulator *ccaR* and a rate-limiting enzyme *cas2*. An improvement of 23.8-fold in CA production was observed, which was a considerable yield in comparison with the previously obtained by amplifying single genes or use of multicopy plasmids. Li and Townsend [78] inactivated the genes *gap1* and *gap2* encoding glyceraldehyde 3-phosphate dehydrogenase generating a disruption in the carbon flux along the glycolytic pathway leading to a 2-fold CA improvement, suggesting that such flux was channeled to CA biosynthesis rather than to the glycolysis. Moreover, when arginine was fed to engineered strain CA production was elevated 3-fold higher than the observed in the wild type strain [78]. The overexpression of a putative sigma factor gene *orf21* in the wild-type *S. clavuligerus* increased the CA production by 1.43-fold [79]. The overexpression of *orf21* stimulated the overexpression of the early CA genes, *ceas2* and *cas2* and the regulatory gene *ccaR*, which was consistent with the enhanced production of CA [79]. The overexpression of regulators *ccaR* and *claR* together in the *gap1* mutant strain led to an increase in CA by 5.85-fold, compared with the *gap1* deletion mutant [80]. Additionally, compared with the *gap1* deletion mutant, ornithine increased CA production by 6.51-fold and glycerol increased CA by 6.21-fold; a feed with ornithine and glycerol together increased CA by 7.02-fold [80].

The highest CA titers up to now reported have been achieved by the integrative overexpression of clavaminic acid synthase (*cas2)* gene and two regulatory genes (*ccaR* and *claR)* in a engineered *S. clavuligerus* strain, which was able to reach a CA concentration of 6.690 $g.L^{-1}$ in submerged cultivations [81]. Qin et al. [82] fused a *neo* gene (a promoter-less kanamycin resistance gene) with the regulator *claR*. This so-called NEO strain of *S. clavuligerus* produced 3.26 $g.L^{-1}$ of CA [82]. In that study, after three series of treatment and screening, the authors reported 4.33 $g.L^{-1}$ of CA, which is an increment of 33.8% compared to the initial NEO strain. Cho et al [83] recently reported enhanced CA accumulations by using reverse engineering and overexpression of the regulatory genes *ccaR, claR* in an overexpressed *cas1* industrial strain of *S. clavuligerus*. The mutant strain was able to produce up to 6.01 $g.L^{-1}$ of CA in batch cultivations (4.5 L), value susceptible of being further improved through fed-batch operations.

Despite the studies reported have shown important advances in the knowledge of CA biosynthesis and enhancement of its production, the integration of systemic approaches and novel transformation strategies might lead to further enhancement of CA productivities. However, the *in silico* characterization of metabolic phenotypes must be continuously improved through the adoption of new experimental evidence and new biochemical and genetic knowledge that will allow to improve the predictions and directions of further rational strain improvement strategies.

1.6. Dynamic flux balance analysis (DFBA): a systemic approach for the dynamic study of metabolic scenarios

As previously described, the use of FBA in *S. clavuligerus* has allowed to describe metabolic phenotypes and to explore potential alternatives for the enhancement of the CA yield under pseudo-steady state conditions. Nevertheless, the meaningful results of those FBA approaches, pseudo-steady state modelling approach is not able to capture the time-dependent concentration changes, the dynamic intracellular metabolic responses to external conditions and other related perturbations [84]. On one hand, phenomenological models like those derived from Monod or Michaelis-Menten kinetic rate expression have been widely used to describe the macroscopic microbial growth, substrates consumption and products secretion, but those types of models do not provide information of intracellular flux distributions [85]. On the other hand, the pseudo-steady state approaches could predict the intracellular and exchange reaction fluxes based on stoichiometric mass balance of a metabolic reaction network in a single condition, which is determined by the solution of a constrained linear programming optimization problem.

Accurate metabolic dynamic models have been created with limited experimental data, as for the case of kinetic models based on stimulus-response experiments [86–88], models using *in vitro* parameters available for enzymes on databases (e.g. KEGG and BRENDA) and/or using generic or approximate kinetic rate equations [89,90] . Those models were limited to represent the central carbon metabolism [88,91–93] with small number of reactions, mainly due to the experimental and computational limitations. Another approach considered the integration of dynamic models of central metabolism with steady-state genome scale models for the rest of the metabolic network [90,94,95].

Since cells in a culture are naturally in a dynamic condition, a nonlinear behavior and property variations are expected during the process time. This fact has repercussions on prediction of cell phenotypical states, product yield and bioreactor control. Quantitative mathematical models are needed to describe the process dynamics and the interrelation among relevant variables [96]. A feasible approach for dealing with dynamic metabolic modeling of cellular cultures was proposed by Mahadevan *et al.* [97] considering a dynamic extension of classic FBA. FBA solves a linear programming problem for calculating the steady-state reaction flux distributions along the metabolic network that maximize (or minimizes) a pre-defined objective function, under some constraints. By considering the metabolic network under steady-state, a general formulation for the FBA is [98]:

$$Max\ \boldsymbol{Z} = \boldsymbol{f}^{\boldsymbol{T}}\boldsymbol{v} \tag{1}$$

$$\begin{bmatrix} s.t. & \boldsymbol{S}\boldsymbol{v} = 0 \\ & l_b \leq \boldsymbol{v} \leq u_b \end{bmatrix} \tag{2}$$

where $\boldsymbol{S}_{mxn}$ is the stoichiometric matrix of coefficients for m metabolites and n reactions including the internal and exchange reactions, $\boldsymbol{v}$ is the flux vector of dimension n, Z is the objective function f is a vector of weights , and l_b and u_b are the lower and upper bounds, respectively. The objective function is expected to capture the physiological goal of the organism such as to maximize the ATP production, growth rate or specific metabolite production [98].

For most system biology applications where standard FBA is used, the analysis lies on the maximization of growth rate. Some variations of the traditional FBA (such as the parsimonious and sparse FBA) use a two-stage optimization procedure in order to retrieve a unique and biologically meaningful solution to the FBA problem of growth rate maximization. The first stage of this two-stage optimization solves a FBA standard problem for biomass maximization whereas the second stage deals with the minimization of the fluxes vector, which is mathematically represented as follows:

$$Min \sum v^2 \tag{3}$$

$$\begin{bmatrix} s.t. \boldsymbol{Sv} = 0 \\ \boldsymbol{l_b} \leq \boldsymbol{v} \leq \boldsymbol{l_u} \\ \boldsymbol{f^T v} = \mathbf{Z}_{max} \end{bmatrix} \tag{4}$$

where the norm of vector v is the objective function to be minimized. The stoichiometric matrix $\boldsymbol{S}$ and the upper and lower bound for the flux vector are the same used in the standard FBA (Eq. 1). The last constraint represents the requirement to satisfy the optimal solution of the standard FBA problem. It is important to notice that the assumption underlying the flux minimization principle postulates that cells of living organisms gain functional fitness by fulfilling their functions with minimal effort, and thus assuring an efficient metabolic flux distribution to accomplish a specific pattern of cellular functions [99].

The FBA approach presents some limitations, such as the prediction of cellular growth and product secretion rates only for fixed values of substrate uptake rates and its strict applicability to the balanced growth phase in batch cultures or steady-state growth in continuous cultures. The dynamic flux balance analysis (DFBA) allows prediction of cellular metabolism and metabolite concentrations in batch and fed-batch cultivations, which are the most common operation modes in bioprocess industry [100]. Additionally, the DFBA approach can also incorporate kinetic expressions for the cases with well characterized kinetics [97,100].

DBFA provides a practical framework for incorporation of intracellular features since it is based in the FBA formulation but including a small number of additional parameters, including the formulation of substrate uptake kinetics to account for known regulatory processes [100]. DFBA imposes constraints on fluxes at each time interval, those constraints are typically expressed as kinetic expressions (e.g. Monod or Michaelis-Menten) depending on time-varying concentrations of substrates and products linked to the constrained flux [101].

Two DFBA formulations were proposed by Mahadevan et al.[97]: the Dynamic Optimization Approach (DOA) and the Static Optimization Approach. The DOA performs an optimization solving a nonlinear programming (NLP) problem, which in turn, solves a system of algebraic differential equations once over the entire time period of interest, allowing to obtain time profiles of fluxes and metabolite levels [97]. The SOA divides the total time into several time intervals and solves an instantaneous optimization problem using linear programming (LP) at the beginning of each time interval, followed by integration over the interval, allowing to know the flux distribution at a particular time instant [97]. In the DFBA for a given metabolic network with m metabolites and n fluxes, the mass conservation equations are stated as ordinary differential equations (ODE) as follows [97]:

$$\frac{d\boldsymbol{z}}{dt} = \boldsymbol{A}\boldsymbol{v}X \tag{5}$$

$$\frac{dX}{dt} = \mu X \tag{6}$$

$$\mu = \sum w_i v_i \tag{7}$$

where X is the biomass concentration, $\boldsymbol{v}$ is the vector of metabolic fluxes per gram (Dry Weight) of the biomass, A is the stoichiometric matrix, μ is the growth rate obtained as a weighted sum of the reactions that synthesize the growth precursors, and w_i are the amounts of the growth precursors required per gram (DCW) of biomass. The DFBA problem applying the DOA is formulated as follows [97]:

$$Max \quad \hat{w}_{end}\Phi(\boldsymbol{z},\boldsymbol{v},X)|_{t=t_f} + \hat{w}_{ins}\sum_{j=0}^{M}\int_{t_o}^{t_f} L\big(\boldsymbol{z},\boldsymbol{v},X(t)\big)\delta\big(t-t_j\big)dt \tag{8}$$

$$\begin{bmatrix} s.t.\ \frac{d\boldsymbol{z}}{dt} = \boldsymbol{A}\boldsymbol{v}X \\ \frac{dX}{dt} = \mu X \\ \mu = \sum w_i v_i \\ t_j = t_o + j\frac{t_f - t_o}{M} \\ \boldsymbol{z}(t_o) = \boldsymbol{z}_o \\ X(t_o) = X_o \\ c(\boldsymbol{v},\boldsymbol{z}) \le 0 \quad |\dot{\boldsymbol{v}}| \le |\dot{\boldsymbol{v}}_{max}| \end{bmatrix} \tag{9}$$

where z is the vector of metabolite concentrations, z_o and X_o are the initial conditions for the metabolite concentration and the biomass concentration respectively, $c(v,z)$ is a vector function representing nonlinear constraints that could arise due to consideration of kinetic expressions for fluxes, t_o and t_f are the initial and final times, Φ is the terminal objective function that depends on the end-point concentration, L is the instantaneous objective function, δ is the Dirac-delta function, t_j is the time instant at which L is considered, w_{ins} and w_{end} are the weights associated with the instantaneous and the terminal objective function respectively, and $v(t)$ is the time profile of the metabolic fluxes. If the nonlinear constraint is absent, the problem reduces to an optimization involving a bilinear system but as the size of the network increases, the number of variables and the number of constraints would increase proportionally in the NLP problem [97].

The alternative and simpler SOA formulation extends the FBA approach introducing the flux rate-of-change constraints, and its advantage is a considerable reduction in the number of variables to be solved in comparison with the DOA formulation. In SOA formulation the optimization problem is a LP problem as opposed to the NLP for DOA, then, the SOA is scalable to larger metabolic networks as the case of the genome-scale models [97]. In SOA formulation, the time period is divided in N intervals and, in absence of nonlinear constraints involving the fluxes, the problem becomes into a LP problem, which is solved at the beginning of each time interval for obtaining the fluxes at the given time instant. The problem is formulated as follows:

$$Max \ \sum w_i v_i(t) \tag{10}$$

$$\begin{bmatrix} s.t.\ \boldsymbol{z}(t+\Delta t) \ge 0 \ \ \boldsymbol{v}(t) \ge 0 \\ \boldsymbol{z}(t+\Delta t) = \boldsymbol{z}(t) + \boldsymbol{A}\boldsymbol{v}\Delta t \\ X(t+\Delta t) = X(t) + \mu X(t)\Delta t \\ |\boldsymbol{v}(t) - \boldsymbol{v}(t-\Delta t)| \le \dot{\boldsymbol{v}}_{max}\Delta t \end{bmatrix} \tag{11}$$

where Δt is the length of time interval, the optimization problem is solved in the time interval and the dynamic equations are integrated assuming constant fluxes in the interval. The procedure is then repeated from t_o to t_f [97]. Regardless the formulation (DOA, SOA or other), DFBA provides a framework for modeling the dynamic responses of a metabolic network to various perturbations. DFBA also allows to identify the constraints governing the behavior at the different phases of a culture and the sensitivity to the parameters of the model [97,100,101]. The DFBA approach allows incorporating kinetic expressions available, thus, it can be used to identify regulatory phenomena and obtain information of dynamic of the metabolic pathways. Therefore, changes in the regulatory structure aimed to optimizing the dynamics of a particular metabolic process could be obtained as a solution to a modified DFBA problem [97].

There are no academic reports dealing with the dynamics of metabolic capabilities of *S. clavuligerus* so far. Nevertheless, the DFBA has been used in describing dynamic fluxes distribution

in different organisms. DFBA has been used to model the competition of growth between reducer bacteria *Geobacter sulfurreducens* and *Rhodoferax ferrireducens,* predicting at low rates of acetate flux that *Rhodoferax* will contend with *Geobacter* as long as sufficient ammonium is available, but under high concentrations of acetate *Geobacter* species would predominate. The dynamic model also predicted that under nitrogen fixation, higher carbon and electron fluxes would be diverted toward respiration rather than biomass formation in *Geobacter* [102]. Sánchez et al. [103] identified the DFBA model parameters for a dynamic genome-scale model for *Saccharomyces cerevisiae* in batch and fed-batch cultures in aerobic and anaerobic conditions. The model showed that optimization of consumption, suboptimal growth and production rates are more useful for calibrating the model than using Boolean gene expression rules, biomass requirements and ATP maintenance. Barreto-Rodriguez et al. [96] presented a simplified network for modeling and prediction of gene overexpression in *E.Coli* using DFBA. The model aimed at predicting ethanol concentration profiles in glycerol batch cultivations and the i*n silico* results were successfully validated by overexpressing alcohol/acetaldehyde dehydrogenase (*adhE)*, pyruvate kinase (*pykF)*, pyruvate formate-lyase (*pflB)* and isoleucine-valine enzymes (*ilvC-llvL)*. Robitaille, Chen and Jolicoeur [104] developed and calibrated a dynamic metabolic model for CHO cells using datasets obtained under four different culture conditions, including batch and fed-batch cultures comparing two different culture media. The results suggested that a single model structure with a single set of kinetic parameter values is efficient for estimating the time course of measured and non-measured intracellular and extracellular metabolites. Furthermore, little impact of culture media and the fed-batch strategies on flux distribution was found through DFBA due to absence of differences between exponential and stationary phases for viable cells in batch cultures.

The DOA is still limited to small-scale metabolic models and it is prohibitive in terms of computational power due to the dimensional explosion derived from time discretization of the equations [84]. The SOA is a straight-forward implementation more appropriated for genome-scale model applications, since the static linear programming solution requires much less computational power and time. Therefore the SOA formulation is scalable to larger metabolic networks. SOA allows the external environment to change each time-step, hence adjusting the constraints and/or objective functions according to the modified external environment, allowing to obtain the new solution valid for the interval [84,105,106]. Recently, DFBA-SOA has been successfully applied in the analysis of genome-scale models for prediction and description of phenotypes, as well as culture dynamics of several microorganisms of industrial interest like *S. tsukubaensis* [84], *Clostridium butyricum* [106] and *Chlamydomonas reinhardtii* [107]. Furthermore, the significance of the results is independent of the mathematical approach used, since no significant difference in the concentrations and flux profiles have been observed when comparing the DOA and SOA [97,106].

1.7. Conclusions

In view of the emergence of antibiotics resistance phenomena, the research in antibiotics against resistant bacteria has become more relevant. An overview of CA and S. clavuligerus studies using systemic approaches was presented. The biochemical studies regarding CA biosynthesis has allowed to elucidate most of the reaction steps involved in biosynthesis of clavam metabolites, including CA and clavams 5S. Systemic approaches involving multidisciplinary collaboration of biology, engineering, biochemistry, molecular biology, analytical chemistry and computational biology have contributed to decipher the intrinsic metabolic complexity of *S. clavuligerus* in connection with the antibiotics production at different scales. Metabolic modeling in pseudo-state conditions has revealed important features of *S. clavuligerus* and supported the rational bioprocesses and strain improvements. However, the application of dynamic approaches and integration of experimental information in the regulatory and transcriptomic levels are still missed in the literature. Strain engineering has render important CA productivities enhancements but novel modification strategies and further scale-up of the processes with the engineered strains remain as pending tasks.

Publication: This chapter was partially published as Gómez-Ríos, D.; Ramírez-Malule, H. Bibliometric analysis of recent research on multidrug and antibiotics resistance (2017–2018). *J. Appl. Pharm. Sci.* **2019**, *9*, doi: 10.7324/JAPS.2019.90515

References

1. Banin, E.; Hughes, D.; Kuipers, O.P. Editorial: Bacterial pathogens, antibiotics and antibiotic resistance. *FEMS Microbiol. Rev.* **2017**, *41*, 450–452.
2. Herrera, M.L.; Moya, T.; Vargas, A.; Campos, M.; Marín, J.P. Cepas productoras de beta lactamasa de efecto expandido en el Hospital Nacional de Niños. *Rev. Médica del Hosp. Nac. Niños Dr. Carlos Sáenz Herrera* **2002**, *37*, 19–27.
3. Bush, K.; Bradford, P.A. β-Lactams and β-Lactamase Inhibitors: An Overview. *Cold Spring Harb. Perspect. Med.* **2016**, *6*, a025247.
4. Ramirez-Malule, H.; Restrepo, A.; Cardona, W.; Junne, S.; Neubauer, P.; Rios-Estepa, R. Inversion of the stereochemical configuration (3S, 5S)-clavaminic acid into (3R, 5R)-clavulanic acid: A computationally-assisted approach based on experimental evidence. *J. Theor. Biol.* **2016**, *395*, 40–50.
5. Ozcengiz, G.; Demain, A.L. Recent advances in the biosynthesis of penicillins, cephalosporins and clavams and its regulation. *Biotechnol. Adv.* 2013, *31*.
6. Brown, A..; Butterworth, D.; Cole, M.; Hanscomb, G.; Hood, J..; Reading, C.; Rolinson, G.. Naturally Occurring β-lactamase Inhibitors with Actibacterial Activity. *J. Antibiot. (Tokyo).* **1976**, *29*, 668–669.
7. Saudagar, P.S.; Survase, S.A.; Singhal, R.S. Clavulanic acid: A review. *Biotechnol. Adv.* **2008**, *26*, 335–351.
8. World Health Organization, Global priority list of antibiotic-resistant bacteria to guide research, discovery, and development of new antibiotics.
9. Gómez-Ríos, D.; Ramírez-Malule, H. Bibliometric analysis of recent research on multidrug and antibiotics resistance (2017–2018). *J. Appl. Pharm. Sci.* **2019**, *9*, 112–116.
10. Magira, E.E.; Islam, S.; Niederman, M.S. Multi-drug resistant organism infections in a medical ICU: Association to clinical features and impact upon outcome. *Med. Intensiva* **2018**, *42*, 225–234.
11. Nazari Alam, A.; Sarvari, J.; Motamedifar, M.; Khoshkharam, H.; Yousefi, M.; Moniri, R.; Bazargani, A. The occurrence of blaTEM, blaSHV and blaOXA genotypes in Extended-Spectrum β-Lactamase (ESBL)-producing Pseudomonas aeruginosa strains in Southwest of Iran. *Gene Reports* **2018**, *13*, 19–23.
12. Costa, A.R.; Monteiro, R.; Azeredo, J. Genomic analysis of Acinetobacter baumannii prophages reveals remarkable diversity and suggests profound impact on bacterial virulence and fitness. *Sci. Rep.* **2018**, *8*, 15346.
13. Bassetti, M.; Vena, A.; Russo, A.; Croxatto, A.; Calandra, T.; Guery, B. Rational approach in the management of P.aeruginosa infections. *Curr. Opin. Infect. Dis.* **2018**, *31*, 1.
14. Biswas, D.; Tiwari, M.; Tiwari, V. Comparative mechanism based study on disinfectants against multidrug-resistant Acinetobacter baumannii. *J. Cell. Biochem.* **2018**, *119*, 10314–10326.
15. Reading, C.; Cole, M. Clavulanic acid: a beta-lactamase-inhiting beta-lactam from Streptomyces clavuligerus. *Antimicrob. Agents Chemother.* **1977**, *11*, 852–7.
16. Mutlu, A. Increasing clavulanic acid production both in wild type and industrial Streptomyces clavuligerus strains by amplification of positive regulator claR gene, Middle East Technical University, 2012.
17. Viana Marques, D. de A.; Feitosa Machado, S.E.; Santos Ebinuma, V.C.; Lima Duarte, C. de A.; Converti, A.; Porto, A.L.F. Production of β -Lactamase Inhibitors by Streptomyces Species. *Antibiotics* **2018**, *7*, 1–26.
18. Higgens, C.E.; Kastner, R.E. Streptomyces Clavuligerus sp.nov. a B-Lactam Antibiotic Producer. *Int. J. Syst. Bacteriol.* **1971**, *21*, 326–331.
19. Paradkar, A. Clavulanic acid production by Streptomyces clavuligerus: biogenesis, regulation and strain improvement. *J. Antibiot. (Tokyo).* **2013**, *66*, 411–20.
20. Jensen, S.E. Biosynthesis of clavam metabolites. *J. Ind. Microbiol. Biotechnol.* **2012**, *39*, 1407–1419.
21. Hamed, R.B.; Gomez-Castellanos, J.R.; Henry, L.; Ducho, C.; McDonough, M.A.; Schofield, C.J. The enzymes of β-lactam biosynthesis. *Nat. Prod. Rep.* **2013**, *30*, 21–107.

22. Bachmann, B.; Li, R.; Townsend, C. beta-Lactam synthetase: a new biosynthetic enzyme. *Proc. Natl. Acad. Sci. U. S. A.* **1998**, *95*, 9082–6.
23. Bachmann, B.O.; Townsend, C.A. Kinetic mechanism of the β-lactam synthetase of streptomyces clavuligerus. *Biochemistry* **2000**, *39*, 11187–11193.
24. Tahlan, K.; Park, H.U.; Wong, A.; Beatty, P.H.; Jensen, S.E. Two Sets of Paralogous Genes Encode the Enzymes Involved in the Early Stages of Clavulanic Acid and Clavam Metabolite Biosynthesis in Streptomyces clavuligerus. *Antimicrob. Agents Chemother.* **2004**, *48*, 930–939.
25. Salowe, S.P.; Neil Marsh, E.; Townsend, C.A. Purification and Characterization of Clavaminate Synthase from Streptomyces clavuligerus: An Unusual Oxidative Enzyme in Natural Product Biosynthesis. *Biochemistry* **1990**, *29*, 6499–6508.
26. Busby, R.W.; Chang, M.D.-T.; Busby, R.C.; Wimp, J.; Townsend, C.A. Expression and Purification of Two Isozymes of Clavaminate Synthase and Initial Characterization of the Iron Binding Site. *J. Biol. Chem.* **1995**, *270*, 4262–4269.
27. Zhang, Z.; Ren, J. shan; Harlos, K.; McKinnon, C.H.; Clifton, I.J.; Schofield, C.J. Crystal structure of a clavaminate synthase-Fe(II)-2-oxoglutarate-substrate-NO complex: Evidence for metal centred rearrangements. *FEBS Lett.* **2002**, *517*, 7–12.
28. Caines, M.E.C.; Elkins, J.M.; Hewitson, K.S.; Schofield, C.J. Crystal Structure and Mechanistic Implications of N 2-(2-Carboxyethyl)arginine Synthase, the First Enzyme in the Clavulanic Acid Biosynthesis Pathway. *J. Biol. Chem.* **2004**, *279*, 5685–5692.
29. Wu, T.K.; Busby, R.W.; Houston, T.A.; Mcilwaine, D.B.; Egan, L.A.; Townsend, C.A.; Wu, T.; Busby, R.W.; Houston, T.A.; Ilwaine, D.B.M.C.; et al. Identification, Cloning, Sequencing, and overexpression of the gene encoding proclavaminate amidino hydrolase and characterization of protein function in clavulanic acid biosynthesis. *J. Bacteriol.* **1995**, *177*, 3714–3720.
30. Shrestha, B.; Dhakal, D.; Darsandhari, S.; Pandey, R.P.; Pokhrel, A.R.; Jnawali, H.N.; Sohng, J.K. Heterologous production of clavulanic acid intermediates in Streptomyces venezuelae. *Biotechnol. Bioprocess Eng.* **2017**, *22*, 359–365.
31. Arulanantham, H.; Kershaw, N.J.; Hewitson, K.S.; Hughes, C.E.; Thirkettle, J.E.; Schofield, C.J. ORF17 from the clavulanic acid biosynthesis gene cluster catalyzes the ATP-dependent formation of N-glycyl-clavaminic acid. *J. Biol. Chem.* **2006**, *281*, 279–287.
32. MacKenzie, A.K.; Kershaw, N.J.; Hernandez, H.; Robinson, C. V.; Schofield, C.J.; Andersson, I. Clavulanic Acid Dehydrogenase: Structural and Biochemical Analysis of the Final Step in the Biosynthesis of the β-Lactamase Inhibitor Clavulanic Acid. *Biochemistry* **2007**, *46*, 1523–1533.
33. Zelyas, N.J.; Cai, H.; Kwong, T.; Jensen, S.E. Alanylclavam biosynthetic genes are clustered together with one group of clavulanic acid biosynthetic genes in Streptomyces clavuligerus. *J. Bacteriol.* **2008**, *190*, 7957–7965.
34. Goomeshi Nobary, S.; Jensen, S.E. A comparison of the clavam biosynthetic gene clusters in Streptomyces antibioticus Tü1718 and Streptomyces clavuligerus . *Can. J. Microbiol.* **2012**, *58*, 413–425.
35. Bushell, M.E.; Kirk, S.; Zhao, H.; Avignone-rossa, C.A. Manipulation of the physiology of clavulanic acid biosynthesis with the aid of metabolic flux analysis. *Enzyme Microb. Technol.* **2006**, *39*, 149–157.
36. Ramirez-malule, H.; Junne, S.; Cruz-bournazou, M.N.; Neubauer, P. Streptomyces clavuligerus shows a strong association between TCA cycle intermediate accumulation and clavulanic acid biosynthesis. *Appl. Microbiol. Biotechnol.* **2018**, *102*, 4009–402.
37. Sánchez, C.; Quintero, J.C.; Ochoa, S. Flux Balance Analysis in the Production of Clavulanic Acid by Streptomyces clavuligerus. *Biotechnol. Prog.* **2015**, *31*, 1226–1236.
38. Cavallieri, A.P.; Baptista, A.S.; Leite, C.A.; Araujo, M.L.G. da C. A case study in flux balance analysis: Lysine, a cephamycin C precursor, can also increase clavulanic acid production. *Biochem. Eng. J.* **2016**, *112*, 42–53.
39. Ser, H.-L.; Law, J.W.-F.; Chaiyakunapruk, N.; Jacob, S.A.; Palanisamy, U.D.; Chan, K.-G.; Goh, B.-H.; Lee, L.-H. Fermentation Conditions that Affect Clavulanic Acid Production in Streptomyces clavuligerus: A Systematic Review. *Front. Microbiol.* **2016**, *7*, 522.

40. Bellão, C.; Antonio, T.; Araujo, M.L.G.C.; Badino, A.C. Production of clavulanic acid and cephamycin c by streptomyces clavuligerus under different fed-batch conditions. *Brazilian J. Chem. Eng.* **2013**, *30*, 257–266.
41. Saudagar, P.S.; Singhal, R.S. Optimization of nutritional requirements and feeding strategies for clavulanic acid production by Streptomyces clavuligerus. *Bioresour. Technol.* **2007**, *98*, 2010–2017.
42. Sánchez, C.; Gomez, N.; Quintero, J.C. Producción de Ácido Clavulánico por fermentación de Streptomyces clavuligerus : Evaluación de diferentes medios de cultivo y modelado matemático. *Dyna* **2012**, *79*, 158–165.
43. Saudagar, P.S.; Singhal, R.S. Optimization of nutritional requirements and feeding strategies for clavulanic acid production by Streptomyces clavuligerus. *Bioresour. Technol.* **2007**, *98*, 2010–7.
44. Bussari, B.; Saudagar, P.S.; Shaligram, N.S.; Survase, S.A.; Singhal, R.S. Production of cephamycin C by Streptomyces clavuligerus NT4 using solid-state fermentation. *J. Ind. Microbiol. Biotechnol.* **2008**, *35*, 49–58.
45. da Silva Rodrigues, K.C.; de Souza, A.T.; Badino, A.C.; Pedrolli, D.B.; Cerri, M.O. Biotechnology and Industrial Microbiology Screening of medium constituents for clavulanic acid production by Streptomyces clavuligerus. *Brazilian J. Microbiol.* **2018**, *49*, 832–839.
46. Neto, A.B.; Hirata, D.B.; Cassiano Filho, L.C.M.; Bellão, C.; Badino, A.C.; Hokka, C.O. A study on clavulanic acid production by Streptomyces clavuligerus in batch, FED-batch and continuous processes. *Brazilian J. Chem. Eng.* **2005**, *22*, 557–563.
47. Teodoro, J.C.; Baptista-Neto, A.; Araujo, M.L.G.C.; Hokka, C.O.; Badino, A.C. Influence of glycerol and ornithine feeding on clavulanic acid production by streptomyces clavuligerus. *Brazilian J. Chem. Eng.* **2010**, *27*, 499–506.
48. Domingues, L.C.G.; Teodoro, J.C.; Hokka, C.O.; Badino, A.C.; Araujo, M.L.G.C. Optimisation of the glycerol-to-ornithine molar ratio in the feed medium for the continuous production of clavulanic acid by Streptomyces clavuligerus. *Biochem. Eng. J.* **2010**, *53*, 7–11.
49. Carvalho, V.; Brandão, J.F.; Brandão, R.; Rangel-yagui, C.O.; Couto, J.A.; Converti, A.; Pessoa, A. Stability of clavulanic acid under variable pH , ionic strength and temperature conditions . A new kinetic approach. **2009**, *45*, 89–93.
50. Brethauer, S.; Held, M.; Panke, S. Clavulanic Acid Decomposition Is Catalyzed by the Compound Itself and by Its Decomposition Products. *J. Pharm. Sci.* **2008**, *97*, 3451–3455.
51. Marques, D.A.V.; Oliveira, R.P.S.; Perego, P.; Porto, A.L.F.; Pessoa, A.; Converti, A. Kinetic and thermodynamic investigation on clavulanic acid formation and degradation during glycerol fermentation by Streptomyces DAUFPE 3060. *Enzyme Microb. Technol.* **2009**, *45*, 169–173.
52. Costa, C.L.L.; Badino, A.C. Production of clavulanic acid by Streptomyces clavuligerus in batch cultures without and with glycerol pulses under different temperature conditions. *Biochem. Eng. J.* **2012**, *69*, 1–7.
53. Olmos, E.; Mehmood, N.; Haj Husein, L.; Goergen, J.L.; Fick, M.; Delaunay, S. Effects of bioreactor hydrodynamics on the physiology of Streptomyces. *Bioprocess Biosyst. Eng.* **2013**, *36*, 259–272.
54. Alok S, and I.G. Effect of Different Impellers and Baffles on Aerobic Stirred Tank Fermenter using Computational Fluid Dynamics. *J. Bioprocess. Biotech.* **2014**, *4*, 1.
55. Hristov, H. V; Mann, R.; Lossev, V.; Vlaev, S.D. A simplified CFD for three-dimensional analysis of fluid mixing, mass transfer and bioreaction in a fermenter equipped with triple novel geometry impellers. *Food Bioprod. Process.* **2004**, *82*, 21–34.
56. Jin, B.; van Leeuwen, J.H.; Doelle, H.W.; Yu, Q.M. The influence of geometry on hydrodynamic and mass transfer characteristics in an external airlift reactor for the cultivation of filamentous fungi. *World J. Microbiol. Biotechnol.* **1999**, *15*, 83–90.
57. Lin, Y.H.; Hwang, S.C.J.; Gong, J.T.; Wu, J.Y.; Chen, K.C. Using redox potential to detect microbial activities during clavulanic acid biosynthesis in Streptomyces clavuligerus. *Biotechnol. Lett.* **2005**, *27*, 1791–1795.
58. Rosa, J.C.; Baptista Neto, A.; Hokka, C.O.; Badino, A.C. Influence of dissolved oxygen and shear conditions on clavulanic acid production by Streptomyces clavuligerus. *Bioprocess Biosyst. Eng.* **2005**, 99–104.

59. Xia, X.; Lin, S.; Xia, X.X.; Cong, F.S.; Zhong, J.J. Significance of agitation-induced shear stress on mycelium morphology and lavendamycin production by engineered Streptomyces flocculus. *Appl. Microbiol. Biotechnol.* **2014**, *98*, 4399–4407.
60. Zacchetti, B.; Smits, P.; Claessen, D. Dynamics of pellet fragmentation and aggregation in liquid-grown cultures of Streptomyces lividans. *Front. Microbiol.* **2018**, *9*, 1–10.
61. Manteca, A.; Alvarez, R.; Salazar, N.; Yagüe, P.; Sanchez, J. Mycelium differentiation and antibiotic production in submerged cultures of Streptomyces coelicolor. *Appl. Environ. Microbiol.* **2008**, *74*, 3877–3886.
62. Pinto, L.S.; Vieira, L.M.; Pons, M.N.; Fonseca, M.M.R.; Menezes, J.C. Morphology and viability analysis of Streptomyces clavuligerus in industrial cultivation systems. *Bioprocess Biosyst. Eng.* **2004**, *26*, 177–184.
63. Cerri, M.O.; Badino, A.C. Shear conditions in clavulanic acid production by Streptomyces clavuligerus in stirred tank and airlift bioreactors. *Bioprocess Biosyst. Eng.* **2012**, *35*, 977–984.
64. Park, J.H.; Lee, S.Y.; Kim, T.Y.; Kim, H.U. Application of systems biology for bioprocess development. *Trends Biotechnol.* **2008**, *26*, 404–412.
65. Gómez-Ríos, D.; Navarro, G.; Monsalve, P.; Barrera-Zapata, R.; Ríos-Estepa, R. Aspen Plus Simulation Strategies Applied to the Study of Chitin Bioextraction from Shrimp Waste. *Food Technol. Biotechnol.* **2019**, *57*.
66. Gómez-Ríos, D.; Barrera-Zapata, R.; Ríos-Estepa, R. Comparison of process technologies for chitosan production from shrimp shell waste: A techno-economic approach using Aspen Plus ®. *Food Bioprod. Process.* **2017**, *103*, 49–57.
67. Kirk, S. The physiology of clavulanic acid production by Streptomyces clavuligerus, University of Surrey, 2000.
68. Sánchez, C. Análisis de flux metabólico en la producción de ácido clavulánico a partir de Streptomyces Clavuligerus, Universidad de Antioquia, 2013.
69. Medema, M.H.; Alam, M.T.; Heijne, W.H.M.; Van Den Berg, M.A.; Müller, U.; Trefzer, A.; Bovenberg, R.A.L.; Breitling, R.; Takano, E. Genome-wide gene expression changes in an industrial clavulanic acid overproduction strain of Streptomyces clavuligerus. *Microb. Biotechnol.* **2011**, *4*, 300–305.
70. Toro, L.; Pinilla, L.; Avignone-Rossa, C.; Ríos-Estepa, R. An enhanced genome-scale metabolic reconstruction of Streptomyces clavuligerus identifies novel strain improvement strategies. *Bioprocess Biosyst. Eng.* **2018**, *41*, 657–669.
71. Gómez-Cerón, S.; Galindo-Betancur, D.; Ramírez-Malule, H. Data set of in silico simulation for the production of clavulanic acid and cephamycin C by Streptomyces clavuligerus using a genome scale metabolic model. *Data Br.* **2019**, *24*, 103992.
72. Medema, M.H.; Trefzer, A.; Kovalchuk, A.; van den Berg, M.; Müller, U.; Heijne, W.; Wu, L.; Alam, M.T.; Ronning, C.M.; Nierman, W.C.; et al. The Sequence of a 1.8-Mb Bacterial Linear Plasmid Reveals a Rich Evolutionary Reservoir of Secondary Metabolic Pathways. *Genome Biol. Evol.* **2010**, *2*, 212–224.
73. Ramirez-Malule, H. Quantitative description of the metabolic capabilities of Streptomyces clavuligerus for clavulanic acid production: A combined constraint-based modeling approach and experimental testing. **2016**.
74. Cao, G.; Zhong, C.; Zong, G.; Fu, J.; Liu, Z.; Zhang, G.; Qin, R. Complete Genome Sequence of Streptomyces clavuligerus F613-1, an Industrial Producer of Clavulanic Acid . *Genome Announc.* **2016**, *4*, 4–5.
75. Hwang, S.; Lee, N.; Jeong, Y.; Lee, Y.; Kim, W.; Cho, S.; Palsson, B.O.; Cho, B.-K. Primary transcriptome and translatome analysis determines transcriptional and translational regulatory elements encoded in the Streptomyces clavuligerus genome. *Nucleic Acids Res.* **2019**, *47*, 6114–6129.
76. Song, J.Y.; Jensen, S.E.; Lee, K.J. Clavulanic acid biosynthesis and genetic manipulation for its overproduction. *Appl. Microbiol. Biotechnol.* **2010**, *88*, 659–669.
77. Hung, T.V.; Malla, S.; Park, B.C.; Liou, K.; Lee, H.C.; Sohng, J.K. Enhancement of clavulanic acid by replicative and integrative expression of ccaR and cas2 in Streptomyces clavuligerus NRRL3585. *J. Microbiol. Biotechnol.* **2007**, *17*, 1538–45.
78. Li, R.; Townsend, C.A. Rational strain improvement for enhanced clavulanic acid production by genetic engineering of the glycolytic pathway in Streptomyces clavuligerus. **2006**, *8*, 240–252.

79. Jnawali, H.N.; Liou, K.; Sohng, J.K. Role of σ-factor (orf21) in clavulanic acid production in Streptomyces clavuligerus NRRL3585. *Microbiol. Res.* **2011**, *166*, 369–379.
80. Jnawali, H.N.; Lee, H.C.; Sohng, J.K. Enhancement of Clavulanic Acid Production by Expressing Regulatory Genes in gap Gene Deletion Mutant of Streptomyces clavuligerus NRRL3585. *J. Microbiol. Biotechnol.* **2010**, *20*, 146–152.
81. Kurt-Kizildoğan, A.; Vanli-Jaccard, G.; Mutlu, A.; Sertdemir, I.; Özcengiz, G. Genetic engineering of an industrial strain of Streptomyces clavuligerusfor further enhancement of clavulanic acid production. *Turkish J. Biol.* **2017**, *41*, 342–353.
82. Qin, R.; Zhong, C.; Zong, G.; Fu, J.; Pang, X.; Cao, G. Improvement of clavulanic acid production in Streptomyces clavuligerus F613-1 by using a claR - neo reporter strategy. *Electron. J. Biotechnol.* **2017**, *28*, 41–46.
83. Cho, H.S.; Jo, J.C.; Shin, C.-H.; Lee, N.; Choi, J.-S.; Cho, B.-K.; Roe, J.-H.; Kim, C.-W.; Kwon, H.J.; Yoon, Y.J. Improved production of clavulanic acid by reverse engineering and overexpression of the regulatory genes in an industrial Streptomyces clavuligerus strain. *J. Ind. Microbiol. Biotechnol.* **2019**, *46*, 1205–1215.
84. Wang, C.; Liu, J.; Liu, H.; Wang, J.; Wen, J. A genome-scale dynamic flux balance analysis model of Streptomyces tsukubaensis NRRL18488 to predict the targets for increasing FK506 production. *Biochem. Eng. J.* **2017**, *123*, 45–56.
85. Villegas, A.; Arias, J.P.; Aragón, D.; Ochoa, S.; Arias, M. Structured model and parameter estimation in plant cell cultures of Thevetia peruviana. *Bioprocess Biosyst. Eng.* **2017**, *40*, 573–587.
86. Theobald, U.; Mailinger, W.; Baltes, M.; Rizzi, M. In Vivo Analysis of Metabolic Dynamics in Saccharomyces cerevisiae : I . Experimental Observations. **1997**.
87. Ghorbaniaghdam, A.; Henry, O.; Jolicoeur, M. A kinetic-metabolic model based on cell energetic state: Study of CHO cell behavior under Na-butyrate stimulation. *Bioprocess Biosyst. Eng.* **2013**, *36*, 469–487.
88. Chassagnole, C.; Noisommit-Rizzi, N.; Schmid, J.W.; Mauch, K.; Reuss, M. Dynamic modeling of the central carbon metabolism of Escherichia coli. *Biotechnol. Bioeng.* **2002**, *79*, 53–73.
89. Costa, R.S.; Machado, D.; Rocha, I.; Ferreira, E.C. Hybrid dynamic modeling of Escherichia coli central metabolic network combining Michaelis-Menten and approximate kinetic equations. *BioSystems* **2010**, *100*, 150–157.
90. Adiamah, D.A.; Schwartz, J.M. [2012 Schwartz]Construction of a Genome-Scale Kinetic ...erculosis Using Generic Rate Equations.pdf. *Metabolites* **2012**, *2*, 382–397.
91. Singh, V.K.; Gosh, I. Kinetic modeling of tricarboxylic acid cycle and glyoxylate bypass in Mycobacterium tuberculosis, and its application to assessment of drug targets. *Theor. Biol. Med. Model.* **2006**, *3*, 1–11.
92. Khodayari, A.; Zomorrodi, A.R.; Liao, J.C.; Maranas, C.D. A kinetic model of Escherichia coli core metabolism satisfying multiple sets of mutant flux data. *Metab. Eng.* **2014**, *25*, 50–62.
93. Machado, D.; Herrgard, M.J.; Rocha, I. Modeling the Contribution of Allosteric Regulation for Flux Control in the Central Carbon Metabolism of E. coli. *Front Bioeng Biotechnol* **2015**, *3*, 154.
94. Mannan, A.A.; Toya, Y.; Shimizu, K.; McFadden, J.; Kierzek, A.M.; Rocco, A. Integrating kinetic model of E. coli with genome scale metabolic fluxes overcomes its open system problem and reveals bistability in central metabolism. *PLoS One* **2015**, *10*, 1–36.
95. Adiamah, D.A.; Handl, J.; Schwartz, J.M. Streamlining the construction of large-scale dynamic models using generic kinetic equations. *Bioinformatics* **2010**, *26*, 1324–1331.
96. Barreto-Rodriguez, C.M.; Ramirez-Angulo, J.P.; Gomez Ramirez, J.M.; Achenie, L.; Molina-Bulla, H.; González Barrios, A.F. Dynamic Flux Balance Analysis for Predicting Gene Overexpression Effects in Batch Cultures. *J. Biol. Syst.* **2014**, *22*, 1–12.
97. Mahadevan, R.; Edwards, J.S.; Doyle, F.J. Dynamic flux balance analysis of diauxic growth in Escherichia coli. *Biophys. J.* **2002**, *83*, 1331–1340.
98. Orth, J.D.; Thiele, I.; Palsson, B.O. What is flux balance analysis? *Nat. Biotechnol.* **2010**, *28*, 245–248.
99. Holzhütter, H.G. The principle of flux minimization and its application to estimate stationary fluxes in metabolic networks. *Eur. J. Biochem.* **2004**, *271*, 2905–2922.

100. Henson, M.A.; Hanly, T.J. Dynamic flux balance analysis for synthetic microbial communities. *IET Syst. Biol.* **2014**, *8*, 214–29.
101. Villegas, R.M.; Martinez, R. Identification of Dynamic Metabolic Flux Balance Models Based on Parametric Sensitivity Analysis by, University of Waterloo, 2016.
102. Zhuang, K.; Izallalen, M.; Mouser, P.; Richter, H.; Risso, C.; Mahadevan, R.; Lovley, D.R. Genome-scale dynamic modeling of the competition between Rhodoferax and Geobacter in anoxic subsurface environments. *ISME J.* **2011**, *5*, 305–16.
103. Sánchez, B.J.; Pérez-Correa, J.R.; Agosin, E. Construction of robust dynamic genome-scale metabolic model structures of Saccharomyces cerevisiae through iterative re-parameterization. *Metab. Eng.* **2014**, *25*, 159–173.
104. Robitaille, J.; Chen, J.; Jolicoeur, M. A single dynamic metabolic model can describe mAb producing CHO cell batch and fed-batch cultures on different culture media. *PLoS One* **2015**, *10*.
105. Feng, X.; Xu, Y.; Chen, Y.; Tang, Y.J. Integrating flux balance analysis into kinetic models to decipher the dynamic metabolism of shewanella oneidensis MR-1. *PLoS Comput. Biol.* **2012**, *8*.
106. Serrano-Bermúdez, L.M.; González Barrios, A.F.; Montoya, D. Clostridium butyricum population balance model: Predicting dynamic metabolic flux distributions using an objective function related to extracellular glycerol content. *PLoS One* **2018**, *13*, e0209447.
107. Salguero, D.A.M.; Fernández-Niño, M.; Serrano-Bermúdez, L.M.; Melo, D.O.P.; Winck, F. V.; Caldana, C.; Barrios, A.F.G. Development of a Chlamydomonas reinhardtii metabolic network dynamic model to describe distinct phenotypes occurring at different CO2 levels. *PeerJ* **2018**, *2018*, 1–25.

Chapter 2

Evaluation of the Environmental Conditions and Culture Media Composition on Clavulanic Acid Biosynthesis in *Streptomyces clavuligerus,* at Laboratory Scale

Abstract: Clavulanic acid (CA) is a β-lactam antibiotic inhibitor of β-lactamase enzymes responsible for antibiotics resistance in several pathogenic bacteria. In this chapter, submerged cultures of a wild type strain of *Streptomyces clavuligerus* were performed in synthetic and complex media for the evaluation of biomass accumulation and CA productivity. The effect of the agitation rate on biomass and CA production was also explored. In summary, this chapter aimed at presenting all the preliminary experimental work at lab scale, which was the basis for the experimental work at bioreactor scale. In shake flask cultures a synthetic media mainly composed of glycerol, glutamate, ammonium, phosphate and trace elements produced the lowest biomass concentration, but the highest CA production among the media tested. The Fed-batch operation mode favored biomass maintenance and CA accumulation compared with the batch operation, in which CA degradation rate prevented the stability of CA secretion. Increase of agitation velocity from 200 to 220 and 250 rpm showed positive effect on biomass and CA accumulations possibly related to moderate shear stress and an enhanced mass transfer. In contrast, high shear stress caused by addition of glass beads inhibited completely biomass growth and CA production.

2.1. Introduction

Different nutritional and environmental conditions have been explored as an attempt to improve the understanding of the biosynthesis of CA by secreted *Streptomyces clavuligerus (S. clavuligerus).* As reviewed by Ser et al. [1], media containing glycerol have been reported as favoring CA biosynthesis based on the direct utilization of glyceraldehyde-3-phosphate as an early precursor of its biosynthetic pathway. When comparing the CA production using glycerol and sucrose as carbon sources, glycerol promotes higher CA titers up to 5-fold than those observed in cultivations with starch [2,3]. Nevertheless, substrate inhibition can occur at concentrations of glycerol higher than 50 $g.L^{-1}$ [3]. The production of CA is enhanced by amino-acids supplementation [4,5] and complex nitrogen sources such as soy protein and soy flour [2,3]. Saudagar and Singhal found that glutamic acid has the greater statistic effect on CA production regarding the production medium and confirmed the repression of CA biosynthesis when increasing the phosphate concentration in the media over 100 $mmol.L^{-1}$ [5]. A complex culture medium is a source of important amounts of free or hydrolyzed amino acids, which act not only as nitrogen sources but also as secondary carbon sources. Complex nitrogen sources, as those containing soy protein, favor considerably the CA accumulation in contrast to the chemically defined media [3].

CA production is preferably carried out in batch or fed-batch operation. In all cases, the media design must consider phosphate limitation to promote CA accumulation. Batch cultivations are, in general, less efficient in terms of CA accumulation since this kind of operation is limited by the substrate starvation, biomass decline and product degradation [1,6]. Conversely, the fed-batch operation by adding glycerol led to higher CA concentrations in comparison with the batch control [2,5,6].

Other factors apart from culture media could affect the CA accumulation in submerged cultures of *S. clavuligerus.* The CA molecule shows susceptibility to temperature and ionic strength in

aqueous solutions, which compromises the CA titers attained during cultivations [7,8]. The pH culture conditions seem to affect CA yield, possibly more linked to molecule degradation than biosynthesis inhibition [9]. The maximum concentration of CA has been reported at neutral or slightly acidic pH conditions (6.8), regardless the substrates used during the cultivations [1]. Low temperatures favor the molecule stability; in this regard, higher titers have been reported during operating fermentations at 20°C but the growth rate at such temperature is lower than that observed at 28°C [10].

Agitation and oxygen mass transfer are also considered as factors potentially affecting the CA production. An increase of 50% in oxygen transfer in shake flask cultures increased 2-fold the CA production [11]. For the case of bioreactor operation, Rosa et al. [12] found that intense agitation rates i.e., 800 - 1000 rpm, favored CA accumulation in stirred tank bioreactors. The volumetric mass transfer coefficient (k_La) observed in airlift reactors operated in the range from 3 to 5 vvm, is comparable to those in stirred tank bioreactors, operating in the range of 600 to 1000 rpm; both conditions promote CA accumulation. In this work, the use of different media was explored for determination of the most favorable cultivation conditions regarding the CA production, aimed to obtain reproducible and stable growth and detectable concentrations of CA for further studies at bioreactor scale.

2.2. Materials and Methods

2.2.1 Activation of the strain

A cryostock of S. clavuligerus ATCC 27064 mycelial suspension (1.2 mL) stored in glycerol sterile solution (16.7%) at -80 °C was used for inoculation of batch and fed-batch cultivation in the shake flask scale. Activation of the strain was performed in seed medium prepared as follows (in $g.L^{-1}$, distilled water): glycerol, 15; soy peptone, 15; sodium chloride, 3 and calcium carbonate, 1; pH was adjusted at 6.8. Mycelial suspension was inoculated in 20 mL of seed medium disposed in 100 mL baffled Erlenmeyer flasks and then incubated at 28 °C for 24 h at 200 rpm in orbital shaker (MaxQ400, Thermo Scientific, Waltham, MA USA).

2.2.2 Media composition

Three different production media reported in the literature as suitable for CA production were tested. Two synthetic media were used in addition to a complex medium. The first synthetic medium considered was the glycerol-sucrose-proline-aspartate (GSPA) [18] prepared as follows (concentration in $g.L^{-1}$, distilled water): glycerol, 15; sucrose, 20; NaCl, 5.0; L- proline, 2.5; K_2HPO_4, 2.0; $MgSO_4 \cdot 7H_2O$, 1.0; $CaCl_2$, 0.4; $MnCl_2 \cdot 4H_2O$, 0.1; $FeCl_3 \cdot 6H_2O$, 0.1; $ZnCl_2$, 0.05; 3-(N-morpholino) propanesulfonic acid (MOPS), 20.9 and aspartic acid, 1.5. The second synthetic medium used was the one formulated by Roubos et al. [19] and adapted by Ramírez-Malule et al. [14], (concentrations in $g.L^{-1}$, distilled water): glycerol, 9.3; K_2HPO_4, 0.8; $(NH_4)_2SO_4$, 1.26; monosodium glutamate, 9.8; $FeSO_4 \cdot 7H_2O$, 0.18; $MgSO_4 \cdot 7H_2O$, 0.72; MOPS, 10.5 and trace elements solution (1.44 mL). The trace elements solution contained ($g.L^{-1}$): H_2SO_4, 20.4; monosodium citrate$\cdot 1H_2O$, 50; $ZnSO_4 \cdot 7H_2O$, 16.75; $CuSO_4 \cdot 5H_2O$, 2.5; $MnCl_2 \cdot 4H_2O$, 1.5; H_3BO_3, 2; and $Na_2MoO_4 \cdot 2H_2O$, 2. Finally, the complex medium referred as isolate soy protein (ISP) [18] was also used, prepared as follows (concentrations in $g.L^{-1}$, distilled water): glycerol, 15.0; soy protein isolate, 10.0; malt extract, 10.0; yeast extract, 1.0; K_2HPO_4, 2.5; $MgSO_4 \cdot 7H2O$, 0.75; $MnCl_2 \cdot 4H_2O$, 0.001; $FeSO_4 \cdot 7H_2O$, 0.001; $ZnSO4 \cdot 7H2O$, 0.001; MOPS, 21.0. In all cases, the feed medium used in the fed-batch operation was composed of ($g.L^{-1}$, distilled water): glycerol, 120; K_2HPO_4, 2; and $(NH_4)_2SO_4$, 8.

2.2.3 Operation conditions

Pre-cultures were performed in 45 mL of production media after inoculation of 5 mL of mycelial suspension from seed cultures for a total operating volume of 50 mL. The pre-cultures were

performed in 250 mL baffled shake flasks during 20 h at 200 rpm in an orbital shaker. Initially, batch and fed-batch cultivations were performed in duplicates maintaining agitation at 200 rpm for selecting the culture medium yielding the highest CA accumulation. Batch cultivations were performed during 160 h with 50 mL operation volume, inoculated with 10% v/v of mycelial suspension from pre-culture in identical medium. For the case of fed-batch operation, the starting volume was 50 mL; the initial batch operation lasted up to 33 h, then addition of 50 mL of feed media was accomplished in the subsequent 104 h. Finally, a starvation phase of 23 h was followed prior to the end of the cultivation at 160 h. Once the more suitable medium was selected, additional experiments were performed at 200, 220 and 250 rpm in order to explore the effect of agitation on S. clavuligerus growth and CA production.

2.2.4 Analytical methods

Culture samples (1 mL) were taken at intervals of approximately 12 h and then centrifuged at 15,000 rpm and 4 °C for 10 min; wet biomass was washed with 0.9 % NaCl and centrifuged. Test tubes were dried overnight at 75 °C for dry cell weight (DCW) determination. CA was determined by HPLC using an Agilent 1200 Series equipped with a Diode Array Detector, using a reverse phase column ZORBAX Eclipse XDB-C18 (4.6 x 150 mm, 18 μm). The mobile phase was a 96% v/v KH_2PO_4 (50 mM, pH 3.2) and 6% v/v methanol solution at a flow rate of 1 $mL.min^{-1}$. The supernatant samples (300 μL) were derivatized with 100 μL of imidazole reagent (99.0%) and allowed to stand for 15 min at 30 °C. After incubation, 20 μL were injected into the HPLC unit. The CA derivative was detected at 311 nm [20].

2.2.5 Mass balances for specific growth and productivity

Starting from the dynamic general mass balance in fed-batch reactor for component i:

$$\frac{dC_i}{dt} = \frac{F}{V}(C_{i,f} - C_i) + r_i + GTR \tag{1}$$

where C_i is the concentration of component i in the reactor, V the volume, $C_{i,f}$ concentration in the feed (F), r_i the volumetric reaction rate and GTR the gas transfer rate if i is a gas component, otherwise GTR is zero. The mass balance (Eq. 1) applied to biomass:

$$\frac{dX}{dt} = \frac{F}{V}(-X) + \mu X \tag{2}$$

where X is biomass concentration and μ is specific growth rate. Similarly for the product p:

$$\frac{dC_p}{dt} = \frac{F}{V}(C_{p,f} - C_p) + r_p \tag{3}$$

For batch operation the specific growth rate and product specific production (q_p) by approximating the derivatives to finite differences:

$$\mu = \frac{1}{X}\left(\frac{\Delta X}{\Delta t}\right) + \frac{F}{V} \tag{4}$$

$$q_p = \frac{r_p}{X} = \frac{1}{X}\left(\frac{\Delta C_p}{\Delta t} + \frac{F}{V}C_p\right) \quad (5)$$

For the case of batch operation *F=0* leading to the expressions applicable for batch cultures. Equations 4 and 5 were used for the specific growth rate and productivity determinations in batch and fed-batch cultures.

2.3. Results and discussion

The growth and CA concentrations were followed in all cultivations, using the procedures previously described in the Materials and Methods section. In batch conditions, the highest biomass accumulation was observed in cultures performed with the ISP medium, perhaps due to the high concentration of carbon sources (glycerol and proteins), attaining a maximum biomass of 23.2 gDCW.L^{-1}; this is approximately 2-fold the maximum biomass observed in the cultivations with the poorer Roubos synthetic medium. Similarly, the maximum specific growth rate was observed in the ISP medium with 0.110±0.004 h^{-1}, followed by the GSPA medium (0.082±0.005 h^{-1}) and the Roubos medium (0.071±0.006 h^{-1}). An accelerated growth phase was observed in the ISP medium in comparison with the other media tested. Nevertheless, the accelerated growth led to early starvation condition and, therefore, a decline of growth after reaching the maximum biomass value at 46 h. In the case of GSPA, the concentration of carbon and nitrogen sources was lower than those of the ISP medium. Similar growth and decline trends were observed for the case of ISP and GSPA media. The maximum biomass accumulated was 17.0 gDCW.L^{-1} and the decline of biomass was less pronounced.

The Roubos medium has less substrate concentration; therefore, the strain exhibited lower specific growth rate and the exponential phase lasted up to 45 h. Interestingly, the biomass decline was less pronounced after finishing the exponential phase with maximum biomass of 10.4 gDCW.L^{-1}. In all cases, the biomass started to decline between 115 and 130 h after substrate depletion. Biomass time courses for batch cultures of *S. clavuligerus* are presented in Figure 2.1, in all cases no lag phase was observed, most likely due to high biomass concentration in the inoculum leading to a quasi-linear trend.

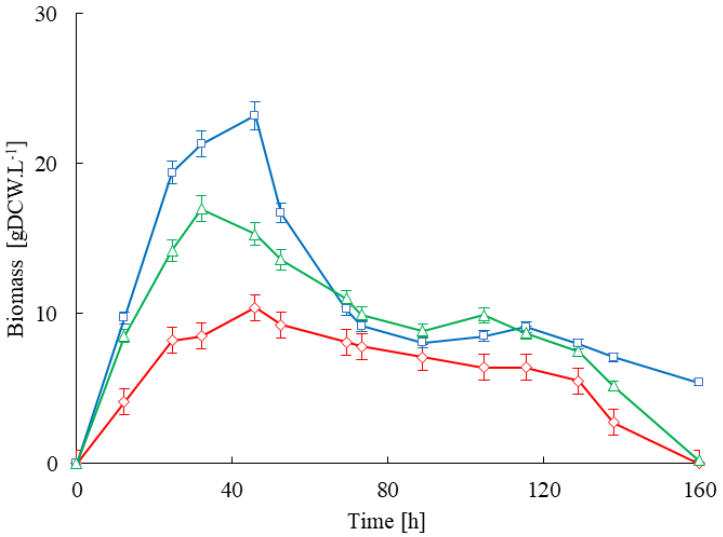

Figure 2.1. *S. clavuligerus* biomass growth in batch cultures (50 mL shake flasks). GSPA medium (triangles), ISP medium (squares) and Roubos medium (diamonds).

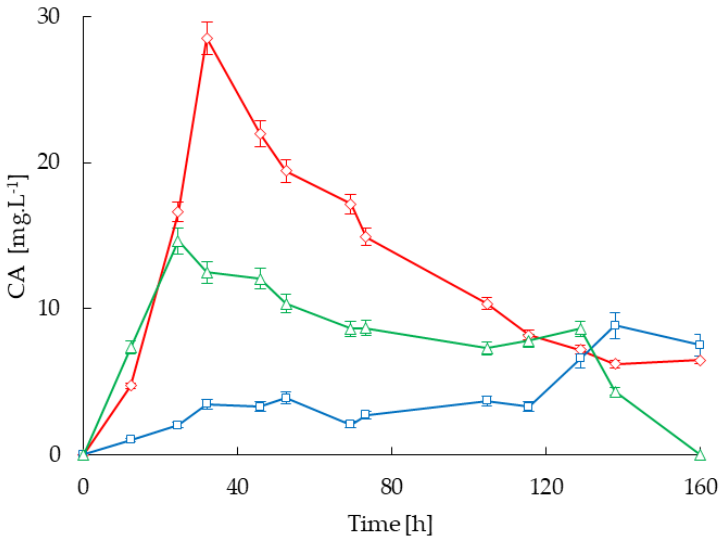

Figure 2.2. CA production in batch cultures (50 mL shake flasks) of *S. clavuligerus*. GSPA medium (triangles), ISP medium (squares) and Roubos medium (diamonds).

CA time courses in batch cultivations are presented in Figure 2.2. The Roubos medium led to a more specific CA production, considering the lower biomass accumulation 0.240±0.026 mg.(gDCW.h)$^{-1}$. The maximum CA concentration in batch cultures in the Roubos medium was 28.5 mg.L^{-1}. Cultures in GSPA and ISP media reached 14.6 and 8.8 mg.L^{-1}, respectively. The productivity of CA was 0.140±0.010 mg.(gDCW.h)$^{-1}$ in the ISP medium and 0.101+0.016 mg.(gDCW.h)$^{-1}$ in the GSPA medium. These results show that CA biosynthesis is favored under nutritional restrictions, mainly phosphate limitation, but maintaining a sufficient supply of carbon and nitrogen flux through central metabolism. It is documented that CA secretion is triggered as a response to stress conditions imposed by nutrient starvation, e.g., phosphate and amino-acids [13]. In this regard, the Roubos medium is designed to provide glycerol and glutamate, which are directly incorporated in the oxidative direction of glycolysis and tricarboxylic acids (TCA) cycle, respectively, thus favoring the synthesis of carboxyethyl arginine as the starting point of the clavams pathway, and finally leading to CA synthesis [14]. Moreover, this medium is P-limited while nitrogen as ammonium is readily available during the culture. In many actinomycetes, the stress response due to nutritional and environmental factors triggers secondary metabolism and antibiotics production; in some instances, this response is also linked to morphological differentiation [15].

Fed-batch has been reported as an operation mode that enhances CA production in *S. clavuligerus* cultures when provided with glycerol and some amino-acids related with arginine metabolism, as the C-5 precursor of CA [1]. Since the phosphate depletion is considered one of the main factors triggering CA secretion, the fed-batch operation was tested in cultivations with the Roubos, ISP and GSPA media, once the phosphate limitation started between 32 and 46 h. A feed medium containing glycerol, ammonium and phosphate was used for all the cultivation operated in fed-batch. The feeding medium was designed to maintain the glycerol and ammonium supply based on the C/N ratio of the batch medium, with a minimum amount of phosphate for maintenance purposes, since it has been reported that total phosphate starvation inhibits completely growth and CA production [5].

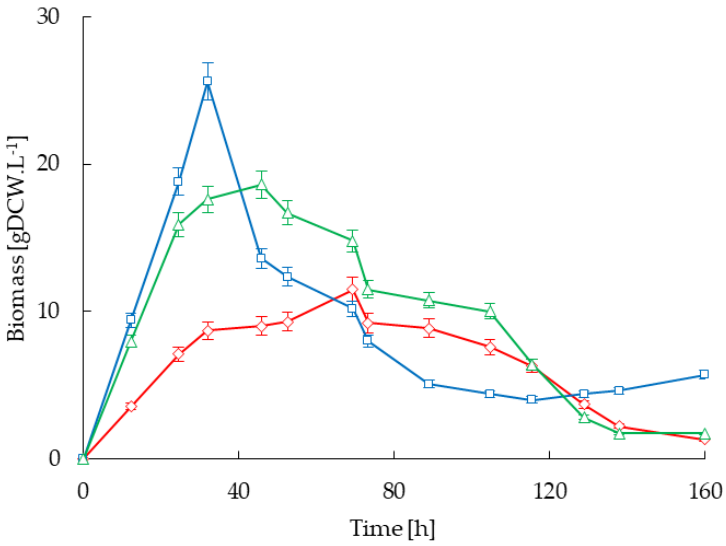

Figure 2.3. *S. clavuligerus* biomass accumulation in shake-flask fed-batch cultures (50 to 100 mL). GSPA medium (triangles), ISP medium (squares) and Roubos medium (diamonds).

Similar to batch cultivations, the highest biomass accumulation was observed in the cultures with the ISP medium (25.6 gDCW.L^{-1}). However, the extensive growth was not able to continue even under the feeding conditions. The maximum biomass attained in the GSPA medium was 17.6 gDCW.L^{-1} during the batch phase; the growth reached 18.6 gDCW.L^{-1} during the fed-batch. The feeding condition delayed the pronounced decline of biomass until t=70 h, maintaining the biomass concentration over 11 gDCW.L^{-1}; this circumstances was not observed in batch cultivations. Feeding with the Roubos medium supported the growth until t=69 h, allowing to reach higher biomass values (11.5 gDCW.L^{-1}) and higher specific growth rate (0.091±0.006 h^{-1}) than those obtained in batch cultures. Additionally, the biomass decline was less pronounced than in batch cultures. For the case of synthetic media, stopping the feeding led to a rapid decline of biomass after t=105 h. Biomass time courses for fed-batch cultivations are presented in Figure 2.3.

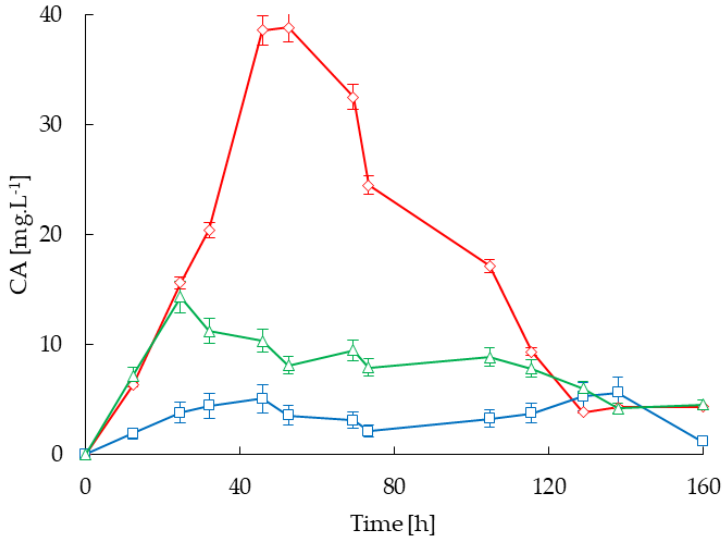

Figure 2.4. CA production in fed-batch cultures (50 to 100 mL shake flasks) of *S. clavuligerus*. GSPA medium (triangles), ISP medium (squares) and Roubos medium (diamonds).

The CA production was enhanced in the fed-batch operation mode using the Roubos medium. The maximum CA concentration was 36% higher than that obtained in the batch cultures. The CA accumulation for the case of GSPA and ISP media were similar to that observed in the batch

operation, considering the dilution effect of the feeding. The specific CA production in the Roubos medium was 0.390±0.002 mg.(gDCW.h)$^{-1}$; in the GSPA and ISP media they were 0.070±0.007 and 0.022±0.005 mg.(gDCW.h)$^{-1}$, respectively.

The highest concentration attained in fed-batch operation using the defined Roubos medium, was 38.9 mg.L^{-1}. Notice that, in batch operation, a higher CA concentrations was also reached. Further, the defined GSPA medium promoted CA production but the concentrations attained were approximately half of the CA concentrations compared with those obtained from the Roubos-medium cultivations. The lowest production of CA was observed in the complex media, probably due to a high availability of nutrients that does not allowed to reach limiting conditions that may trigger CA production. In Figure 2.4, the time courses of CA production in Roubos, GSPA and ISP media are presented. The CA concentration was considerably more stable for the case of fed-batch cultivations, since a continuous synthesis could occur, thus reducing the CA degradation rate due through hydrolysis. Although high CA concentrations were also reached in batch cultivations, a rapid degradation seems to take place once the maximum concentration was reached. Thus, the CA production, attained with the Roubos medium, was considerably higher than that observed with the GSPA and ISP media for the operating conditions, considered in this study.

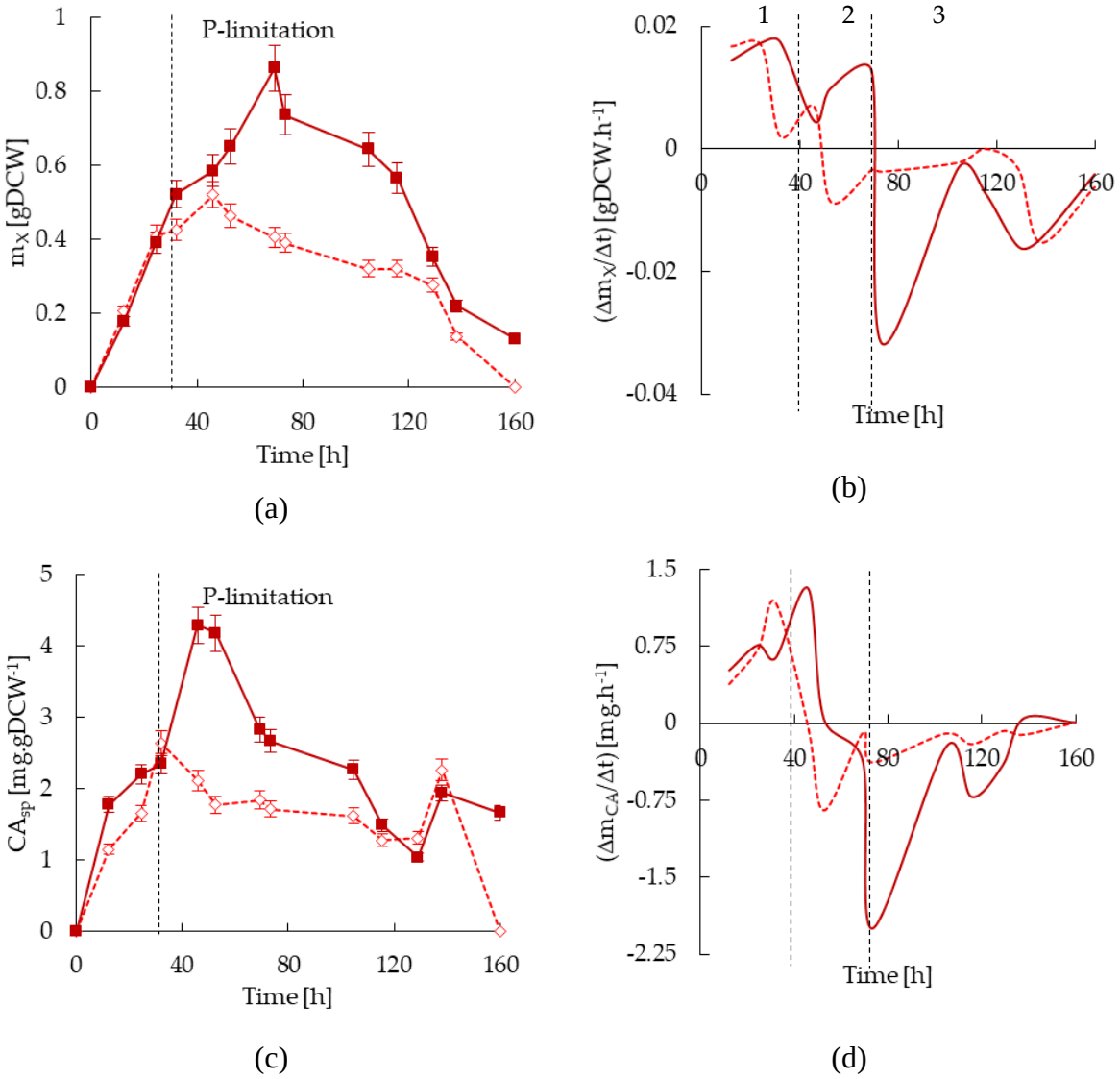

Figure 2.5. CA and biomass production in batch (open symbols, dashed lines) and fed-batch (closed symbols, continuous line). (a) Total biomass (m_X); (b) biomass accumulation rates ($\Delta m_X/\Delta t$); (c) specific CA concentration (CA_{sp}) and (d) CA mass accumulation rates ($\Delta m_{CA}/\Delta t$).

According to the previous results, the medium formulated by Roubos et al. favored higher CA concentrations in fed-batch cultures, but lower biomass concentration in comparison with GSPA and ISP media. In order to compare the performance of batch and fed-batch operating modes regarding CA and biomass production, the total biomass (m_x), specific CA concentration (CA_{sp}), biomass and CA mass accumulations rates ($\Delta m/\Delta t$) are showed in Figure 2.5. Total biomass (Figure 2.5a) behave similar in both cases before the start of the fed-batch operation (phase 1); after starting the feed (phase 2), a considerable increase in total biomass and biomass accumulation rate (Figure 2.5b) were observed, since more carbon and nitrogen were available in the environment. A decreasing trend was observed in the batch operation after 70 h when glutamate limitation was reached (phase 3), leading to a sustained fall in biomass production. However, the death rate seems to be reduced by the supply of nutrients.

CA production correlates with biomass as observed in Figures 2.5c and 2.5d. The maximum CA production is attained before reaching the maximum biomass value. In the case of fed-batch operation, CA production might be enhanced by the nutrients supply under phosphate limitation, immediately after the feeding started (phase 2). However, the CA production seems to be also affected by the glutamate availability, since this amino-acid is incorporated in the urea cycle as C-5 precursor. Similarly, total CA started to decline before than biomass. This suggests a that CA net accumulation might be the result of production and degradation rates, as occurs in biomass synthesis. Thus explaining the total loss of CA at the end of the culture, the coincidence with the fall in biomass, as well as the maximum CA accumulation observed prior to reaching the maximum biomass point.

Moreover, it is expected that CA increases the demand for oxygen and the biomass profiles in batch and fed-batch conditions suggest that oxygen limitation, inherent to shake flask cultivations, is present due to their low k_La values; this environment is limiting for cell growth, even under substrate availability. The extensive growth observed in GSPA and ISP medium might lead to oxygen starvation due to the high biomass concentration, triggering the subsequent pronounced biomass decline added to the dilution factor. For the case of the Roubos medium, the growth and biomass accumulation were lower than that attained from the GSPA and ISP media; therefore, oxygen starvation most likely did not occur. This is consistent with the observed less pronounced biomass decline and large CA biosynthesis. Indeed, the aeration and agitation rates are closely related with CA production and biomass accumulation, due to the strictly aerobic metabolism of *S. clavuligerus* [16]. As a consequence, CA production in shake flasks is usually below 70 $mg.L^{-1}$ as a result of mass transfer limitations [1].

As observed in Figure 2.6, the biomass production with the Roubos medium in fed-batch operation at different agitation rates is rather similar to the dilution factor due to feeding, leading to approximately constant biomass concentration during the fed-batch. The k_La can be enhanced by increasing the oxygen dissolution into the liquid phase by larger agitation rates [12]. Nevertheless, excessive shear stress could negatively affect *S. clavuligerus* growth [17]. The effect of agitation on biomass and CA production was explored by performing fed-batch cultivations of *S. clavuligerus* using the Roubos medium and modifying the agitation rates from 220 to 250 rpm. The time course of biomass at 200, 220 and 250 rpm are showed in Figure 2.6.

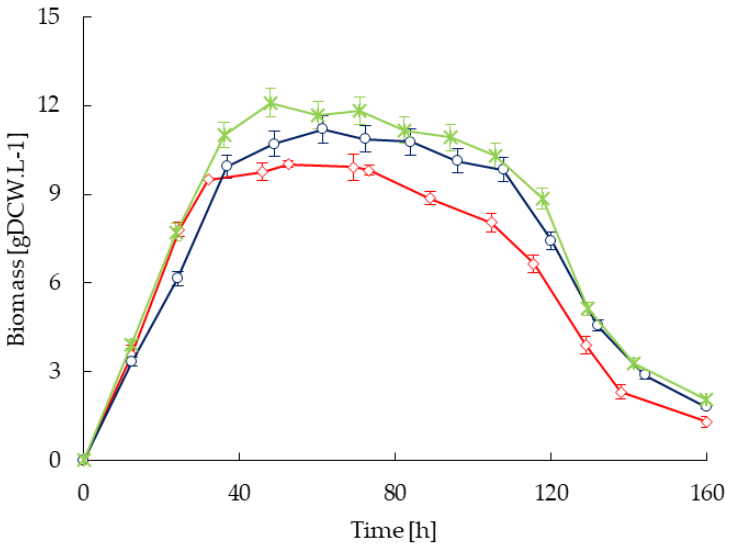

Figure 2.6. *S. clavuligerus* biomass accumulation in fed-batch cultures (50 to 100 mL shake flasks) at agitation rates of 200 (diamonds), 220 (circles) and 250 rpm (stars).

Increasing the agitation rate entailed a positive effect on biomass concentration as observed in Figure 2.6. The maximum biomass obtained at 220 and 250 rpm were 12.8 and 20.9 % higher than that observed at 200 rpm, respectively. Similar values of maximum growth rates were observed at 220 rpm (0.17 h^{-1}) and 250 rpm (0.16 h^{-1}). The decline of biomass was more pronounced at 250 rpm, suggesting that, after 106 h of cultivation, shear stress affected cell viability under substrate starvation.

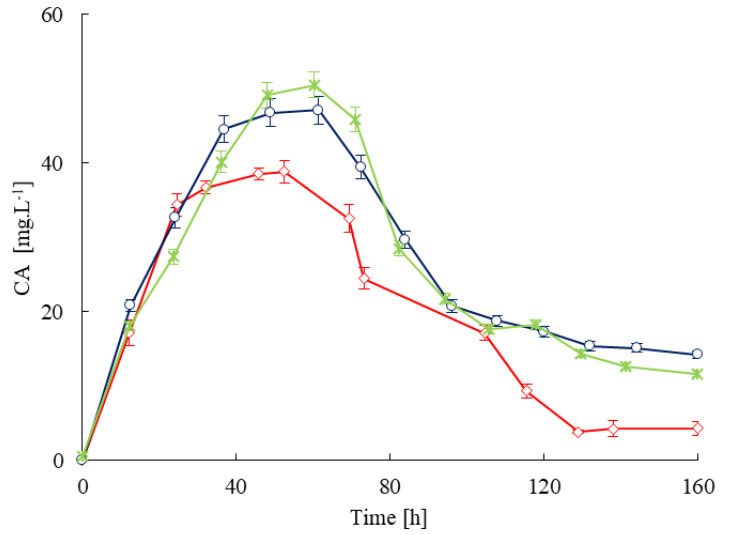

Figure 2.7. CA production in fed-batch cultures (50 to 100 mL shake-flasks) of *S. clavuligerus* at agitation rates of 200 (diamonds), 220 (circles) and 250 rpm (stars).

The highest CA concentration was obtained at 250 rpm (50.55 $mg.L^{-1}$) with a specific production of 0.37 $mg.(gDCW.h)^{-1}$. The highest CA productivity occurred in cultivations at 220 rpm (0.50 $mg.(gDCW.h)^{-1}$) yielding a maximum CA concentration of 47.13 $mg.L^{-1}$ at 61.5 h, coinciding with the end of the exponential phase. In all cases, the CA production seems to decrease with biomass decay and product degradation accelerates the fall of CA content. The highest degradation rate occurred at 250 rpm showing a rapid CA reduction after reaching the maximum concentration. The CA decline in cultivations at 220 and 250 rpm showed a similar trend, suggesting that CA secretion continues at

a rate that is lower than the degradation rate. For the case of cultivations at 200 rpm, the lower CA secretion led to low CA content at the end of the culture. CA production is potentially favored by the enhanced k_La attributable to the higher agitation rate.

Difference in both, biomass and CA accumulations between 220 and 250 rpm, were not statistically significant, as indeed occurred between 200 and 220 rpm. Higher agitation rates could enhance CA production, but only if an adequate aeration is provided. The low increase in biomass and CA accumulations at 250 rpm might be the result of insufficient air content in the shake flasks that did not enhance the dissolved oxygen in the liquid phase despite the higher agitation velocity. However, a positive effect of moderate increase of agitation rate in *S. clavuligerus* growth and CA secretion.

In order to explore the effect of a high shear stress on *S. clavuligerus* cultures in shake flasks, batch cultivations at 220 rpm in Roubos medium were performed, adding glass beads (5 %v/v) as a mechanism to increase the shear stress over the cells. The enhanced shear stress inhibited totally the growth of *S. clavuligerus*, showing a negative control respect to the cultivations at 220 rpm. The negative effect of increased shear stress was reported by Roubos et al. in bioreactors when volumetric power dissipation exceeded 1.7 $kW.m^{-3}$ [17].

2.4. Conclusions

The three media formulations tested supported biomass synthesis accordingly to the initial substrate concentration. The ISP medium provides complex carbon sources as amino-acids and hydrolyzed proteins that promote high specific growth rate but not necessarily enhance the CA production possibly linked to low activity of secondary metabolism. The defined media as the case of GSPA and Roubos lead to specific nutrients starvation (mainly phosphate and amino-acids) that act as stress factors potentially triggering the CA secretion. The chemically defined Roubos media allowed reaching the highest CA accumulations in batch and fed-batch cultivations. This synthetic medium supported more stable growth even under phosphate limitation.

Fed-batch operation of cultures with defined media favored the biomass and CA synthesis. Moreover, the feeding contributes to maintain more stable values of biomass and CA concentrations during the fed-batch phase since this operation mode assure the supply of carbon and nitrogen sources to the central metabolism required for growth and maintenance, without eliminating the nutritional restrictions that activate the secondary metabolism and promote the antibiotics secretion.

Moderate increase in agitation velocities showed positive effects on CA production possibly as a consequence of moderate shear stress and enhanced mass transfer capacity. Nevertheless, high shear stress generated by the application of glass beads inhibited completely the growth of the microorganism. The oxygen dissolution seems to be a limiting factor when increasing the agitation velocities in shake flasks cultivations. Thus, the impact of agitation and shear stress in *S. clavuligerus* cultivations and its relationship with mass transfer and CA production must be further studied in bioreactors under controlled conditions of aeration and agitation.

References

1. Ser, H.-L.; Law, J.W.-F.; Chaiyakunapruk, N.; Jacob, S.A.; Palanisamy, U.D.; Chan, K.-G.; Goh, B.-H.; Lee, L.-H. Fermentation Conditions that Affect Clavulanic Acid Production in Streptomyces clavuligerus: A Systematic Review. *Front. Microbiol.* **2016**, *7*, 522.
2. Bellão, C.; Antonio, T.; Araujo, M.L.G.C.; Badino, A.C. Production of clavulanic acid and cephamycin c by streptomyces clavuligerus under different fed-batch conditions. *Brazilian J. Chem. Eng.* **2013**, *30*, 257–266.
3. Sánchez, C.; Gomez, N.; Quintero, J.C.; Sanchez, C.; Gomez, N.; Quintero, J.C. Producción de Ácido Clavulánico por fermentación de Streptomyces clavuligerus : Evaluación de diferentes medios de cultivo y modelado matemático. *Dyna* **2012**, *79*, 158–165.
4. Bushell, M.E.; Kirk, S.; Zhao, H.; Avignone-rossa, C.A. Manipulation of the physiology of clavulanic acid biosynthesis with the aid of metabolic flux analysis. *Enzyme Microb. Technol.* **2006**, *39*, 149–157.

5. Saudagar, P.S.; Singhal, R.S. Optimization of nutritional requirements and feeding strategies for clavulanic acid production by Streptomyces clavuligerus. *Bioresour. Technol.* **2007**, *98*, 2010–7.
6. Neto, A.B.; Hirata, D.B.; Filho, L.C.M.C.; Bellão, C.; Júnior, A.C.B.; Hokka, C.O.; Cassiano Filho, L.C.M.; Bellão, C.; Badino, A.C.; Hokka, C.O. A study on clavulanic acid production by Streptomyces clavuligerus in batch, FED-batch and continuous processes. *Brazilian J. Chem. Eng.* **2005**, *22*, 557–563.
7. Carvalho, V.; Brandão, J.F.; Brandão, R.; Rangel-yagui, C.O.; Couto, J.A.; Converti, A.; Pessoa, A. Stability of clavulanic acid under variable pH , ionic strength and temperature conditions . A new kinetic approach. **2009**, *45*, 89–93.
8. Brethauer, S.; Held, M.; Panke, S. Clavulanic Acid Decomposition Is Catalyzed by the Compound Itself and by Its Decomposition Products. *J. Pharm. Sci.* **2008**, *97*, 3451–3455.
9. Marques, D.A.V.; Oliveira, R.P.S.; Perego, P.; Porto, A.L.F.; Pessoa, A.; Converti, A. Kinetic and thermodynamic investigation on clavulanic acid formation and degradation during glycerol fermentation by Streptomyces DAUFPE 3060. *Enzyme Microb. Technol.* **2009**, *45*, 169–173.
10. Costa, C.L.L.; Badino, A.C. Production of clavulanic acid by Streptomyces clavuligerus in batch cultures without and with glycerol pulses under different temperature conditions. *Biochem. Eng. J.* **2012**, *69*, 1–7.
11. Lin, Y.H.; Hwang, S.C.J.; Gong, J.T.; Wu, J.Y.; Chen, K.C. Using redox potential to detect microbial activities during clavulanic acid biosynthesis in Streptomyces clavuligerus. *Biotechnol. Lett.* **2005**, *27*, 1791–1795.
12. Rosa, J.C.; Baptista Neto, A.; Hokka, C.O.; Badino, A.C. Influence of dissolved oxygen and shear conditions on clavulanic acid production by Streptomyces clavuligerus. *Bioprocess Biosyst. Eng.* **2005**, 99–104.
13. Lebrihi, A.; Germain, P.; Lefebvre, G. Phosphate repression of cephamycin and clavulanic acid production by Streptomyces clavuligerus. *Appl. Microbiol. Biotechnol.* **1987**, *26*, 130–135.
14. Ramirez-malule, H.; Junne, S.; Cruz-bournazou, M.N.; Neubauer, P. Streptomyces clavuligerus shows a strong association between TCA cycle intermediate accumulation and clavulanic acid biosynthesis. *Appl. Microbiol. Biotechnol.* **2018**, *102*, 4009–402.
15. Manteca, Á.; Yagüe, P. Streptomyces Differentiation in Liquid Cultures as a Trigger of Secondary Metabolism. *Antibiotics* **2018**, *7*, 1–13.
16. Marques, D.A.V.; Santos-ebinuma, V.C.; Pessoa-Junior, A.; Porto, A.L.F.; Rivas Torres, B.; Concerti, A. Effect of Aeration and Agitation on Extractive Fermentation of Clavulanic Acid by Using Aqueous Two-phase System. *Biotechnol. Prog.* **2016**, *32*, 1444–1452.
17. Roubos, J. a; Krabben, P.; Luiten, R.G.M.; Verbruggen, H.B.; Joseph A Quantitative Approach to Characterizing Cell Lysis Caused by Mechanical Agitation of <I>Streptomyces clavuligerus</I>. *Biotechnol. Prog.* **2001**, *17*, 336–347.
18. Pinilla, L.; Toro, L.F.; Avignone-rossa, C.; Peñuela, M.; Ríos-estepa, R. Streptomyces clavuligerus strain selection for clavulanic acid biosynthesis : a study based on culture composition effects and statistical analysis • biosíntesis de ácido clavulánico : un estudio basado en los efectos de la composición del medio de cultiv. **2018**, *85*, 111–118.
19. Roubos, J.A.; Krabben, P.; De Laat, W.; Heijnen, J.J. Clavulanic Acid Degradation in Streptomyces clavuligerus Fed-Batch Cultivations. *Biotechnol. Prog.* **2002**, *18*, 451–457.
20. Ramirez-Malule, H.; Junne, S.; López, C.; Zapata, J.; Sáez, A.; Neubauer, P.; Rios-Estepa, R. An improved HPLC-DAD method for clavulanic acid quantification in fermentation broths of Streptomyces clavuligerus. *J. Pharm. Biomed. Anal.* **2016**, *120*, 241–247.

Chapter 3

Characterization of the Metabolic Response of *Streptomyces clavuligerus* to Shear Stress in Stirred Tank and Single-Use 2-D Rocking Motion Bioreactors for Clavulanic Acid Production

Abstract: *Streptomyces clavuligerus* (*S. clavuligerus*) is a Gram-positive filamentous bacterium notable for producing clavulanic acid (CA), an inhibitor of β-lactamase enzymes, which confers resistance to bacteria against several antibiotics. Here we present a comparative analysis of the morphological and metabolic response of *S. clavuligerus* linked to the CA production under low and high shear stress conditions in 2-D rocking-motion single-use bioreactor (CELL-tainer) and stirred tank bioreactor (STR), respectively. The CELL-tainer guarantees high turbulence and enhanced volumetric mass transfer at low shear stress, which allows, different from the use of bubble columns, the investigation of the impact of shear stress without oxygen limitation. The results indicate that high shear forces do not compromise the viability of *S. clavuligerus* cells; even higher specific growth rate, biomass and specific CA production rate were observed in the STR. Under low shear forces in the CELL-tainer the mycelial diameter increased considerably (average diameter 2.27 μm in CELL-tainer vs. 1.44 μm in STR). This suggests that CA production may be affected by a lower surface to volume ratio which would lead to lower diffusion and transport of nutrients, oxygen and product. The present study shows that there is a strong correlation between macromorphology and CA production, which should be an important aspect to consider in industrial production of CA.

3.1. Introduction

Shear conditions in CA production by *S. clavuligerus* have been previously explored in airlift [1] and stirred tank reactors [2]. However, the physiological response of *S. clavuligerus* to shear forces and its relationship with CA secretion is not completely understood. Many efforts have been carried out to increase the yield of CA since not only nutritional, but also environmental and degradation factors compromise the product yield in submerged cultivations of *S. clavuligerus* [3,4].

In microbial cultivations the effects of shear forces are particularly important since they affect the growth rate, broth rheology and transport of nutrients, leading to specific morphological responses. Therefore, knowledge about the effect of shear stress on microorganisms of industrial interest is essential for the appropriate design and operation of the bioprocesses. The physiological and metabolic responses to shear stress are strain-dependent. In the case of *Streptomyces* sp. numerous studies have focused on the effects of nutritional factors on the production of antibiotics, but few studies have correlated hydrodynamic stress with antibiotic production, although these two conditions are strongly coupled in bioreactors [5]. A rocking-motion bioreactor is a technology that allows the investigation of the effect of low shear forces on macromorphology apart from oxygen starvation, which is not the case for STRs or airlift reactors at higher cell concentration. Additionally, the gas mass transfer is considerably higher than in the bubble columns, which also create low shear stress, but also low mass gas transfer. Additionally, antibiotics production in *Streptomyces* cultures also depends on an appropriate setup of the biophysical parameters e.g., pH, viscosity, agitation and dissolved oxygen (DO), which affect morphological differentiation and metabolite secretion [6].

Some studies explored the impact of mechanical stress on *Streptomyces* morphology in suspension cultures, showing that high shear stress typically leads to the formation of small mycelial particles while clumping or pellet formation occurs at low shear stress [7,8]. Such pellets favor the accumulation of actinorhodin in *S. coelicolor*, nystatin in *S. noursei*, retamycin in *S. olindensis*, and

nikkomycin in *S. tendae* as Manteca et al. [9] previously reviewed. In the case of *S. clavuligerus*, little is known about the relationship between shear stress, growth, morphology and metabolites secretion. The dispersed mycelial morphology has been observed more often in *S. clavuligerus* cultivations performed in bioreactors and, in contrast to other phylogenetically related species, pellet formation seems to be related with a decrease in the CA production rate [10,11].

Single-use technology has emerged as an interesting alternative for biotechnological production of drugs due to its flexibility, scalability, availability of different stirring configurations, easy handling, reduced incidence of cross-contamination and savings in operational costs and time [12,13]. Several single-use bioreactor types are currently commercially available [12,14]; the gas mass transfer of some of them is based on stirring, while it relies on shaking in others [15,16]. In particular, 2-D rocking-motion bioreactors, which create a wave or cause eddy formation at the vessel wall for the suction of air into the liquid phase, exhibited comparably higher gas mass transfer rates while mechanical shear forces are considerably lower than in stirred tank bioreactors. This leads to an altered micromorphology and subsequently different growth and product synthesis rates as observed in cultivations performed in the two-dimensional rocking-motion bioreactor concept CELL-tainer® [13,17,18]. In this regard, the filamentous fungus *Aspergillus niger* (*A. niger*) cultivated in this low shear-force environment, showed a similar macromorphology as in shake flask cultures, while large pellets were formed. When talcum was added into the cultivation medium, a rather dispersed growth was achieved similar to the macromorphology obtained in stirred tank reactors [19]. While a fed-batch mode can be conducted, and the DO and pH-value can be controlled in a bioreactor more easily than in a shake flask, the effects of an altered shear stress on the cells macromorphology can be investigated in the 2-D rocking-motion bioreactor independently from changes on gas mass transfer. If cultivations in a stirred tank reactor are compared with cultivations in 2-D rocking-motion bioreactors, the relationship between shear forces, macromorphology and growth as well as product synthesis can be determined.

So far, to our knowledge, there are no reports in the literature addressing the effects of low shear forces in single-use systems on the physiology and morphology of *Streptomyces* species. The present study aims at performing a comparative analysis of the metabolic response *of S. clavuligerus* and the production of CA, to the shear stress effects in a 2-D rocking-motion single-use bioreactor (low-shear stress condition) and a stirred tank reactor (high-shear stress condition), since the hydrodynamic condition is an important parameter to consider in industrial production of CA. For acquiring an equitable comparison, fed-batch cultivations of *S. clavuligerus* were carried out under identical operating conditions in both bioreactors.

3.2. Materials and Methods

3.2.1 Strain and cultivation procedures

S. clavuligerus DSM 41826, stored at -80 °C in a glycerol solution (16.7% v/v), was inoculated for activation in seed medium as described by Roubos et al. [20]. Two cultivation cycles (seed and preculture) were carried out prior to reactor inoculation. Cryotube cell suspensions (1.2 mL) were inoculated into 50 mL of seed medium in a 250 mL Ultra-Yield™ shake flask (Thomson Instrument Company, Oceanside, CA). Cells were grown in a rotary shaker incubator for 26 h at 200 rpm and 28 °C. For the preculture, 2500 mL Ultra Yield shake flasks were filled with 450 mL of chemically defined medium, inoculated with 50 mL of cultivated seed broth. Cells were grown for 20 h using identical conditions [10].

Fed-batch cultivations were carried out in duplicate in a 15 L stirred tank bioreactor (STR), (Techfors S, Infors AG, Bottmingen, Switzerland) and in a 20 L single-use 2-D rocking-motion bioreactor CELL-tainer® (CT), (CELL-tainer Biotech BV, Winterswijk, The Netherlands) both operated at 5 L initial filling volume. Bioreactors were inoculated at 10% v/v from preculture. A chemically defined medium, formulated as follows, was used (per L): glycerol (9.3 g), K_2HPO_4 (0.8 g), $(NH_4)_2SO_4$ (1.26 g), monosodium glutamate (9.8 g), $FeSO_4 \cdot 7H_2O$ (0.18 g), $MgSO_4 \cdot 7H_2O$ (0.72 g) and

trace elements solution (1.44 mL). The trace elements solution contained (per L): H_2SO_4 (20.4 g), monosodium citrate·$1H_2O$ (50 g), $ZnSO_4 \cdot 7H_2O$ (16.75 g), $CuSO_4 \cdot 5H_2O$ (2.5 g), $MnCl_2 \cdot 4H_2O$ (1.5 g), H_3BO_3 (2 g), and $Na_2MoO_4 \cdot 2H_2O$ (2 g) (all from Carl Roth GmbH, Karlsruhe, Germany). Antifoam 204 (Sigma Inc., St. Louis, MO, USA) was used at concentration of 1:1000 v/v, pH was controlled at 6.8 by using 4 M solutions of either NaOH or HCl. Aeration was provided at 0.6 vvm and temperature was controlled at 28 °C. Reactors were equipped with pH (Polylite Plus) and dissolved oxygen (DO – VisiFerm) probes (Hamilton Inc., Bonaduz, Switzerland). Outgas analysis was performed by O_2 and CO_2 gas sensors coupled to an exhaust gas analyzer (BlueInOne Ferm, BlueSens GmbH, Herten, Germany).

Batch operation was carried out during the first 37 h of cultivation, followed by fed-batch operation during the next 77 h. The feed medium had the following composition (per L): glycerol (120.0 g), K_2HPO_4 (2.0 g), $(NH_4)_2SO_4$ (8.0 g); the feeding rate was set at 35 mL h^{-1}. The batch and fed-batch media were designed for achieving phosphate limitation around 40 h considering the phosphate/carbon ratio of biomass composition [10]. Once the fed-batch stage ended, cultivation continued without any feeding for 43 h (total cultivation time of 157 h). Agitation was controlled manually in the range of 300-500 rpm in the STR and 12-25 rpm in the CT; DO was maintained between 50 and 70 %, avoiding the sudden oscillations of agitation originated by the DO automatic control. Culture samples (2 mL) were taken at 12 h intervals and centrifuged at 15,000 rpm and 4 °C for 10 min; wet biomass was washed with 0.9 % NaCl and centrifuged. Test tubes were dried overnight at 75 °C for dry cell weight (DCW) determination.

The rheological parameters of the broth were determined according to Campesi et al. [21] and Cerri & Badino [1]. The k_La was calculated using the stationary method from exhaust gas data analysis [18,19]. The estimation of shear stress in both reactors was performed according to the methodology established for STR [22–25] and correlation of data for single-use bioreactors [26–28].

3.2.2 Mycelium measurement and products quantification

The time courses of changes in mycelial diameter was followed by random measurement of individual mycelia for each cultivation sample and replicates. *S. clavuligerus* mycelia directly taken from cultivation samples were stained with crystal violet, observed and photographed using a Nikon Eclipse Ti2 inverted microscope (Nikon Instruments Inc., Amsterdam, The Netherlands) at 400x magnification in order to capture a wide field of the sample. Post-processing of images and measurement of mycelial diameter were performed in ImageJ by applying digital zoom up to 250% and using the built-in measurement tool (NIH, Maryland, USA) [29]. Four different pictures were observed for each sample and at least 100 measurements of individual mycelia were performed per picture. Then, the mean values and standard deviations (SD) of mycelial diameter for each time point were calculated.

Quantifications of CA concentration in supernatant samples were carried out by HPLC equipped with a diode array detector (DAD, 1200 Series, Agilent Technologies GmbH, Waldbronn, Germany), using a Zorbax Eclipse XDB-C-18 chromatographic column (Agilent Technologies) and a C-18 guard column (Phenomenex® GmbH, Aschaffenburg, Germany) operated with a flow rate of 1 mL/min at 30 °C. The mobile phase, consisted of H_2PO_4 (50 mM, pH 3.2) and methanol (HPLC grade). HPLC analyses were performed by using the gradient method described by Ramirez-Malule [30]. Imidazole was used for derivatization of CA. The clavulanate-imidazole chromophore was detected at 311 nm.

Glycerol, pyruvate and succinate were quantified with an Agilent 1200 Series HPLC system equipped with a refractive index detector (RID) and operated at 15 °C using a HyperREZ™ XP carbohydrate H+ column (Thermo Scientific, Waltham, MA, USA) at a constant flow rate of 0.5 mL/min using 5 mM sulfuric acid solution as mobile phase [31]. Quantification of glutamate was performed with an Agilent 1260 Series Infinity HPLC system (Agilent Technologies), equipped with a fluorescence detector (FLD) with an excitation wavelength of 340 nm and emission wavelength of 450 nm. o-Phthaldialdehyde was used for precolumn derivatization of samples. A C18 Gemini®

column with a SecurityGuard™ precolumn (Phenomenex) were used, operated at a flow rate of 1 mL/min and 40 °C. The mobile phase consisted of NaH_2PO_4 (40 mM , pH 7.8) as polar eluent and a solution of methanol (45% vol.), acetonitrile (45% vol.) and water (10% vol.) as nonpolar eluent [32]. The semi-quantitative determination of phosphate and ammonium ions was performed by using phosphate and ammonia tests (MQuant™; Merck KgaA, Darmstadt, Germany). Statistical analysis of results was performed in terms of standard deviations and averages.

3.2.3 Oxygen mass transfer coefficient (k_La) and broth reology

According to Enfors [33], the kLa can be estimated by the gas balance method from online measurements of exhaust gas and DO (Eq. 1).

$$k_L a\, C^* = \left(\frac{Q_i v_{O2,i} - Q_o v_{O2,o}}{V}\right)\left(\frac{DO^*}{DO^* - DO}\right) \quad (1)$$

where Q_i and Q_o are the gas flowrates at inlet and outlet, respectively. $v_{O2,i}$ and $v_{O2,o}$ are the volume fractions of oxygen in the gas, respectively. DO* represents the dissolved oxygen of the liquid in equilibrium with the gas bubbles in the reactor according to Eq. 2, total pressure and volumetric fractions of oxygen at the outlet and at calibration conditions (100% saturation, usually 20.9 % v/v).

$$DO^* = \frac{v_{O2,o}}{v_{cal}}\frac{P_T}{P_{cal}} \quad (2)$$

where C^* is the oxygen concentration in the gas-liquid interface calculated as follows:

$$C^* = 55.5\,\frac{Y_{O2,o} P_T}{H} \quad (3)$$

where H is the Henry constant and $Y_{O2,o}$ is the mole fraction of oxygen at outlet. Similarly, the respiratory quotient (RQ) is defined as the ratio between carbon dioxide production rate (q_{CO2}) and oxygen uptake rate (q_{O2}):

$$RQ = \frac{q_{CO2}}{q_{O2}} \quad (4)$$

The rheology of the fermentation broth may have a large impact on the oxygen transfer as the stirrer rotates in a reactor it imposes a shear stress and a shear rate on the liquid. *S. clavuligerus* fermentation broth is characterized by high viscosity, exhibiting rheological properties of a pseudoplastic fluid according to Eq. 4, where n is the mean behavior index of the fermentation broth and K the consistency index depending on biomass concentration and shear conditions. The apparent viscosity of the broth is defined by Eq. 5.

$$\tau = K\gamma^n \quad (5)$$

$$\mu_{app} = K\gamma^{(n-1)} \quad (6)$$

3.3. Results

3.3.1. Biomass and morphology

S. clavuligerus was cultivated at bench scale in stirred tank reactor (STR) and rocking-motion single-use bioreactor CELL-tainer® (CT) to investigate the impact of shear forces on macromorphology and CA production. Figure 3.1 shows the time course of biomass concentration during 6.5 days of cultivation in both reactors. Difference in growth trends observed in both cultivations was not statistically significant. Slightly higher growth rates were attained in the STR, showing also a higher maximum biomass concentration (12.3 gDCW.L^{-1}) compared to CT cultivations where the maximum biomass was 11.5 gDCW.L^{-1}. The maximum specific growth rates for the STR and CT during fed-batch operation were 0.050 h^{-1} and 0.042 h^{-1}, respectively. The exponential growth phase started at 14 h in both reactors and the stationary phase coincided with phosphate and glutamate starvation between 60 and 70 h. Only a small amount of phosphate (~0.47 mmol.h^{-1}) was fed to the reactor during the fed-batch stage for maintenance without repressing CA biosynthesis. For both cultivations, a slight decline of biomass occurred from 133 h onwards and the final biomass concentration at 157 h was rather the same (10.2 gDCW.L^{-1}) in both bioreactors.

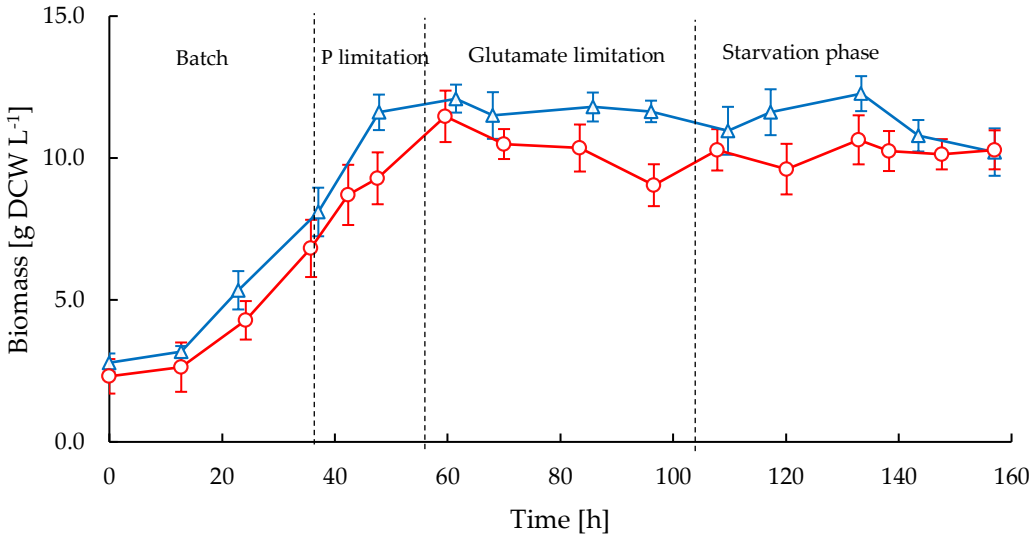

Figure 3.1. Time course of biomass in STR (triangles) and CT (circles) in fed-batch cultivations of S. clavuligerus.

In all the experiments performed in the STR and CT reactors a mycelial morphology was observed as the dominant or only form. Highly fragmented and less branched mycelial structures were observed in the STR after 86 h of cultivation (Figure 3.2b) compared with the mycelial in the early stages of cultivation (Figure 3.2a). In the CT samples the preservation of macromorphology along the cultivation is notable (Figures 3.2c and 3.2d) showing less fragmentated, more branched and slightly aggregated mycelia. In contrast to what was observed in the STR, a significant increment of filament diameter along the cultivation time was measured in CT samples (Figure 3.2e). A clear decrease in the filament diameter of 22.5% was measured in the STR varying from 1.86 ± 0.30 μm to 1.44 ± 0.21 μm during the course of the cultivation. In contrast, the filaments diameter increased by 30.6% in CT cultivations in the same time, varying from 1.74 ± 0.25 μm to 2.27 ± 0.31 μm.

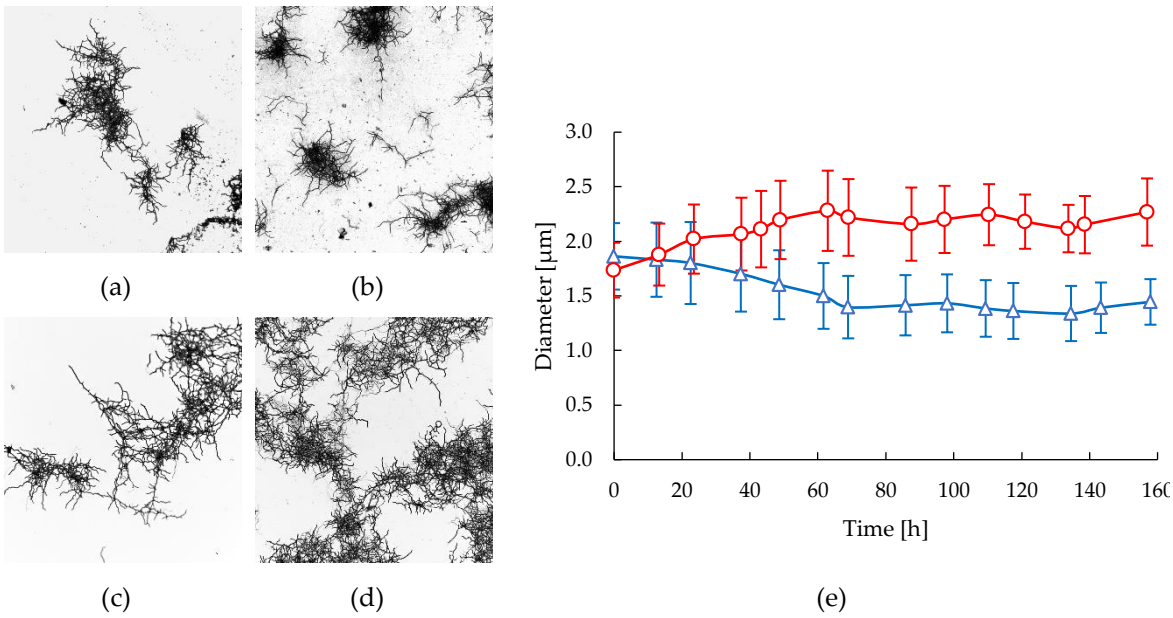

Figure 3.2. Morphological response of *S. clavuligerus* in STR (triangles) and CT (circles) bioreactors: (a) Mycelia in STR at 22 h; (b) Mycelia in STR at 86 h; (c) Mycelia in CT at 23 h. (d) Mycelia in CT at 87 h; (e) Time course of mycelial diameter in STR (blue) and CT (red).

3.3.2. Shear stress and oxygen transfer

During the experiments, the DO was used as an indicator of oxygen availability in the medium and it was also selected as the control variable to assure the comparability of both cultivations even under different hydrodynamic conditions, as it can be observed in Fig. 3a. Since the CT provided a high capacity to increase the DO in the media, only small changes of rocking velocity were applied when needed to maintain the DO values closer to those of the STR. A minimum set-point of 20 % for the DO was defined for all cultivations, but it was preferred to maintain the DO between 50 and 70 % by controlling the agitation speed between 300 and 500 rpm in the STR and 15 to 25 rpm in the CT, respectively. This was done in order to maintain moderate shear forces on the strain, avoiding extreme agitation values that could affect the cell or favor CA degradation.

Table 3.1 Biomass as dry cell weight (DCW), culture volume (V), agitation velocity (N), volumetric mass transfer coefficient (kLa), maximum shear stress (τ_{max}) and apparent viscosity (μ_{app}) of fermentation broths in STR and CT cultivations.

Bioreactor	t(h)	DCW (g L^{-1})	V (L)	N (rpm)	k_La (h^{-1})	τ_{max} (Pa)	μ_{app} (Pa s)
CT	0	0.5	5.0	12	73.25 ± 7.40	0.066 ± 0.010	0.0011 ± 0.0005
	25	2.1	5.0	15	43.90 ± 0.92	0.102 ± 0.068	0.0012 ± 0.0001
	36	3.4	5.0	17	61.71 ± 8.13	0.222 ± 0.016	0.0021± 0.0013
	46	4.7	5.1	20	80.52 ± 8.86	0.147 ± 0.041	0.0041 ± 0.0015
	53	9.3	5.8	25	208.10 ± 28.79	0.572 ± 0.033	0.0055 ± 0.0005
	69	10.1	6.1	22	121.88 ± 3.26	0.747 ± 0.079	0.0083 ± 0.0007
	108	10.3	7.8	22	83.73 ± 7.15	0.634 ± 0.029	0.0096 ± 0.0007
STR	0	1.9	5.0	300	39.11 ± 2.80	1.472 ± 0.061	0.0013 ± 0.0001
	23	4.3	5.0	320	35.49 ± 1.99	3.091 ± 0.228	0.0034 ± 0.0003
	37	6.5	5.0	410	50.57 ± 2.40	5.047 ± 0.538	0.0051 ± 0.0006
	48	7.7	5.2	450	58.61 ± 3.46	5.883 ± 0.645	0.0058 ± 0.0016
	86	9.3	6.4	500	61.92 ± 3.78	6.460 ± 0.381	0.0088 ± 0.0017
	109	12.1	7.8	500	54.85 ± 0.26	7.563 ± 0.255	0.0145 ± 0.0010

Table 3.1 shows the estimated volumetric oxygen transfer coefficient (k_La) values, the apparent viscosity (μ_{app}) of the broth and the maximum shear stress (τ_{max}) at different mixing velocities (N). The mass transfer is limited by the increasing viscosity of the broth, therefore the requirement of increasing the agitation velocity to maintain DO and k_La values. Agitation in both reactor underwent a turbulent flow according to the calculated values of Reynolds number at the operating conditions. The maximum Reynolds numbers at 500 rpm in STR and 22 rpm in CT were 13582 and 15896, respectively. The k_La values were considerably higher in the rocking-motion reactor than those attained from the STR, during all experiments. Therefore, only small changes in agitation speed in the CT showed a significant increase in the k_La and DO values. Interestingly, it was also observed that despite the differences in the volumetric oxygen transfer attained in both reactors, the growth rate of *S. clavuligerus* was not significantly affected by an enhanced oxygen transport. The RQ (see Fig. 3b) was close to 1 during the early stages of cultivation. After 40 h for the STR and 50 h for the CT cultivations the RQ decreased presumably linked to glutamate and phosphate depletion during glycerol feeding. Despite the observation that the reduction of RQ occurred in both reactors; in the CT the RQ remained 15 % higher after glutamate exhaustion in comparison with the STR. The lower RQ in the STR cultivations during the fed-batch phase coincided also with comparatively higher glycerol uptake as showed in Fig. 4.

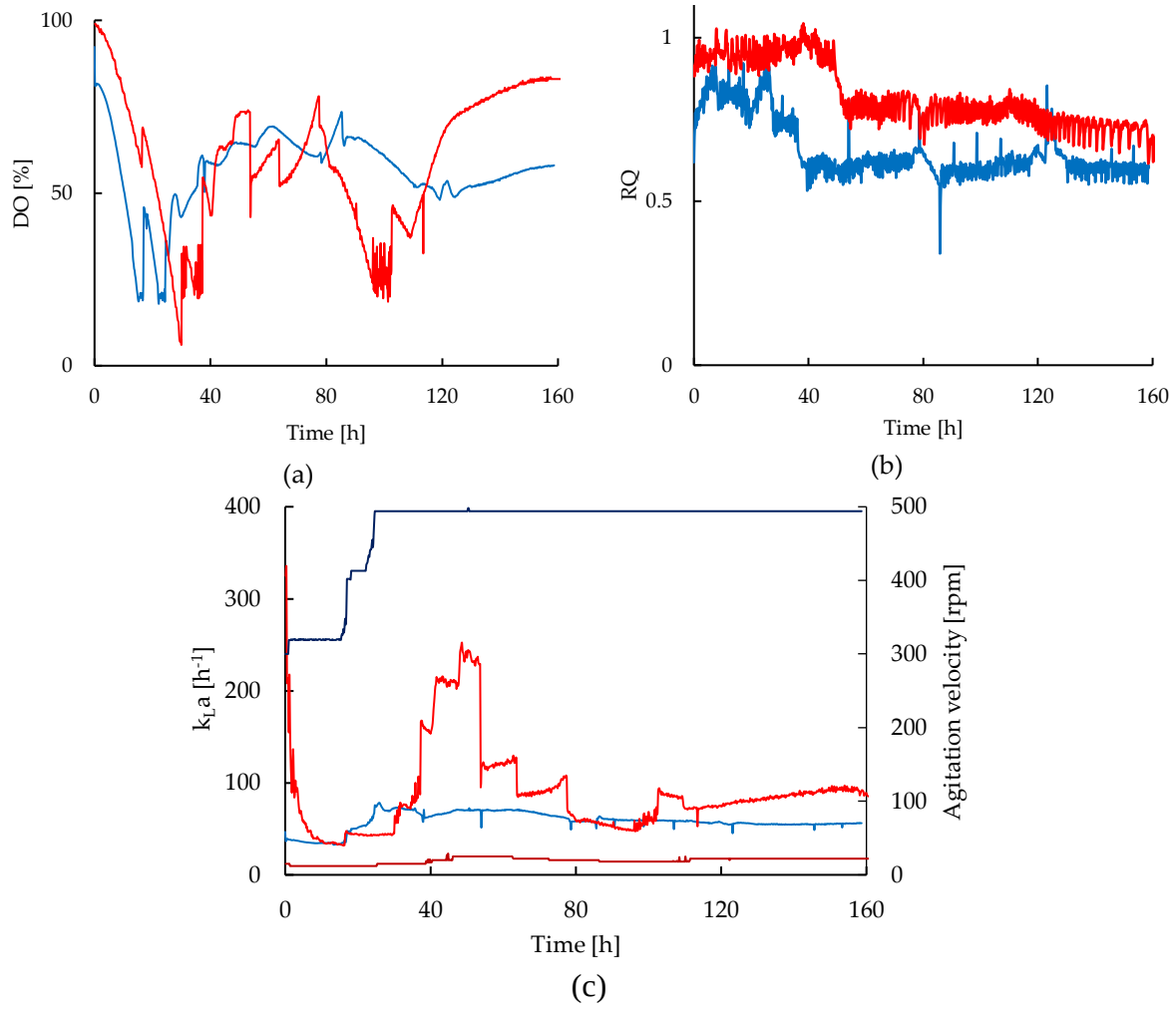

Figure 3.3. Dynamic profiles of oxygen in liquid and exhaust gas in fed-batch cultivations of *S. clavuligerus*: (a) DO in STR (blue) and CT (red) cultivations; (b) RQ in STR (blue) and CT (red) cultivations; (c) kLa in STR (blue) and CT (red), agitation velocity in STR (dark blue) and CT (dark red).

The mean behavior index (n) of the fermentation broth was 0.318 and the consistency index (K) ranged between 0.1 and 1.5 Pa s^n. As presented in Table 3.1, the initial apparent viscosity of the broth was rather close to the value of water at the operating temperature (0.001 Pa s) and then increased with cellular growth. The shear stress values (τ_{max}) in the STR reactor were in the range from 1.4 to 7.6 Pa. In the case of CT the shear stress ranged between 0.06 and 0.63 Pa.

3.3.3 Substrates and products

All cultivations were operated in fed-batch mode suppling glycerol as the main carbon source and following a constant feeding pattern of 35 mL h^{-1}. Fig. 4 shows the time courses of glycerol and glutamate concentrations in the culture media in both bioreactors. The glycerol consumption was mainly correlated with biomass accumulation, showing a rapid depletion after 14 h, i.e. after starting the exponential phase in the batch stage. Since glycerol is fed in excess, during the fed-batch stage a constant accumulation of glycerol was observed from 37 h onwards up to 110 h when the feeding was stopped. After 110 h a sustained decline in glycerol occurred indicating that even during the stationary phase the metabolic activity was rather high, which agrees with the observed continuous CA secretion until the end of the cultivations.

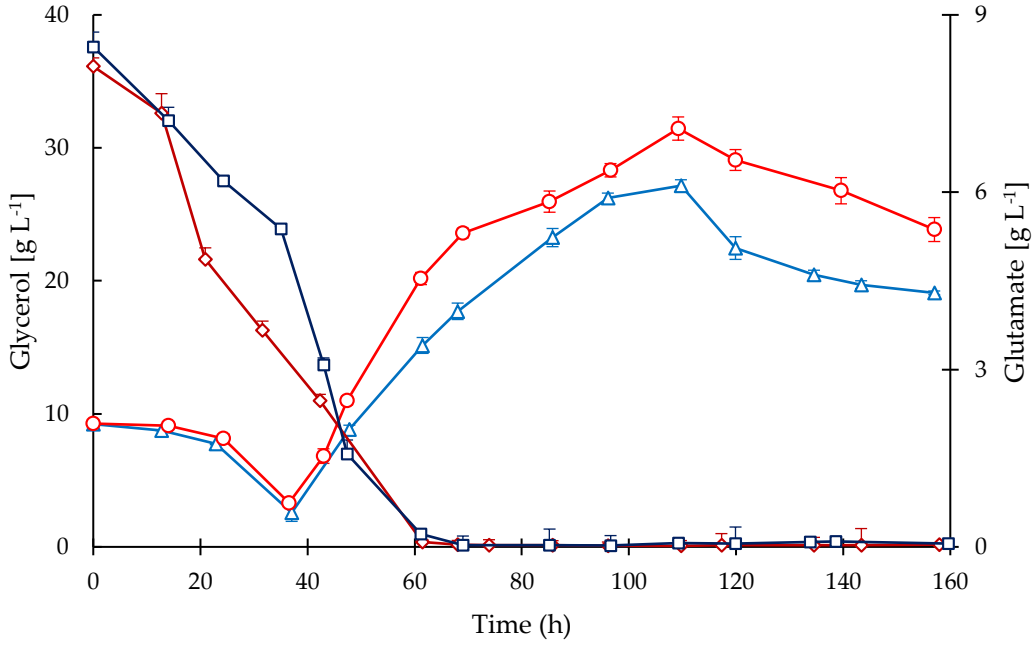

Figure 3.4. Time courses of substrates in the culture media for fed-batch cultivations of *S. clavuligerus*. Glycerol in STR (triangles) and CT (circles), glutamate in STR (squares) and CT (diamonds).

A high concentration of glutamate was provided initially in the media but not in the feedings. Therefore, a rapid decline of glutamate concentration (Figure 3.4) was observed during the exponential phase in both bioreactors and it remained up to 70 h of cultivation; during this phase the glutamate was depleted. Similar to glycerol, glutamate uptake was higher during the first 45 h of cultivation in STR, which is congruent with a higher growth rate and biomass concentration. Note that growth rate (Figure 3.1) declined in both cultivations when glutamate became exhausted (Figure 3.4); in contrast, the accumulation of CA was not affected by glutamate starvation as observed in Figure 3.5. Although the nutritional conditions in both reactors were similar regarding glycerol, glutamate, ammonium and phosphate, the accumulation of CA was considerably lower in CT cultivations. The secretion of CA was triggered after 24 h of cultivation, coinciding with a drop in phosphate concentration of at least 80%. Then, the CA concentration increased throughout the cultivation time and the maximum accumulation was obtained at the end of the process (157 h). The

maximum mean concentrations of CA attained were 187.2 mg L^{-1} for the CT and 422.7 mg L^{-1} for the STR cultivations. The maximum CA specific production rates were 0.697 and 0.358 mg (g DCW)$^{-1}$ h^{-1} in the STR and CT, respectively.

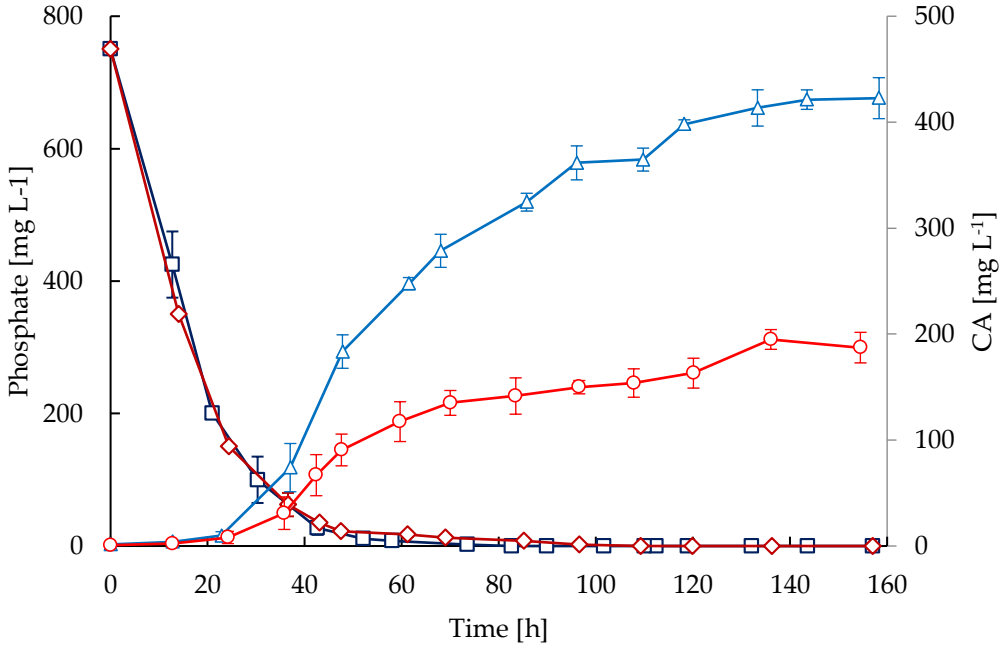

Figure 3.5. Time courses of CA and phosphate in fed-batch cultivations of *S. clavuligerus*. CA in STR (triangles) and CT (circles), phosphate in STR (squares) and CT (diamonds).

Pyruvate and succinate were observed to accumulate differently in the STR and CT cultivations (Figure 3.6). The CT cultivations showed higher pyruvate levels compared to the STR. In both cultures the concomitant accumulation of succinate and CA were observed (Figures 3.5 and 3.6), although succinate levels were considerably higher in the STR compared to the CT cultivations.

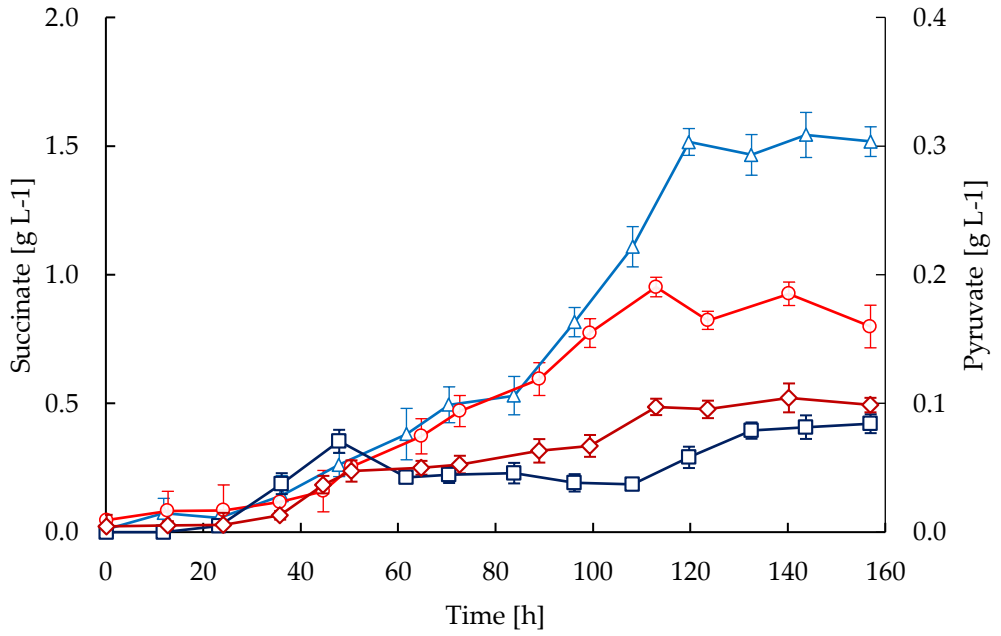

Figure 3.6.. Time courses of succinate and pyruvate accumulations in fed-batch cultivations of *S. clavuligerus*. Succinate in STR (triangles) and CT (circles), pyruvate in STR (squares) and CT (diamonds).

3.4. Discussion

Previous studies have extensively explored different cultivation conditions for promoting *S. clavuligerus* optimal growth and enhanced CA production. However, given the relationship between morphology and secondary metabolite secretion in the *Streptomyces* genus a better understanding of the factors influencing the morphology in submerged cultures is required for the identification of optimal bioprocessing conditions. This has a special importance also for a later scale up of the process to an industrial environment, as the fluid dynamic conditions change with scale.

It is known that glycerol is the most suitable carbon source for *S. clavuligerus*, supplying glyceraldehyde-3-phosphate as an early C-3 precursor and substrate for energy metabolism and growth [34]. Thus, a constant feeding of carbon source was implemented to provide glycerol in excess for growth and maintenance, so as to promote CA biosynthesis. Additionally, a high initial concentration of glutamate was used in the production medium as a secondary carbon and nitrogen source, although it played an important role as early C-5 precursor favoring the metabolic fluxes through amino acids metabolism and the urea cycle during the exponential growth phase. Note that growth rate (Figure 3.1) declined in both cultivations when glutamate became exhausted (Figure 3.4) despite the high availability of glycerol. This is the time that we interpret as the beginning of the stationary phase. This observation clearly indicates the importance of glutamate as a precursor of biomass when using a defined media.

S. clavuligerus is a strictly aerobic organism; thus, the oxygen transfer to the liquid medium in the reactor is a critical parameter to ensure proper growth and productivity [2]. In *streptomycetes*, the production of antibiotics is strongly affected by the balance of nutrients and oxygen availability in the medium, which can affect the growth rate, the induction of secondary metabolism and maximum concentrations of secondary metabolites [5]. In this regard, determination of the k_La in bioreactors is an important parameter when assessing the oxygen mass transfer characteristics in connection with mixing and reactor geometry. In STRs, the increase of k_La implies vigorous stirring to favor mass transfer from gas to liquid phase by increasing the turbulence of the system, thus increasing shear stress on the medium and cells [35,36]. In contrast, wave and rocking-motion reactors are characterized by up to 100-fold lower shear forces compared to STRs [15,16,27] and especially 2-D rocking-motion bioreactors provide higher k_La values compared to simple wave systems that are comparable to those obtained in STRs at high stirring speed [17–19].

As shown in Table 3.1, lower shear stress was experienced by the liquid phase and the cells of *S. clavuligerus* cultivated in the CT in comparison with the STR. The predominant filamentous morphology in liquid cultures of *Streptomyces* leads to an increase in broth viscosity and appearance of non-Newtonian rheology concomitant with cell growth [5]. The average shear stresses estimated for the fermentation broths were 0.44 and 4.92 Pa for the CT and STR, respectively. The oxygen transfer from the gas to the liquid phase is clearly favored by the 2-D wave pattern generated during rocking motion. Nevertheless, the effect of oxygen mass transfer on the secondary metabolism of *S. clavuligerus* is not completely clear. The activities of deacetoxycephalosporin C synthase and isopenicillin-N synthetase increases at oxygen saturation and hence, the production of cephamycin C and penicillin N [37], while oxygen limitation (~10% DO) leads to inhibition of CA production [2]. Considering the requirement of molecular oxygen during CA biosynthesis, an operational window regarding DO values between 20% and 80% can be assumed as suitable for CA production, since the repression of CA at low DO values and the activation of the penicillin, cephalosporin and cephamycin biosynthesis occur when operating at oxygen saturation [2,37]. Increase of reaction fluxes through penicillin and cephalosporins pathways would potentially reduce the carbon flux toward CA biosynthesis due to an increasing demand of amino acid precursors.

The shear stress values (τ_{max}) in the STR reactor presented in Table 3.1 were consistent with results from previous studies on cultivation of filamentous organisms in stirred tank bioreactors [1,38]. Shear stress higher than 6 Pa, as observed in STR reactors, triggers stress responses in sensitive strains like CHO cells. Nevertheless, the limits for cell damage and lysis are in the order of 100 Pa [39]. Previous studies have shown that *S. clavuligerus* can be cultivated in STR reactors at mixing

velocities up to 800 rpm without compromising cell viability [40,41]. In contrast with STR, it has been widely reported that shear forces in rocking and wave reactors are considerably lower than those arising in reactors with axial or orbital agitation [27,28], which is also in agreement with our results considering the calculated maximum shear stress ranging between 0.06 and 0.63 Pa. For the sake of comparison, the typical shear stress for water as a fluid model in wave reactors is in the range of 0.01 to 0.1 Pa at agitation rates from 15 to 30 rpm [27,28]. The shear stress in the fermentation broth is not just a function of the shear rate of mixing; but also an increasing viscosity changes drastically the shear stress conditions to which the cells are exposed [21,25]. Therefore, the shear forces in *S. clavuligerus* fermentation broths were expected to exceed the values reported for Newtonian fluids at similar agitation conditions in STR and single-use reactors [16,27,28].

It is well known for *S. clavuligerus* that cultivation under intensive agitation and optimal nutritional conditions lead to the prevalence of mycelial morphology [42]. Exponential growth of *Streptomyces* in mycelial form takes place by a combination of tip growth and branching of multicellular hyphal sections connected in compartments [43,44]. Under mechanical stress the adhesive forces between hyphae may be weakened making the filaments prone to fragmentation [8]. Thus, intense agitation causes fragmentation resulting in formation of short hyphae capable of growing and reproducing under nutrients availability, otherwise those fragments would eventually die [5,7].

The higher biomass production and apparent viscosity observed in STR (Figure 3.1) compared with the CT in our opinion are a consequence of the extensive hyphal fragmentation caused by the mechanical shear forces, which led to a great number of viable hyphal fragments. Additionally, the enhanced oxygen transfer entailed a positive effect on growth, possibly compensating for the potential shear damage caused by agitation nearby the impeller or reactor wall. In contrast, under mild agitation the individual hyphae tend to become longer and branched and slightly aggregated, resulting in a decrease of mass and heat transfer [5,7].

The macromorphology and product biosynthesis in submerged cultivations of filamentous organisms is a multifactorial process affected by the bioprocessing conditions [19]. Several *Streptomyces* species have a marked tendency to aggregate due to bio-adhesive properties of hyphae; such is the case for *S. avermitilis* [45], *S. lividans* [8], *S. toxytricini* [46] and *S. coelicolor* [9] among others. Furthermore, the morphological changes associated with the increase in shear stress are related to different physiological activities [7]. Specifically, in streptomycetes, the production of many secondary metabolites is affected by agitation frequency and power dissipation suggesting a possible relationship between agitation, macromorphology and product secretion [5]. An increase of the agitation rate in the range from 200 to 600 rpm was observed to favor the production of neomycin in STR cultivations of *S. fradiae,* but a negative effect was reported for agitation values above 600 rpm [47]. Similarly, natamycin production by *S. natalensis* increased up to 7-fold when the agitation was increased from 50 to 250 rpm in a STR [48,49]. In shake flask cultures of *S. pristinaespiralis*, the increase in power dissipation between 2 and 5 kW m^{-3} increased pristinamycin accumulation [50]. For all cases, a threshold in the yield was observed when the agitation rate was increased, indicating that cell damage and loss of viability might occur when exceeding the tolerable agitation limits [5]. In *Saccharopolyspora erythraea*, considered as a streptomyces specie formerly, it was observed previously that both the size and the branching rate affect the susceptibility of the hyphal fragments to breakage and antibiotic production. Since highly branched hyphae produced were less susceptible to breakage and, at higher stirrer speeds, the rate of breakage of larger hyphal fragments was less than that of the smaller fragments [51]. Thus, the adverse condition might select a subpopulation of mycelium better able to survive. Similarly, in our case a more resilient population able to adapt to high shearing conditions and to secrete more antibiotic could be present in the reactor.

We observed thinner and dispersed mycelia at high shear stress in the STR and this was coincident with a high CA productivity. During the lag and early exponential phases no statistical differences were observed in the morphology of *S. clavuligerus* cultivated in either the STR or CT reactors despite the significant difference in shear forces. The increase of agitation speed from 300 to

500 rpm in the STR led to an increase of shear stress, thus causing a sustained decrease of mycelial diameter during the exponential growth (Figure 3.2e) and a higher growth rate, in comparison with the CT cultivations. Conversely, the mycelial morphology in the CT cultivations suggests that a reproduction mechanism of elongation, branching and thickening of existent mycelia is favored under low shear forces, also promoting slight aggregation due to adhesive properties of the hyphae [8]. In contrast, continuous fragmentation in the STR avoids reaching significant elongation, thickening and branching of mycelia. Interestingly, morphological differentiation induced by the hydrodynamic regime was observed to stop when glutamate was exhausted, coinciding with the start of the stationary phase. Therefore, the filament diameter acquired up to this point (60 h), remained rather constant during the rest of the cultivations as shown in Figure 3.2e.

It is known that antibiotic production in streptomycetes is initiated by stress conditions e.g., essential nutrients limitation [7,43]. Although the nutritional conditions in both reactors were similar regarding glycerol, glutamate, ammonium and phosphate, the accumulation of CA was considerably lower in CT cultivations. It has been widely reported that phosphate is a strong repressor of CA biosynthesis [1,2,34,52]; indeed the secretion of CA was triggered after 24 h of cultivation, coinciding with a drop in phosphate concentration of at least 80%. According to our observations, CA production was enhanced by the shear conditions present in the STR. Although nutritional conditions were the same in the cultivations performed in both reactors and phosphate limitation triggered the CA secretion at approximately the same time, the CA production rate in STR was 2.5-fold the observed in the CT cultivations. Presumably two factors are linked to the observed low CA biosynthesis: i) under the environmental conditions of the CT reactor, cellular activity might be catabolizing nutrients for growth regulation through mycelial thickening and branching, leaving, as a consequence, a smaller net amount for cell production, as indicated by the lower specific growth rate observed; ii) the difference in the RQ values observed in CT and STR reactors suggests a limited oxygen transfer to the intracellular environment in the CT cultivations probably due to adhesion of the more branched filaments and lower surface to volume ratio given the observed mycelial thickening, leading to higher RQ values in comparison to those observed in the STR. Similar observations regarding the secretion of secondary metabolites and RQ values linked to filaments aggregation have been reported for the filamentous organism *A. niger* cultivated at low shear forces [19]. Additionally, a lower uptake of glycerol and glutamate were also observed in the CT cultivations, suggesting that CA production may be affected by the lower surface to volume ratio of mycelia which would lead to lower diffusion and transport of nutrients, oxygen and product secretion.

Additionally, intracellular availability of oxygen plays a key role in CA biosynthesis, considering the oxidation steps catalyzed by the enzyme clavaminate synthase [53]. According to Li et al. [54], the RQ values close to 1 observed in both reactors during the first hours of cultivation (see Figure 3.3b), indicate a balanced metabolism consistent with the aerobic oxidation of glycerol and glutamate as carbon sources present in the media. During the fed-batch operation the appearance of phosphate limitation led to a rapid decline in the RQ showing the increase of oxygen uptake in this stage. The increase in glycerol concentration during the feeding added to the phosphate and glutamate depletions led to a metabolic imbalance between the glycolysis and TCA cycle, accompanied by an increase in the glycerol uptake since it is the only carbon source available in the media. The latter favors the substrate level phosphorylation as an alternative for ATP production under phosphate limitation [55].

It has been previously reported that activation of secondary metabolism under phosphate limitation in streptomycetes is also accompanied by a decline in the RQ [56]. Therefore, the accumulation of intermediates derived from the metabolic imbalance between glycolysis and the TCA cycle would promote the biosynthesis of antibiotics [56,57]. In our case, the decline in RQ was accompanied by a slight decrease in the specific growth rate (Figure 3.1), and the accumulation of pyruvate and succinate, respectively (Figure 3.6). Previously, Ramirez-Malule et al. [10] also reported the accumulation of succinate during CA production in continuous cultures (V=0.3 L) at different

dilution rates; however pyruvate was not observed to be accumulated under such conditions. According to Viollier et al [57] the secretion of glycolytic and TCA intermediates in *Streptomyces* evidences the metabolic imbalance in the central metabolism. Moreover, the trends in the accumulation of pyruvate and succinate were opposite in the CT and STR reactors. The higher accumulation of pyruvate in CT cultivations (Figure 3.6) might be related to a catabolic repression as a consequence of the reduced oxygen uptake, which would lead to a decrease in the reaction fluxes along the TCA cycle and hence, in the respiratory chain.

Molecular oxygen is part of CA biosynthetic pathway, and Ives and Bushell [58] observed that CA was abolished under oxygen limitation in 25 mL cultures due to an insufficiency of TCA-derived precursors. Dunstan et al [59] found in oxygen-limited cultures of *Amycolatopsis orientalis* that oxygen assimilation rate was only sufficient for biomass production, during the phase when secondary metabolic pathways were induced, leaving insufficient oxygen for vancomycin synthesis, which is also oxygen depend antibiotic; thus, the lack of oxygen under these conditions may also have prevented the induction of the enzymes needed for the terminal biosynthetic steps. Similarly, in our *S. clavuligerus* the oxygen uptake was lower in CA non-producing cultivations while biomass was not affected. Therefore, the enzymes related to oxygen dependent steps during CA biosynthesis could not be expressed under low oxygen transfer conditions. The oxygen dependent step in CA biosynthesis catalyzed by the clavaminate synthase oxidizes 2-oxoglutarate to succinate, explaining the accumulation of succinate in STR cultivations with high CA productivity.

Interestingly, the decrease in the RQ was considerably less pronounced in the CT cultivations corresponding with the lower oxygen and glycerol uptake during the fed-batch stage, which also coincided with a lower CA biosynthesis rate compared with the STR cultivations. Indeed, adhesion of mycelia in *Streptomyces* limits the mass transfer of nutrients and reduces the oxygen uptake as a consequence of a higher resistance to diffusion, which not only affects the growth, but also the antibiotics production [5,46]. In contrast, the looser and thinner mycelial structures of *S. clavuligerus*, cultivated at high shear conditions, impose less resistance to oxygen diffusion from the medium to the intracellular compartment allowing the cultures to effectively respond to the higher uptake for oxygen, in accordance with the RQ values, which ranged from 0.5 to 0.7 during CA production in STR. These results suggest the RQ as an additional parameter to consider in *S. clavuligerus* cultivations for CA production in connection with the macromorphology and the hydrodynamic conditions. In this regard, an online RQ-control approach could be applied to *S. clavuligerus* as a strategy to promote changes in carbon fluxes and therefore, the synthesis of the desired products [54,60].

3.5. Conclusions

The results of this study indicate that low shear forces did not lead to significant hyphal fragmentation or lysis in *S. clavuligerus*, on the contrary, it promoted mycelial thickening and branching mechanisms of growth, hence favoring the preservation of macromorphology during the cultivation. The motion pattern of the rocking-motion single use bioreactor CELL-tainer is able to provide high values of volumetric mass transfer coefficient, facilitating oxygen dissolution even at low rocking speeds, while exerting low shear stress on the cells and the liquid. Under low shear forces in the CELL-tainer the mycelial diameter increased considerably (average diameter 2.27 in CELL-tainer vs. 1.44 μm in STR). This suggests that CA production may be affected by a lower surface to volume ratio, which would lead to lower diffusion and transport of nutrients, oxygen and product.

In addition to phosphate limitation, oxygen transport from liquid phase to the cells seems to be also a critical factor for CA biosynthesis. Thickening of the mycelium reduce the surface to volume ratio, therefore limiting the oxygen transport, leading to a decrease in the oxygen uptake and consequently to a low production rate of CA. Thus, the high shear forces attained in the stirred tank bioreactor prevented mycelial adhesion and promoted high uptakes of glycerol and oxygen required for CA production. The notable production of CA observed at RQ values between 0.5 and 0.7, suggests that RQ is a useful parameter for obtaining information about the oxidative metabolism of the bacteria and activation of secondary metabolism.

Here we presented a methodology for the analysis of the effect of shear forces on the bioprocess performance of *S. clavuligerus* without introducing other disturbances on the process, allowing the study of the physiological and metabolic response of the strain to the environmental shear conditions. The results can be valuable for other studies focused on strain and process optimization. Additionally, further application of an online RQ-control approach would help to redistribute carbon fluxes on primary metabolism and eventually contribute to increase the product synthesis.

Publication: This chapter was published as Gómez-Ríos, D.; Junne, S.; Neubauer, P.; Ochoa, S.; Ríos-Estepa, R.; Ramírez-Malule, H. Characterization of the Metabolic Response of *Streptomyces clavuligerus* to Shear Stress in Stirred Tanks and Single-Use 2D Rocking Motion Bioreactors for Clavulanic Acid Production. *Antibiotics* **2019**, *8*, 168.

References

1. Cerri, M.O.; Badino, A.C. Shear conditions in clavulanic acid production by Streptomyces clavuligerus in stirred tank and airlift bioreactors. *Bioprocess Biosyst. Eng.* **2012**, *35*, 977–984.
2. Rosa, J.C.; Baptista Neto, A.; Hokka, C.O.; Badino, A.C. Influence of dissolved oxygen and shear conditions on clavulanic acid production by Streptomyces clavuligerus. *Bioprocess Biosyst. Eng.* **2005**, 99–104.
3. Gómez-Ríos, D.; Ramírez-Malule, H.; Neubauer, P.; Junne, S.; Ríos-Estepa, R. Degradation Kinetics of Clavulanic Acid in Fermentation Broths at Low Temperatures. *Antibiotics* **2019**, *8*, 6.
4. Gómez-Ríos, D.; Ramírez-Malule, H.; Neubauer, P.; Junne, S.; Ríos-Estepa, R. Data of clavulanic acid and clavulanate-imidazole stability at low temperatures. *Data Br.* **2019**, *23*, 103775.
5. Olmos, E.; Mehmood, N.; Haj Husein, L.; Goergen, J.L.; Fick, M.; Delaunay, S. Effects of bioreactor hydrodynamics on the physiology of Streptomyces. *Bioprocess Biosyst. Eng.* **2013**, *36*, 259–272.
6. Manteca, Á.; Yagüe, P. Streptomyces Differentiation in Liquid Cultures as a Trigger of Secondary Metabolism. *Antibiotics* **2018**, *7*, 1–13.
7. Xia, X.; Lin, S.; Xia, X.X.; Cong, F.S.; Zhong, J.J. Significance of agitation-induced shear stress on mycelium morphology and lavendamycin production by engineered Streptomyces flocculus. *Appl. Microbiol. Biotechnol.* **2014**, *98*, 4399–4407.
8. Zacchetti, B.; Smits, P.; Claessen, D. Dynamics of pellet fragmentation and aggregation in liquid-grown cultures of Streptomyces lividans. *Front. Microbiol.* **2018**, *9*, 1–10.
9. Manteca, A.; Alvarez, R.; Salazar, N.; Yagüe, P.; Sanchez, J. Mycelium differentiation and antibiotic production in submerged cultures of Streptomyces coelicolor. *Appl. Environ. Microbiol.* **2008**, *74*, 3877–3886.
10. Ramirez-malule, H.; Junne, S.; Cruz-bournazou, M.N.; Neubauer, P. Streptomyces clavuligerus shows a strong association between TCA cycle intermediate accumulation and clavulanic acid biosynthesis. *Appl. Microbiol. Biotechnol.* **2018**, *102*, 4009–402.
11. Pinto, L.S.; Vieira, L.M.; Pons, M.N.; Fonseca, M.M.R.; Menezes, J.C. Morphology and viability analysis of Streptomyces clavuligerus in industrial cultivation systems. *Bioprocess Biosyst. Eng.* **2004**, *26*, 177–184.
12. Eibl, R.; Kaiser, S.; Lombriser, R. Disposable bioreactors : the current state-of-the-art and recommended applications in biotechnology. **2010**, 41–49.
13. Junne, S.; Solymosi, T.; Oosterhuis, N.; Neubauer, P. Cultivation of Cells and Microorganisms in Wave-Mixed Disposable Bag Bioreactors at Different Scales. *Chemie Ingeniur Tech.* **2012**, *85*, 57–66.
14. DeFife, K.; Leigh, P. Versatility of a Single-Use Bioreactor Platform for Culture of Diverse Cell Types. *BioPharm Int.* **2009**, *22*.
15. Löffelholz, C.; Kaiser, S.C.; Kraume, M.; Eibl, R.; Eibl, D.; Löffelholz, C.; Eibl, Á.S.C.K.Á.R.E.Á.D. Dynamic Single-Use Bioreactors Used in Modern Liter- and m 3 - Scale Biotechnological Processes : Engineering Characteristics and Scaling Up. **2013**.
16. Odeleye, A.O.O.; Marsh, D.T.J.; Osborne, M.D.; Lye, G.J.; Micheletti, M. On the fluid dynamics of a laboratory scale single-use stirred bioreactor. *Chem. Eng. Sci.* **2014**, *111*, 299–312.
17. Hillig, F.; Porscha, N.; Junne, S.; Neubauer, P. Growth and docosahexaenoic acid production performance of the heterotrophic marine microalgae Crypthecodinium cohnii in the wave-mixed single-use reactor CELL-tainer. *Eng. Life Sci.* **2014**, *14*, 254–263.

18. Westbrook, A.; Scharer, J.; Moo-young, M.; Oosterhuis, N.; Chou, C.P. Application of a two-dimensional disposable rocking bioreactor to bacterial cultivation for recombinant protein production. *Biochem. Eng. J.* **2014**, *88*, 154–161.
19. Kurt, T.; Maria, A.; Ardébol, M.; Turan, Z.; Neubauer, P.; Junne, S.; Meyer, V. Rocking Aspergillus : morphology - controlled cultivation of Aspergillus niger in a wave - mixed bioreactor for the production of secondary metabolites. *Microb. Cell Fact.* **2018**, 1–9.
20. Roubos, J.A.; Krabben, P.; De Laat, W.; Heijnen, J.J. Clavulanic Acid Degradation in Streptomyces clavuligerus Fed-Batch Cultivations. *Biotechnol. Prog.* **2002**, *18*, 451–457.
21. Campesi, A.; Cerri, M.O.; Hokka, C.O.; Badino, A.C. Determination of the average shear rate in a stirred and aerated tank bioreactor. *Bioprocess Biosyst. Eng.* **2009**, *32*, 241–248.
22. Kumar, B. Energy Dissipation and Shear Rate with Geometry of Baffled Surface Aerator. *Chem. Eng. Res. Bull.* **2010**, *14*, 92–96.
23. Tamphasana, T.; Kumar, B. Engineering Science and Technology , an International Journal Mass transfer and power characteristics of stirred tank with Rushton and curved blade impeller. *Eng. Sci. Technol. an Int. J.* **2017**, *20*, 730–737.
24. Sánchez Pérez, J.A.; Rodríguez Porcel, E.M.; Casas López, J.L.; Fernández Sevilla, J.M.; Chisti, Y. Shear rate in stirred tank and bubble column bioreactors. *Chem. Eng. J.* **2006**, *124*, 1–5.
25. Buffo, M.M.; Corrêa, L.J.; Esperança, M.N.; Cruz, A.J.G.; Farinas, C.S.; Badino, A.C. Influence of dual-impeller type and configuration on oxygen transfer, power consumption, and shear rate in a stirred tank bioreactor. *Biochem. Eng. J.* **2016**, *114*.
26. Eibl, D.; Eibl, R. *Disposable Bioreactors II*; Scheper, T., Ed.; Springer, 2014; Vol. 138; ISBN 978-3-642-45157-7.
27. Öncul, A.A.; Kalmbach, A.; Genzel, Y.; Reichl, U.; Thévenin, D. Characterization of flow conditions in 2 L and 20 L wave bioreactors?? usingcomputational fluid dynamics. *Biotechnol. Prog.* **2010**, *26*, 101–110.
28. Zhan, C.; Hagrot, E.; Brandt, L.; Chotteau, V. Study of hydrodynamics in wave bioreactors by computational fluid dynamics reveals a resonance phenomenon. *Chem. Eng. Sci.* **2019**, *193*, 53–65.
29. Rasband, W.S.; U. S. National Institutes of Health ImageJ 2018.
30. Ramirez-Malule, H.; Junne, S.; López, C.; Zapata, J.; Sáez, A.; Neubauer, P.; Rios-Estepa, R. An improved HPLC-DAD method for clavulanic acid quantification in fermentation broths of Streptomyces clavuligerus. *J. Pharm. Biomed. Anal.* **2016**, *120*, 241–247.
31. Junne, S.; Klingner, A.; Kabisch, J.; Schweder, T.; Neubauer, P. A two-compartment bioreactor system made of commercial parts for bioprocess scale-down studies : Impact of oscillations on Bacillus subtilis fed-batch cultivations. *Biotechnol. J.* **2011**, *6*, 1009–1017.
32. Lemoine, A.; Martınez-Iturralde, N.M.; Spann, R.; Neubauer, P. Response of Corynebacterium glutamicum Exposed to Oscillating Cultivation Conditions in a Two- and a Novel Three-Compartment Scale- Down Bioreactor. *Biotechnol. Bioeng.* **2015**, *112*, 1220–1231.
33. Enfors, S.-O. *Fermentation Process Engineering*; School of Biotechnology, Royal Institute of Technology: Stockholm, Sweden, 2011;
34. Bushell, M.E.; Kirk, S.; Zhao, H.; Avignone-rossa, C.A. Manipulation of the physiology of clavulanic acid biosynthesis with the aid of metabolic flux analysis. *Enzyme Microb. Technol.* **2006**, *39*, 149–157.
35. Daub, A.; Böhm, M.; Delueg, S.; Mühlmann, M.; Schneider, G.; Büchs, J. Characterization of hydromechanical stress in aerated stirred tanks up to 40 m(3) scale by measurement of maximum stable drop size. *J. Biol. Eng.* **2014**, *8*, 17.
36. Baldi, S.; Yianneskis, M. On the quantification of energy dissipation in the impeller stream of a stirred vessel from fluctuating velocity gradient measurements. *Chem. Eng. Sci.* **2004**, *59*, 2659–2671.
37. Rollins, M.J.; Jensen, S.E.; Westlake, D.W.S. Effect of dissolved oxygen level on ACV synthetase synthesis and activity during growth of Streptomyces clavuligerus. *Appl. Microbiol. Biotechnol.* **1991**, *35*, 83–88.
38. Duobin, M.; Yuping, M.; Lujing, G.; Aijing, Z.; Jianqiang, Z.; Chunping, X. Fermentation characteristics in stirred-tank reactor of exopolysaccharides with hypolipidemic activity produced by Pleurotus geesteranus 5#. *An. Acad. Bras. Cienc.* **2013**, *85*, 1473–1481.
39. Chisti, Y. Hydrodynamic damage to animal cells. *Crit. Rev. Biotechnol.* **2001**, *21*, 67–110.

40. Teodoro, J.C.; Baptista-Neto, A.; Araujo, M.L.G.C.; Hokka, C.O.; Badino, A.C. Influence of glycerol and ornithine feeding on clavulanic acid production by streptomyces clavuligerus. *Brazilian J. Chem. Eng.* **2010**, *27*, 499–506.
41. Costa, C.L.L.; Badino, A.C. Production of clavulanic acid by Streptomyces clavuligerus in batch cultures without and with glycerol pulses under different temperature conditions. *Biochem. Eng. J.* **2012**, *69*, 1–7.
42. Yagüe, P.; López-García, M.T.; Rioseras, B.; Sánchez, J.; Manteca, Á. Pre-sporulation stages of Streptomyces differentiation: State-of-the-art and future perspectives. *FEMS Microbiol. Lett.* 2013, *342*.
43. Barka, E.A.; Vatsa, P.; Sanchez, L.; Gaveau-vaillant, N.; Jacquard, C.; Klenk, H.; Clément, C.; Ouhdouch, Y.; Wezel, P. Van Taxonomy , Physiology , and Natural Products of Actinobacteria. *Microbiol. Mol. Biol. Rev.* **2016**, *80*, 1–44.
44. Veiter, L.; Rajamanickam, V.; Herwig, C. The filamentous fungal pellet — relationship between morphology and productivity. *Appl. Microbiol. Biotechnol.* **2018**, *102*, 2997–3006.
45. Yin, P.; Wang, Y.H.; Zhang, S.L.; Chu, J.; Zhuang, Y.P.; Chen, N.; Li, X.F.; Wu, Y. Bin Effect of mycelial morphology on bioreactor performance and avermectin production of Streptomyces avermitilis in submerged cultivations. *J. Chinese Inst. Chem. Eng.* **2008**, *39*, 609–615.
46. Kumar, P.; Dubey, K.K. Mycelium transformation of Streptomyces toxytricini into pellet: Role of culture conditions and kinetics. *Bioresour. Technol.* **2017**, *228*, 339–347.
47. Ohta, N.; Park, Y.S.; Yahiro, K.; Okabe, M. Comparison of neomycin production from Streptomyces fradiae cultivation using soybean oil as the sole carbon source in an air-lift bioreactor and a stirred-tank reactor. *J. Ferment. Bioeng.* **1995**, *79*, 443–448.
48. Elsayed, E.A.; Farid, M.A.; El-Enshasy, H.A. Enhanced Natamycin production by Streptomyces natalensis in shake-flasks and stirred tank bioreactor under batch and fed-batch conditions. *BMC Biotechnol.* **2019**, *19*, 46.
49. El Enshasy, H.; Farid, M.; Elsayed, E. *Influence of inoculum type and cultivation conditions on natamycin production byStreptomyces natalensis*; 2000; Vol. 40;.
50. Mehmood, N.; Olmos, E.; Marchal, P.; Goergen, J.L.; Delaunay, S. Relation between pristinamycins production by Streptomyces pristinaespiralis, power dissipation and volumetric gas-liquid mass transfer coefficient, kLa. *Process Biochem.* **2010**, *45*, 1779–1786.
51. Wardell, J.N.; Bushell, M.E. Kinetics and manipulation of hyphal breakage and its effect on antibiotic production. *Enzyme Microb. Technol.* **1999**, *25*, 404–410.
52. Saudagar, P.S.; Singhal, R.S. Optimization of nutritional requirements and feeding strategies for clavulanic acid production by Streptomyces clavuligerus. *Bioresour. Technol.* **2007**, *98*, 2010–7.
53. Arulanantham, H.; Kershaw, N.J.; Hewitson, K.S.; Hughes, C.E.; Thirkettle, J.E.; Schofield, C.J. ORF17 from the clavulanic acid biosynthesis gene cluster catalyzes the ATP-dependent formation of N-glycyl-clavaminic acid. *J. Biol. Chem.* **2006**, *281*, 279–287.
54. Li, X.; Yu, C.; Yao, J.; Wang, Z.; Lu, S. An Online Respiratory Quotient-Feedback Strategy of Feeding Yeast Extract for Efficient Arachidonic Acid Production by Mortierella alpina. *Front. Bioeng. Biotechnol.* **2018**, *5*, 1–11.
55. Hodgson, D. a Primary metabolism and its control in streptomycetes: a most unusual group of bacteria. *Adv. Microb. Physiol.* **2000**, *42*, 47–238.
56. Gamboa-Suasnavart, R.A.; Valdez-Cruz, N.A.; Gaytan-Ortega, G.; Cereceda-Reynoso, G.I.; Cabrera-Santos, D.; López-Griego, L.; Klöckner, W.; Büchs, J.; Trujillo-Roldán, M.A. The metabolic switch can be activated in a recombinant strain of Streptomyces lividans by a low oxygen transfer rate in shake flasks. *Microb. Cell Fact.* **2018**, 1–12.
57. Viollier, P.H.; Minas, W.; Dale, G.E.; Folcher, M.; Thompson, C.J. Role of Acid Metabolism in Streptomyces coelicolor Morphological Differentiation and Antibiotic Biosynthesis. *J. Bacteriol.* **2001**, *183*, 3184–3192.
58. Bushell, M.E.; Kirk, S.; Zhao, H.-J.; Avignone-Rossa, C.A. Manipulation of the physiology of clavulanic acid biosynthesis with the aid of metabolic flux analysis. *Enzyme Microb. Technol.* **2006**, *39*, 149–157.
59. Dunstan, G.H.; Avignone–Rossa, C.; Langley, D.; Bushell, M.E. The Vancomycin biosynthetic pathway is induced in oxygen-limited Amycolatopsis orientalis (ATCC 19795) cultures that do not produce antibiotic. *Enzyme Microb. Technol.* **2000**, *27*, 502–510.

60. Xiao, J.; Shi, Z.; Gao, P.; Feng, H.; Duan, Z.; Mao, Z. On-line optimization of glutamate production based on balanced metabolic control by RQ. *Bioprocess Biosyst. Eng.* **2006**, *29*, 109–117.

Chapter 4

A Combined Constraint-based Modeling and Experimental Approach Clears up the Metabolic Relationship Between the TCA Cycle Intermediates, Amino-acid Biosynthesis, Phosphate and Oxygen Uptakes, during CA Production

Abstract: Antibiotics biosynthesis in the *Streptomyces* genus is usually triggered by nutritional and environmental perturbations. For this chapter, a new genome scale metabolic network of *Streptomyces clavuligerus* was reconstructed and used to study the experimentally observed effect of oxygen and phosphate concentrations on clavulanic acid biosynthesis under high and low shear stress. A flux balance analysis based on experimental evidence revealed that the clavulanic acid biosynthetic pathway is activated by phosphate limitation and connected with an increased uptake of oxygen. Phosphate limitation leads to an increase of the carbon flux through the phosphate producing reactions in order to maintain a stoichiometric supply of intracellular phosphate for the central anabolic and catabolic reactions, thus increasing the oxygen demand and favoring clavulanic acid biosynthesis.

4.1. Introduction

A common approach for studying the effect of nutritional, genetic and environmental perturbations on metabolism is the genome-scale metabolic modeling by using flux balance analysis (FBA) [1]. In the case of *S. clavuligerus*, metabolic network models have been reconstructed and/or updated for this purpose [2–5], providing insights about the metabolic features of the species and possible genetic targets for further strain improvement. Nevertheless, the referred models share a common origin and some of their inconsistencies persisted between them without being corrected.

Starting from recent advances in genome-scale model reconstruction and available genetic information, a new and improved genome-scale model of the *S. clavuligerus* metabolism has been developed. In this work, a novel top-down reconstruction tool proposed by Machado et al. [6] was used for the generation of an initial model based on the genome assembly for *S. clavuligerus* by Cao et al [7]. The initial reconstruction was systematically and manually curated for inclusion of missing reactions and the removal of inconsistencies, especially those of thermodynamic nature, for the purpose of obtaining a more realistic representation of the complexity of the *S. clavuligerus* metabolism. This model was used in a combined approach of experimental and modeling work for investigating the connection between the different nutritional conditions observed in *S. clavuligerus* cultivations and CA biosynthesis. For this, fed-batch cultivations in defined media were performed in stirred tank and single-use rocking-motion bioreactors. Subsequently, the experimentally observed metabolic scenarios were simulated by using the constructed and validated genome-scale model of *S. clavuligerus* in order to identify putative connections between the central carbon and amino acid metabolism, nutrient limiting conditions and CA production.

4.2. Materials and Methods

4.2.1. Generation of a new genome scale model of S. clavuligerus

An initial Genome-Scale Metabolic Network (GSMN) was generated from the representative genome of S. clavuligerus sequenced by Cao et al. [7] and currently available in the NCBI database (refseq GCA_001693675.1). This initial reconstruction was performed by using CarveMe, an

automated tool for GSMN reconstruction developed by Machado et al. [6]. The reconstruction pipe-line of this novel tool is defined as a top-down approach, in which the probable reactions of the organism-specific metabolic network are scored according to the Gene-Protein-Reaction (GPR) associations from the organism genome assembly [6]. For the initial reconstruction of the GSMN of S. clavuligerus, the script of CarveMe was executed in the Anaconda Python distribution for Linux, externally the Diamond sequence aligner [8] and IBM CPLEX v12.9 for Linux were also required.

The initial GSMN was manually curated by following a systematic procedure in order to improve the *in silico* representation of the physiology of the organism. The missing reactions and metabolites in the secondary metabolism, which correspond to penicillin-cephalosporin biosynthesis, clavulanic acid biosynthesis and 5S-clavams bifurcation were manually added and associated to the corresponding genes, while maintaining the connectivity of the model, and the mass and charge balances, respectively.

The flux distribution, obtained by solving a standard FBA optimization, frequently include thermodynamic infeasible cycles (TICs) that represent slopes of reactions like a perpetual motion machine that violate the Second Law of Thermodynamics. This heavily distorts the reaction fluxes predictions. It has been demonstrated that the number of infeasible loops grows rapidly with the network size [9]. Therefore, the construction of larger metabolic models usually implies a considerable number of TICs. Some FBA strategies are currently available for avoiding the TICs, e.g., the thermodynamic FBA that imposes an extra set of constraints for ΔGr and reaction directionality if necessary [10,11]. The loopless FBA and CycleFreeFlux approaches do not require extra parameters in the model [9,12]. However, those might not eliminate all TICs in the network, although it can improve the FBA predictions [11]. In this work a Matlab® implementation of the Flux Variability Analysis methodology proposed by Schellenberger et al. [9] for TICs identification was used in order to determine reactions that appear in one or more TICs. Within this methodology, the TICs are a set of reactions linked to unbounded metabolic fluxes with no specificity for substrate uptake when applying flux variability analysis [94]. Therefore, we performed flux variability analysis constraining the substrate uptake in 1.0 mmol.(g DCW.h)$^{-1}$.

The set of unbounded reactions which are part of the TICs were used to define a stoichiometric matrix. Its null space was used for the individual identification of TICs composed by two or more reactions. The manual curation of the TICs was performed by (i) elimination of linearly dependent reversible reactions resulting in redundancy due to erroneous identification of GPR during the automated reconstruction, and (ii) restriction of the reaction directionality by calculation of the correspondent Standard Gibbs free energy of reaction (ΔGr°) using the NExT (Network-Embedded Thermodynamic analysis) algorithm [13].

The final GSMN denoted as iDG1237 was reviewed with the MC3 Consistency Checker algorithm, which implements stoichiometric-based identification and flux variability analysis to determine single connected and dead end metabolites in the network, as well as the consistent coupled and inconsistent coupled/zero-flux reactions [14]. The iDG1237 genome-scale model for *S. clavuligerus* is available in SBML (xml) and MS Excel (xlslx) file formats in the supplementary material S1.

4.2.2. Flux Balance Analysis

In the FBA studies the external/internal exchange reactions were constrained to represent *in silico* the environmental conditions observed in *S. clavuligerus* cultivations at high and low shear stress conditions. FBA solves a linear programming problem for calculating the steady-state reaction flux distributions along the metabolic network that maximizes (or minimizes) a pre-defined objective function, under specific constraints. The objective function shall reflect the achievement of a meaningful physiological state of the organism like a maximal ATP production, growth rate, or specific metabolite production [15]. In most cases the objective function is the maximum biomass production, that is the specific growth rate under non-limiting conditions. Some variations of the traditional FBA, such as the parsimonious and sparse FBA, use a two-stage optimization procedure

in order to retrieve a unique and biologically meaningful solution to the FBA problem of growth rate maximization. In this work a two-stage approach involving biomass maximization and FBA and flux minimization, as presented in Equation 1.

$$Min \ \sum v^2 \qquad \begin{bmatrix} s.t. \boldsymbol{Sv} = 0 \\ l_b \leq v \leq l_u \\ f^T v = Z_{max} \end{bmatrix} \tag{1}$$

where $\boldsymbol{S}$ is the stoichiometric matrix of coefficients for m metabolites and n reactions, v is the flux vector of dimension n, Z_{max} represents the biomass maximization, f is a vector of weights , and l_b and u_b are the lower and upper bounds, respectively. Thus, in the first stage the FBA standard problem for biomass maximization is solved, whereas the second stage deals with the minimization of the vector of fluxes. It is important to notice that the assumption underlying the objective function minimization, postulates that living organisms gain functional fitness by fulfilling their functions with maximal efficiency, and thus assuring a minimal energy requirement to accomplish a specific pattern of cellular functions [16]. All FBA problems were solved in COBRA Toolbox 3.0 synchronized with MATLAB; the Gurobi 5.7 and IBM CPLEX v12.9 optimization plugins were required for solution of FBA and flux variability analysis, respectively.

4.2.3. Microorganism, cultivation media and experimental conditions

S. clavuligerus DSM 41826, cryo-preserved at −80°C in glycerol solution (16.7% v/v), was inoculated for activation in seed medium as described by Roubos et al. [17]. Cultivations were carried out in duplicate in a 15 L stirred tank bioreactor (STR) (Techfors S, Infors AG, Bottmingen, Switzerland) and 20 L single-use rocking-motion bioreactor CELL-tainer® (CT) (Cell-tainer Biotech BV, Winterswijk, The Netherlands) both operated at 5 L initial filling volume. Cultivation and analytical procedures were described in detail in the chapter 3.

4.3. Results and discussion

4.3.1. Development of a new and improved genome scale model of S. clavuligerus

Firstly, this study aims for a novel GSMN for *S. clavuligerus* in order to improve the *in silico* representation of its metabolism in comparison to previously reported GSMNs. It considers the current state-of-the-art in genetics and biochemistry. The reconstruction process is based on an initial functional and high-quality universal model, in which infeasible reactions for *S. clavuligerus* were removed and constraints were added [6]. Nevertheless, this organism-specific model reconstruction presented numerous gaps in pathways and gene annotations in addition to a considerable number of TICs. The initial reconstruction included 1956 metabolic reactions, 233 internal/external exchange reactions and 1234 GPR associations. After a preliminary manual curation of reactions, the model considered 2004 metabolic reactions, 243 internal/external exchange reactions and 1257 GPR.

The previous GSMN share a common origin, the model iMM865 reported by Medema et al [18]). Since that assembly contained a lower number of identified genes, the derived models have a lower number of GPR associations, metabolites and reactions than the reconstruction as presented in Table 4.1. After first manual curation, a total of 1018 unbounded reactions taking part in 124 TICs were identified and reactions participating in infeasible loops were reviewed for linear independence, directionality and essentiality for growth. The manual curation of TICs allowed to eliminate 70 linearly dependent reactions associated to cofactors and prosthetic group biosynthesis, alternate carbon metabolism, amino acid metabolism, membrane lipid metabolism and erroneous inner membrane transport reactions. Additionally, the directionality of 20 reactions was restricted according to the calculated ΔGr°. After implementing those changes, the number of unbounded

reactions was reduced to 86 and the TICs were curated in 93%. The remaining loops could not be removed due to their intrinsic connectivity with essential reactions in the network.

The resulting GSMN of *S. clavuligerus* named iDG1237 consists of 2177 reactions, including 543 internal/external metabolite exchange reactions and 1237 annotated genes. The metabolites were annotated according with their correspondent BIGG identifiers; similarly the genes were annotated with their Refseq identifiers when available. The model consistency statistics for the iDG1237 model and the previous models for *S. clavuligerus* are presented in Table 4.1.

Table 4.1. Model consistency statistics of *S. clavuligerus* genome-scale metabolic models.

Feature	iMM865	iLT1021	iGG1534	iDG1237
Metabolites	1173	1162	1199	1518
Reactions	1492	1494	1534	2177
Reversible reactions	1492	576	610	707
Dead-end metabolites	311	333	338	48
Coupled reactions	0	422	338	880
Inconsistent coupling	0	127	35	0
Zero-flux reactions	383	473	486	105
Unbounded reactions	1024	496	598	86
TICs	411	135	185	9

The improved connectivity of the model is reflected in a lower number of dead-end metabolites. In the case of the iDG1237 GSMN, the number of dead-end metabolites is considerably lower (3%) compared to previously reported GSMNs (~27%). Additionally, the number of zero-flux reactions and inconsistent coupling was approximately 80% lower than in previous reconstructions. Therefore, the full consistent coupling allows a better determination of relationships among reactions and pathways, connections between nutritional factors and desired metabolites, analysis of potential knockouts, as well as further regulatory and expression studies [14,19]. The number of infeasible loops is also considerably lower in the iDG1237 model and therefore, the loopless condition in FBA simulations might be easily satisfied, leading to more consistent metabolic phenotype predictions. In summary, the iDG1237 model presents fewer inconsistencies (dead-end metabolites, inconsistent coupling, unbounded reactions, zero-flux reactions and TICs) in the context of pseudo steady-state modelling than the previous models reported for *S. clavuligerus*.

4.3.2. Model validation

The model validation was performed by comparing the fluxes predicted by the iDG1237 model and the previous GSMNs against experimental data of S. clavuligerus in a chemostat mode, using the experimental data published by Bushell et al. [20] and Ramirez-Malule et al. [5]. Simulations were performed under the two-stage optimization approach. The experimental specific growth rate in chemostat cultures were compared with model predictions. Exchange fluxes of nutrients were constrained accordingly to the experimental media compositions, including glycerol ($v_{ex,Glyc}$) and phosphate ($v_{ex,Pi}$), since CA is majorly secreted under phosphate limitation [5,20]. The values of the experimental (μ_{exp}) and in silico (μ) growth rates, CA secretion fluxes ($v_{ex,CA}$) and cumulative mean square error (MSE) between the experimental and in silico data, are presented in Table 4.2. The O_2 demand and CO_2 excretion were also considered in the model evaluation (data available in supplementary material S2.

Table 4.2. Comparison of experimental and *in silico* growth rates for *S. clavuligerus* models.

Constraints		iMM865		iLT1021		iGG1534		iDG1237		μ_{exp}	Reference
$v_{ex,Pi}$	$v_{ex,Glyc}$	μ	$v_{ex,CA}$	μ	$v_{ex,CA}$	μ	$v_{ex,CA}$	μ	$v_{ex,CA}$		
-0.20	0.50	1.60	0	0.03	0	0.92	0	0.03	0	0.04	[20]
-0.20	0.60	1.61	0	0.04	0	0.93	0	0.04	0	0.05	[20]
-0.20	0.93	1.67	0	0.06	0	0.97	0	0.05	0	0.07	[20]
-0.20	2.18	2.44	0	0.12	0	1.55	0	0.09	0	0.09	[20]
0	0.72	2.97	0	0.05	0	1.94	0	0.05	0.03	0.05	[5]
0	1.11	2.90	0	0.05	0	1.90	0	0.05	0.04	0.05	[5]
0	0.97	2.75	0	0.05	0	1.78	0	0.05	0.03	0.04	[5]
MSE		1.506		0.393		0.700		0.172			

v in [mmol.(g DCW.h)$^{-1}$], D and μ in [h^{-1}].

The iDG1237 had the lowest MSE with respect to experimental data. Furthermore, none of the models previously published was able to calculate reaction fluxes through the CA biosynthesis and clavams pathways, under phosphate limitation. Therefore, iDG1237 model exhibited better representation capabilities of CA producing scenarios. This is most likely due to the completeness of the metabolic network, its higher connectivity and few unrealistic loops that allow a closer representation of the metabolic events that the cell experiences under nutritional and genetic constraints.

4.3.3. S. clavuligerus cultivation under high and low shear stress conditions

Experimental results of growth, CA production and phosphate limitation in batch and fed-batch stages of cultivations under high shear (STR) and low shear stress (CT) conditions are shown in Figures 1A and 1B, respectively. The maximum growth rates of S. clavuligerus observed in STR were 0.104 h^{-1} and 0.028 h^{-1} for the batch and fed-batch stages, respectively. Those were slightly higher in comparison with the 0.102 h^{-1} and 0.024 h^{-1} attained in the CT cultivations during the batch and fed-batch phases, respectively. At the end of the fed-batch operation, the maximum biomass was lower in the CT (9.0 gDCW.L^{-1}) than the observed in STR (11.9 gDCW.L^{-1}). The glycerol and glutamate-concentration time courses are presented in Figure 1c. In this regard, glycerol and glutamate were consumed rapidly during the exponential growth phase but feeding of glycerol in excess (after 37 h) led to accumulation during the fed-batch stages. The high glycerol and glutamate uptakes were consistent with the maximum growth rates and biomass concentrations. The maximum uptake fluxes of glycerol in STR and CT were 1.93 and 1.92 mmol.(g DCW.h)$^{-1}$, respectively. Similarly, the maximum uptake fluxes of glutamate in STR and CT were 1.34 and 1.29 mmol.(g DCW.h)$^{-1}$.

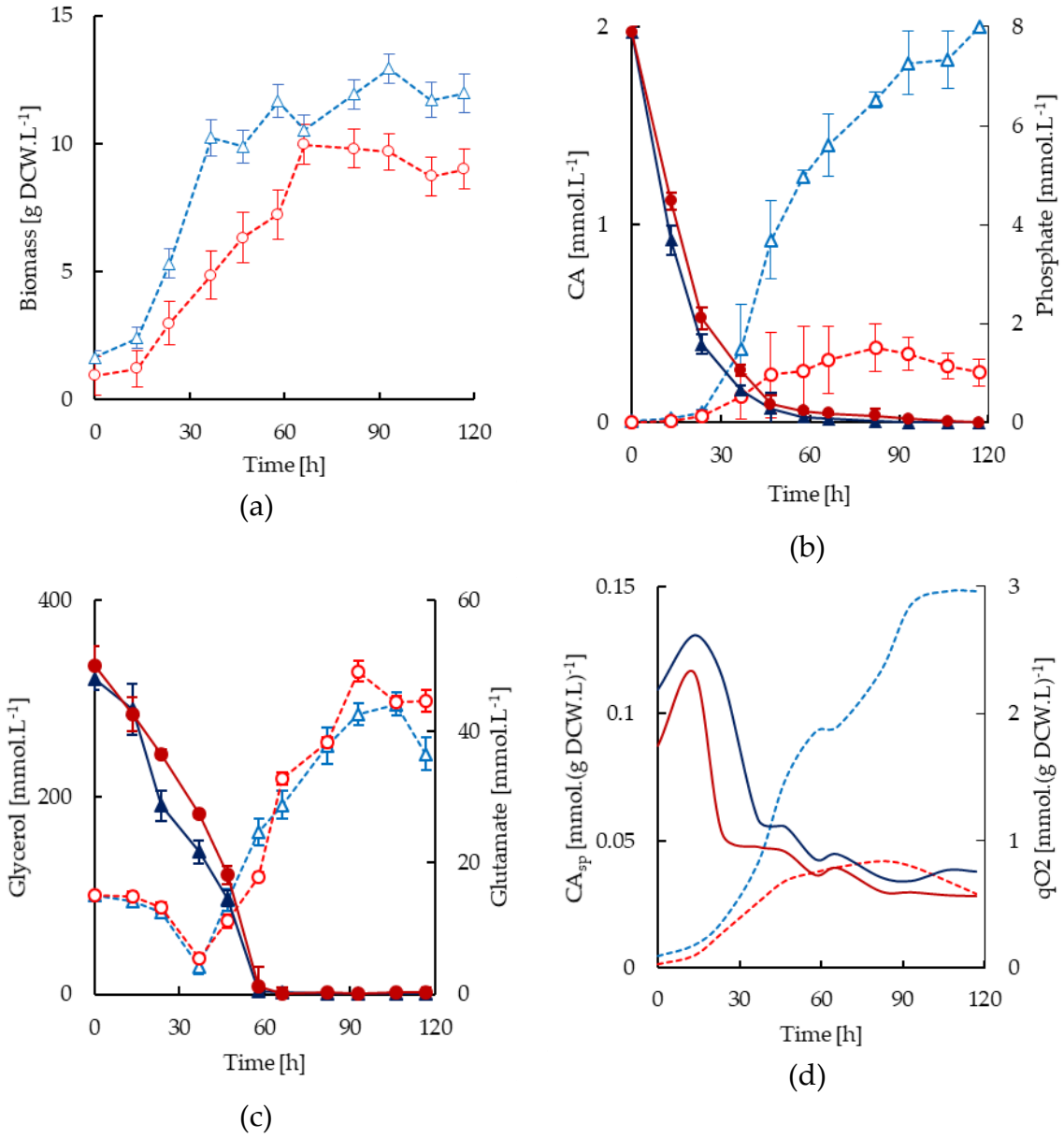

Figure 4.1. Growth and physiological profiles for fed-batch cultivations of *S. clavuligerus* in STR (triangles, blue line) and CT (circles, red line). (**a**) Biomass; (**b**) CA (open symbols) and phosphate (filled symbols); (**c**) Glycerol (open symbols) and glutamate (filled symbols); (**d**) Mean specific CA (CAsp) (discontinuous lines) and oxygen uptake (qO2) (continuous lines). STR: Stirred tank reactor; CT: CELL-tainer.

The phosphate limitation was expected to be reached around 40-50 h and the specific CA production typically starts to increase with the phosphate depletion as observed in Figures 1B and 1D. The phosphate uptake was slightly lower in the CT cultivations and therefore the phosphate exhaustion took place later (66 h) in comparison to the STR cultivations (47 h). Despite the fact that equivalent conditions of phosphate depletion and glycerol availability were attained in both reactors, the CA production did not increase significantly in the CT reactor beyond 37 h. The oxygen uptake (qO_2) in STR cultivations was higher when CA was continually produced as showed in Figure 1D. In this regard, oxygen limitation decreases the antibiotic production in filamentous organisms [21]. CA biosynthesis might decrease if oxygen is limited in the broth [22]. In the previous chapter, it was reported that the low shear forces, as attained in the CT cultivation, promoted

mycelia thickening and branching; therefore, oxygen diffusion from the media to the inner core of cells might be reduced due to the higher barrier for penetration [23].

Organic acids secretion in *streptomycetes* (Figures 2A and 2B) is related to an imbalance in between glycolysis and the tricarboxylic acids (TCA) cycle, observed in abundance of carbon source due to glycerol accumulation. It is also related with the activation of secondary metabolism [24,25]. Shut down of TCA cycle reactions like the catalyzed by the citrate synthase (CS), in addition to activation of anaplerotic reactions, have been proposed as metabolic mechanisms to deal with excessive carbon uptake; while promotes substrate phosphorylation as an energy producing mechanism and leading to secretion of acids such as pyruvate and succinate [24,25]. In fact, the fed-batch stage led to an excess of carbon source and some accumulation of succinate and oxaloacetate (Figure 2A), in addition to malate and pyruvate (Figure 2B).

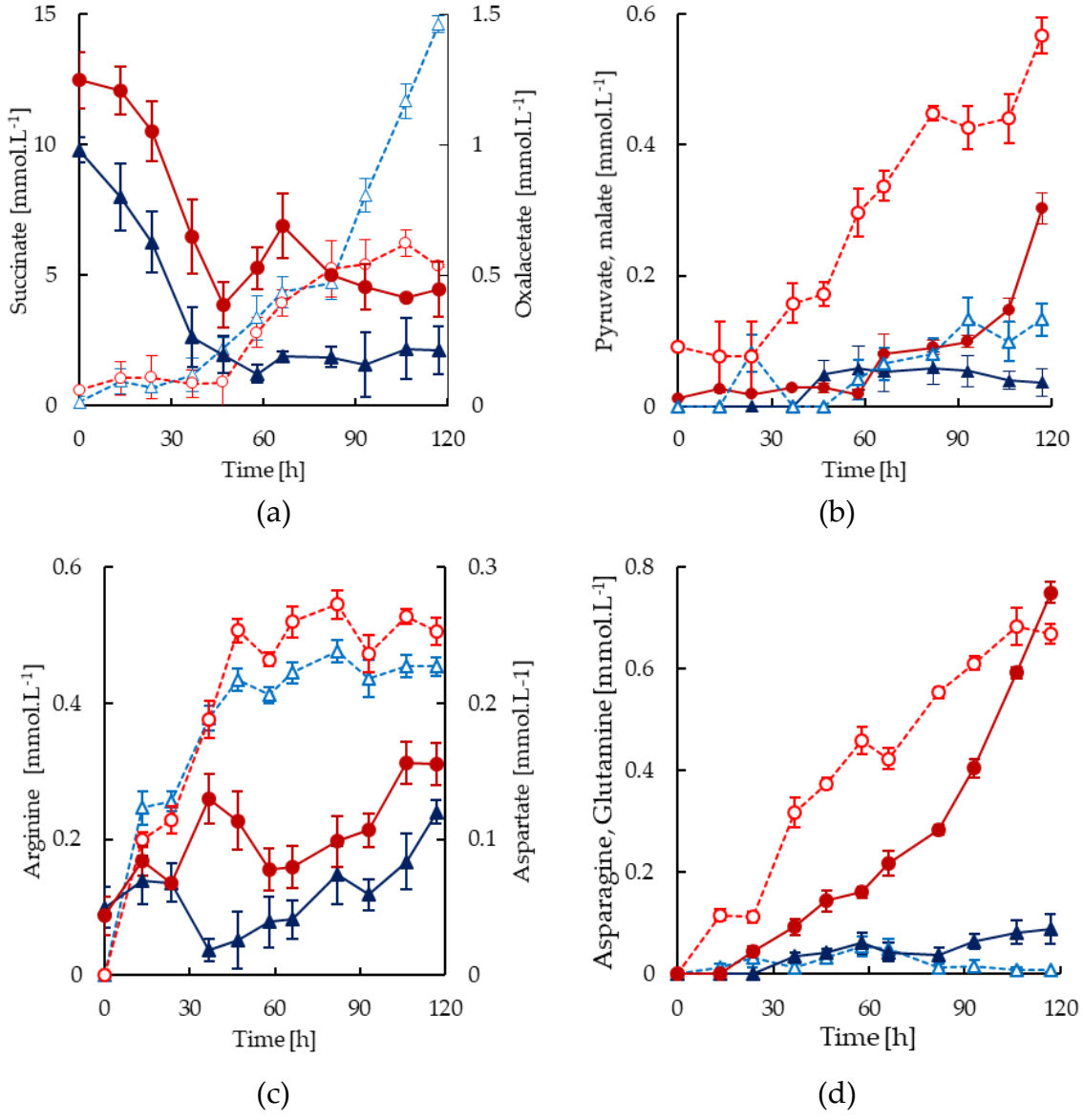

Figure 4.2. TCA intermediates and amino acids profiles for fed-batch cultivations of *S. clavuligerus* in STR (triangles, blue line) and CT (circles, red line). (**a**) Succinate (open symbols) and oxaloacetate (filled symbols); (**b**) Pyruvate (open symbols) and malate (closed symbols); (**c**) Arginine (open symbols) and aspartate (closed symbols); (**d**) Asparagine (open symbols) and glutamine (closed symbols). STR: Stirred tank reactor; CT: CELL-tainer.

The q_{O2} difference between both reactors is in average 20% SD=13%. However, it is expected that most of the oxygen is required for primary metabolism and biomass production [21]; even if a certain oxygen limitation is occurring due to the thicker mycelia and more viscous broth. Ramírez-Malule et al. (2018) showed in a previous work, that pyruvate is not significantly accumulated during clavulanic production. In this case pyruvate was not accumulated in STR cultivations while it was accumulated in CT cultivation. Thus, pyruvate accumulation might indicate a certain repression in connection with mycelia thickening and some oxygen limitation from 30 h onwards, that further affects the CA production.

Moreover, the accumulation of these acids might promote the occurrence of the down-stream reactions related to urea cycle and hence, the arginine and ornithine biosynthesis. CA biosynthesis and clavams pathways would act as a sink for glycerol via GAP and for nitrogen and TCA intermediates through arginine and 2-oxoglutarate consumption. Therefore, lower activity of CA, clavams and Penicillin-cephalosporin pathways might increase the up-stream accumulation of acids and amino acids.

In this study, accumulation of succinate was observed during CA production (Figures 1B and 2A). In STR cultivations where the CA accumulation was sustained during the complete fed-batch stage, the accumulation of succinate showed the same increasing trend. In contrast, the CT cultivations showed lower succinate accumulations and lower synthesis rate of CA. It is known that succinate is a byproduct of some reactions in the amino acids metabolism and in *S. clavuligerus* it is also produced by the reactions catalyzed by clavaminate synthase (CAS) and even in the Cephalosporin-Penicillins pathway; in both cases the reactions require 2-oxoglutarate as substrate [5,26,27].

During growth and CA production it was expected some accumulation of oxaloacetate originated from TCA cycle and phosphoenolpyruvate carboxylase (PPC) reactions; it has been shown that this anaplerotic reaction is responsible of oxaloacetate accumulations in *streptomycetes*, acting also as source of inorganic phosphate (Pi) [5,24]. Interestingly, the accumulation of oxaloacetate was also lower when higher CA production was observed (Figures 1B and 2A), suggesting a higher consumption of this precursor to satisfy the demand for arginine from urea cycle, which also would require aspartate from the reaction catalyzed by aspartate transaminase (ASPTA). In fact, these accumulations are consistent with the accumulation of aspartate and arginine observed in Figure 2C. In all cases, the accumulation of precursors was higher in the CT cultivations (with exception of succinate), probably due to the presence of a flux bottleneck in the CA pathway leading to up-stream accumulations of early CA precursors. In this regard, the reactions catalyzed by the CAS are rate-limiting steps and they are oxygen and 2-oxoglutarate dependent [28]. The activity of CAS controls directly the flux reaction along the clavulanic acid and 5S clavams pathways [28,29] .

Glutamate fuels the urea cycle as C-5 precursor yielding aspartate and hence arginine, which is the second early precursor of CA. Under glutamate limitation ($t > 58$ h), a pool of aspartate is expected to be formed from fumarate and ammonium since the cultivations were not nitrogen-limited. In this scenario, the demand for glutamate and aspartate might also be satisfied to a lesser extent from glutamine and asparagine (Figure 2D). In this regard, lower accumulations of arginine, aspartate, glutamine and asparagine were observed at higher CA biosynthesis rates suggesting a higher demand for those amino acids when the CA production is active.

4.3.4. Effect of oxygen uptake, phosphate and glutamate depletions in CA biosynthesis

Previous experimental studies have shown that phosphate has a potential repressive effect on CA biosynthesis [30–32]. Therefore, the phosphate limitation is an essential condition for CA production in all scales and operation modes. However, phosphate depletion does not necessarily trigger the CA production if sufficient oxygen does not reach the intracellular compartment. The above depends not only on the k_La and the DO values attained in the cultivation, but on the

mycelium thickness and aggregation that potentially limits the diffusion of oxygen towards the intracellular environment [23].

Based on the experimental results for *S. clavuligerus* cultivations in defined medium performed in STR and CT bioreactors, six metabolic scenarios corresponding to different phases during the cultivation time course were considered for the *in silico* metabolic flux analysis. The complete results of FBA simulations are available in the supplementary material S3. The selected scenarios coincide with different nutritional and environmental conditions attained in the bioreactor cultivations aiming at providing insights regarding the effect of oxygen and phosphate uptakes on the carbon fluxes along the metabolic network in connection with the CA biosynthesis and secretion. Experimental results showed that growth, nutrient uptake and metabolite secretion is essentially the same during the first 37 h of cultivation in both bioreactors. Thus, two scenarios of growth without nutrient limitation were considered for this interval: scenario 1 (SC1): initial growth phase in defined medium without nutrient limitation (0-12 h), and scenario 2 (SC2): exponential growth in defined medium without nutrient limitation (22-37 h). From 37 h onwards, the effect of nutritional and environmental conditions on growth and CA biosynthesis rate is more notorious. Then, two metabolic scenarios were selected as representative of the cultivation stages occurring between 48 and 62 h - scenario 3 (SC3): exponential growth in glycerol and glutamate with phosphate limitation in STR, and scenario 4 (SC4): exponential growth in glycerol and glutamate with phosphate limitation and respiratory quotient (RQ) =1 in CT cultivations. Similarly, two additional scenarios were explored based on the cultivation stage between 62 and 85 h - scenario 5 (SC5): growth in glycerol with phosphate limitation in STR, and scenario 6 (SC6): growth in glycerol with phosphate limitation and RQ=1 in CT bioreactor.

The scenarios with RQ=1 (SC 4 and SC6) were observed in the CT cultivations after 37 h as a consequence of a lower oxygen uptake with respect to carbon dioxide secretion. The lower and upper bounds of the exchange fluxes of the components of the defined medium were constrained between -1 and 1, respectively. The main nutrients uptakes, i.e. glycerol, glutamate, phosphate and ammonium, were set as equality constraints according to the experimentally observed flux since these are the main exchange fluxes in the network. For the case of the simulations with RQ=1, the exchange flux of carbon dioxide was also constrained to satisfy the RQ constraint. The constrained flux values and simulation results for specific growth rate, CA and oxygen exchange flux values are summarized in Table 4.3.

Table 4.3. Summary of experimental constraints and *in silico* growth rate, CA secretion and oxygen uptake using the iDG1237 model.

Scenario	t (h)	Mode	Bioreactor	Experimental constraints				Results			
				$v_{ex,Glyc}$	$v_{ex,Pi}$	$v_{ex,NH4}$	$v_{ex,Glu}$	μ	$v_{ex,CA}$	$v_{ex,O2}$	RQ*
SC1	0-22	Batch	STR &CT	-0.5	-0.1	-0.2	-0.5	0.06	0	-1.6	1.01
SC2	22-37	Batch	STR &CT	-2.0	-0.1	-0.9	-0.5	0.13	0	-3.84	1.20
SC3	37-68	Fed-batch	STR	-0.6	0	-0.2	-0.1	0.02	0.02	-0.53	0.94
SC4	37-68	Fed-batch	CT	-0.6	0	-0.2	-0.1	0.02	$6x10^{-3}$	-0.48	1.01
SC5	68-93	Fed-batch	STR	-0.6	0	-0.2	0	0.01	$9x10^{-3}$	-0.48	0.87
SC6	68-93	Fed-batch	CT	-0.6	0	-0.2	0	0.01	0	-0.42	1.01
MSE								$1.8x10^{-4}$	$9.8x10^{-5}$	0.28	0.02

*v in [mmol (g DCW.h)$^{-1}$] and μ in [h^{-1}]. RQ was constrained in scenarios SC4 and SC6 by matching the exchange flux of CO_2 with the uptake of O_2.

The specific production of CA varied because of a nutrient-specific effect in each metabolic scenario. The experimental evidences and FBA simulations showed no significant reaction flux towards CA biosynthesis prior to phosphate limitation (SC1 and SC2, between 0 and 37 h). Moreover, the oxygen uptake has an important influence on carbon flux distribution along the

central carbon metabolism. Under identical scenarios of phosphate limitation, decrease of oxygen uptake impacted negatively the carbon fluxes through the urea cycle, aspartate and arginine biosynthesis and carboxyethyl arginine as early precursor of CA. Additionally, under glutamate and phosphate depletions, the carbon fluxes through the glycolytic and TCA cycle also decrease as effect of reduced oxygen uptake. The main carbon fluxes along central metabolism are summarized in Figure 3 for the metabolic scenarios simulated under the constraints shown in Table 4.3.

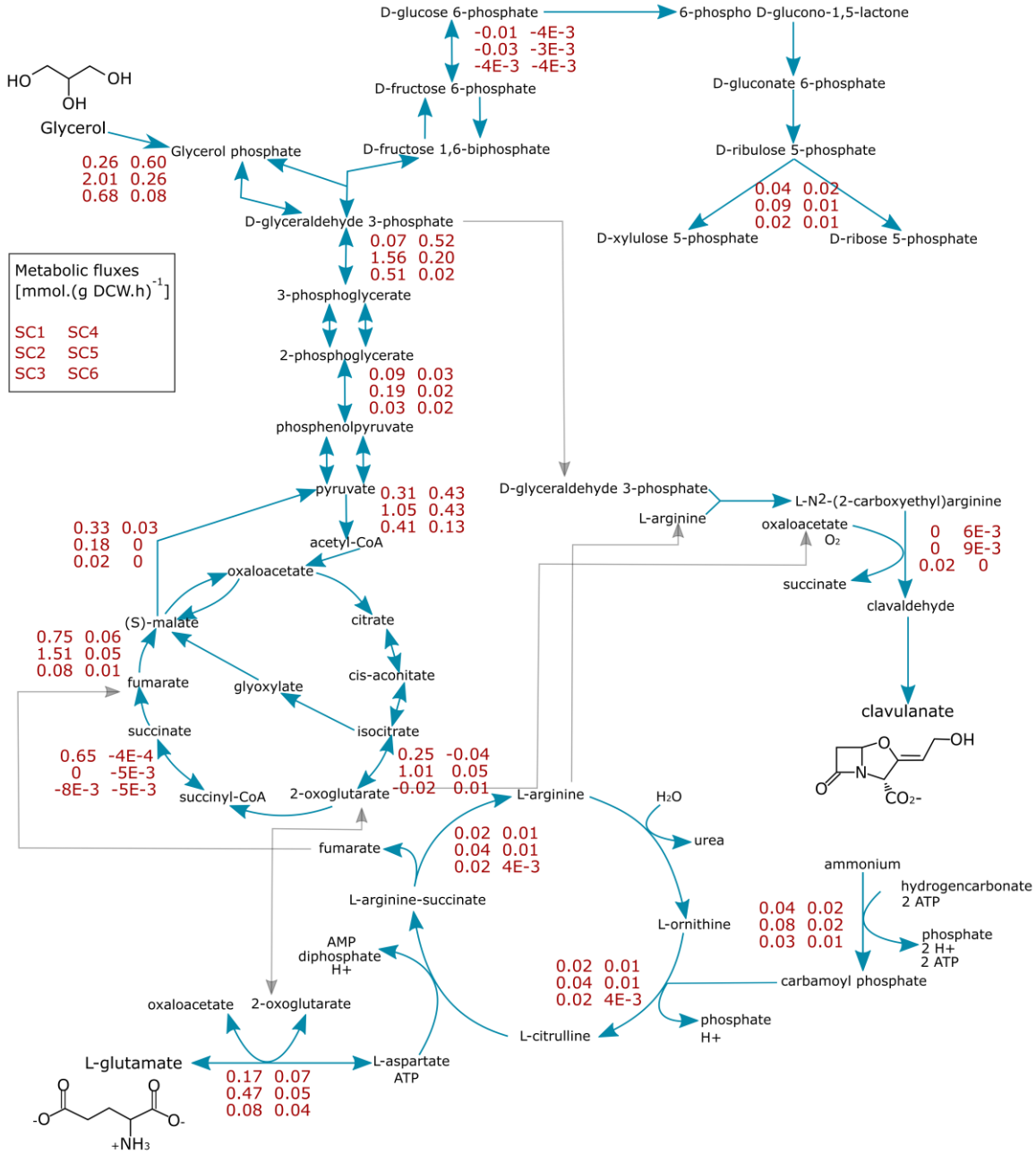

Figure 4.3. Summary of *in silico* carbon flux distribution throughout central metabolism and CA biosynthesis for *S clavuligerus* for the metabolic scenarios (SC1-SC6).

The simulation of SC1 and SC2 showed that the flux ratio between the pay-off phase of the glycolysis and the first oxidation in the TCA cycle, as well as the RQ approached to 1, most likely indicating a balanced metabolism. According to Li [33], an approximation of the RQ to 1 is expected as the C/N ratio decreases. This is consistent with higher nitrogen and amino acid uptakes with respect to glycerol uptake during the early stages of the cultivations. In these scenarios, the oxidative direction of TCA cycle was preferred, considering the oxidation of the carbon sources to promote the growth. FBA indicates that anaplerotic reactions catalyzed by PPC, citrate lyase (CITL) and the glyoxylate shunt are not activated under the described conditions.

Simulation of SC2 represented the exponential growth between 22 and 50 h. A significant increase in the glycerol uptake in this phase was experimentally verified. This condition led to an RQ=1.2 due to the increase in the CO_2 secretion associated to the significant carbon sources (glycerol and glutamate) oxidations linked to the maximum specific growth rate. Previous reports suggested that RQ values between 1 and 1.2 are characteristic of growth without nutrients limitation, while values out of this range are associated to limitation whether nitrogen or phosphate, affecting also the growth rate [33,34]. As expected, the high availability of nutrients derives in significant fluxes along lipids metabolism, membrane lipids and cell envelope biosynthesis. Synthesis of amino acids derived from glutamate (aspartate, ornithine and glycine) is favored in this scenario, activating the urea cycle in the biosynthetic direction to support the extensive biomass synthesis. The flux ratio between the carbon uptake and oxidation in the TCA cycle was 0.95 indicating higher fluxes through the TCA cycle in the oxidative direction aiming to provide the reduced cofactors and intermediates to the biosynthetic pathways. Under these conditions, the flux towards the secondary metabolism is not favored, indicating the dominancy of the biomass synthesis as observed in the experimental data (Figures 1 and 2). Therefore, activation of numerous reactions associated to membrane, lipids, nucleotides and amino acids biosynthesis were observed in addition to the highest activity observed throughout the respiratory chain, 9.5 mmol (g DCW.h)$^{-1}$. The exponential growth causes a rapid phosphate depletion, which then stimulates the production of CA from 37 h onwards.

The highest reaction flux towards the CA pathway (0.02 mmol (g DCW.h)$^{-1}$) was observed in SC3 coinciding with the maximum experimental CA production observed (Figure 1). This scenario was macroscopically characterized by a decrease of growth rate, glycerol and glutamate uptakes probably due to the phosphate limitation and the decline in the extracellular glutamate concentration and in the RQ down to 0.94. FBA showed a higher specific demand of oxygen in SC3 compared with SC4. Since, the only difference between SC3 and SC4 is the constraint related to the RQ, the observed changes in intracellular reaction fluxes are only attributable to the difference in oxygen uptake. The metabolic imbalance caused by the higher oxygen uptake (+10%) in SC3 coincided *in silico* with the highest CA production rate and with a slight flux depletion (<6%) in 83% of the active reactions in comparison with SC4. In *S. clavuligerus* cultivations the ammonium salts are commonly used as nitrogen source. Therefore, amino acids biosynthesis and urea cycle are activated by the constant fluxes of ammonium and intermediates from TCA cycle, scenario also favored by the intracellular accumulation of glutamate. Interestingly, under the conditions of SC3, most of the flux-increasing reactions are related to TCA cycle, amino acids metabolism and CA biosynthesis. Additionally, the higher oxygen uptake derived in a mean increase along the dehydrogenases of the respiratory chain of 5%, as for the case of cytochrome BD (CYTBD). In this regard, CA biosynthesis requires molecular oxygen for carrying out the oxidation steps catalyzed by the CAS, increasing at the same time the demand for reduced cofactors, given likely the final NADPH-dependent reduction of clavulanate-9-aldehyde into CA by the clavulanate dehydrogenase (CAR) [35].

Interestingly, the fluxes of reactions dependent on glutamate as substrate were up to 1.7 higher in SC3 in comparison with SC4. Those reactions include the catalyzed by ASPTA and glutamine synthetase (GLNS) reacting in the direction of aspartate and glutamine production, respectively. The formation of a pool of glutamine impulses the reaction catalyzed by the Carbamoyl-phosphate synthase (CBPS) towards carbamoyl phosphate, increasing also the availability of glutamate. Thus, the glutamate, glutamine, carbamoyl phosphate and aspartate pools direct the urea cycle to arginine

succinate lyase (ARGSL), whose flux is 1.7-fold the observed in SC4. The large availability of arginine and GAP from glycerol promotes the flux in the CA biosynthesis pathway, increasing the reaction flux up to 2.6-fold compared with SC4. During CA biosynthesis, the carbon flux towards asparagine synthase (ASNS) decreases, hence reducing the pool of asparagine as consequence of the observed high fluxes of aspartate and glutamine into the urea cycle. These FBA results are consequent with the experimentally observed lower accumulations of arginine, aspartate and glutamine and asparagine in the STR reactor (Figure 2), since the demand for these products from urea cycle mainly, would avoid their extensive accumulation during CA production.

Accumulations of oxaloacetate, succinate, aspartate, asparagine, arginine and glutamine were observed when CA is produced. Those experimental results are consistent with the *in silico* observed increments in the reaction fluxes along their producing pathways. Nevertheless, the extensive accumulation of those products during the cultivations might indicate the downstream repression of CA biosynthesis due to nutritional down-regulation in conditions of reduced oxygen uptake. Succinate accumulation due to high formation fluxes increases the reaction fluxes of fumarate, malate, oxaloacetate and succinyl-CoA in the TCA cycle [5]. Succinyl-CoA accumulation displaces the reversible reaction of 2-oxoglutarate dehydrogenase (AKG) towards 2-oxoglutarate production while reducing the fluxes of aconitase (ACONT) and isocitrate dehydrogenase (ICDH). Thus generating a pool of 2-oxoglutarate, which is further demanded during amino acids metabolism and CA biosynthesis. The higher reaction fluxes observed in the reactions dependent on malate and oxaloacetate, as the case of malate dehydrogenase (MDH) and ASPTA, agree with the lower accumulations of these intermediates in the STR cultivations compared with CT cultivations (Figure 2). Figure 4 displays the reaction fluxes of representative enzymes of central and amino-acids metabolism in metabolic scenarios SC3, SC4, SC5 and SC6 referred to glycerol uptake.

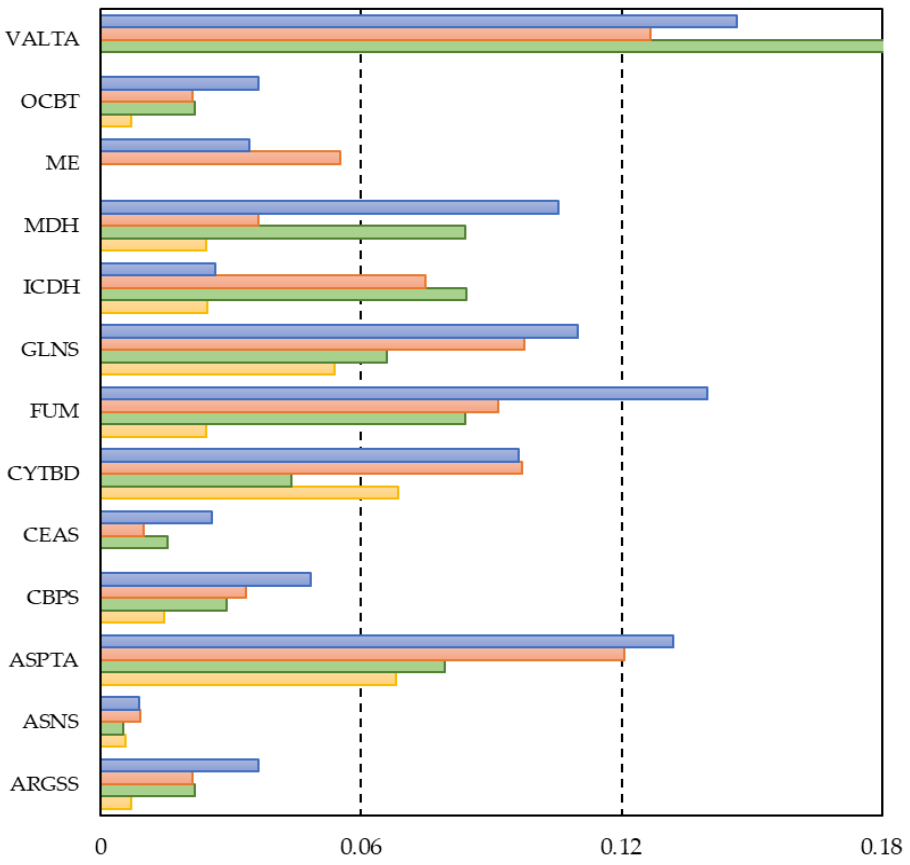

Figure 4.4. In silico flux ratio respect to glycerol uptake of representative enzymes in simulated scenarios of phosphate limitation and reduced oxygen uptake; SC3 (blue), SC4 (red), SC5 (green), SC6 (orange).

A differentiation between phosphate limited and non-limited scenarios is plausible. Under identical constrains, FBA simulations shows that oxygen uptake increases during phosphate limitation up to 17%, leading to an increase in the activity of dehydrogenases of at less 6%. It is known that Pi promotes the biomass accumulation but prevents the production of secondary metabolites in Streptomyces species, which is sometimes reflected in the transcription of biosynthetic gene clusters [36,37]. The role of phosphate repression in *Streptomyces sp.* and its relationship with activation of antibiotics biosynthetic pathways is still an open matter, since complex signaling and regulation cascades presumably respond to phosphate depletion to maintain the cellular functions, the energetic balance and to activate defense mechanisms [38]. In the case of *S. clavuligerus,* phosphate represses not only the CA biosynthesis but also the biosynthesis of cephamycin C [39].

Apart from transcriptomic and proteomic evidence, FBA shows a stoichiometric relationship between the phosphate depletion and activation of CA biosynthesis. The phosphate exhaustion necessarily implies the activation of reactions to compensate the lack of Pi [37,38]. Simulations showed that phosphate limited metabolic scenarios increase the fluxes in several glutamate-dependent reactions, contributing to supply Pi or PPi from ATP hydrolysis. This is the case of N-acetyl-γ-glutamyl-phosphate reductase (AGPR), ornithine carbamoyltransferase (OCBT), argininesuccinate synthase (ARGSS), CBPS and GLNS, which also increase the flux of urea cycle towards the production of arginine. Additionally, the reactions catalyzed by the 2-(2-carboxyethyl) arginine synthase (CEAS) and the (carboxyethyl) arginine beta-lactam-synthase (BLS) are activated under phosphate limitation, since they produce Pi and PPi as by-products. PPi is further hydrolyzed by the inorganic diphosphatase (PPA), whose flux increases 43% under P-limitation. Moreover, on the early stage of cultivation (SC1) the phosphate availability and low accumulation of succinate direct the reaction catalyzed by the succinyl-CoA (SUCOAS) synthetase towards ATP and succinate formation, but the opposite occurs if phosphate is depleted, the reaction is reversed to generate succinyl-CoA and Pi. Presumably, the demand for Pi from essential reactions activate fluxes from secondary reactions having Pi as product, and then these metabolites are synthetized. Thus, CA biosynthesis might be favored by the stoichiometric requirements for maintaining the intracellular pool of Pi.

The primary response to phosphate limitation in the phylogenetic related *Streptomyces coelicolor* (*S. coelicolor)* involves upregulation of genes involving phosphate mediated reactions in order to obtain phosphate from different sources [37,38]. In this regard, transcriptomics and proteomic analysis of wild type *S. coelicolor* under P-limitation showed upregulation of SUCD, cytochrome B, phosphoglycerate mutase (PGM), glyceraldehyde dehydrogenase (GAPD), adenylate kinase (ADK), GLNS, MDH, SUCOAS and several aminotransferases [37]. Additionally, the downregulations of cysteine and histidine synthesis, as well as the cytochrome bd oxidase (CYTBD) were observed [37]. Those results obtained in the transcription level for the model organism *S. coelicolor* coincide with the FBA results of our simulations of P-limited scenarios for the related species *S. clavuligerus*.

In the case of limited synthetic media, the amino acid feed is aimed to increase the flux in the direction of the biosynthetic pathways hence improving the product yield respect to non-supplemented cultures [20]. Simulation of SC6 and SC7 considered the glutamate exhaustion observed in the STR and CT cultivations after 68 h.

FBA results suggest that availability of glutamate affects positively the carbon flux towards CA biosynthesis since this amino acid is downstream related with arginine as the C-5 precursor of CA. Indeed, the highest biosynthesis rate of CA was observed in the STR cultivations when both conditions, phosphate limitation and glutamate availability, coexisted. In this regard,

Rodriguez-García et al. [37] reported that transcriptomic analysis of phosphate limitation in *S. coelicolor* indicated up-regulation of genes encoding the glutamate transporters [37].

Simulation of SC5 showed that glutamate starvation increases the flux along the glycolysis due to a reduction in the pool of acetyl-CoA. The demand for TCA intermediates, mainly oxaloacetate and 2-oxoglutarate, implies a higher requirement for acetyl-CoA from pyruvate, increasing 10% the flux through the enolase (ENO) and downstream pyruvate kinase (PYK) and pyruvate dehydrogenase (PDH). Consequently, in the reactions of TCA catalyzed by CS, ACONT and ICDH, increased their fluxes up to 70% with respect to SC3. Since glutamate is constantly demanded to feed the urea cycle, valine degradation might act as an auxiliary supply of glutamate. This is evidenced by the increase of reaction fluxes through valine transaminase (VALTA) and valine dehydrogenase (VALDH) under glutamate depletion. As expected, the lower supply of carbon in SC5 and SC6 leads to a decrease in the global activity of dehydrogenases of the respiratory chain up to 55% with respect to SC3 and SC4. Glutamate starvation also favor the activation of PPC as consequence of the increase in the carbon flux in the glycolysis, providing oxaloacetate for the amino acids metabolism when CA is produced.

The lower oxygen uptake in SC6 might originate from a decreased TCA cycle activity leading to a lower demand of oxygen as electrons receptor in the respiratory chain, coinciding also with a lower activity in dehydrogenases like ICDH and MDH, as well as in the CYTBD (Figure 4). Moreover, the increase of the flux (45%) towards pentose-phosphate and gluconeogenesis pathways shown in Figure 3 are coincident with the reduction along the pay-off phase of glycolysis and TCA, since inhibition of CA production decrease the downstream demand for precursors coming from glycerol catabolism.

4.4. Conclusions

In this work, we developed a new and improved computational genome-scale model of *S. clavuligerus* by using a state-of-the-art top-down approach during the reconstruction. The reconstruction started from the most-recent genome assembly reported for *S. clavuligerus* and it was manually curated for a more realistic representation of the cell metabolism. The resultant iDG1237 model showed better predictive capabilities compared with its predecessors in relation to biomass and product biosynthesis, network topology, thermodynamic consistency and simulation of metabolic scenarios of nutritional limitation. The present model constitutes a new basis for computer-aided analysis and design of CA production scenarios as well as strain engineering.

The *in silico* and experimental results of this study provide new insights to the understanding of the role of nutritional regulation in CA production by *S. clavuligerus,* based on an *in silico* stoichiometric analysis of the effects of phosphate and oxygen limitations experimentally observed in cultures performed in stirred tank and single-use rocking-motion biorreactors. The phosphate depletion leads to a considerable increase of fluxes through the reactions involving phosphate and pyrophosphate to stoichiometrically supplied phosphate to central metabolism and biosynthetic pathways. CA biosynthesis might be favored by such stoichiometric requirements, since the phosphate producer reactions mediated by CEAS and the BLS would contribute to maintain the intracellular pool of Pi. Specifically, in the context of growth in defined media, the glutamate availability would increase the reaction fluxes along glutamate degradation and urea cycle pathways, increasing at the same time the pool of Pi and arginine, and triggering CA biosynthesis.

Moreover, the experimental evidence showed that the stoichiometric effect of phosphate depletion does not enhance itself CA production, as it requires molecular oxygen in the oxidation reactions catalyzed by the CAS, otherwise CA production is not favored. The present combined experimental and modelling approach highlighted the importance of the metabolic relationship between the TCA cycle intermediates, amino-acids biosynthesis, phosphate and oxygen uptakes and CA production. Further exploration of metabolic scenarios considering nutritional and genetic regulation of metabolism could contribute to stablish suitable conditions for obtaining CA-overproducer strains.

Publication: This chapter was accepted to be published as *Gómez-Rios, D; López-Agudelo, V.A.; Ramírez-Malule, H.; Neubauer, P.; Junne, S.; Ochoa, S.; *Ríos-Estepa, R. A genome-scale insight into the effect of shear stress during the fed-batch production of clavulanic acid by *Streptomyces clavuligerus*. *Microorganisms* **2020.**

References

1. López-Agudelo, V.A.; Baena, A.; Ramirez-Malule, H.; Ochoa, S.; Barrera, L.F.; Ríos-Estepa, R. Metabolic adaptation of two in silico mutants of Mycobacterium tuberculosis during infection. *BMC Syst. Biol.* **2017**, *11*, 1–18.
2. Medema, M.H.; Alam, M.T.; Heijne, W.H.M.; Van Den Berg, M.A.; Müller, U.; Trefzer, A.; Bovenberg, R.A.L.; Breitling, R.; Takano, E. Genome-wide gene expression changes in an industrial clavulanic acid overproduction strain of Streptomyces clavuligerus. *Microb. Biotechnol.* **2011**, *4*, 300–305.
3. Toro, L.; Pinilla, L.; Avignone-Rossa, C.; Ríos-Estepa, R. An enhanced genome-scale metabolic reconstruction of Streptomyces clavuligerus identifies novel strain improvement strategies. *Bioprocess Biosyst. Eng.* **2018**, *41*, 657–669.
4. Gómez-Cerón, S.; Galindo-Betancur, D.; Ramírez-Malule, H. Data set of in silico simulation for the production of clavulanic acid and cephamycin C by Streptomyces clavuligerus using a genome scale metabolic model. *Data Br.* **2019**, *24*, 103992.
5. Ramirez-malule, H.; Junne, S.; Cruz-bournazou, M.N.; Neubauer, P. Streptomyces clavuligerus shows a strong association between TCA cycle intermediate accumulation and clavulanic acid biosynthesis. *Appl. Microbiol. Biotechnol.* **2018**, *102*, 4009–402.
6. Machado, D.; Andrejev, S.; Tramontano, M.; Patil, K.R. Fast automated reconstruction of genome-scale metabolic models for microbial species and communities. *Nucleic Acids Res.* **2018**, *46*, 7542–7553.
7. Cao, G.; Zhong, C.; Zong, G.; Fu, J.; Liu, Z.; Zhang, G.; Qin, R. Complete Genome Sequence of Streptomyces clavuligerus F613-1, an Industrial Producer of Clavulanic Acid . *Genome Announc.* **2016**, *4*, 4–5.
8. Buchfink, B.; Xie, C.; Huson, D.H. Fast and sensitive protein alignment using DIAMOND. *Nat. Methods* **2014**, *12*, 59.
9. Schellenberger, J.; Lewis, N.E.; Palsson, B. Elimination of thermodynamically infeasible loops in steady-state metabolic models. *Biophys. J.* **2011**, *100*, 544–553.
10. Henry, C.S.; Broadbelt, L.J.; Hatzimanikatis, V. Thermodynamics-based metabolic flux analysis. *Biophys. J.* **2007**, *92*, 1792–1805.
11. Noor, E. Removing both Internal and Unrealistic Energy-Generating Cycles in Flux Balance Analysis. *arXiv:1803.04999v1* 2018.
12. Desouki, A.A.; Jarre, F.; Gelius-Dietrich, G.; Lercher, M.J. CycleFreeFlux: Efficient removal of thermodynamically infeasible loops from flux distributions. *Bioinformatics* **2015**, *31*, 2159–2165.
13. Martínez, V.S.; Nielsen, L.K. NExT : Integration of Thermodynamic Constraints and Metabolomics Data into a Metabolic Network. In *Metabolic Flux Analysis. Methods in Molecular Biology (Methods and Protocols)*; Krömer, J., Nielsen, L., Blank, L., Eds.; Humana Press: New York, NY, 2012; Vol. 1191, pp. 65–78 ISBN 9781617796173.
14. Yousofshahi, M.; Ullah, E.; Stern, R.; Hassoun, S. MC3: A steady-state model and constraint consistency checker for biochemical networks. *BMC Syst. Biol.* **2013**, *7*.
15. Orth, J.D.; Thiele, I.; Palsson, B.O. What is flux balance analysis? *Nat. Biotechnol.* **2010**, *28*, 245–248.
16. Holzhütter, H.G. The principle of flux minimization and its application to estimate stationary fluxes in metabolic networks. *Eur. J. Biochem.* **2004**, *271*, 2905–2922.
17. Roubos, J.A.; Krabben, P.; De Laat, W.; Heijnen, J.J. Clavulanic Acid Degradation in Streptomyces clavuligerus Fed-Batch Cultivations. *Biotechnol. Prog.* **2002**, *18*, 451–457.
18. Medema, M.H.; Trefzer, A.; Kovalchuk, A.; van den Berg, M.; Müller, U.; Heijne, W.; Wu, L.; Alam, M.T.; Ronning, C.M.; Nierman, W.C.; et al. The Sequence of a 1.8-Mb Bacterial Linear Plasmid Reveals a Rich Evolutionary Reservoir of Secondary Metabolic Pathways. *Genome Biol. Evol.* **2010**, *2*, 212–224.
19. Marashi, S.A.; Bockmayr, A. Flux coupling analysis of metabolic networks is sensitive to missing reactions. *BioSystems* **2011**, *103*, 57–66.
20. Bushell, M.E.; Kirk, S.; Zhao, H.; Avignone-rossa, C.A. Manipulation of the physiology of clavulanic acid biosynthesis with the aid of metabolic flux analysis. *Enzyme Microb. Technol.* **2006**, *39*, 149–157.

21. Dunstan, G.H.; Avignone–Rossa, C.; Langley, D.; Bushell, M.E. The Vancomycin biosynthetic pathway is induced in oxygen-limited Amycolatopsis orientalis (ATCC 19795) cultures that do not produce antibiotic. *Enzyme Microb. Technol.* **2000**, *27*, 502–510.
22. Ives, P.R.; Bushell, M.E. Manipulation of the physiology of clavulanic acid production in Streptomyces clavuligerus. *Microbiology* **1997**, *143*, 3573–3579.
23. Gómez-Ríos, D.; Junne, S.; Neubauer, P.; Ochoa, S.; Ríos-Estepa, R.; Ramírez-Malule, H. Characterization of the Metabolic Response of Streptomyces clavuligerus to Shear Stress in Stirred Tanks and Single-Use 2D Rocking Motion Bioreactors for Clavulanic Acid Production. *Antibiotics* **2019**, *8*, 168.
24. Hodgson, D. a Primary metabolism and its control in streptomycetes: a most unusual group of bacteria. *Adv. Microb. Physiol.* **2000**, *42*, 47–238.
25. Viollier, P.H.; Minas, W.; Dale, G.E.; Folcher, M.; Thompson, C.J. Role of Acid Metabolism in Streptomyces coelicolor Morphological Differentiation and Antibiotic Biosynthesis. *J. Bacteriol.* **2001**, *183*, 3184–3192.
26. Zhang, Z.; Ren, J. shan; Harlos, K.; McKinnon, C.H.; Clifton, I.J.; Schofield, C.J. Crystal structure of a clavaminate synthase-Fe(II)-2-oxoglutarate-substrate-NO complex: Evidence for metal centred rearrangements. *FEBS Lett.* **2002**, *517*, 7–12.
27. Ozcengiz, G.; Demain, A.L. Recent advances in the biosynthesis of penicillins, cephalosporins and clavams and its regulation. *Biotechnol. Adv.* 2013, *31*.
28. Kurt-Kizildoğan, A.; Vanli-Jaccard, G.; Mutlu, A.; Sertdemir, I.; Özcengiz, G. Genetic engineering of an industrial strain of Streptomyces clavuligerusfor further enhancement of clavulanic acid production. *Turkish J. Biol.* **2017**, *41*, 342–353.
29. Arulanantham, H.; Kershaw, N.J.; Hewitson, K.S.; Hughes, C.E.; Thirkettle, J.E.; Schofield, C.J. ORF17 from the clavulanic acid biosynthesis gene cluster catalyzes the ATP-dependent formation of N-glycyl-clavaminic acid. *J. Biol. Chem.* **2006**, *281*, 279–287.
30. Bushell, M.E.; Kirk, S.; Zhao, H.-J.; Avignone-Rossa, C.A. Manipulation of the physiology of clavulanic acid biosynthesis with the aid of metabolic flux analysis. *Enzyme Microb. Technol.* **2006**, *39*, 149–157.
31. Kirk, S.; Avignone-rossa, C.A.; Bushell, M.E. Growth limiting substrate affects antibiotic production and associated metabolic fluxes in Streptomyces clavuligerus. *Biotechnol. Lett.* **2000**, *22*, 1803–1809.
32. Saudagar, P.S.; Singhal, R.S. Optimization of nutritional requirements and feeding strategies for clavulanic acid production by Streptomyces clavuligerus. *Bioresour. Technol.* **2007**, *98*, 2010–2017.
33. Li, X.; Yu, C.; Yao, J.; Wang, Z.; Lu, S. An Online Respiratory Quotient-Feedback Strategy of Feeding Yeast Extract for Efficient Arachidonic Acid Production by Mortierella alpina. *Front. Bioeng. Biotechnol.* **2018**, *5*, 1–11.
34. Xiao, J.; Shi, Z.; Gao, P.; Feng, H.; Duan, Z.; Mao, Z. On-line optimization of glutamate production based on balanced metabolic control by RQ. *Bioprocess Biosyst. Eng.* **2006**, *29*, 109–117.
35. MacKenzie, A.K.; Kershaw, N.J.; Hernandez, H.; Robinson, C. V.; Schofield, C.J.; Andersson, I. Clavulanic Acid Dehydrogenase: Structural and Biochemical Analysis of the Final Step in the Biosynthesis of the β-Lactamase Inhibitor Clavulanic Acid. *Biochemistry* **2007**, *46*, 1523–1533.
36. Bibb, M.J. Regulation of secondary metabolism in streptomycetes. *Curr. Opin. Biotechnol.* **2005**, *8*, 208–215.
37. Rodríguez-García, A.; Barreiro, C.; Santos-Beneit, F.; Sola-Landa, A.; Martín, J.F. Genome-wide transcriptomic and proteomic analysis of the primary response to phosphate limitation in Streptomyces coelicolor M145 and in a ΔphoP mutant. *Proteomics* **2007**, *7*, 2410–2429.
38. Barreiro, C.; Martínez-Castro, M. Regulation of the phosphate metabolism in Streptomyces genus: impact on the secondary metabolites. *Appl. Microbiol. Biotechnol.* **2019**, *103*, 1643–1658.
39. Saudagar, P.S.; Survase, S.A.; Singhal, R.S. Clavulanic acid: A review. *Biotechnol. Adv.* **2008**, *26*, 335–351.

Chapter 5

Implementation of a Dynamic Genome-Scale Metabolic Modeling Approach for the Phenotypical Description and Analysis of the Metabolic Performance of *Streptomyces clavuligerus* for Clavulanic Acid Production

Abstract: *Streptomyces clavuligerus (S. clavuligerus)* is a filamentous Gram-positive bacterium producer of the β-lactamase inhibitor clavulanic acid (CA). Antibiotics biosynthesis and secretion in the *Streptomyces* genus is closely related with nutritional and environmental perturbations. In this work, the integration of a dynamic flux balance analysis approach (DFBA) with a validated genome scale metabolic network (GSMN) of *S. clavuligerus* was used for the description of its intracellular metabolic performance during batch and fed-batch cultures. The application of the DFBA framework provided insights about the role of central metabolism in CA biosynthesis and allowed to study the impact of the operation mode and potential genetic modifications on CA production. The experimental testing of fed-batch cultivations in synthetic media and under glutamate and phosphate limitations enhanced the CA secretion.

5.1. Introduction

Secondary metabolism of *S. clavuligerus* expressed under nutritional restrictions, mainly under phosphate limitation, lead to secretion of two main β-lactam antibiotics: (i) cephamicyn C (CephC), a cephem type compound, and (ii) clavulanic acid (CA), a β-lactamase inhibitor with an oxapenam bicyclic ring. Due to the clinical importance of CA and low titers when cultivating the wild-type strain, considerable efforts have been dedicated in order to improve the nutritional and environmental cultivation conditions, as previously reviewed by Saudagar et al [1], Paradkar [2] and more recently by Ser et al [3]. Genetic engineering has been also explored as alternative for rational strain design showing that modification of metabolic and regulatory features could increase the CA production in the laboratory scale [4–6].

The systems biology approach constitutes a rational framework for studying the effect of genetic and environmental perturbations on metabolism through the application of mathematic, biochemical and biologic knowledge. In this regard, the large-scale genome analyses and the genome-scale constraint-based modeling allow the *in silico* evaluation of the global physiology of a cell with respect to nutritional and environmental perturbations in connection with cellular regulations at different levels, e.g. gene expression, transcriptional regulation and metabolic fluxes distribution [7]. This analysis can provide information of suitable bioprocessing conditions or also it can be used to predict potential metabolic targets for further application of genetic engineering approaches.

The pseudo-steady state genome-scale modeling - through application of flux balance analysis (FBA) - has contributed to understand the physiology of *S. clavuligerus* regarding nutritional conditions, gene essentiality, activation of secondary metabolism and antibiotics secretion [8,9]. Despite the meaningful results of those FBA approaches, they are not capable of capturing the time-dependent concentration changes, the dynamic intracellular metabolic responses to external conditions and other related perturbations [10], mostly due to the pseudo-steady state assumption during the model derivation and mathematical solution. Unstructured models, like those derived from Monod or Michaelis-Menten kinetic rate expressions, have been widely used to describe the macroscopic microbial growth, substrates consumption and products secretion in dynamic models. However, this kind of models do not provide information of intracellular fluxes distribution. The

pseudo-steady state approaches could predict the intracellular and exchange reaction fluxes based on stoichiometric mass balance of a metabolic reaction network in a single condition, which is determined by the solution of a constrained Linear Programming (LP) optimization problem. Therefore, the traditional FBA approach presents some limitations, such as the prediction of cellular growth and product secretion rates only for fixed values of substrate uptake rates and its strict applicability to the balanced growth phase in batch cultures or steady-state growth in continuous cultures.

Since cells in a culture are naturally in a dynamic condition, a nonlinear behavior and property variations are expected during the process time. This fact has repercussions on prediction of cell phenotypical states, product yield and bioreactor control. Quantitative mathematical models are needed to describe the dynamics process and the interrelation among relevant variables [11]. A feasible approach for dealing with dynamic metabolic modeling of cellular cultures was proposed by Mahadevan *et al.* [12], considering a dynamic extension of classic FBA. The dynamic flux balance analysis (DFBA) is aimed to predict the time-dependent intracellular reaction fluxes and metabolite concentrations of unsteady state bioprocess, e.g. batch and fed-batch cultivations, which are the most common operation modes in bioprocessing industry [13]. Additionally, the DFBA approach can also incorporate kinetic expressions for the cases with well characterized kinetics [12,13].

DBFA includes the dynamic description of intracellular and extracellular process by means of kinetic equations with a small number of additional parameters, including the formulation of substrate uptake kinetics to account for known regulatory processes [13]. DFBA imposes constraints on fluxes at each time interval, those constraints are typically expressed as kinetic expressions (e.g. Monod or Michaelis-Menten) depending on time-varying concentrations of substrates and products linked to the constrained flux [14].

Two DFBA formulations were proposed by Mahadevan *et al.*[12]: the Dynamic Optimization Approach (DOA) and the Static Optimization Approach (SOA). The DOA performs an optimization solving a Nonlinear Programming (NLP) problem, which in turn, solves a system of algebraic differential equations once over the entire time period of interest, allowing to obtain time profiles of fluxes and metabolite levels [12]. The SOA divides the total time into several time intervals and solves an instantaneous optimization problem using LP at the beginning of each time interval, followed by integration over the interval, allowing to know the flux distribution at a particular time instant [12].

The DOA is still limited to small-scale metabolic models and it is restrictive in terms of computational power due to the dimensional explosion derived from time discretization of the equations [10]. The SOA is a straight-forward implementation more appropriated for genome scale metabolic network (GSMN) applications, since the static LP solution requires much less computational power and time. Therefore, the SOA formulation is scalable to larger metabolic networks. SOA allows the external environment to change each time-step, hence adjusting the constraints and/or objective functions according to the modified external environment, allowing to obtain the new solution valid for the interval [10,15,16]. Moreover, the significance of the results is independent of the mathematical approach used, since no significant difference in the concentrations and flux profiles have been observed when comparing the DOA and SOA [12,16]. Recently, DFBA-SOA has been successfully applied in the analysis of GSMN for prediction and description of phenotypes, as well as culture dynamics of several microorganisms of industrial interest like *Streptomyces tsukubaensis* [10], *Clostridium butyricum* [16] and *Chlamydomonas reinhardtii* [17]. In this work, a DFBA framework was used for the analysis of dynamic characteristics of *S. clavuligerus* metabolism in connection with CA production and cultivation operation mode aimed to explore potential metabolic scenarios that might lead to the enhancement of CA production in wild-type and *in silico* engineered strains.

5.2. Materials and Methods

5.2.1 Microorganism, cultivation media and experimental conditions

S. clavuligerus DSM 41826, cryo-preserved at −80°C in glycerol solution (16.7% v/v), was inoculated for activation in seed medium as described by Roubos et al. [17]. Cultivations were carried out in duplicate in a 15 L stirred tank bioreactor (STR) (Techfors S, Infors AG, Bottmingen, Switzerland) and 20 L single-use rocking-motion bioreactor CELL-tainer® (CT) (Cell-tainer Biotech BV, Winterswijk, The Netherlands) both operated at 5 L initial filling volume. Cultivation and analytical procedures were described in detail in the chapter 3.

Additionally, batch (50 h) and fed-batch (110 h) cultivations of *S. clavuligerus* ATCC 27064 wild-type were carried out by duplicate in a 1 L stirred tank bioreactor (STR) (BIOSTAT® A, Sartorius, Göttingen, Germany) operated at 0.5 L (batch volume) with the previously chemically defined medium. Fed-batch operation was carried out using non-supplemented and glutamate-supplemented feeding media. In the case of fed-batch operation with glutamate-supplemented medium, the feeding was implemented at 34 h up to reaching a final volume of 0.75 L. Modified feeding defined medium was prepared as follows (in $g.L^{-1}$ deionized and distilled water): glycerol, 120.0; K_2HPO_4, 2.0; $(NH_4)_2SO_4$, 8.0 and monosodium glutamate, 100.

5.2.2 Genome scale metabolic model and FBA simulations

The GSMN iDG1237 reconstructed from the genome reference for *S. clavuligerus* (NCBI refseq GCA_001693675.1) was used for the DFBA simulations with the SOA. The iDG1237 model consists of 2177 reactions, including 543 internal/external metabolite exchange reactions and 1237 annotated genes. This model was previously checked and manually curated for improving the thermodynamic consistency and connectivity. Then, it was validated in pseudo-steady state conditions with experimental chemostat data. To check the sensitivity of the GSMN to the dynamic constrains to be further applied, FBA simulations were performed for exploring the effect of varying the key nutrients uptakes on biomass synthesis (Z) and CA secretion flux ($v_{CA,e}$) as objective functions, formulated as presented in Eqs. 1 and 2, respectively.

$$\begin{bmatrix} Max\ Z = f^T v \\ s.t.\quad S \cdot v = 0 \\ l_b \leq v \leq u_b \end{bmatrix} \tag{1}$$

$$\begin{bmatrix} Max\ v_{CA\_ex} \\ s.t.\quad S \cdot v = 0 \\ l_b \leq v \leq u_b \end{bmatrix} \tag{2}$$

Additionally, the GSMN was used for identification of potential metabolic targets for gene knockout, dampening and/or overexpression that might favor the CA biosynthesis in *S. clavuligerus* cultures. Initially, a gene essentiality analysis in synthetic medium was performed, which was followed by the application of the RoBoKoD (Robust, Overexpression, Knockout and Dampening) pipeline for determination of the potential gene candidates [40]. The RoBoKoD method has been used previously for *in silico* strain design of *S. clavuligerus* (iLT1021) and *Escherichia coli* (iNS142) [9,40].

5.2.3 Kinetic model

A first-principles based model of *S. clavuligerus* growth was constructed considering the consumption of glycerol and glutamate as carbon sources so as other nutrients like ammonium, phosphate and oxygen. Glycerol ($C_3H_8O_3$) and glutamate ($C_5H_9O_4$) are used as carbon sources during the exponential growth phase while ammonium (NH_4^+) is required as nitrogen source for growth in glycerol while glutamate provides both, carbon and nitrogen. Phosphate (H_2PO_4) is required in small

amounts to support biomass synthesis. Since *S. clavuligerus* is a strictly aerobic microorganism, it requires molecular oxygen (O_2) for respiration, hence producing CO_2 and water [32]. Based on the simplified stoichiometry of biomass synthesis, a kinetic Monod model was proposed for describing the growth, nutrients consumption and by-products excretion. The resultant system of ordinary differential equations (ODE) describing the mass balances is presented in Eq. 3-10.

$$\frac{dV}{dt} = F \tag{3}$$

$$\frac{dX}{dt} = X\left(\mu_{Glyc} + \mu_{Glu} - k_d\right) - \left(\frac{F}{V}\right)X \tag{4}$$

$$\frac{dC_{Glyc}}{dt} = X\left(\frac{-\mu_{Glyc}}{Y_{X/Glyc}}\right) + \left(\frac{F}{V}\right)\left(C_{Glyc,f} - C_{Glyc}\right) \tag{5}$$

$$\frac{dC_{Glu}}{dt} = X\left(\frac{-\mu_{Glu}}{Y_{X/Glu}}\right) + \left(\frac{F}{V}\right)\left(C_{Glu,f} - C_{Glu}\right) \tag{6}$$

$$\frac{dC_{Pi}}{dt} = X\left(\frac{-\mu_{Glyc}}{Y_{X/Pi,Glyc}} + \frac{-\mu_{Glu}}{Y_{X/Pi,Glu}}\right) + \left(\frac{F}{V}\right)\left(C_{Pi,f} - C_{Pi}\right) \tag{7}$$

$$\frac{dC_{O2}}{dt} = X\left(\frac{-\mu_{Glyc}}{Y_{X/O2,Glyc}} + \frac{-\mu_{Glu}}{Y_{X/O2,Glu}}\right) + OTR \tag{8}$$

$$\frac{dC_{NH3}}{dt} = X\left(\frac{-\mu_{Glyc}}{Y_{X/NH4,Glyc}} + \frac{\mu_{Glu}}{Y_{X/NH4,Glu}}\right) + \left(\frac{F}{V}\right)\left(C_{NH4,f} - C_{NH4}\right) \tag{9}$$

$$\frac{dC_{CO2}}{dt} = X\left(\frac{\mu_{Glyc}}{Y_{X/CO2,Glyc}} + \frac{\mu_{Glu}}{Y_{X/CO2,Glu}}\right) + GTR \tag{10}$$

The specific growth rates in glycerol and glutamate were defined according to the usual Monod rate expression, as showed in Eqs. 11 to 13, respectively. The total growth rate (μ_{Kin}), defined by Eq. 15, is the sum of individual growth rates in each carbon source:

$$\mu_{Glyc} = \frac{\mu_{Glyc,max}\, C_{Glyc}}{K_{Glyc}X + C_{Glyc}} \tag{11}$$

$$\mu_{Glu} = \frac{\mu_{Glu,max}\, C_{Glu}}{K_{Glu}X + C_{Glu}} \tag{12}$$

$$\mu_{Kin} = \mu_{Glyc} + \mu_{Glu} \tag{13}$$

The parameters of the kinetic model comprised by Eqs. 3 to 13 were identified by the minimization of least square error using the Levenberg-Marquadt method using the experimental data of *S. clavuligerus* cultivations in 2.5 L shake flasks performed by duplicate with 0.5 L of operating volume.

5.2.4 DFBA implementation

The application of the SOA for DFBA underlies in the assumption of pseudo-steady state condition in each interval where the FBA problem would be solved. This assumption implies that intracellular kinetics are several orders of magnitude faster than extracellular kinetics [10]. Thus, the time-dependent reaction fluxes are discretized by solving a FBA for the GSMN in short integration periods, i.e. the step size. A set of dynamic constrains is defined by the kinetic model, whose

integration provide the extracellular concentrations of specified nutrients or metabolites and therefore, the exchange fluxes for constraining the FBA problem in each interval. Additionally, the usual steady-state constrains defined by the exchange reactions bounds for the FBA problem were maintained when dynamic constrains were not defined. It has been reported that classic objective function of biomass maximization in FBA could overestimate the specific growth rate and, in some cases, generate a large number of unbounded reaction fluxes [15]. Then the parsimonious enzyme usage assumption is a straightforward alternative applicable to FBA to overcome the issues related with the biomass maximization objective function [42,43]. In order to integrate those two approaches in the DFBA-SOA problem definition, a trade-off between the biomass maximization and parsimonious enzyme usage has been proposed to account for the sub-optimal growth by introducing a soft-constraint (α) into the objective function of the FBA optimization problem [10,15].

In this work, the DFBA-SOA formulation proposed by Feng et al [15] was implemented in the dynamic analysis of the metabolic features of *S. clavuligerus*. A quadratic programming (QP) problem was defined aimed to minimize the error between the growth rate predicted via FBA and the solution of the dynamic equations. This QP problem contains the FBA optimization defined for each interval in the integration range, but considering the dynamic constraints determined by the previously derived kinetic model. The formulation of the DFBA-SOA problem is presented in Eq. 14:

$$
\begin{aligned}
&min \sum \left(\mu_{kin}(t) - \mu_{FBA}(t)\right)^2 \\
&\quad s.t \\
&\quad \begin{cases} min[-\alpha\mu_{FBA} + (1-\alpha)\sum_{i=1}^{n} {v_i}^2] \\ \quad s.t \quad S \cdot v_n = 0 \\ \qquad\quad lb \le v_{n-m} \le ub \\ \qquad\quad v_m = \frac{1}{X}\left(\frac{dC_m}{dt}\right) \\ \qquad\quad 0 \le \alpha \le 1 \end{cases}
\end{aligned}
\tag{14}
$$

The vector of fluxes v_m is the link between the kinetic model and the FBA for each interval acting as equality constraints for the key nutrients, obtained as rates from the kinetic equations Eqs. 5-12. Additionally, the growth rate predicted by the FBA (μ_{FBA}) is forced to approach to the calculated by the kinetic model (μ_{kin}). The flux vector v_{n-m} is constrained assuming the pseudo-steady state condition for those metabolites. Since the mass conservation is assured for both, the kinetic and pseudo-steady state models, realistic predictions are expected by implementing this formulation of the DFBA-SOA. The QP optimization problem was solved with Gurobi 7.5 MATLAB API by using the Simplex algorithm for QP. All the FBA optimization problems were solved in COBRA Toolbox 3.0 for MATLAB. Data sets of *S. clavuligerus* cultivations in batch mode (0.5 L) in STR, fed-batch mode in STR from 5.0 to 7.8 L and 2-D rocking-motion bioreactor CELL-tainer® (CT) from 5.0 to 7.8 L were used for validation of the proposed DFBA-GSMN approach.

5.3. Results and discussion

5.3.1 Pseudo-steady state simulation (FBA)

In FBA simulations, the effects of glycerol, glutamate, oxygen, ammonium and phosphate flux uptakes on biomass synthesis and CA secretion as objective functions were explored. Additionally, the effects of CephC and clavam-2-carboxylate biosynthesis as products of cephalosporins and clavams 5S pathways were also considered, since the synthesis of these compounds is expected to compete with CA biosynthesis. Results of the effect of the above-mentioned variables on growth rate are presented in Figure 5.1.

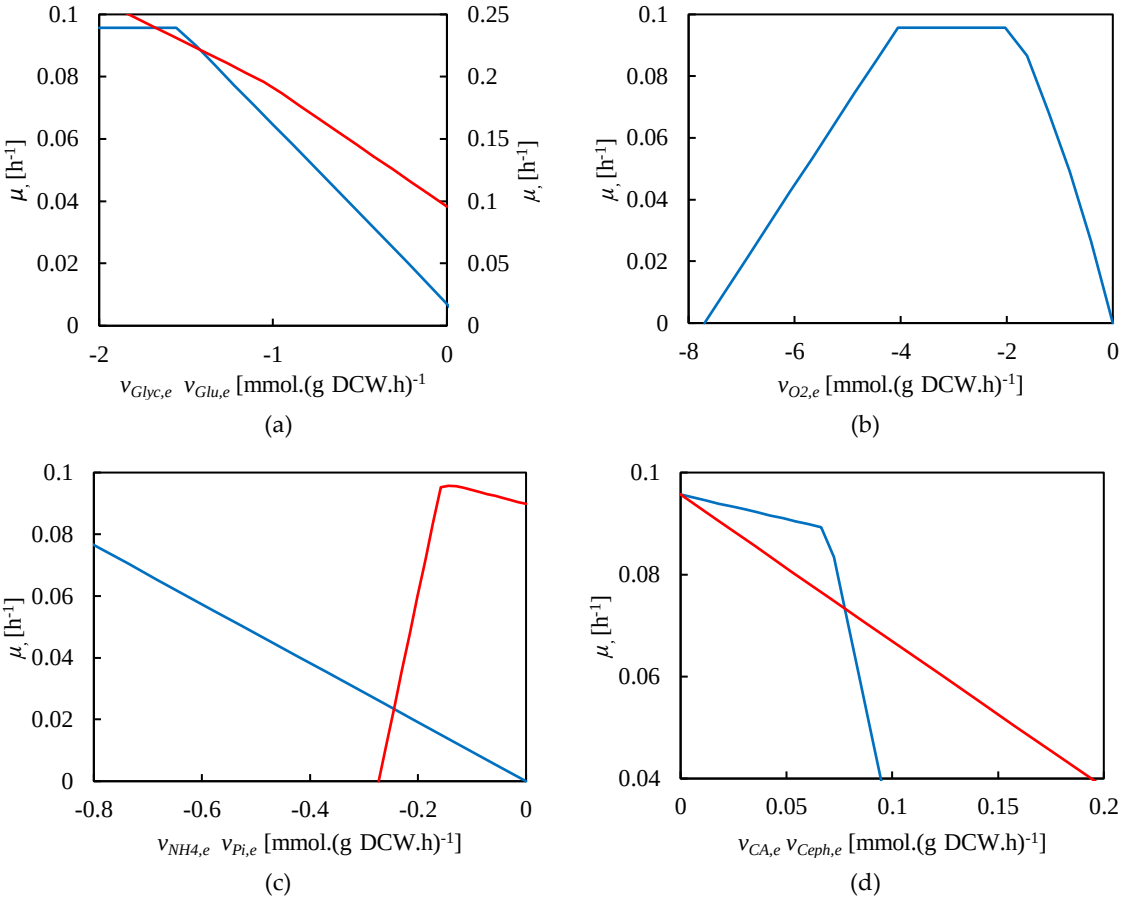

Figure 5.1. Effect of nutrients uptake, cephamycin C and CA secretion on *S. clavuligerus* growth rate. (a) Glycerol (blue) and glutamate (red); (b) Oxygen (blue); (c) Ammonium (red) and phosphate (blue); and (d) CA (blue) and cephamycin C (red).

As expected, glycerol and glutamate as the main biomass precursors in the synthetic media showed a direct effect on growth rate (Figure 5.1a). The increase in glycerol in-flux support biomass synthesis up to 0.095 h^{-1}. Moreover, glutamate, due to its content of carbon and nitrogen, could enhance more the growth rate up to 0.25 h^{-1}. Since *S. clavuligerus* is a strictly aerobic organism, the oxygen uptake favors biomass synthesis. However, this augmentation must be accompanied of an increase of substrate influx to push the energetic metabolism, otherwise it would affect growth rate negatively, as observed in Figure 5.1b, for flux values higher than 4 mmol.(g DCW.h)$^{-1}$. Ammonium influx as the main nitrogen source is essential for growth and promotes growth as long as enough carbon is provided as showed in Figure 5.1c. As pointed out by Saudagar et al [18], there exists a threshold in the phosphate influx to support the biomass accumulation and CA biosynthesis. As presented in Figure 5.1c, phosphate is a biomass precursor but uptake rates over 0.2 mmol.(g DCW.h)$^{-1}$ inhibit growth; also, phosphate secretion affects growth rate. Similar *in silico* results were reported by Toro et al [9]. The antibiotics biosynthesis use substrates that are simultaneously required for growth, such as glyceraldehyde-3-phosphate (GAP), arginine and TCA intermediates [19]. Thus, the increase in CA secretion is expected to affect the biomass synthesis as showed in Figure 5.1d. However, feasible phenotypes producing either CA or CephC can be attained at specific growth rates higher than 0.04 h^{-1} and lower than 0.9 h^{-1}, as it has been observed in our batch and fed-batch cultivations (see Results section, Chapter 3).

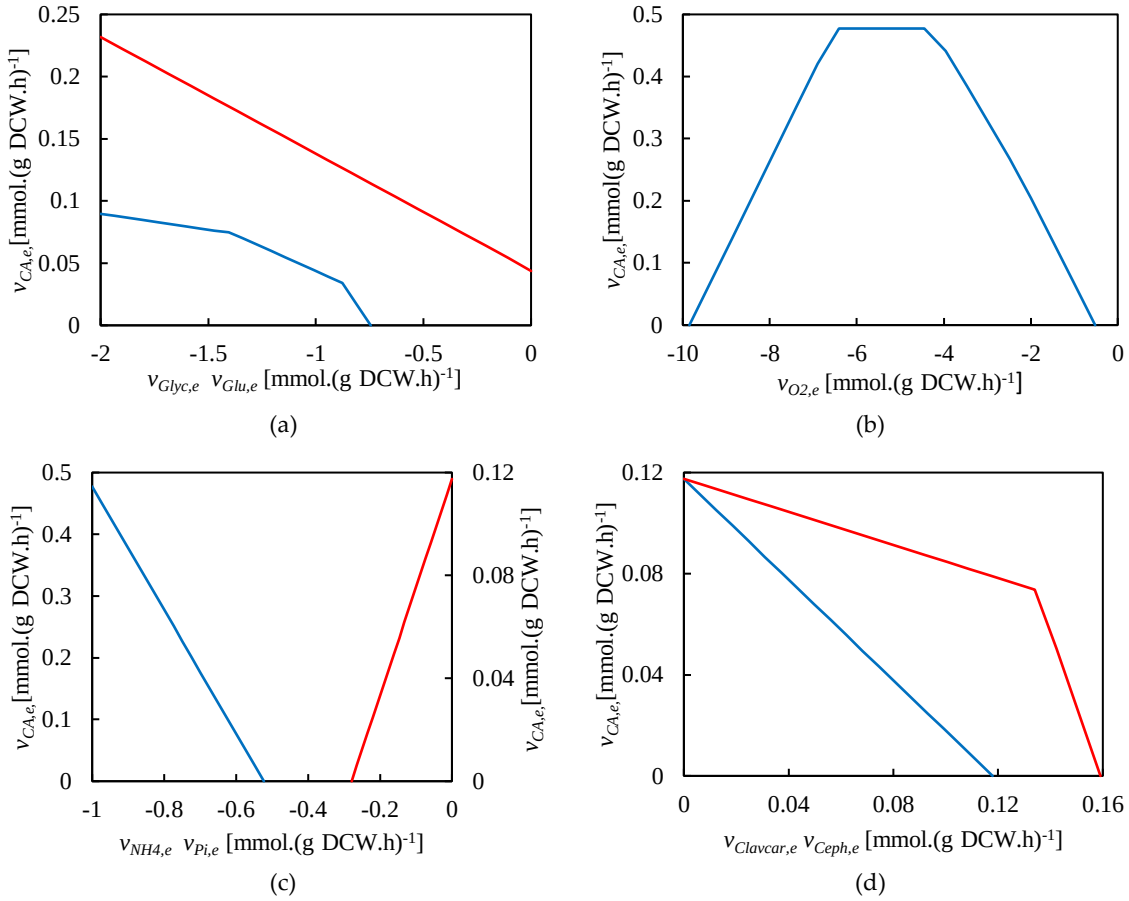

Figure 5.2. Effect of nutrients uptake, clavam-2-carboxylic acid and cephamycin C secretions on CA production. a) Glycerol (blue) and glutamate (red); b) Oxygen (blue); c) Ammonium (blue) and phosphate (red); and d) Clavam 2-carboxylic acid (blue) and cephamycin C (red).

According to experimental observations, previously discussed in Chapters 2 and 3, a minimum specific growth rate of 0.05 h^{-1} was defined for the analysis of CA production scenarios, since antibiotic biosynthesis with no cell growth is biologically unfeasible. CA production is not possible without providing glycerol; thus, as observed in Figure 5.2a, an increase in the glycerol uptake would favor the CA secretion up to a maximum of 0.48 mmol.(g DCW.h)$^{-1}$. The simultaneous availability of glutamate enhances the CA production (Figure 5.1a). The assimilation of glutamate increases the flux towards arginine in the urea cycle, which is an early precursor of CA. This result is coincident with the observations reported by Bushell et al [20] when supplementing glutamate in chemostat cultivations. CA biosynthesis involves several oxidation reactions requiring oxygen [21]. Thus, an increase in CA biosynthesis is usually accompanied by an increase in oxygen uptake (Figure 5.2b). However, an increase in oxygen influx higher than 6 mmol.(g DCW.h)$^{-1}$ would affect the CA production possibly linked to a decline in biomass as observed in Figure 5.1b. Assimilation of ammonium is essential for secondary metabolism, therefore, an increase in the uptake is expected to impact positively the CA production as it can be observed in Figure 5.2c. Phosphate limitation has been reported as a condition triggering the antibiotics biosynthesis in several species of streptomyces [22]. *In silico* results presented in Figure 5.2c shows that maximum CA production is attained when the limitation condition is reached, and no production occurs at phosphate uptakes higher than 0.26 mmol.(g DCW.h)$^{-1}$. CephC biosynthesis has been reported as a competitor pathway of CA biosynthesis, although both can be secreted under appropriated nutritional conditions [23]. Experimental results reported by Bellão et al. [23] showed that the higher the CA production the lower the cephamycin C secretion. This is probably linked to the consumption of 2-oxoglutarate and oxygen in oxidation reactions, as also occurs in CA biosynthesis. Moreover, the biosynthesis of early

precursors of CephC; valine, cysteine and lysine, requires glutamate. This is similar to the case of arginine in the urea cycle, which uses aspartate directly produced from glutamate. The clavam-2-carboxylate is a product of the 5S clavams pathway. Figure 5.2d shows that the higher the clavam 2-carboxylate production the lower the CA secretion. The 5S clavams pathway is competitor of CA biosynthesis since both pathways use the same precursor, clavaminic acid, whose synthesis acts a bifurcation point between both pathways [24].

The reaction essentiality analysis showed that 216 reactions (9.7 %) are essential for growth in the synthetic medium; these reactions are associated to 109 genes, which is 8.8 % of the genes annotated in the iDG1237 GSMN. The critical reactions are showed in Supplementary material S4. In the context of pseudo-steady state, 96 reactions were identified as potential targets for single or double knockout and 72 for overexpression or dampening linked to the enhancement of CA production. The biomass and CA to glycerol ratio ($\mu.v_{CA,e}/v_{Glyc,e}$) was used as indicator for selecting the best potential candidates for genetic engineering of the strain. For the case of the wild-type a ratio of 0.0024 was attained; the best candidate, i.e. overexpression of CEAS, showed 0.028. A summary of the best potential reaction candidates for strain engineering is presented in Table 5.1.

Recent studies have focused on the genetic engineering of expression levels of genes directly associated with the biosynthetic pathway of CA or its regulation. Consistent with what has been reported by other authors, overexpression of the regulatory genes associated with the CA synthesis would generate significant increases in its production [25–28]. In our study, the best ranking in connection with the enhancement of CA secretion was obtained for the overexpression of the early steps of CA biosynthesis pathway. The overexpression of N2-(2-carboxyethyl)-arginine synthase (CEAS) leads to an increase of the carbon flux along the complete CA pathway leading to an increase in the CA secretion. In our simulations (see chapter 4), under phosphate limitation and adequate carbon, nitrogen and oxygen supply there are no significant fluxes through the 5S clavams pathway. Therefore, all the carbon flux directed to CEAS is impacting directly the CA biosynthesis. As suggested by the results showed in Table 5.1, the dampening of phosphoglycerate kinase (PGK) would improve the flux of GAP as the C-3 precursor of CA while the flux of aspartate synthetized from glutamate will maintain the flux of the C-5 precursor required for CA production.

The analysis of potential strain modifications, presented in Table 5.1, indicates that a lower increase in CA production could be achieved by overexpressing the putative pyridoxal phosphate-dependent aminotransferase catalyzing the production of clavulanate-1-aldehyde, either by single overexpression or in combination with other modifications. In this regard, the synthesis of (3R, 5R) clavaldehyde has not been completely elucidated. However, this step might be related with the *orf17* cluster encoding the N-glycyl-clavaminate synthetase, which has been proposed as one enzymes catalyzing the reactions leading to (3R, 5R) clavaldehyde [21,29]. Moreover, the clavaminic acid synthesis is the bifurcation point between 5S clavams and CA biosynthesis; therefore, overexpression of regulatory or encoding genes linked to clavaldehyde synthesis would drive the carbon flux preferably towards CA instead of 5S clavams. Similarly, the single overexpression of clavaldehyde dehydrogenase (CAR) also would potentially increase de CA secretion. Comparable results were obtained *in silico* by Toro et al [9], showing that overexpression of genes controlling the late steps in CA biosynthesis are suitable candidates for enhancing CA production. Since the demand for reducing cofactors increases when enhancing the CA production, these modifications could be accompanied by attenuations that reduce the cost of these cofactors in other reactions without compromising cell growth such as ferredoxin and glutarate-semialdehyde oxidoreductase. Likewise, in order to preserve the intracellular pool of intermediates required for the biosynthesis of CA, some decarboxylases can also be attenuated, such as pyruvate decarboxylase and ornithine decarboxylase.

Table 5.1. Potential reaction targets for enhancement of CA production by strain engineering of *S. clavuligerus*.

Modifications	Strategy	Enzyme	Reaction ID Model iDG1237	NCBI protein ID	*Ratio* ($\mu.v_{CA,e}/v_{Glyc,e}$)
Single	Overexpression	N2-(2-carboxyethyl)-arginine synthase	CEAS	ANW18135	0.02756
Single	Knockout	Pyruvate kinase	PYK	ANW20351.1	0.02041
Single	Dampening	Phosphoglycerate kinase	PGK	ANW20748.1	0.01821
Double	Overexpression	Claviminate aminotransferase (hypothetical)	CV1		0.00905
	Dampening	Ferredoxin (NADP)	FRNDPR2r	ANW18690.1	
Triple	Overexpression	Claviminate aminotransferase (hypothetical)	CV1		0.00697
	Dampening	Pyridoxal 5-phosphate phosphatase	PYDXPP	ANW19305.1	
	Dampening	Glutarate-semialdehyde:NAD+ oxidoreductase	OXPTNDH	ANW21404.1	
Double	Overexpression	Claviminate aminotransferase (hypothetical)	CV1		0.00507
	Dampening	Pyruvate decarboxylase	PYRDC	ANW18804.1	
Double	Overexpression	Claviminate aminotransferase (hypothetical)	CV1		0.00448
	Dampening	Ornithine Decarboxylase	ORNDC	ANW19435.1	
Single	Overexpression	Clavulanate dehydrogenase	CAR	ANW18142	0.00435
Double	Knockout	Phosphoglycerate mutase	PGM	ANW17043.1	0.00300
	Knockout	Gamma-glutamyl-gamma aminobutyric acid dehydrogenase	GGGABADr	ANW18767.1	
Double	Knockout	Enolase	ENO	ANW19850.1	0.00255
	Knockout	Cystathionine beta synthase	CYSTS	ANW19434.1	
Single	Dampening	Succinil Coa synthetase	SUCOAS	ANW17690.1	0.00245

Previous reports showed that a significant increase in the production of CA can be achieved by disrupting the GAPD enzyme, directing part of the flux of GAP to CA biosynthesis [27,30]. Our *in silico* analysis summarized in Table 5.1 showed that the single deletion of the gene encoding the reaction catalyzed by pyruvate kinase (PYK) would also improve the flux of GAP towards CA biosynthesis. This modification implies the regulation of the flux passing from glycolysis to TCA cycle through the phosphoenolpyruvate carboxylase (PPC) in order to maintain the oxidative metabolism in the TCA. The knockout of phosphoglycerate mutase (PGM) cuts the conversion of 3-phosphoglycerate to 2-phosphoglycerate by alternatively activating the alcohol dehydrogenase for the use of glycerol as the sole source of carbon. This pathway is conducive to the formation of 2-phosphoglycerate via glycerate in three reactions, which is also a shorter route than glycolysis itself, so the flow of carbon to TCA is not compromised. The consequent accumulation of 2-phosphoglycerate and 3-phosphoglycerate favors the synthesis of amino acids and 2-oxoglutatarate, both widely required by secondary metabolism. Similarly, formation of a pool of 3-phosphoglycerate is favored by the deletion of the cystathionine beta synthase, avoiding the supply of 3-phosphoglycerate as precursor in the serine-cysteine pathway. The gamma-glutamyl-gamma aminobutyric acid dehydrogenase (GABA) connects succinate from TCA cycle with glutamate metabolism; its dampening would reduce the carbon flux from glutamate to TCA cycle, favoring the flux towards the urea cycle. The deletion of enolase would cause the repression of phosphoenolpyruvate production from 2-phosphoglycerate, generating the accumulation of this intermediate, then increasing the production of CA. The *in-silico* modifications with the highest ratio of CA to glycerol usage were further assessed under a DFBA approach.

5.3.2 Parameters estimation

As presented in Chapter 2, the growth of *S. clavuligerus* and CA production in batch and fed-batch modes were explored in the shake-flask scale, showing similar trends in exponential growth, substrate and nutrients consumption during the first 45 h of cultivation. The feeding implemented in the fed-batch cultivations promoted the maintenance of the stationary phase and CA production for longer time when compared with the batch cultivations. The fed-batch operation did not enhance significantly the observed biomass accumulation, the specific growth rate or the nutrients uptake, but also supported the metabolic activity leading to a durable stationary phase, in which the CA secretion is sustained.

S. clavuligerus growth in submerged cultivations is significantly affected by shear forces [31]. Under appropriated nutritional conditions, the increase in the shear stress leads to higher growth rate, biomass accumulation and, therefore, higher uptake of nutrients and CA secretion. Parameters of the dynamic first-principles based model, described by Eqs. 5-12, were estimated from experimental data sets of *S. clavuligerus* cultivations in 2.5 L shake-flasks with 500 mL of operation volume in batch mode using synthetic media. Note that only nutritional factors were considered in the formulation of the dynamic equations with Monod type reaction kinetics. According to previous results of fed-batch cultivation of *S. clavuligerus* in STR and CT bioreactors, the change of hydrodynamic conditions affects macroscopically the specific growth rate and morphology, then leading to changes in the nutrients uptakes and metabolites secretion [31]. The estimated parameters for the proposed unstructured model representing the *S. clavuligerus* growth using glycerol and glutamate as carbon sources are presented in Table 5.2 and 5.3, respectively. The time courses of model predictions and experimental data are presented in Figure 5.3, including the calculation of normalized root mean square error (NRMSE) for the data set. The mean error between the predictions of the kinetic model and the experimental data was 6.7%, showing a good fit of the model.

Table 5.2. Kinetic parameters estimated for *S. clavuligerus* growth on glycerol.

Symbol	Description	Value	Units
$\mu_{Glyc,max}$	Maximum specific growth rate on glycerol	0.38 μ_{max}	h^{-1}
k_d	Global specific death constant	0.010 ±0.005	h^{-1}
$Y_{X/Glyc}$	Glycerol yield coefficient referred to biomass	1.634±0.013	C-mmol X.(mmol glycerol^{-1})
$Y_{X/O2,Glyc}$	Oxygen yield coefficient referred to biomass	0.582±0.023	C-mmol X.(mmol O_2^{-1})
$Y_{X/NH4,Glyc}$	Ammonium yield coefficient referred to biomass	2.755±0.016	C-mmol X.(mmol $NH_4^{+\,-1}$)
$Y_{X/CO2,Glyc}$	Carbon dioxide yield coefficient referred to biomass	0.485±0.005	C-mmol X.(mmol CO_2^{-1})
$Y_{X/H2O,Glyc}$	Water yield coefficient referred to biomass	0.698±0.045	C-mmol X.(mmol H_2O^{-1})
$Y_{X/Pi,Glyc}$	Phosphate yield coefficient referred to biomass	33.300±0.066	C-mmol X.(mmol Pi^{-1})
K_{Glyc}	Monod saturation constant	0.003±0.001	mmol.L^{-1}

Table 5.3. Kinetic parameters estimated for *S. clavuligerus* growth on glutamate.

Symbol	Description	Value	Units
$\mu_{Glu,max}$	Maximum specific growth rate on glutamate	0.62 μ_{max}	h^{-1}
$Y_{X/Glu}$	Glutamate yield coefficient referred to biomass	1.953±0.021	C-mmol X.(mmol glutamate^{-1})
$Y_{X/O2,Glu}$	Oxygen yield coefficient referred to biomass	1.330±0.016	C-mmol X.(mmol O_2^{-1})
$Y_{X/NH4,Glu}$	Ammonium yield coefficient referred to biomass	4.001±0.058	C-mmol X.(mmol $NH_4^{+\,-1}$)
$Y_{X/CO2,Glu}$	Carbon dioxide yield coefficient referred to biomass	1.869±0.033	C-mmol X.(mmol CO_2^{-1})
$Y_{X/H2O,Glu}$	Water yield coefficient referred to biomass	0.610±0.074	C-mmol X.(mmol H_2O^{-1})
$Y_{X/Pi,Glyc}$	Phosphate yield coefficient referred to biomass	33.300±0.066	C-mmol X.(mmol Pi^{-1})
K_{Glu}	Monod saturation constant	0.086±0.011	mmol.L^{-1}

5.3.3 Dynamic fluxes distributions in batch and fed-batch operation

The standard FBA approach assumes pseudo-steady state conditions; thus, it is able represent the cell conditions for a single time. Nevertheless, the extension of FBA to DFBA is required if time-courses of flux distributions and responses to time-dependent perturbations are aimed to be analyzed. The implementation of a DFBA approach allowed to study the time-dependent intracellular fluxes distribution in batch and fed-batch operation of *S. clavuligerus* cultures in STR and CT bioreactors. According to our observations the specific growth rate can be affected by cultivation conditions, mainly by the shear forces due to agitation mechanism. Therefore, for more accurate results when using the DFBA framework, the value of observed growth rate must be provided according to the experience cultivating the strain. The vector of initial values for integration of the kinetic model is presented in Table 5.4. Figure 5.4 shows the predicted and experimental time-courses of biomass, glycerol, glutamate and CA concentrations for batch cultures in STR (0.5 L) and fed-batch cultures in STR (5.0 – 7.8 L) and CT (5.0 – 7.8 L) bioreactors.

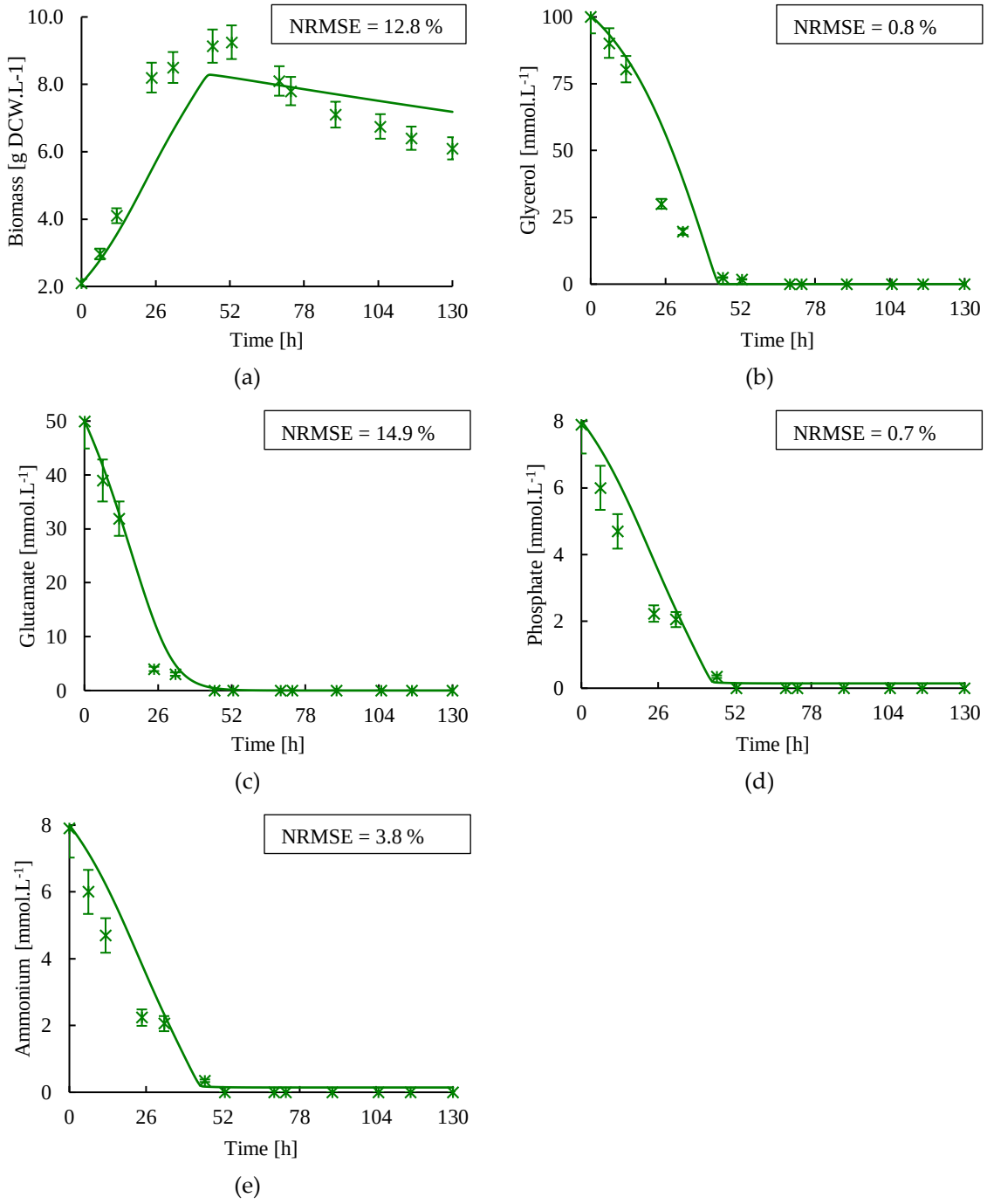

Figure 5.3. Experimental data (stars) for parameters estimation of *S. clavuligerus* unstructured model and predicted time-courses of substrates and products (solid lines). a) Biomass; b) Glycerol; c) Glutamate; d) Phosphate and e) Ammonium.

Table 5.4. Parameters and initial conditions for solving the dynamic unstructured model of *S. clavuligerus* growth.

Symbol	Description	Value	Units
μ_{max} (STR, batch)	Mean maximum specific growth rate in STR (0.5 L)	0.080	h^{-1}
μ_{max} (STR, fed-batch)	Mean maximum specific growth rate in STR (5-7.8 L)	0.070	h^{-1}
μ_{max} (CT, fed-batch)	Mean maximum specific growth rate in CT (5-7.8 L)	0.065	h^{-1}
F	Feed rate	0.035	$L.h^{-1}$
$C_{Glyc,f}$	Concentration of glycerol in feeding medium	1304	$mmol.L^{-1}$
$C_{Pi,f}$	Concentration of phosphate in feeding medium	11.48	$mmol.L^{-1}$
$C_{NH4,f}$	Concentration of ammonium in feeding medium	121.08	$mmol.L^{-1}$
$C_{Glyc,f}$	Concentration of glutamate in supplemented feeding medium	100*	$mmol.L^{-1}$
t_f	Start of fed-batch operation	37-34*	h
X(t=0)	Initial biomass concentration	1.89	$g\ DCW.L^{-1}$
C_{Glyc} (t=0)	Initial glycerol concentration in medium	100.5	$mmol.L^{-1}$
$C_{Glu,}$ (t=0)	Initial glutamate concentration in medium	50	$mmol.L^{-1}$
$C_{Pi,}$ (t=0)	Initial phosphate concentration in medium	8	$mmol.L^{-1}$
C_{NH4} $(t=0)_o$	Initial ammonium concentration in medium	40	$mmol.L^{-1}$
V(t=0)	Initial operation volume	5	L

* Applicable only in the simulation scenario considering fed-batch operation using medium supplemented with glutamate.

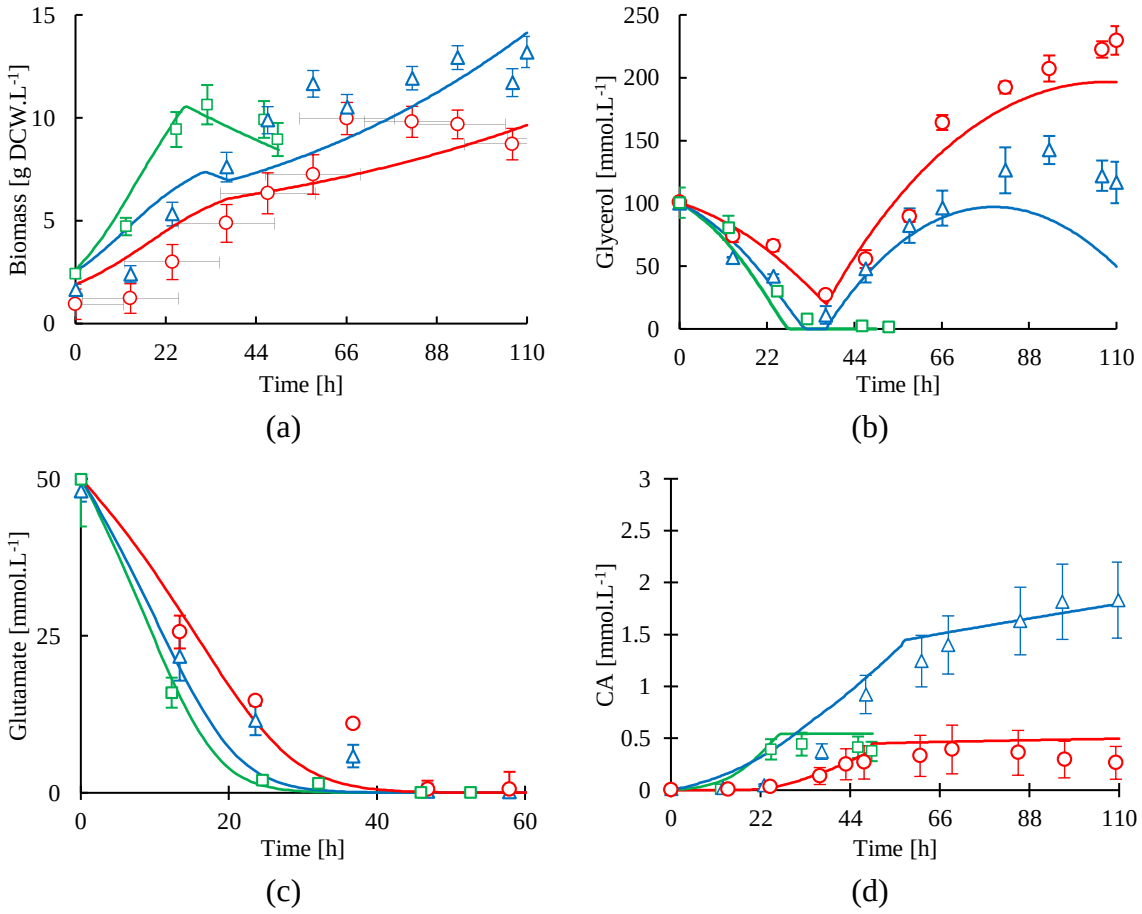

Figure 5.4. DFBA simulated and experimental time-courses of substrates and products in *S. clavuligerus* cultivations. a) Biomass in STR batch (green), STR fed-batch (blue) and CT fed-batch (red); b) Glycerol in STR batch (green), STR fed-batch (blue) and CT fed-batch (red); c) Glutamate in STR batch (green), STR fed-batch (blue) and CT fed-batch (red) and d) CA in STR batch (green), STR fed-batch (blue) and CT fed-batch (red).

The kinetic parameters estimated for *S. clavuligerus* growth, substrate consumption and product formation are in the range of those previously reported by other authors for the same organism [32,33]. In general, the prediction of extracellular compounds agreed the experimental observations, presented in Figure 5.4. The nutritional conditions attained in the batch operation does not assure a supply of carbon and nitrogen sources beyond 30 h. According to our experimental observations, the growth rate in all cases decreases after glycerol and glutamate starvation. Nevertheless, growth can continue if at less one carbon source is still available in the medium as the case of fed-batch operation. Thus, biomass synthesis continues when glycerol is fed, as it can be observed in Figures 5.4a and 5.4b. However, growth proceeds at lower rate due to the lack of extracellular amino-acids that act as direct precursors of biomass. For the case of batch operation, starvation of glycerol occurs first, at approximately 30 h followed by glutamate exhaustion around 44 h, thus leading to a clear biomass decline (Figures 5.4a and 5.4b). The dynamic model shows that batch operation generates low titers of CA as consequence of poor nutritional conditions that prevent the continuous activity of the secondary metabolism.

As showed in Figure 5.4c for fed-batch operations, the glycerol feeding causes a decrease in the demand for glutamate. Therefore, in contrast with batch cultivations, glutamate depleted at 50-60 h approximately. As discussed in Chapter 3, the environmental conditions in the rocking-motion bioreactor CT cause an increase in the mycelial diameter, limiting the oxygen transfer rate (OTR) and uptake of nutrients, impacting negatively the growth rate and CA production. The consideration of the OTR in the kinetic model allowed to represent the low CA production in this kind of reactor (Figure 5.4d) as a consequence of the reduced oxygen and nutrients uptake.

DFBA simulations shows that in the cultivations with the highest growth rates (STR), the substrate starvation causes a sudden drop in the reaction fluxes of glycolysis, TCA and urea cycles decreasing the flux in the CA pathway. In the case of batch cultures in STR, this drop supposes a decrease in the metabolic activity as consequence of nutrients depletion and the pronounced decline in the specific growth rate, conditions leading to a low CA biosynthesis (Figure 5.5). In the fed-batch cultivations in STR, the intense metabolic activity also leads to a starvation point evidenced in the drop of all fluxes around the 35th h. Interestingly, the feeding from 37 h onwards, restores the metabolic activity to values closer to those observed prior to substrate depletion. The DFBA shows that at the beginning of the fed-batch operation (from 37 to 48 h) a reactivation of the metabolic fluxes occurs due to the increasing concentration of glycerol, in addition to the remaining extracellular glutamate that boosts the urea cycle in arginine direction. This availability of substrate causes a favorable peak in the fluxes of the central metabolism of approximately 6 h that finishes when glutamate is finally depleted and promotes higher fluxes towards CA biosynthesis (see CEAS in Figure 5.5) . Once glutamate has depleted (after 48 h), a new but less pronounced drop in the metabolic activity is observed. After this last drop, the fed-batch operation stabilizes the biomass concentration, generating presumably a sub-optimal phenotype that is able to maintain a stable secretion of CA. Although the reaction fluxes along the CA pathway are lower than those attained during the exponential phase, at this point a high number of producer cells is present in the culture vessel with enough availability of primary carbon and nitrogen sources, thus leading to a significant volumetric production rate that contributes to attain higher CA titers than in batch operations, as shows the dynamics of CA accumulation showed in Figure 5.4.

In CT cultivations lower growth rate and nutrients uptake were observed (Figure 5.4). In this case, the fed-batch operation started before the glycerol and glutamate starvations. The DFBA shows that no drop in the metabolic fluxes occur if the complete limitation of substrate is not reached (Figure 5.5). This could be an indicator of a more balanced metabolism, as previously suggested for this kind of cultivations in connection with the observed respiratory quotient and the reaction fluxes calculated for the glycolysis and the TCA cycle, as discussed in Chapters 3 and 4 [31]. Similarly to STR cultivations, the late glutamate depletion caused a drop in the metabolic fluxes, stabilizing the reaction fluxes at lower rates than in STR, mostly due to the lower nutrients uptake and biomass accumulation.

Figure 5.5 summarizes the dynamic fluxes distribution along the central metabolism and CA biosynthesis. As discussed in Chapter 4, The CA accumulation is favored by phosphate depletion coexisting with availability of carbon and nitrogen sources. This is consequent with the increasing trend in the reaction flux along the CA biosynthesis pathway as it can be observed in the dynamics of reaction catalyzed by CEAS showed in Figure 5.5. Moreover, the availability of glutamate promotes a high flux through the TCA and urea cycles so as in CA pathway and the lack of this C-5 precursor affects not only the biomass synthesis but also the CA production rate, as observed in the fluxes of aspartate transaminase (ASPTA) and arginine-succinate synthase (ARGSS) showed in Figure 5.5. The highest reaction fluxes in the CEAS occur when both precursors, glycerol and glutamate, are available in the medium, since those substrate boost the TCA and urea cycles favoring the CA accumulation up to the 48 h, when the glutamate starvation occurs. However, if this condition does not coexist with phosphate limitation, the fluxes are not directed significantly to CA biosynthesis as observed in STR batch and CT fed-batch cultivations, prior to the 23th h. The rapid phosphate depletion in the batch cultivations led to a pronounced increase in the flux reaction through CEAS from 12 to 27 h, but this condition coincides with a low biomass concentration, which does not lead to a significant CA production rate.

For all the cultivations, the highest reaction fluxes along the glycolysis are observed in the early stages of cultivation when attaining the highest specific growth rates and highest substrate uptakes, prior to glycerol starvation (at 34 h approximately). The fluxes-trend through pyruvate dehydrogenase (PDH) and TCA enzymes succinyl CoA synthetase (SUCOAS) and succinate dehydrogenase (SUCD) are coincident with the trends of substrate uptakes, starting at high values and decreasing accordingly with the carbon source depletion. Similar trends are observed in the fluxes of urea cycle enzymes as the case ARGSS and ASPTA. In batch operation, due to the irreversible mechanism of citrate synthase (CS), the flux through this enzyme increases markedly with the glutamate depletion, leading to an increase in ammonium uptake up to the 22th h, indicating a higher demand for intermediates related to amino acids synthesis. Indeed, the glutamate depletion also affects slightly the activity of glyceraldehyde-3-phosphate dehydrogenase (GAPD), isocitrate dehydrogenase (IDH) and malate dehydrogenase (MDH). Interestingly, this glutamate limitation condition led also to an increase in the CEAS activity, but this is not sustained due to extensive nutrients depletion. These conditions were observed with less intensity in fed-batch operation, since the glutamate depletion is delayed by the feeding containing ammonium and glycerol.

In all cases, during the exponential growth no significant fluxes are directed to the pentose-phosphate pathway (PPP), which is verified in the low activity of the glucose-6-phosphate dehydrogenase (G6PD). In this phase, the central metabolism is majorly activated in the oxidative direction, providing also the intermediates and reduced cofactors required for biomass accumulation and also for antibiotic biosynthesis. After glutamate depletion, the carbon fluxes through the primary metabolism stabilizes with a slightly negative slope. Interestingly, in this phase the PPP is activated presumably due to the low activity of NAD-dependent dehydrogenases.

The role of amino acids in nutritional regulation of CA production is not completely understood. Studies involving different media and amino acids supplementation showed that CA production could vary depending on the amount and the amino acids added in both, medium and feeding. The amino acids stoichiometrically related with the urea cycle such as ornithine, arginine, aspartate and glutamate could enhance the CA production in comparison with non-supplemented media [3,20,34]. Moreover, from regulatory standpoint, it is likely that *S. clavuligerus* responds to amino acid starvation by inducing production of the phosphorylated nucleotides like the guanosine pentaphosphate (ppGpp), whose synthesis is regulated by factors RelA and RshA that positively influence CA production by mechanisms that need to be further elucidated [2,25]. The DFBA applied to batch and fed-batch cultivation scenarios revealed an important stoichiometric role of glutamate limitation in CA production, especially in regulating the fluxes in the urea cycle (see ARGSS and ASPTA in Figure 5.5). The glutamate depletion stimulates the ammonium uptake and the metabolic activity of IDH increasing the production rate of 2-oxoglutarate, which is an important precursor in amino acids metabolism and also of CA biosynthesis. This is reflected in the increasing flux of CEAS,

observed when coexisting phosphate and glutamate limitations under availability of glycerol, ammonium and adequate oxygen transfer conditions.

The precursors of CA biosynthesis are mostly derived from primary metabolism, then it is suitable to maintain or even, stimulate the carbon fluxes towards the glycolytic, TCA and urea pathways aimed to provide the intermediates required for CA biosynthesis. The DFBA suggests that a suitable scenario for the enhancement of CA production involves a fed-batch operation starting in the point of phosphate, glycerol and glutamate limitations, but without reaching the starvation point, i.e. approximately at 34 h of cultivation in the case of the wild-type strain cultivated in chemically defined medium. Additionally, feeding medium formulation should consider the supply of enough glycerol and ammonium while maintaining a phosphate and glutamate limited scenario. Such conditions potentially would preserve the highest activity along the CEAS and downstream in the complete CA biosynthesis pathway. Moreover, high glutamate concentrations would promote the extensive biomass synthesis and in the other hand, lack of glutamate would cause a decay on the metabolic activity. Thus, low glutamate concentrations would promote the CA accumulation during the stationary phase. A similar effect has been observed in the related species *Streptomyces platensis*, in which, antibiotics synthesis was stimulated by maintaining L-aspartate concentrations in a narrow range around 0.5 $mg.L^{-1}$, i.e. under aspartate-limited conditions. In that case, it was observed that L-aspartate concentrations out of that operative range decreased the antibiotics secretion [35].

Based on this analysis, DFBA simulations were conducted considering the same feeding medium composition but adding glutamate supplementation at low concentration (100 $mmol.L^{-1}$). The same kinetic parameters were maintained in the simulation and the fed-batch operation started prior the substrates exhaustion (34 h). Since a higher amount of carbon is supplied during the supplemented fed-batch operation, an increase in the biomass was expected (Figure 5.6a). The feeding medium supplemented with glutamate leads to slightly lower uptake of glycerol in comparison with the non-supplemented medium (Figure 5.6b), in which case glycerol is the only carbon source. Nevertheless, it was observed that the higher metabolic activity in the supplemented culture causes a faster depletion of glycerol at the end of the cultivation. As expected, the supplementation of glutamate during the fed-batch leads to a slight accumulation of this amino acid during the cultivations (Figure 5.6c). The model showed a potential increase in CA accumulation of approximately 1.4-fold the observed in the STR fed-batch cultivation using non-supplemented feeding medium (Figure 5.6d).

Considering that fed-batch operation using a medium with glycerol, ammonium and glutamate is suitable for the enhancement of CA production and based on previous identification of potential reaction targets leading to enhancement of CA production, an *in silico* analysis of two strain engineering strategies was performed. Specifically, *in silico* single overexpression of *ceas*2 and single deletion of *pyk* showed the best ratio of glycerol usage and CA secretion. Therefore, overexpression of *ceas*2 (2-fold) and single deletion of *pyk* were *in silico* studied as potential strategies for *S. clavuligerus* strain engineering. DFBA simulations were conducted maintaining the same kinetic parameters and the fed-batch operation with supplemented medium from the 34^{th} h of cultivations. For the sake of comparison, Figure 5.6 presents the simulated time-courses of biomass, glycerol, glutamate and CA concentrations for wild-type, and *in-silico S. clavuligerus Δceas2* and *Δpyk.* The uptake of glycerol, glutamate and even the biomass accumulation remained mostly unmodified after applying the *in silico* modifications (Figures 5.6a-c). Interestingly, the CA secretion was different in all cases (Figure 5.6d), indicating a flux redistribution that impacts positively the CA biosynthesis but not the biomass accumulation. The highest *in-silico* CA concentration was observed in the fed-batch cultivation supplemented with glutamate for the *S. clavuligerus Δceas2*, whose maximum concentration was 1.9-fold the calculated for the wild-type strain (see Figure 5.6d). The knockout of the *pyk* also would increase the CA production but in a lesser extent, showing a maximum increase of 1.1-fold the concentration of the supplemented wild-type cultivation (Figure 5.6d).

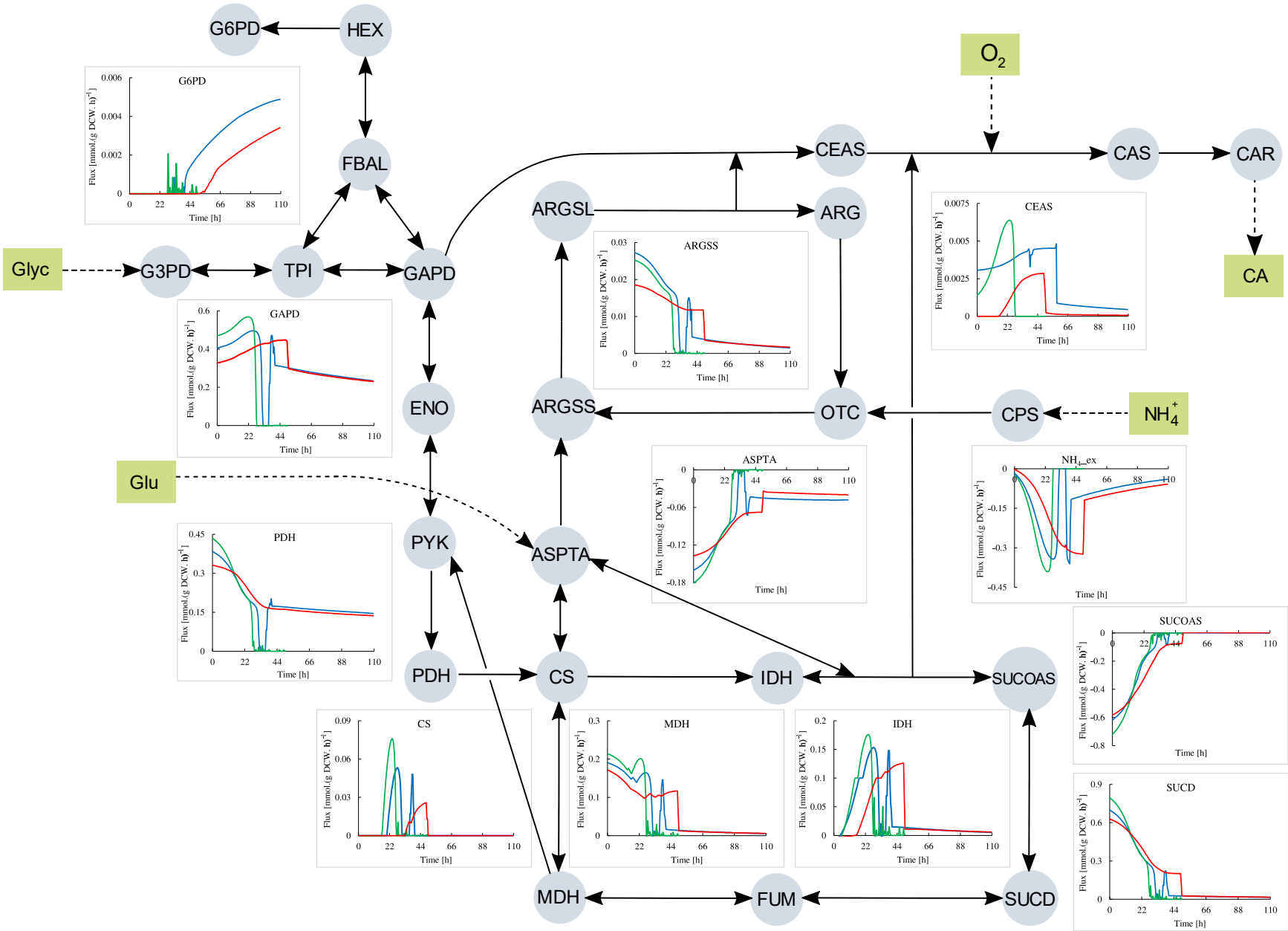

Figure 5.5. In silico dynamic fluxes distribution in central metabolism and CA biosynthesis in batch (blue) and fed-batch cultures of *S.clavuligerus* in STR (blue) and CT (red) bioreactors

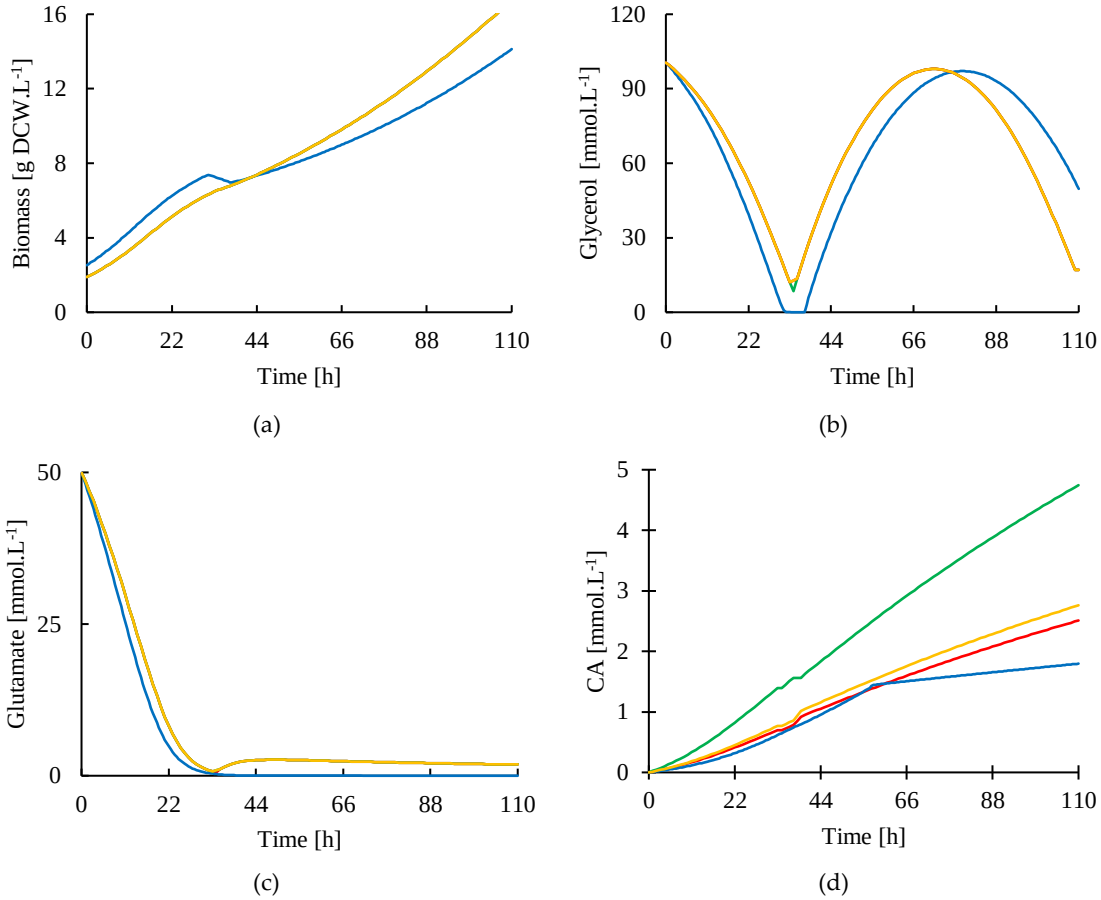

Figure 5.6. DFBA simulated time-courses of substrates and products in fed batch cultivations of S. clavuligerus: wild-type non-supplemented (blue), wild-type supplemented (red), Δceas2 supplemented (green) and Δpyk supplemented (orange.) a) Biomass; b) Glycerol; c) Glutamate and d) CA.

Figure 5.7 summarizes the dynamic fluxes distribution along primary metabolism and CA biosynthesis. Results showed that an increase in CA production rate would be possible by maintaining more stable fluxes along the glycolysis where the C-3 precursor GAP is produced and the urea cycle where the C-5 (arginine) precursor is synthesized as show the fluxes of GAPD, PDH, ARGSS and ASPTA in Figure 5.7. Furthermore, this condition avoids the previously observed drop caused by the carbon sources depletion in the STR fed-batch non-supplemented cultures. The implementation of fed-batch operation at 34 h, i.e. before the carbon sources starvation, might lead to a higher and more stable metabolic activity in most of the enzymes, contributing also to maintain higher fluxes along the CA biosynthesis. Despite the glutamate limitation condition (40 h) still causes a drop in the metabolic fluxes, this drop is considerably less pronounced than the observed in the simulations of fed-batch non-supplemented cultures. Additionally, higher reaction fluxes could be maintained during all the cultivation time.

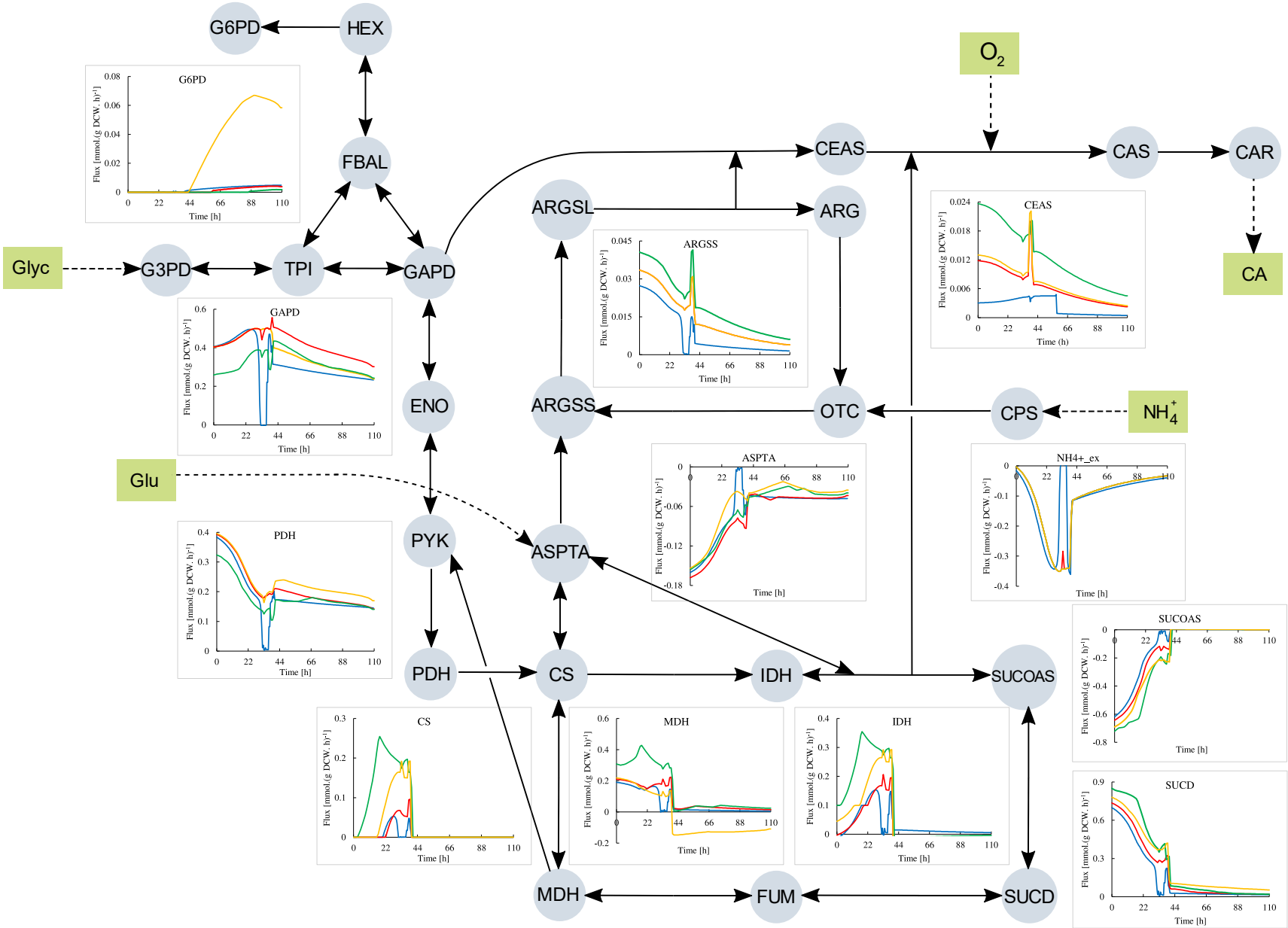

Figure 5.7. In silico dynamic fluxes distribution in central metabolism and CA biosynthesis for fed-batch non supplemented (blue) and supplemented (red) cultures with wild-type strain and fed-batch supplemented cultures with *Δceas2* (green) and *Δpyk* (orange) modified strains.

The fluxes through the PPP decrease due to the supplemented feeding, evidencing a higher demand for carbon from glycolysis and TCA cycle throughout the cultivations. Interestingly, the fluxes in the reactions catalyzed by the ARGSS and specially in the CEAS, were the highest observed between the *in silico* experiments considering the wild-type strain as observed in Figure 5.7. Indeed, transcriptomic evidence has shown upregulation of CEAS, BLS, CAS and CAR when CA in synthetized under extensive amino acids supply [36]. The carbon flux in the CA pathway is less affected by the glutamate depletion than the reactions of central metabolism, suggesting that maintaining a constant supply of glutamate at low concentration might favor the continuity of secondary metabolism without promoting a substantial increase in biomass, since the latter is more favored by a high activity of primary metabolism.

The simulation of cultivations with *Δceas2* shows less carbon flux along the glycolysis in comparison with the *Δpyk* and wild-type strains, observable in the lower reaction fluxes of GAPD and PDH in Figure 5.7. This is due to a considerable demand for GAP directly from CEAS. Additionally, this modification would also cause an increase in the demand for TCA cycle, 2-oxoglutarate and arginine, leading to an increase in the reaction fluxes of most of the enzymes in the TCA and urea cycle. The demand for carbon from central metabolism and CA biosynthesis also reduces considerably the fluxes towards the PPP. Indeed, the highest fluxes for the CS, IDH, SUCOAS, SUCD, MDH, ARGSS and CEAS were observed for the *Δceas2* that, in turn, showed the highest CA production.

The deletion of *pyk* causes a redistribution of metabolic fluxes by cutting the pyruvate synthesis from phosphoenolpyruvate. Thus, the carbon flux is redistributed towards PPP, CA biosynthesis and PPC. Actually, the flux through the G6PD was the highest observed among all the simulations as showed in Figure 5.7. In the case of the glycolysis, the PPC must act as the auxiliary connection point between the glycolysis and TCA maintaining the carbon flux to the oxidative metabolism and the intermediates supply to the urea cycle and CA biosynthesis. Additionally, the demand for pyruvate from PDH and TCA cycle is compensated by the malic enzyme, increasing the demand for malate, then causing the flux inversion of the MDH. Thus, the flux throughout the TCA cycle does not decrease despite the deletion of the last reaction of the glycolysis. The lower CA biosynthesis in comparison with the *Δceas2* strain is concordant with the lower activity of ARGSS, ASPTA and CEAS in connection with a lower demand for C-5 precursors. Experimental validation of cultivation with the modified feeding medium with glutamate (100 mmol.L^{-1}) maintaining the same feed-rate (0.035 L.h^{-1}) showed an increase of CA productivity up to 1.09-fold the attained in the fed-batch cultivations with feeding without glutamate supplementation (Figure 5.8b).

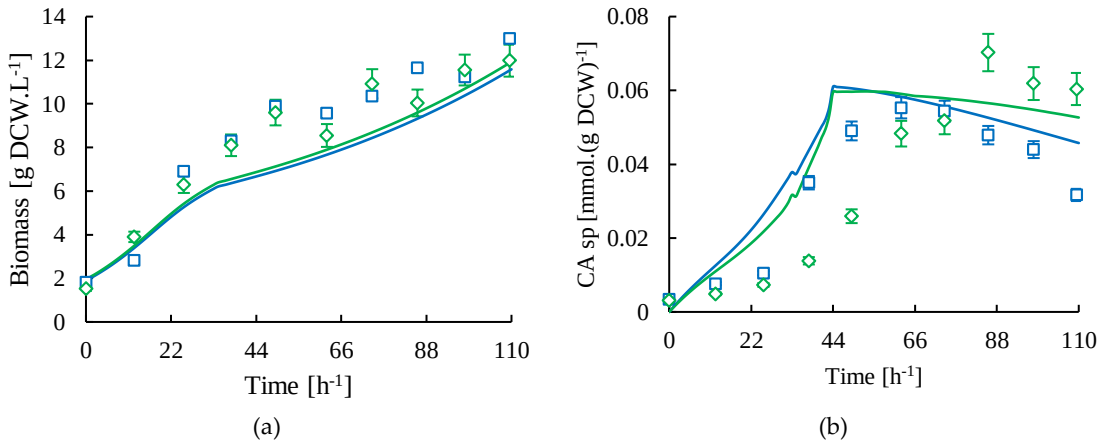

Figure 5.8. Experimental and simulated time-courses of fed-batch cultivations of *S. clavuligerus*. a) Biomass time-courses of cultivation with non- supplemented feeding (blue) and glutamate-supplemented feeding (green); b) Specific CA time-courses of cultivation with non-supplemented feeding (blue) and glutamate-supplemented feeding (green)

5.4. Conclusions

A DFBA approach linked to a previously validated GSMN of *S. clavuligerus* was used for the determination intracellular fluxes distribution based on macroscopic bioprocess variables. Initially, pseudo-steady state simulations allowed to analyze the sensitivity of the GSMN to constrains associated to the environmental cultivation conditions. Furthermore, potential metabolic targets were determined using the GSMN in pseudo-steady state conditions. The dynamic extension of the proposed model predicted correctly the substrates consumption, growth and antibiotic secretion in *S. clavuligerus* cultures under different environmental conditions. The dynamic flux distribution revealed the crucial role of TCA cycle and urea cycle in the CA biosynthesis. Moreover, the dynamic simulations indicated that fed-batch operation with glutamate supplementation entails positive effects on CA production by stimulating the reaction fluxes in the primary metabolism and CA biosynthesis.

DFBA simulations showed that single perturbations of CEAS and PYK reactions would cause a redistribution of metabolic fluxes that potentially would lead to higher CA secretion. Experimental studies using an engineered strain and implementing the fed-batch operation scenario deducted from DFBA simulations showed an improvement in CA production by approximately 1.09-fold the obtained with the wild-type strain. Our DFBA-GSMN provide complementary perspectives regarding the metabolic changes occurring during the bioprocess aimed to improve the antibiotic production levels. This is the first work involving the DFBA application to a *S. clavuligerus* GSMN. The results of this study provided insights about the dynamic metabolic state of *S. clavuligerus* cells, especially in non-steady state processes like the case of batch and fed-batch operations. The proposed model constitutes a valuable tool for the further analysis of effects of genetic, environmental and nutritional perturbations on the metabolism of the organism in connection with antibiotics secretion.

References

1. Saudagar, P.S.; Survase, S.A.; Singhal, R.S. Clavulanic acid: A review. *Biotechnol. Adv.* **2008**, *26*, 335–351.
2. Paradkar, A. Clavulanic acid production by Streptomyces clavuligerus: biogenesis, regulation and strain improvement. *J. Antibiot. (Tokyo).* **2013**, *66*, 411–20.
3. Ser, H.-L.; Law, J.W.-F.; Chaiyakunapruk, N.; Jacob, S.A.; Palanisamy, U.D.; Chan, K.-G.; Goh, B.-H.; Lee, L.-H. Fermentation Conditions that Affect Clavulanic Acid Production in Streptomyces clavuligerus: A Systematic Review. *Front. Microbiol.* **2016**, *7*, 522.
4. Kurt-Kizildoğan, A.; Vanli-Jaccard, G.; Mutlu, A.; Sertdemir, I.; Özcengiz, G. Genetic engineering of an industrial strain of Streptomyces clavuligerusfor further enhancement of clavulanic acid production. *Turkish J. Biol.* **2017**, *41*, 342–353.
5. Jnawali, H.N.; Yoo, J.C.; Sohng, J.K. Improvement of clavulanic acid production in Streptomyces clavuligerus by genetic manipulation of structural biosynthesis genes. *Biotechnol. Lett.* **2011**, *33*, 1221–1226.
6. Qin, R.; Zhong, C.; Zong, G.; Fu, J.; Pang, X.; Cao, G. Improvement of clavulanic acid production in Streptomyces clavuligerus F613-1 by using a claR - neo reporter strategy. *Electron. J. Biotechnol.* **2017**, *28*, 41–46.
7. Park, J.H.; Lee, S.Y.; Kim, T.Y.; Kim, H.U. Application of systems biology for bioprocess development. *Trends Biotechnol.* **2008**, *26*, 404–412.
8. Ramirez-malule, H.; Junne, S.; Cruz-bournazou, M.N.; Neubauer, P. Streptomyces clavuligerus shows a strong association between TCA cycle intermediate accumulation and clavulanic acid biosynthesis. *Appl. Microbiol. Biotechnol.* **2018**, *102*, 4009–402.
9. Toro, L.; Pinilla, L.; Avignone-Rossa, C.; Ríos-Estepa, R. An enhanced genome-scale metabolic reconstruction of Streptomyces clavuligerus identifies novel strain improvement strategies. *Bioprocess Biosyst. Eng.* **2018**, *41*, 657–669.
10. Wang, C.; Liu, J.; Liu, H.; Wang, J.; Wen, J. A genome-scale dynamic flux balance analysis model of Streptomyces tsukubaensis NRRL18488 to predict the targets for increasing FK506 production. *Biochem. Eng. J.* **2017**, *123*, 45–56.

11. Barreto-Rodriguez, C.M.; Ramirez-Angulo, J.P.; Gomez Ramirez, J.M.; Achenie, L.; Molina-Bulla, H.; González Barrios, A.F. Dynamic Flux Balance Analysis for Predicting Gene Overexpression Effects in Batch Cultures. *J. Biol. Syst.* **2014**, *22*, 1–12.
12. Mahadevan, R.; Edwards, J.S.; Doyle, F.J. Dynamic flux balance analysis of diauxic growth in Escherichia coli. *Biophys. J.* **2002**, *83*, 1331–1340.
13. Henson, M.A.; Hanly, T.J. Dynamic flux balance analysis for synthetic microbial communities. *IET Syst. Biol.* **2014**, *8*, 214–29.
14. Villegas, R.M.; Martinez, R. Identification of Dynamic Metabolic Flux Balance Models Based on Parametric Sensitivity Analysis by, University of Waterloo, 2016.
15. Feng, X.; Xu, Y.; Chen, Y.; Tang, Y.J. Integrating flux balance analysis into kinetic models to decipher the dynamic metabolism of shewanella oneidensis MR-1. *PLoS Comput. Biol.* **2012**, *8*.
16. Serrano-Bermúdez, L.M.; González Barrios, A.F.; Montoya, D. Clostridium butyricum population balance model: Predicting dynamic metabolic flux distributions using an objective function related to extracellular glycerol content. *PLoS One* **2018**, *13*, e0209447.
17. Salguero, D.A.M.; Fernández-Niño, M.; Serrano-Bermúdez, L.M.; Melo, D.O.P.; Winck, F. V.; Caldana, C.; Barrios, A.F.G. Development of a Chlamydomonas reinhardtii metabolic network dynamic model to describe distinct phenotypes occurring at different CO2 levels. *PeerJ* **2018**, *2018*, 1–25.
18. Saudagar, P.S.; Singhal, R.S. Optimization of nutritional requirements and feeding strategies for clavulanic acid production by Streptomyces clavuligerus. *Bioresour. Technol.* **2007**, *98*, 2010–2017.
19. Gómez, D.; Ramirez-malule, H.; Junne, S.; Neubauer, P.; Rios-estepa, R.; Junne, S.; Neubauer, P.; Rios-estepa, R. Accumulation of TCA cycle intermediates during Clavulanic Acid biosynthesis in batch cultures of Streptomyces clavuligerus. **2016**, 17.
20. Bushell, M.E.; Kirk, S.; Zhao, H.; Avignone-rossa, C.A. Manipulation of the physiology of clavulanic acid biosynthesis with the aid of metabolic flux analysis. *Enzyme Microb. Technol.* **2006**, *39*, 149–157.
21. Arulanantham, H.; Kershaw, N.J.; Hewitson, K.S.; Hughes, C.E.; Thirkettle, J.E.; Schofield, C.J. ORF17 from the clavulanic acid biosynthesis gene cluster catalyzes the ATP-dependent formation of N-glycyl-clavaminic acid. *J. Biol. Chem.* **2006**, *281*, 279–287.
22. Barreiro, C.; Martínez-Castro, M. Regulation of the phosphate metabolism in Streptomyces genus: impact on the secondary metabolites. *Appl. Microbiol. Biotechnol.* **2019**, *103*, 1643–1658.
23. Bellão, C.; Antonio, T.; Araujo, M.L.G.C.; Badino, A.C. Production of clavulanic acid and cephamycin c by streptomyces clavuligerus under different fed-batch conditions. *Brazilian J. Chem. Eng.* **2013**, *30*, 257–266.
24. Tahlan, K.; Anders, C.; Wong, A.; Mosher, R.H.; Beatty, P.H.; Brumlik, M.J.; Griffin, A.; Hughes, C.; Griffin, J.; Barton, B.; et al. 5S Clavam Biosynthetic Genes Are Located in Both the Clavam and Paralog Gene Clusters in Streptomyces clavuligerus. *Chem. Biol.* **2007**, *14*, 131–142.
25. Gomez-Escribano, J.P.; Martin, J.F.; Hesketh, A.; Bibb, M.J.; Liras, P. Streptomyces clavuligerus relA-null mutants overproduce clavulanic acid and cephamycin C: negative regulation of secondary metabolism by (p)ppGpp. *Microbiology* **2008**, *154*, 744–755.
26. Jnawali, H.N.; Liou, K.; Sohng, J.K. Role of σ-factor (orf21) in clavulanic acid production in Streptomyces clavuligerus NRRL3585. *Microbiol. Res.* **2011**, *166*, 369–379.
27. Jnawali, H.N.; Lee, H.C.; Sohng, J.K. Enhancement of Clavulanic Acid Production by Expressing Regulatory Genes in gap Gene Deletion Mutant of Streptomyces clavuligerus NRRL3585. *J. Microbiol. Biotechnol.* **2010**, *20*, 146–152.
28. Song, J.Y.; Jensen, S.E.; Lee, K.J. Clavulanic acid biosynthesis and genetic manipulation for its overproduction. *Appl. Microbiol. Biotechnol.* **2010**, *88*, 659–669.
29. Ramirez-Malule, H.; Restrepo, A.; Cardona, W.; Junne, S.; Neubauer, P.; Rios-Estepa, R. Inversion of the stereochemical configuration (3S, 5S)-clavaminic acid into (3R, 5R)-clavulanic acid: A computationally-assisted approach based on experimental evidence. *J. Theor. Biol.* **2016**, *395*, 40–50.
30. Li, R.; Townsend, C.A. Rational strain improvement for enhanced clavulanic acid production by genetic engineering of the glycolytic pathway in Streptomyces clavuligerus. **2006**, *8*, 240–252.
31. Gómez-Ríos, D.; Junne, S.; Neubauer, P.; Ochoa, S.; Ríos-Estepa, R.; Ramírez-Malule, H. Characterization of the Metabolic Response of Streptomyces clavuligerus to Shear Stress in Stirred Tanks and Single-Use 2D Rocking Motion Bioreactors for Clavulanic Acid Production. *Antibiotics* **2019**, *8*, 168.
32. Baptista-Neto, A.; Gouveia, E.R.; Badino-Jr, A.C.; Hokka, C.O. Phenomenological model of the

clavulanic acid production process utilizing Streptomyces clavuligerus. *Brazilian J. Chem. Eng.* **2000**, *17*, 809–818.
33. Sánchez, C.; Gomez, N.; Quintero, J.C.; Sanchez, C.; Gomez, N.; Quintero, J.C. Producción de Ácido Clavulánico por fermentación de Streptomyces clavuligerus : Evaluación de diferentes medios de cultivo y modelado matemático. *Dyna* **2012**, *79*, 158–165.
34. Teodoro, J.C.; Baptista-Neto, A.; Araujo, M.L.G.C.; Hokka, C.O.; Badino, A.C. Influence of glycerol and ornithine feeding on clavulanic acid production by streptomyces clavuligerus. *Brazilian J. Chem. Eng.* **2010**, *27*, 499–506.
35. Falzone, M.; Crespo, E.; Jones, K.; Khan, G.; Korn, V.L.; Patel, A.; Patel, M.; Patel, K.; Perkins, C.; Siddiqui, S.; et al. Nutritional control of antibiotic production by Streptomyces platensis MA7327: Importance of l-aspartic acid. *J. Antibiot. (Tokyo).* **2017**, *70*, 828–831.
36. Pinilla, L.; Toro, L.F.; Laing, E.; Alzate, J.F.; Ríos-Estepa, R. Comparative Transcriptome Analysis of Streptomyces Clavuligerus in Response to Favorable and Restrictive Nutritional Conditions. *Antibiotics* **2019**, *8*, 96.
37. Ramirez-Malule, H.; Junne, S.; López, C.; Zapata, J.; Sáez, A.; Neubauer, P.; Rios-Estepa, R. An improved HPLC-DAD method for clavulanic acid quantification in fermentation broths of Streptomyces clavuligerus. *J. Pharm. Biomed. Anal.* **2016**, *120*, 241–247.
38. Junne, S.; Klingner, A.; Kabisch, J.; Schweder, T.; Neubauer, P. A two-compartment bioreactor system made of commercial parts for bioprocess scale-down studies : Impact of oscillations on Bacillus subtilis fed-batch cultivations. *Biotechnol. J.* **2011**, *6*, 1009–1017.
39. Lemoine, A.; Martınez-Iturralde, N.M.; Spann, R.; Neubauer, P. Response of Corynebacterium glutamicum Exposed to Oscillating Cultivation Conditions in a Two- and a Novel Three-Compartment Scale- Down Bioreactor. *Biotechnol. Bioeng.* **2015**, *112*, 1220–1231.
40. Stanford, N.J.; Millard, P.; Swainston, N. RobOKoD: Microbial strain design for (over)production of target compounds. *Front. Cell Dev. Biol.* **2015**, *3*, 1–12.
41. Coze, F.; Gilard, F.; Tcherkez, G.; Virolle, M.-J.; Guyonvarch, A. Carbon-Flux Distribution within Streptomyces coelicolor Metabolism: A Comparison between the Actinorhodin-Producing Strain M145 and Its Non-Producing Derivative M1146. *PLoS One* **2013**, *8*, e84151.
42. Holzhütter, H.G. The principle of flux minimization and its application to estimate stationary fluxes in metabolic networks. *Eur. J. Biochem.* **2004**, *271*, 2905–2922.
43. López-Agudelo, V.A.; Baena, A.; Ramirez-Malule, H.; Ochoa, S.; Barrera, L.F.; Ríos-Estepa, R. Metabolic adaptation of two in silico mutants of Mycobacterium tuberculosis during infection. *BMC Syst. Biol.* **2017**, *11*, 1–18.

Chapter 6

Degradation Kinetics of Clavulanic Acid in Fermentation Broths at Low Temperatures

Abstract: Clavulanic acid (CA) yield in submerged cultures and downstream processing are compromised by a degradation phenomenon, which is not yet completely elucidated. In this contribution, a study of degradation kinetics of CA at low temperatures (–80, –20, 4, and 25 °C) and pH 6.8 in chemically-defined fermentation broths is presented. Samples of CA in the fermentation broths showed a fast decline of concentration during the first 5 h followed by a slower, but stable, reaction rate in the subsequent hours. A reversible-irreversible kinetic model was applied to explain the degradation rate of CA, its dependence on temperature and concentration. Kinetic parameters for the equilibrium and irreversible reactions were calculated and the proposed kinetic model was validated with experimental data of CA degradation ranging 16.3 mg/L to 127.0 mg/L. Degradation of the chromophore CA-imidazole, which is commonly used for quantifications by High Performance Liquid Chromatography, was also studied at 4 °C and 25 °C, showing a rapid rate of degradation according to irreversible first-order kinetics. A hydrolysis reaction mechanism is proposed as the cause of CA-imidazole loss in aqueous solutions.

6.1. Introduction

CA production is usually performed in submerged cultures of *S. clavuligerus* under aerobic conditions with glycerol as carbon source, maintaining controlled conditions of pH and temperature [5–9]. Previous studies have shown that CA stability increases at slightly acidic pH values [10,11]; several authors found a pH of 6.8 as favorable for obtaining high titers of CA in submerged cultures [5,7,9,12–16].

CA chemical instability largely depends on the pH-value owing to the presence of a carbonyl group linked to the β-lactam ring, which is susceptible to acid or basic catalyzed water attacks [17]. CA is also susceptible to moderate temperature increments, since they accelerate the rate of degradation regardless of the source [10]. Ishida et al. [18] showed that CA is unstable in production media, which contains ammonium ions and amine groups due to the presence of ammonium salts and amino acids.

Bersanetti et al. [10] investigated CA degradation at 10, 20, 25, 30, and 40 °C and pH values of 6.2 and 7.0. The results fitted an irreversible first-order kinetics accounting for the relationship between the degradation rate constant and the temperature. The highest CA stability was found at slightly acid conditions (pH 6.2) and low temperatures (10 °C). It was also observed that CA which originated from fermentation broth, degraded faster than the pure reagent and the commercial medicine [10].

The decomposition kinetics of CA in concentrations between 2.5 and 20 g/L was investigated by Brethauer et al [19]. A first-order kinetic model was proposed where the kinetic constant increased while increasing the initial CA concentration, indicating that CA accelerated its own decomposition [19]. Carvalho et al. [17] explored the CA long-term stability under different conditions of pH (4.0–8.0), temperature (20–45 °C) and ionic strength. The optimal conditions for achieving a low degradation rate were pH 6.0–7.2 and 20 °C; in contrast, addition of inorganic salts (NaCl, Na_2SO_4, $CaCl_2$, and $MgSO_4$) increased instability of CA, possibly due to the higher rate of collisions between molecules within the solution [17].

Marques et al. [11] studied the thermal effect on CA production during fermentation in the temperature range from 24 to 40 °C. The highest rates of CA formation and degradation were observed at relatively high temperatures (32 and 40 °C). The course of CA concentration fitted irreversible first-order kinetics and the temperature dependence followed an Arrhenius-type behavior [11].

Similarly, Costa and Badino [16] investigated the impact of temperature reduction from 30 to 25 °C, 30 to 20 °C, and 25 to 20 °C on CA titers during cultivation. The authors observed that temperature reduction had a stronger impact on CA production rather than on the reduction of CA degradation [16].

Different hypotheses regarding CA degradation have been proposed. It has been reported that amino acids and other metabolites or compounds present in the culture media affect the CA degradation, their effect is attributed to the polar groups probably attacking the four-ring lactam carboxyl group of CA to open the β-lactam ring [18,20]. The β-lactam compounds are susceptible to acid–base catalysis and contain groups such as amino or hydroxyl, which can act as catalysts leading to a self-catalyzed decomposition [19].

Due to the wide use of CA in pharmaceutical industry, its production is an intensive field of research [1]. CA stability in fermentation broths is of interest, especially for downstream processing, analysis, conservation and storage. Kinetics of CA degradation in fermentation broths at low temperatures have not been explored so far. This contribution is aimed at modeling and studying the kinetics of CA degradation at low temperatures (−80, −20, 4, and 25 °C) and pH 6.8 in chemically defined fermentation broths, as well as during the imidazole–derivatized conditions.

6.2. Materials and Methods

S. clavuligerus DSM 41826 cryo-preserved at −80 °C in glycerol solution (16.7% *v*/*v*) was inoculated for activation in seed medium as described by Roubos et al. [20]. Batch fermentations were carried out in a 15 L stirred tank bioreactor (Techfors S, Infors AG, Bottmingen, Switzerland) operated at 5 L filling volume. Chemically defined media, composed as follows, were used [35]: glycerol (9.3 g/L), K_2HPO_4 (0.8 g/L), $(NH_4)_2SO_4$ (1.26 g/L), monosodium glutamate (9.8 g/L), $FeSO_4 \cdot 7H_2O$ (0.18 g/L), $MgSO_4 \cdot 7H_2O$ (0.72 g/L) and trace element solution (1.44 mL). Trace elements solution contained: H_2SO_4 (20.4 g/L), monosodium citrate·$1H_2O$ (50 g/L), $ZnSO_4 \cdot 7H_2O$ (16.75 g/L), $CuSO_4 \cdot 5H_2O$ (2.5 g/L), $MnCl_2 \cdot 4H_2O$ (1.5 g/L), H_3BO_3 (2 g/L), and $Na_2MoO_4 \cdot 2H_2O$ (2 g/L). Antifoam 204 was used at a concentration of 1:1000 *v*/*v*, pH was controlled at 6.8 by using NaOH 4M and HCl 4M. Aeration was provided at 0.6 VVM and temperature was controlled in 28 °C.

Two samples (50 mL) of fermentation broth were withdrawn at 36 h of cultivation coinciding with phosphate limitation and exponential phase of growth, both conditions leading to the highest specific CA production and metabolic activity of the strain. Biomass and particulate material were separated by centrifugation at 12000 rpm and filtration using 0.2 μm pore size filters. Supernatants containing CA were adjusted to pH 6.8 and then vortexed and divided in 2 mL aliquots in Eppendorf tubes, according to the experimental design. Dilutions (1:2 and 1:5) were also prepared; finally, samples were divided into four groups and stored at the corresponding exposition temperatures.

A factorial experimental design was proposed; concentration and temperature were defined as factors varying at three and four levels, respectively. The concentration of the supernatant was set as the highest level; dilutions 1:2 and 1:5 were set as the medium and low levels, respectively. Twelve experimental runs were performed by duplicate. Supernatant samples were stored at −80 °C, −20 °C, 4 °C, and 25 °C, respectively, for 43 h. Supernatant samples were withdrawn at 3.1 h, 5.4 h, 18.3 h, 31.0 h, and 42.1 h of storage, derivatized with imidazole solution 20% during 30 min at 30 °C and 800 rpm in a mixing block and immediately analyzed by HPLC. To test the degradation profile at a higher CA concentration than that of the experimental design, an additional duplicate run of supernatant samples with higher CA content (127 mg/L) from a different batch produced with identical medium and conditions was also exposed to the referred temperatures and treated as previously indicated.

For the study of CAI stability, a 2-squared factorial design with duplicates was used. CA samples from fermentation broth with initial concentration of 127.0 mg/L (0.636 mM) and 61.7 mg/L (0.310 mM) were treated as previously described and derivatized. The derivatized samples were stored at 4 °C and 25 °C, aliquots were withdrawn at five different times in a time span of 46 h and analyzed by HPLC.

All the analyses of samples were carried out in an HPLC equipped with a DAD detector (1200 Series, Agilent Technologies, Waldbronn, Germany), using a Zorbax Eclipse XDB-C-18 chromatographic column (Agilent Technologies, Waldbronn, Germany) and a C-18 guard column (Phenomenex®, Aschaffenburg, Germany). The quantification of samples was carried out according to the gradient method described by Ramirez-Malule et al. [36].

The statistical analysis of the data for 95% of confidence was performed in Statgraphics Centurion XVII (Statgraphics Technologies, Inc. The Plains, Virginia, USA). Kinetic parameters were calculated by linear regression of experimental data with the least squares method; consistency was checked by determination of correlation coefficient (r^2) and residual analysis.

6.3. Results and Discussion

6.3.1. Clavulanic Acid Degradation

Previous studies have shown the susceptibility of CA to be decomposed in solution and fermentation broths when temperature ranges from 10 °C to 40 °C [10–12]. As far as we know, kinetics of CA degradation in fermentation broths at low temperatures have not been explored. The initial CA concentrations (CA_o) in supernatant samples included in the experimental design were 65.48 ± 0.04 mg/L (high level), 25.29 ± 0.03 mg/L (medium level), and 16.33 ± 0.04 mg/L (low level). An additional sample of higher concentration (CA_o =126.67 ± 0.04 mg/L) was included in the study. The experimental data presented in Figure 6.1 showed that the degradation proceeded at the highest rate during the first 5–6 h. Product loss was between 8 and 12% during this time. Interestingly, the rate of decomposition tended to slow down markedly as CA_o decreased, which was also confirmed in the statistical analysis. As expected, the degradation of CA was considerably accelerated when temperature increased; thus, at the highest temperature of exposition (25 °C), the accumulated loss of product reached 35% at 42 h at the highest initial CA_o. Comparable results were obtained by Ishida et al. [18] and Roubos et al. [20] in fermentation broths at 28°C with similar composition. In contrast, at the lowest temperature that was evaluated (−80 °C), the exhibited degradation rate was minimum, since less than 4% was lost in 42 hours. This is a desirable condition for long-term conservation of supernatant fermentation samples, assuring a stability of the product of interest.

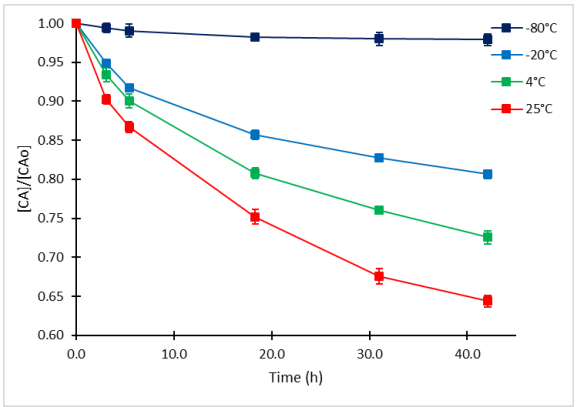

(a)

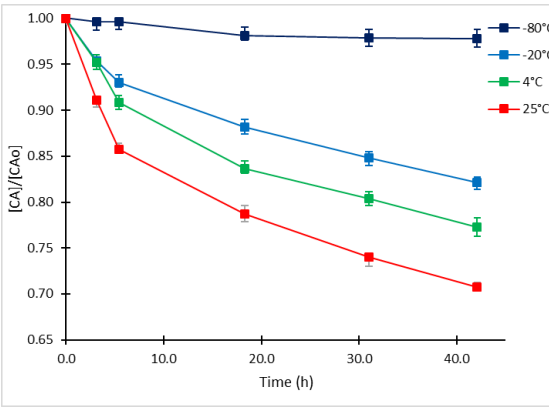

(b)

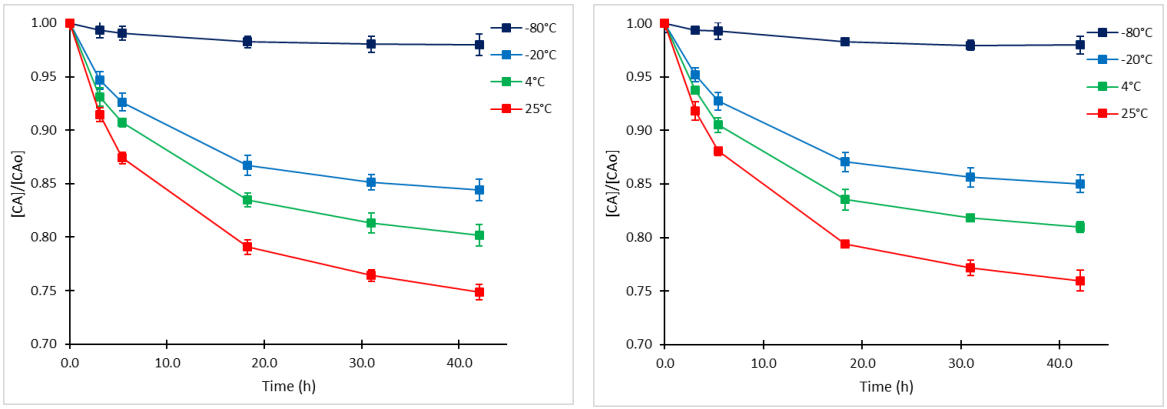

(c) (d)

Figure 6.1. Time courses of relative CA concentration at −80, −20, 4 and 25°C and different CA initial concentrations (CA_o). (**a**) CA_o= 126.7 mg/L; (**b**) CA_o= 65.5 mg/L; (**c**) CA_o= 25.3 mg/L; and (**d**) CA_o= 16.3 mg/L.

The high degradation rate at −20 °C was not initially expected; however, similar behavior was observed for other beta lactam antibiotics in aqueous solutions and CA in its pharmaceutical form [21–23]. This behavior might be caused by the expulsion of the solute to the liquid portion of the mixture, which can form a layer on the surface of ice or can be trapped between growing ice grain [24]. Thus, CA degradation would continue in the liquid portions. Additionally, given the continuous reduction of the liquid volume, the local concentration of the solute in this limited volume increases significantly also increasing the reaction rate [24]. Nevertheless, this condition must not remain for a long time since complete crystallization of the solution will necessarily stop the reaction. This condition might also explain the trends of degradation at −80 °C and its stabilization beyond 20 h.

The statistical analysis with 95% of confidence (r_2 = 0.996) indicates that both, temperature and CA_o, affect the degradation of CA in the time range explored (0 to 42.1 h.). The Pareto standardized chart (Figure 6.2) represents graphically the analysis of variance, showing the significant effects on the response variable, i.e., final CA concentration. The results of the analysis of variance show that the temperature effect is much more significant than CA_o and the combined interaction effect, influencing the final CA concentration negatively in the period between 0 and 42 h.

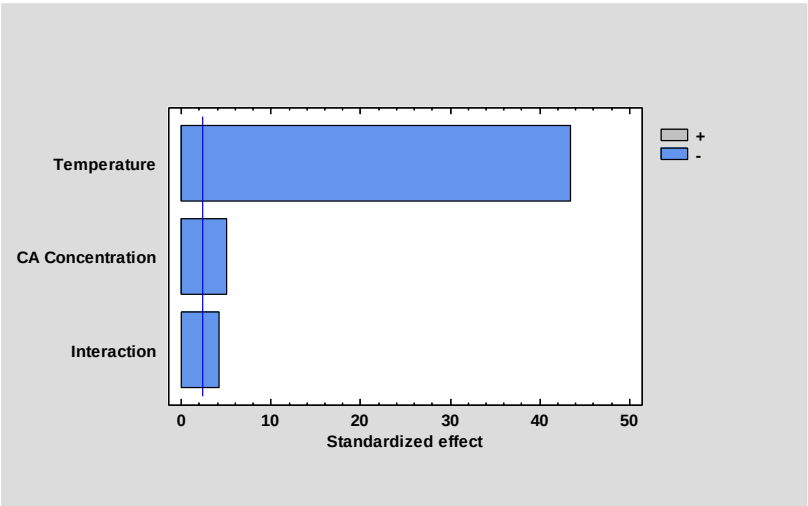

Figure 6.2. Temperature and concentration effects on CA final concentration

The trends of CA decomposition in fermentation broth seem to deviate from first and pseudo-first-order kinetics previously reported for CA solutions prepared with standard reactant or commercial formulations [10,19,23,25–27]. Similar behaviors to those observed in this work can be observed in the data presented by other authors for CA from fermentation broths in the range of 10 to 40 °C [10,17]. The rate of CA degradation is susceptible to medium composition, exhibiting higher degradation rates in supplemented and complex media [10,11,16]. In the present study, the degradation rate was expected to be low since the substances present in the supernatants would be considerably less.

Due to experimental limitations regarding the analysis of the products of CA decomposition, only the time course of CA concentration could be properly followed. Initial CA concentration of 65.5 mg/L was chosen as the base case for the estimation of the kinetic parameters of degradation for being in the middle of the range of concentrations under study. In Figure 6.3, a semi-log representation of CA at different temperatures is presented. A more pronounced slope of the line is attained during the first 5–6 h of exposition, the slope decreased substantially thereafter. Thus, two kinetic constants ($k_{obs,1}$ and $k_{obs,2}$) were determined by means of a linear regression from data plotted in Figure 6.3. The results of the observed rate constants $k_{obs,1}$ for $t < 5.5$ h and $k_{obs,2}$ for $t > 5.5$ h are presented in Table 6.1.

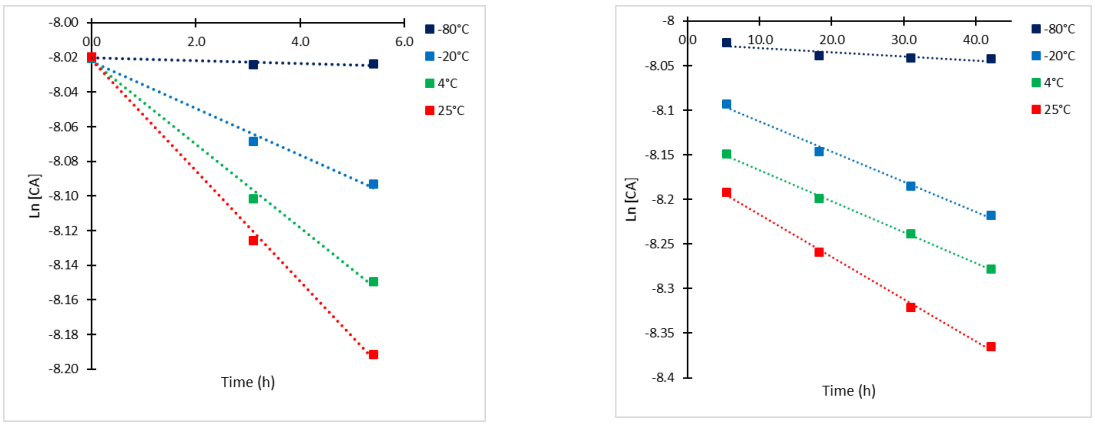

(a) (b)

Figure 6.3. Semi-log plots of CA concentration (CA_o = 65.5 mg/L) at −80, −20, 4 and 25 °C. (**a**) t ≤ 6 h; and (**b**) t > 6 h.

Table 6.1. Observed reaction rate constants for t < 5.5 h (kobs,1) and t > 5.5 h (kobs,2) at −80, −20, 4 and 25 °C.

Temperature	t < 5.5 h		t > 5.5 h	
	$k_{obs,1}$ (h^{-1})	r^2	$k_{obs,2}$ (h^{-1})	r^2
−80 °C	0.0009	0.969	0.0005	0.924
−20 °C	0.0135	0.991	0.0034	0.992
4 °C	0.0241	0.996	0.0035	0.998
25 °C	0.0320	0.998	0.0047	0.997

6.3.2. Kinetic Approach of CA Degradation

The increase of the reaction rate with temperature rise is typical of Arrhenius type kinetics and the significant effect of CA_o can be attributed to self-catalysis [19] or degradation reaction with stoichiometric coefficient higher than one. In this case, the dynamics of CA concentration at different temperatures do not fit with irreversible first-order or pseudo-first-order models; rather they are similar to those observed in two consecutive equilibrium-irreversible first-order reactions (Equations (1)

and (3)). A similar approach was also proposed by Carvalho et al. [17] for degradation of CA solutions prepared with standard reactant, at temperatures ranging from 20 to 40 °C. The observed time courses of CA degradation are typical of consecutive equilibrium-irreversible reactions in which the reaction rate of the irreversible reaction is considerably low in comparison to the equilibrium reaction (i.e., $k_2 < k_1 < k_{-1}$) [17]. Under these conditions, irreversible reaction would be the rate-limiting step, hence the reactant and the intermediate would be in equilibrium condition. Based on this analysis, the following kinetic mechanism of CA degradation was considered: a first step occurs in equilibrium, in which CA produces an active intermediate (I*), hereinafter this intermediate reacts irreversibly with an additional CA molecule to form the degradation product (D).

$$CA \leftrightarrows I^* \qquad r_1 = k_1[CA] - k_{-1}[I^*] \tag{1}$$

$$K_{eq} = \frac{k_1}{k_{-1}} \tag{2}$$

$$I^* + CA \rightarrow D \qquad r_2 = k_2[CA] \tag{3}$$

This kinetic approach is consequent with a feasible chemical mechanism of reaction for CA in aqueous solutions, characterized by several equilibrium steps (Figure 6.4) [28,29]. Additionally, this molecule has different potential candidate nodes (C atoms bonded to N and/or O) for suffering nucleophilic attacks from the substances present in the medium, e.g., CA itself, amino acids, and other metabolites with electronegative groups. In this regard, Zhong et al. [30] proposed a mechanism of formation of the degradation product known as substance E; this mechanism involves several steps, including the irreversible reaction of an active intermediate with an additional molecule of CA leading to the reported decomposition product.

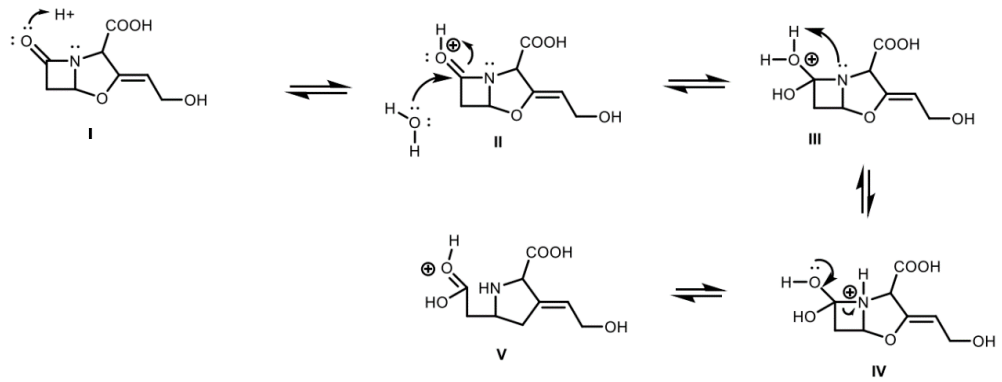

Figure 6.4. Early steps of CA degradation: (I). Protonation of carbonyl group in the β-lactam ring. (II). Nucleophilic attack of water to carbonyl group. (III). Deprotonation of water–protonation of the nitrogen. (IV–V). Breaking of C–N bond in the β-lactam ring.

In the general case, the early steps of CA degradation must involve the equilibrium reaction of opening of the β-lactam ring, via protonation of oxygen and nucleophilic attack of a water molecule to the carbonyl group (Figure 6.4). Once the open intermediate is formed, several irreversible possibilities can occur like nucleophilic attacks by nitrogen on other CA molecules or amino acids, imine formation via decarboxylation or attack of other substances present in the medium [31].

Under this kinetic approach, two kinetic rate constants were determined from experimental data: the equilibrium constant (K_{eq}) and the irreversible rate constant (k_2). During the first 5–6 h of exposition, and according to Equation (1), the equilibrium reaction is favoring the formation of intermediate I*, which is converted irreversibly into product D at lower reaction rate, thus the irreversible reaction (Equation (2)) is the rate-limiting step. This condition, allowed to determine the rate constant

(k_2) for the irreversible reaction from semi-log plot of CA concentration at each temperature (Figure 6.3a) [17]. Values of the irreversible rate constant (k_2) were previously determined as $k_{obs,1}$.

The significant concentration of intermediate I* after 6 shifts the equilibrium towards CA and hence, the equilibrium reaction (Equation (1)) is the rate-limiting step [17]. In the case of the equilibrium constant (K_{eq}), values were determined from experimental time courses of CA concentration by applying parameter estimation using the Levenberg-Marquadt method for least squares minimization. The summary of kinetic parameters for the two-reaction model for CA degradation is presented in Table 6.2.

Table 6.2. Kinetic constants for the Equilibrium-Irreversible reaction model of CA degradation.

Temperature	Equilibrium constant K_{eq}	Irreversible rate constant k_2 (h^{-1})
−80 °C	0.018	0.0009
−20 °C	0.162	0.0135
4 °C	0.210	0.0241
25 °C	0.280	0.0320

The estimated values of equilibrium constant confirmed the initial assumption of $k_2 < k_1 < k_{-1}$, since all the calculated values for k_2 were lower than K_{eq}, and all the estimated values of K_{eq} were lower than 1. For the case of the irreversible reaction (Equation (3)), the dependence of rate constant k_2 on temperature and activation energy were determined through linear regression of data in the Arrhenius plot (Figure 6.5). The activation energy (E_a) calculated for the irreversible process of degradation was 16.512 kJ/mol which is close to previous reports for CA in fermentation broths [10,17]. The corresponding frequency factor (A) was 26.97 h^{-1} with a correlation coefficient (r^2) of 0.961. The standard Gibbs free energy of activation for the reversible reaction (ΔG°) was determined assuming the previously determined equilibrium at 25 °C as the standard condition yielding a value of 3.155 kJ/mol. This shows that decomposition via a transition state is thermally activated. Marques et al. [11] pointed out that ΔG° values for CA formation are slightly higher than those for CA degradation and at moderate temperatures the degradation of CA would be practically unavoidable. This fact explains the accumulation of CA in the fermentation broth while the microorganism is active despite the continuous degradation. Yet, when the production rate decreases, CA would eventually disappear from the broth due to decomposition.

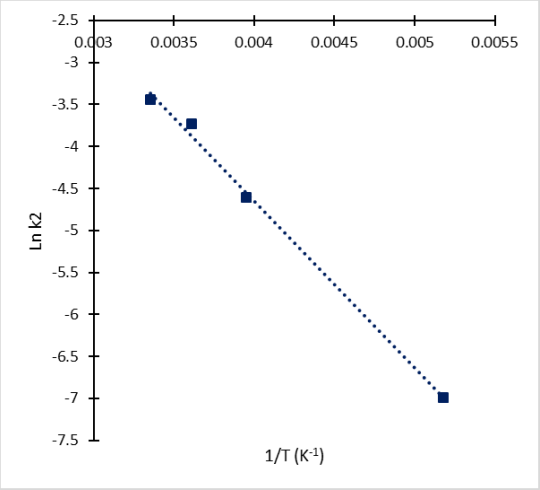

Figure 6.5. Arrhenius plot for determination of kinetic parameters (Ea and A) for the irreversible reaction of CA degradation.

6.3.3. Kinetic Model Validation

The proposed kinetic approach was validated with all the experimental data of CA degradation obtained in this study. Numerical simulations of the kinetic model were performed, and their results were compared with the experimental results of CA degradation at all temperatures and CA_o values. The CA relative concentration time courses and the corresponding experimental points are presented in Figure 6.6. The normalized-root-mean-square error (NRMSE) calculated between the complete experimental dataset and model predictions was used for assessing the accuracy of the kinetic model (Table 6.3).

Table 6.3. Normalized-root-mean-square error (NRMSE) for the kinetic model of CA degradation.

Concentration (mg/L)	Temperature (°C)	NRMSE (%)	Shelf life (t_{90})
126.7	−80	1.87	5.1 months
126.7	−20	3.22	9.0 h
126.7	4	2.18	6.5 h
126.7	25	3.78	4.5 h
65.5	−80	1.95	9.8 months
65.5	−20	4.98	9.7 h
65.5	4	4.93	6.6 h
65.5	25	4.45	4.6 h
25.3	−80	1.92	2.1 years
25.3	−20	3.36	9.9 h
25.3	4	3.27	6.7 h
25.3	25	3.40	4.7 h
16.3	−80	3.89	3.1 years
16.3	−20	1.98	10 h
16.3	4	2.53	6.8 h
16.3	25	2.42	4.8 h

As observed in Figure 6.6, the simulated time course of CA concentration shows a good approximation to the experimental values, notwithstanding the assumptions made for the determination of kinetic parameters. The proposed model of degradation simplified the decomposition of CA to only one intermediate product and one decomposition product following equilibrium and irreversible first-order kinetics; hence, deviations were expected between experimental and simulated data. Nevertheless, in the range of the concentrations and temperatures evaluated, the model showed a good fit, since the deviation of the predicted and measured concentrations was less than 5% in all cases. As it can be observed in Table 6.3, under this kinetic mechanism, the shelf-life of the product is highly dependent on temperature and initial CA concentration and not only on the rate constant as the case of the irreversible first-order reactions. The results obtained for the shelf-lives of CA in fermentation broth are comparable to the data obtained by Jerzsele and Nagy [26] for aqueous solutions of standard clavulanate, Bersanetti et al. [10], Ishida et al. [18] and Roubos et al. [20] for CA degradation in fermentation broths at room temperature. The shelf lives obtained at −20 °C confirm the significant degradation rate at this temperature, similar observations were reported in the temperature range from –7 to –25 °C for CA solutions of pharmaceutical CA [23] and other β-lactam compounds [21,22]. In all cases, the shelf lives of the CA in supernatants are considerably lower than those reported for CA aqueous solutions prepared with pharmaceutical formulations [24,25,32], possibly due to the addition of some stabilizing components to assure a long life in the commercial product.

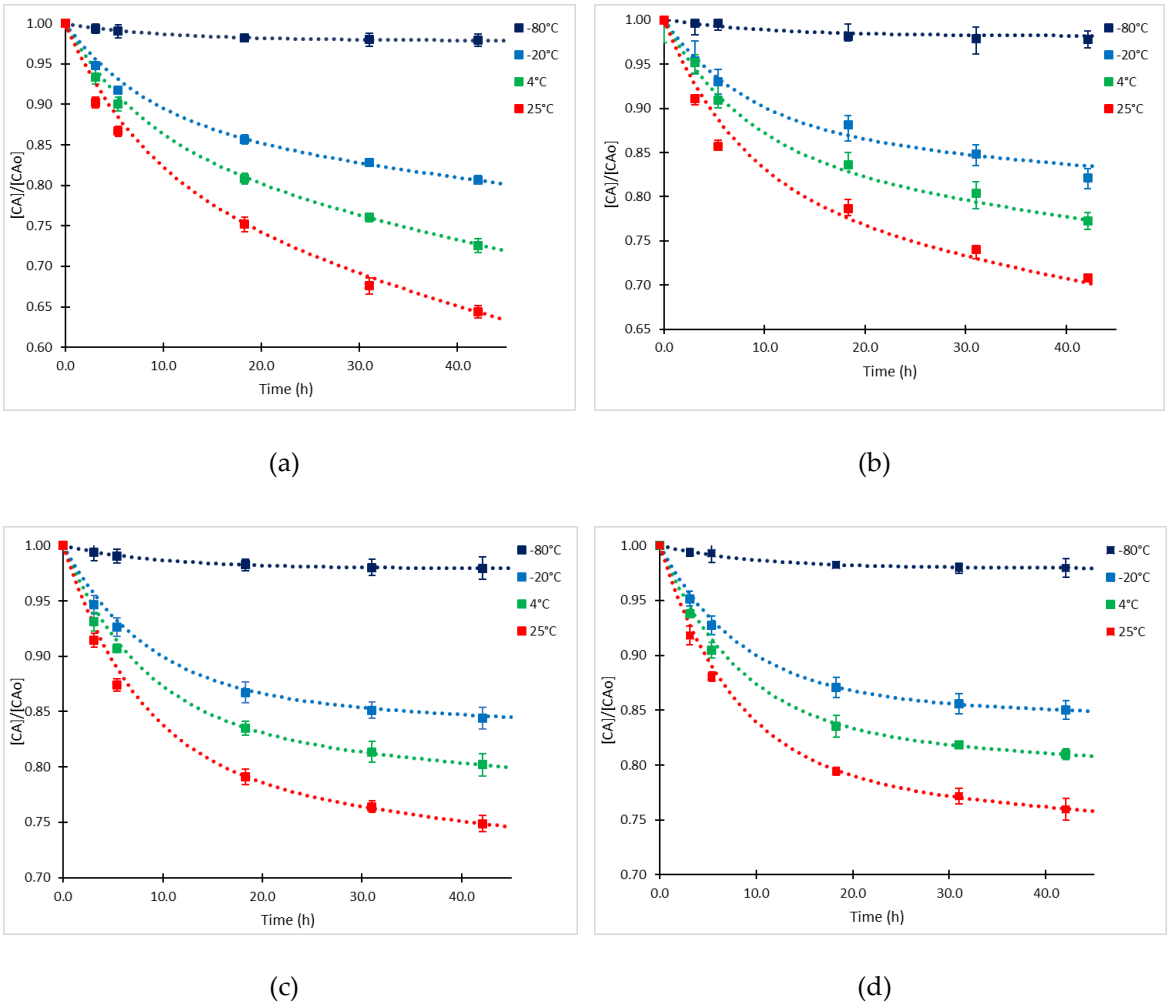

Figure 6.6. Experimental points (squares) and model prediction (dashed line) of CA degradation at −80, −20, 4 and 25 °C. (a) CAo= 126.7 mg/L; (b) CAo= 65.5 mg/L; (c) CAo= 25.3 mg/L; and (d) CAo= 16.3 mg/L.

The proposed kinetic approach for CA degradation explains the observed effect of increase in the reaction rate with increasing CA_o. The equilibrium-irreversible reaction model fits not only the hypothetical chemical reaction mechanisms involving equilibrium steps, but also the potential enzymatic degradation of CA in fermentation broths at temperatures higher than 4 °C, since Michaelis-Menten kinetics represents a special case of this kind of reactions. However, the most significant effect on CA degradation seems to be the chemical mechanism, considering the rapid degradation also observed in standard solutions and (aqueous) pharmaceutical products, where the presence of enzymes or proteins is discarded. Moreover, Ishida et al. [18] found no influence of exocellular proteins (in the culture broth) on the degradation of CA; hence, the enzymatic effect would not be considered as a degradation factor. Presence of free amino acids and decomposition products in CA solutions increase the degradation rate [18,19]; this might be an indicator of susceptibility of CA molecules to nucleophilic attacks added to the variable catalytic effect of pH [10,17,23,25].

6.3.4. Derivatized Clavulanate-Imidazole Degradation Kinetics

CA is poorly retained in C-18 reverse-phase columns for High Performance Liquid Chromatography (HPLC) and it does not produce distinctive peaks. Therefore, derivatization of CA is required to generate the chromophore clavulanate-imidazole (CAI), which is detectable at a

wavelength of 311 nm. During derivatization the β-lactam ring of CA is opened, yielding decarboxylation and formation of an amido group as shown in Figure 6.7.

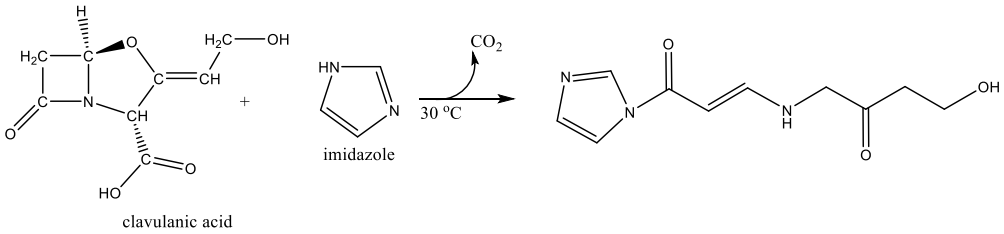

Figure 6.7. Derivatization of CA with imidazole: Alkylation of secondary nitrogen in the imidazole.

Considering the structural difference between the CAI and CA, it was observed that the chromophore is also unstable over time, following a different kinetic mechanism to the untreated CA. Statistical analysis with 95% of confidence (r^2 = 0.998) indicated that solely temperature had a significant effect on the final concentration of the analyzed CAI, showing a typical Arrhenius-type behavior. Time courses for CAI with initial concentrations (CAI_o) of 0.636 mM and 0.310 mM at 4 and 25 °C exhibited higher degradation rates than those for CA. In this case, the CAI showed linear dependency on concentration as it can be observed in the semi-log plot of relative concentrations for the CAI analyzed at different times (Figure 6.8), therefore, the degradation rate of the derivatized CA exhibited a first-order kinetics.

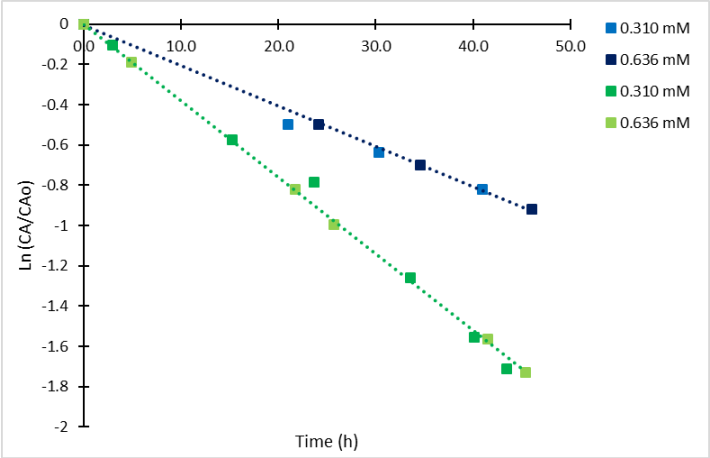

Figure 6.8. Semi-log plot of relative concentrations of derivatized CA at 4 °C (blue) and 25 °C (green).

The calculated kinetic rate constants were 0.020 h^{-1} (r^2 = 0.989) and 0.039 h^{-1} (r^2 = 0.994) at 4 °C and 25 °C. Both values are closer to those calculated for the irreversible step of reaction in CA degradation at the same temperatures (Table 6.2). Regarding the Arrhenius parameters (r^2 = 0.997), the calculated E_a was 21.85 kJ/mol, which is also close to the calculated value for the irreversible step for CA, the corresponding frequency factor (A) was 262.43 h^{-1}. The trend of the time course of degradation for the CAI does not suggest an equilibrium process as for the case of CA, possibly due to the structural chemical modification; other degradation products are formed following a different mechanism. The results indicate a loss of 56% of CAI complex during the first 24 h, reaching a maximum of 82% at 45h and 25 °C. Usually, HPLC autosamplers provide samples cooling at 4 °C. However, at this temperature, the rate of degradation is also significant showing a 40% decay in 24 h and a maximum of 60% in 46 h. As expected, the degradation rate constant and hence, the half-life of the chromophore are independent from the initial CA concentration. The half-lives of the complex were 34.5 h and 17.8 h at 4 °C and 25 °C, respectively. Nevertheless, the degradation process is slowed down by cooling down the solution at 4°C; 10% of the CAI formed is lost in 5 h. These results suggest

that it is convenient to spend a short time between sample derivatization and its injection in the HPLC column for assuring accurate quantification of CA, even if the sampler is cooled to 4 °C.

Since the chemical structure of the CA molecule is modified in the derivatization procedure, a different mechanism of reaction might be operating in the degradation of the chromophore. N-alkyl-imidazoles are hydrolytically unstable and they react under water-catalyzed, base-catalyzed (Figure 6.9), or acid-catalyzed (Figure 6.10) reaction mechanisms [33,34]. Therefore, it is probable that the degradation of the chromophore CAI occurs under one of those mechanisms depending on pH condition. CA is commonly produced and analyzed at slightly acidic conditions, hence, the degradation of the chromophore CAI would follow the mechanism presented in Figure 6.10. The irreversible hydrolysis of the complex might lead to underestimations of CA concentration of samples and/or overestimation of CA degradation rates due to the waiting time of the derivatized samples until the analyses are performed. The summary of experimental data and simulated data-points are presented in Supplementary material S5.

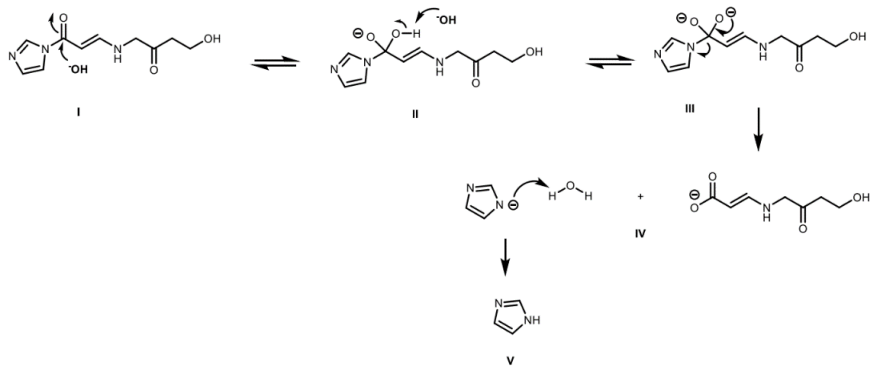

Figure 6.9. Base catalyzed hydrolysis of CAI: (I) Nucleophilic attack of hydroxyl to carbonyl group of CAI; (II) hydroxyl deprotonation and protonation of tertiary nitrogen; (III–IV) configuration of carboxyl group and elimination of imidazole ring; and (V) protonation of imidazole.

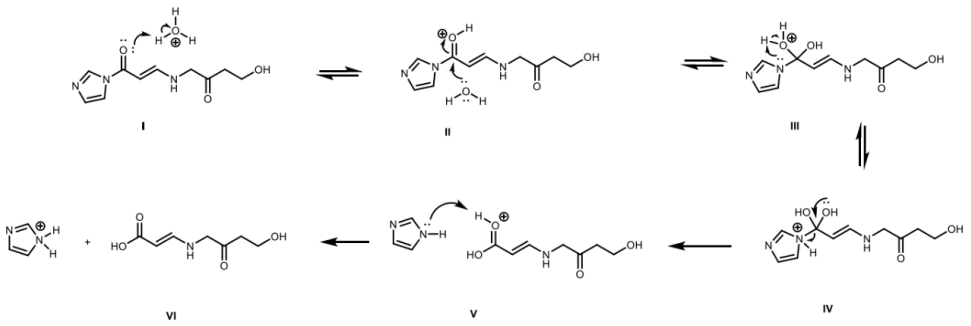

Figure 6.10. Acid catalyzed hydrolysis of CAI: (I) Protonation of carbonyl group of CAI; (II) Nucleophilic attack of water to carbonyl group of CAI; (III) water deprotonation; (IV) protonation of tertiary nitrogen and configuration or carboxyl group; (V) elimination of imidazole ring; and (VI) deprotonation of the carbonyl group and protonation of imidazole.

6.4. Conclusions

The kinetics of degradation of CA produced by *S. clavuligerus* DSM 41826 in a chemical defined medium was satisfactorily represented by two reaction models: one equilibrium reaction for intermediate formation and one irreversible first-order reaction for the degradation product formation. The equilibrium and irreversible reaction constants increased in parallel with temperature

following the Arrhenius behavior. The proposed model showed a better fit with the experimental points than the traditional irreversible first-order model. Calculated NRMSE values at different temperatures and concentrations were less than 5% in all cases.

The samples of CA in fermentation broth exhibited a fast decline of concentration during the first 5 h followed by a slower but stable reaction rate in the subsequent hours, which had been also observed in previous works. The reaction rate of degradation is dependent on several factors like pH, medium composition and temperature, which explains the high variability in the values of constant rates available in literature. The degradation rate at −80 °C is almost null, thus, this condition is appropriate for long-term storage of supernatants and stock solutions. At −20 °C the degradation rate in the time range explored is rather significant, but this condition is not expected to remain during a long time, since crystallization of the solution will avoid the progress of the reaction.

Although the proposed model simplified the decomposition of CA to only one intermediate product and one decomposition product, it allowed to predict the CA concentration pattern in a rather reliable manner. The model is also able to account for the change in the reaction rate depending on the initial CA concentrations and supports the hypothesis of degradation as consequence of a susceptibility to nucleophilic attacks at specific points of the molecule, which also might coincide with hypothetical enzyme catalyzed reactions at specific conditions.

Finally, the CAI chromophore, commonly used for spectrophotometric and HPLC analysis of CA samples, exhibited lower stability in time than the CA itself, possibly due to the susceptibility of N-alkyl-imidazoles to hydrolysis in aqueous solutions. Thus, a short time span is recommended between the derivatization of CA and the chromatographic analysis. For more reliable analysis of CA samples, after derivatization, the substance shall be conserved at 4 °C until the quantification is performed. Additionally, a temperature of −80 °C is recommended for long time storage of CA samples in order to avoid a significant loss of the product.

Publication: This section was published as Gómez-Ríos, D.; Ramírez-Malule, H.; Neubauer, P.; Junne, S.; Ríos-Estepa, R. Degradation kinetics of clavulanic acid in fermentation broths at low temperatures. *Antibiotics* **2019**, *8*, 6, doi:10.3390/antibiotics8010006.

Gómez-Ríos, D.; Ramírez-Malule, H.; Neubauer, P.; Junne, S.; Ríos-Estepa, R. Data of clavulanic acid and clavulanate-imidazole stability at low temperatures. *Data Br.* **2019**, *23*, 103775, doi:10.1016/j.dib.2019.103775.

References

1. Ramirez-Malule, H. Bibliometric Analysis of Global Research on Clavulanic Acid. *Antibiotics* **2018**, *7*, 1–14.
2. Viana Marques, D. de A.; Feitosa Machado, S.E.; Santos Ebinuma, V.C.; Lima Duarte, C. de A.; Converti, A.; Porto, A.L.F. Production of β -Lactamase Inhibitors by Streptomyces Species. *Antibiotics* **2018**, *7*, 1–26.
3. Takahashi, Y.; Nakashima, T. Actinomycetes, an Inexhaustible Source of Naturally Occurring Antibiotics. *Antibiotics* **2018**, *7*, 1–17.
4. Manteca, Á.; Yagüe, P. Streptomyces Differentiation in Liquid Cultures as a Trigger of Secondary Metabolism. *Antibiotics* **2018**, *7*, 1–13.
5. Ser, H.-L.; Law, J.W.-F.; Chaiyakunapruk, N.; Jacob, S.A.; Palanisamy, U.D.; Chan, K.-G.; Goh, B.-H.; Lee, L.-H. Fermentation Conditions that Affect Clavulanic Acid Production in Streptomyces clavuligerus: A Systematic Review. *Front. Microbiol.* **2016**, *7*, 522.
6. Saudagar, P.S.; Singhal, R.S. Optimization of nutritional requirements and feeding strategies for clavulanic acid production by Streptomyces clavuligerus. *Bioresour. Technol.* **2007**, *98*, 2010–2017.
7. Bellão, C.; Antonio, T.; Araujo, M.L.G.C.; Badino, A.C. Production of clavulanic acid and cephamycin c by streptomyces clavuligerus under different fed-batch conditions. *Brazilian J. Chem. Eng.* **2013**, *30*, 257–266.
8. Teodoro, J.C.; Baptista-Neto, A.; Araujo, M.L.G.C.; Hokka, C.O.; Badino, A.C. Influence of glycerol and ornithine feeding on clavulanic acid production by streptomyces clavuligerus. *Brazilian J. Chem. Eng.* **2010**, *27*, 499–506.
9. Neto, A.B.; Hirata, D.B.; Cassiano Filho, L.C.M.; Bellão, C.; Badino, A.C.; Hokka, C.O. A study on clavulanic acid production by Streptomyces clavuligerus in batch, FED-batch and continuous processes. *Brazilian J. Chem. Eng.* **2005**, *22*, 557–563.

10. Bersanetti, P.A.; Almeida, R.M.R.G.; Barboza, M.; Araújo, M.L.G.C.; Hokka, C.O. Kinetic studies on clavulanic acid degradation. *Biochem. Eng. J.* **2005**, *23*, 31–36.
11. Marques, D.A.V.; Oliveira, R.P.S.; Perego, P.; Porto, A.L.F.; Pessoa, A.; Converti, A. Kinetic and thermodynamic investigation on clavulanic acid formation and degradation during glycerol fermentation by Streptomyces DAUFPE 3060. *Enzyme Microb. Technol.* **2009**, *45*, 169–173.
12. Rosa, J.C.; Baptista Neto, A.; Hokka, C.O.; Badino, A.C. Influence of dissolved oxygen and shear conditions on clavulanic acid production by Streptomyces clavuligerus. *Bioprocess Biosyst. Eng.* **2005**, 99–104.
13. Teodoro, J.C.; Baptista-Neto, A.; Cruz-Hernández, I.L.; Hokka, C.O.; Badino, A.C. Influence of feeding conditions on clavulanic acid production in fed-batch cultivation with medium containing glycerol. *Appl. Microbiol. Biotechnol.* **2006**, *72*, 450–455.
14. Bushell, M.E.; Kirk, S.; Zhao, H.; Avignone-rossa, C.A. Manipulation of the physiology of clavulanic acid biosynthesis with the aid of metabolic flux analysis. *Enzyme Microb. Technol.* **2006**, *39*, 149–157.
15. Cerri, M.O.; Badino, A.C. Shear conditions in clavulanic acid production by Streptomyces clavuligerus in stirred tank and airlift bioreactors. *Bioprocess Biosyst. Eng.* **2012**, *35*, 977–984.
16. Costa, C.L.L.; Badino, A.C. Production of clavulanic acid by Streptomyces clavuligerus in batch cultures without and with glycerol pulses under different temperature conditions. *Biochem. Eng. J.* **2012**, *69*, 1–7.
17. Carvalho, V.; Brandão, J.F.; Brandão, R.; Rangel-yagui, C.O.; Couto, J.A.; Converti, A.; Pessoa, A. Stability of clavulanic acid under variable pH, ionic strength and temperature conditions. A new kinetic approach. **2009**, *45*, 89–93.
18. Ishida, K.; Hung, T..; Lee, H..; Liou, K.; Shin, C..; Yoon, Y..; Sohng, J. Degradation of Clavulanic Acid During the Cultivation of Streptomyces clavuligerus; Instability of Clavulanic Acid by Metabolites and Proteins from the Strain. *J. Microbiol. Biotechnol.* **2006**, *16*, 590–596.
19. Brethauer, S.; Held, M.; Panke, S. Clavulanic Acid Decomposition Is Catalyzed by the Compound Itself and by Its Decomposition Products. *J. Pharm. Sci.* **2008**, *97*, 3451–3455.
20. Roubos, J.A.; Krabben, P.; De Laat, W.; Heijnen, J.J. Clavulanic Acid Degradation in Streptomyces clavuligerus Fed-Batch Cultivations. *Biotechnol. Prog.* **2002**, *18*, 451–457.
21. Nickolai, D.J.; Lammel, C.J.; Byford, B.A.; Morris, J.H.; Kaplan, E.B.; Hadley, W.K.; Brooks, G.F. Effects of Storage Temperature and pH on the Stability of Eleven b-Lactam Antibiotics in MIC Trays. *J. Clin. Microbiol.* **1985**, *21*, 366–370.
22. Okerman, L.; Van Hende, J.; De Zutter, L. Stability of frozen stock solutions of beta-lactam antibiotics, cephalosporins, tetracyclines and quinolones used in antibiotic residue screening and antibiotic susceptibility testing. *Anal. Chim. Acta* **2007**, *586*, 284–288.
23. Vahdat, L.; Sunderland, V.B. Kinetics of amoxicillin and clavulanate degradation alone and in combination in aqueous solution under frozen conditions. *Int. J. Pharm.* **2007**, *342*, 95–104.
24. Vetráková, Ľ. Study of Processes Associated with Freezing of Aqueous Solutions, Masaryk University, 2017.
25. Vahdat, L.; Sunderland, B. The influence of potassium clavulanate on the rate of amoxicillin sodium degradation in phosphate and acetate buffers in the liquid state. *Drug Dev. Ind. Pharm.* **2009**, *35*, 471–479.
26. Jerzsele, Á.; Nagy, G. The stability of amoxicillin trihydrate and potassium clavulanate combination in aqueous solutions. *Acta Vet. Hung.* **2009**, *57*, 485–493.
27. Nur, A.O.; Hassan, A.A.; Gadkariem, E.A.; Osman, Z. Stability of Co-Amoxiclav Reconstituted Injectable Solution. *Eur. J. Pharm. Med. Res.* **2015**, *2*, 109–123.
28. Haginaka, J.; Yasuda, H.; Uno, T.; Nakagawa, T. Degradation of Clavulanic Acid in Aqueous Alkaline Solution: Isolation and Structural Investigation of Degradation Products. *Chem. Pharm. Bull.* **1985**, *33*, 218–224.
29. Finn, M.J.; Harris, M.A.; Hunt, E. Studies on the Hydrolysis of Clavulanic. *J. Chem. Soc. Perkin Trans. 1* **1984**, *0*, 1345–1349.
30. Zhong, C.; Cao, G.; Jin, X.; Wang, F. Studies on the formation and forming mechanism of the related substance E in potassium clavulanate production by HPLC-MS / MS. **2014**, *50*.
31. Soroka, D.; De La Sierra-Gallay, I.L.; Dubée, V.; Triboulet, S.; Van Tilbeurgh, H.; Compain, F.; Ballell, L.; Barros, D.; Mainardi, J.L.; Hugonnet, J.E.; et al. Hydrolysis of clavulanate by Mycobacterium tuberculosis β-lactamase BlaC harboring a canonical SDN motif. *Antimicrob. Agents Chemother.* **2015**, *59*, 5714–5720.

32. Peace, N.; Olubukola, O.; Moshood, A. Stability of reconstituted amoxicillin clavulanate potassium under simulated in-home storage conditions. *J. Appl. Pharm. Sci.* **2012**, *2*, 28–31.
33. Gour-Salin, B.J. Hydrolysis rates of some acetylimidazole derivatives. *Canadaian J. Chem.* **1983**, *61*, 2059–2061.
34. Joule, J.A.; Mills, K. 1,3-Azoles: Imidazoles, Thiazoles and Oxazoles: Reactions and Synthesis. In *Heterocyclic Chemistry*; John Wiley & Sons, Inc, 2010; pp. 461–467 ISBN 978-1-4051-3300-5.
35. Ramirez-malule, H.; Junne, S.; Cruz-bournazou, M.N.; Neubauer, P. Streptomyces clavuligerus shows a strong association between TCA cycle intermediate accumulation and clavulanic acid biosynthesis. *Appl. Microbilo. Biotechnol.* **2018**, 102, 4009–4023
36. Ramirez-Malule, H.; Junne, S.; López, C.; Zapata, J.; Sáez, A.; Neubauer, P.; Rios-Estepa, R. An improved HPLC-DAD method for clavulanic acid quantification in fermentation broths of Streptomyces clavuligerus. *J. Pharm. Biomed. Anal.* **2016**, *120*, 241–247.

Conclusions

In this work, the combination of experimental studies (at shake flask and bioreactor scales) with constraint-based modeling in pseudo-steady and dynamic conditions was used as strategy for studying the metabolic response of *S. clavuligerus* to environmental and nutritional perturbations in connection with clavulanic acid (CA) biosynthesis.

Despite the extensive experimental studies reported in the literature for CA production, global optimal cultivation conditions have been not identified, especially due to the lack of knowledge about the nutritional regulation of CA biosynthesis. The experimental testing of different cultivation conditions allowed to determine adequate medium formulation, operation mode and agitation for CA production in the shake flask scale. It was observed that the use of defined media led to rapid nutrients limitations, promoting in some extent, CA secretion. Fed-batch operation favored the continued CA secretion even under biomass synthesis deacceleration, as consequence of a constant supply of carbon and nitrogen sources without eliminating the nutritional restrictions that activate the secondary metabolism. Additionally, at shake flask-scale it was observed that moderate increase in agitation rate could also favor CA production. Those observations led us to propose a methodology for the analysis of the effect of shear forces on the bioprocess performance using stirred tank (STR) and 2-D rocking motion (CELL-tainer) bioreactors.

The motion patterns of STR and CELL-tainer bioreactors imply different oxygen transfer mechanisms and shear stress conditions. The results showed that low shear forces do not lead to significant hyphal fragmentation and promote mycelial thickening and branching. Conversely, the high shear forces arisen in STR favor biomass accumulation as consequence of mycelia fragmentation. In addition to phosphate limitation, the oxygen transport was identified as a critical factor for CA biosynthesis owing to the participation of molecular oxygen in CA biosynthesis. The mycelia thickening reduces considerably the surface-to-volume ratio, limiting the oxygen transport towards the cell, affecting the CA production rate. The highest CA production rate observed in STR was consistent with the phosphate depletion and increase of the respiratory quotient (RQ) as consequence of a higher oxygen uptake during CA biosynthesis. The most favorable conditions for CA production were attained during exponential growth when coexisting phosphate limitation, low concentrations of extracellular glutamate, added to glycerol and ammonia feeding under adequate oxygen transfer rate.

A new and enhanced genome-scale network (GSMN) of the *S. clavuligerus* metabolism was developed and curated by using the recent advances in GSMNs reconstruction and new available genetic information. The resultant iDG1237 model showed better predictive capabilities compared with the previous models of *S. clavuligerus* metabolism in relation to biomass and CA biosynthesis in metabolic scenarios of nutritional limitations. Flux balance analysis (FBA) simulations of experimentally observed scenarios during STR and CELL-tainer cultivations showed that phosphate depletion might lead to a considerable increase of fluxes through those reactions producing phosphate and pyrophosphate, configuring a stoichiometric supply of phosphate to primary metabolism under phosphate limitation scenarios. Thus, CA biosynthesis might be favored by such phosphate compensation, since the reactions catalyzed by the N2-(2-carboxyethyl) arginine synthase and the (carboxyethyl) arginine β-lactam synthase produce phosphate as by-products, contributing to maintain the intracellular pool of inorganic phosphate. Furthermore, glutamate availability would increase the reaction fluxes along glutamate metabolism and urea cycle, increasing at the same time the pool of phosphate and arginine as C-5 precursor of CA. The experimental as well as the *in silico* results, suggest that CA secretion is accompanied by an increase in oxygen uptake, and hence, by a carbon flux imbalance between the glycolysis and TCA cycle. Conversely, the RQ remains close to the unity when CA is poorly produced, evidencing a restriction in the supply of molecular oxygen in the clavams pathway.

A dynamic flux balance analysis (DFBA) approach linked to the iDG1237 GSMN of *S. clavuligerus* was used for the determination of intracellular fluxes distribution based on macroscopic bioprocess variables and experimental data for the substrates and important metabolites. The dynamic extension of the proposed GSMN predicted correctly the dynamics of substrates consumption, growth and CA secretion in *S. clavuligerus* cultures under different environmental conditions. The dynamic flux distributions obtained have revealed the crucial role of TCA and urea cycles in the CA biosynthesis. Moreover, the dynamic simulations suggested that a feeding medium modification to include glutamate, would favor CA production by stimulating the reaction fluxes along the primary and secondary metabolism. Besides, the DFBA showed that the overexpression of N2-(2-carboxyethyl) arginine synthase and the deletion of pyruvate kinase enzymes might cause a redistribution of metabolic fluxes along the central metabolism and CA biosynthesis, enhancing CA secretion. Experimental fed-batch cultivations with glutamate-supplemented feeding medium, showed an improvement in CA production by approximately 1.09-fold the obtained with the wild-type strain under identical environmental conditions. Thus, DFBA framework used in this work has provided complementary perspectives regarding the metabolic phenotypes during CA biosynthesis under non-steady state conditions. Furthermore, this is the first work considering dynamic analysis for a GSMN of *S. clavuligerus*. The proposed framework constitutes a valuable tool for further analysis of genetic, environmental and nutritional perturbations on the metabolism of the organism, in connection with the antibiotics secretion.

By using a rational approach, we identified the fed-batch operation with glutamate supplementation as a favorable condition for increasing the CA production in chemically defined medium with both, wild-type and engineered strains. Moreover, the combination of modeling and experimental studies considering a wide spectrum of operating and nutritional conditions could help to clarify the role of specific nutrients in *S. clavuligerus* secondary metabolism. During the quantification of extracellular metabolites, apart from L-arginine, L-aspartate, L-asparagine and L-glutamine, chromatographic peaks of glycine, L-valine, L-serine and L-threonine were detected, but these were out of the detection range; suggesting that also those amino acids could have a role in the regulation of CA biosynthesis and should further be explored. Additionally, previous studies have shown that other carbon sources than glycerol and possibly other amino acids, would stimulate the secondary metabolism and secretion of cephalosporins and penicillins. Since those products are competitors of CA pathway, it is desirable to determine under which conditions are they formed. However, the quantitative analytical techniques for analysis of those metabolites are still not well developed, and this is a necessity for the generation of more accurate constraint-based simulations.

A new approach consisting in a two-reaction model for CA degradation in fermentation broths was proposed: first, an equilibrium reaction forming an active intermediate and second, an irreversible first-order reaction leading to the formation of the consequent degradation product. The proposed model showed a better fit with the experimental points than the irreversible first-order model usually applied to CA degradation. The model was consistent with the concentration dependence of the reaction rate and supports the hypothesis of degradation due to a susceptibility of β-lactam ring to nucleophilic attacks in the carbonyl-group leading to the consequent CA hydrolysis. The clavulanate-imidazole chromophore commonly used for spectrophotometric and HPLC analysis, exhibits lower stability in time than the CA itself. This is possibly due to the susceptibility of N-alkyl-imidazoles to hydrolysis in aqueous solutions. In this regard, a short time span is recommended between the derivatization of CA and the chromatographic analysis for more reliable analysis of CA samples.

Finally, in order to improve further CA productivity, it is important to point out that the CA degradation during the fermentation requires the exploration of different *in-situ* and/or *ex-situ* separation and stabilization strategies aimed to reduce the loss of product during and after the cultivations. The low yields lead to mass transfer limitations and the interference of extracellular metabolites and media components could compromise the efficiency of the separation operations. If high productivities are attained during the cultivations (with either, the wild-type or engineered

strains) and more appropriated nutritional and environmental conditions are implemented, less costly down-streaming operations would be required. Furthermore, the determination of degradation rates during cultivation might help to a better estimation of CA production in submerged cultivations, for soft-sensor development and control purposes for instance.